

**Systems biology of *Streptomyces albus* to produce the  
antituberculosis polyketide pamamycin**

**Dissertation**

zur Erlangung des Grades  
des Doktors der Ingenieurwissenschaften  
der Naturwissenschaftlich-Technischen Fakultät  
der Universität des Saarlandes

von

**Lars Gläser**

Saarbrücken

2021

Tag des Kolloquiums: 03.12.2021

Dekan: Prof. Dr. Jörn Walter

Berichterstatter: Prof. Dr. Christoph Wittmann  
Prof. Dr. Andriy Luzhetskyy

Vorsitz: Prof. Dr. Uli Kazmaier

Akad. Mitarbeiter: Dr. Ruth Kiefer

## Publications

### Peer-reviewed articles:

**Gläser, L.**, Kuhl, M., Jovanovic, S., Fritz, M., Vögeli, B., Erb, T. J., Becker, J., Wittmann, C. (2020) A common approach for absolute quantification of short chain CoA thioesters in prokaryotic and eukaryotic microbes. *Microb. Cell Fact.* **19**, 160.

<https://doi.org/10.1186/s12934-020-01413-1>

**Gläser, L.**, Kuhl, M., Stegmüller, J., Rückert, C., Kalinowski, J., Luzhetskyy, A., Wittmann, C. (2021) Superior production of heavy pamamycin derivatives using a *bkdR* null mutant of *Streptomyces albus* J1074/R2. *Microb. Cell Fact.* **20**, 111.

<https://doi.org/10.1186/s12934-021-01602-6>

Kuhl, M., **Gläser, L.**, Rebets, Y., Rückert, C., Sarkar, N., Hartsch, T., Kalinowski, J., Luzhetskyy, A., Wittmann, C. (2020) Microparticles globally reprogram *Streptomyces albus* toward accelerated morphogenesis, streamlined carbon core metabolism, and enhanced production of the antituberculosis polyketide pamamycin. *Biotechnol. Bioeng.* **117**: 3858– 3875.

<https://doi.org/10.1002/bit.27537>

**The following peer-reviewed articles were co-authored during this work, but are not part of the dissertation:**

Borrero-de Acuña, J. M., Gutierrez-Urrutia, I., Hidalgo-Dumont, C., Aravena-Carrasco, C., Orellana-Saez, M., Palominos-Gonzalez, N., van Duuren, J. B. J. H., Wagner, V., **Gläser, L.**, Becker, J., Kohlstedt, M., Zacconi, F. C., Wittmann, C., and Poblete-Castro, I. (2020) Channeling carbon flux through the *meta*-cleavage route for improved poly(3-hydroxyalkanoate) production from benzoate and lignin-based aromatics in *Pseudomonas putida* H. *Microb. Biotechnol.* <https://doi.org/10.1111/1751-7915.13705>

Gummerlich, N., Manderscheid, N., Rebets, Y., Myronovskiy, M., **Gläser, L.**, Kuhl, M., Wittmann, C., and Luzhetskyy, A. (2021) Engineering the precursor pool to modulate the production of pamamycins in the heterologous host *S. albus* J1074. *Met. Eng.*

<https://doi.org/10.1016/j.ymben.2021.05.004>

Kuhl, M., Rückert, C., **Gläser, L.**, Beganovic, S., Luzhetskyy, A., Kalinowski, J., Wittmann, C. (2021) Microparticles enhance the formation of seven major classes of natural products in native and metabolically engineered actinobacteria through accelerated morphological development. *Biotechnol Bioeng.*

<https://doi.org/10.1002/bit.27818>

## Conference contributions

### Oral presentations

**Gläser, L.**, Kuhl, M., Rebets, Y., Rückert, C., Kalinowski, J., Luzhetskyy, A., and Wittmann, C.: Systems biology of secondary metabolites: Deciphering nutrient impact on pamamycin production in heterologous *Streptomyces albus* strain. 14<sup>th</sup> International Symposium on Genetics of Industrial Microorganisms, 9-11 September 2019, Pisa, Italy.

Beganovic, S., Becker, J., Kuhl, M., **Gläser, L.**, and Wittmann, C. MISSION to Morphology – bioprocess engineering for natural product formation in *Streptomyces*. 13<sup>th</sup> Meeting of the Slovenian Biochemical Society, 24-27 September 2019, Dobrna, Slovenia.

### Poster presentations

**Gläser, L.**, Kuhl, M., Rebets, Y., Rückert, C., Kalinowski, J., Luzhetskyy, A., and Wittmann, C.: Systems biology of secondary metabolites: Deciphering nutrient impact on pamamycin production in heterologous *Streptomyces albus* J1074/R2. HIPS Symposium, 27-28 June 2019, Saarbrücken, Germany

**Gläser, L.**, Kuhl, M., Rebets, Y., Rückert, C., Kalinowski, J., Luzhetskyy, A., and Wittmann, C.: Deciphering nutrient impact on pamamycin production in heterologous *Streptomyces albus* J1074/R2. PhD day Faculty NT, Saarland University, 6 November 2019, Saarbrücken, Germany.

# Danksagung



## Table of content

1	Introduction .....	1
1.1	General introduction .....	1
1.2	Main objectives.....	2
2	Theoretical Background.....	3
2.1	The phylum <i>Actinobacteria</i> .....	3
2.2	<i>Streptomyces</i> and secondary metabolism – The world of bioactive molecules .....	3
2.3	Systems biology of <i>Streptomyces</i> .....	5
2.4	<i>Streptomyces albus</i> J1074 as heterologous workhorse .....	7
2.5	Biosynthesis of the polyketide pamamycin in <i>S. albus</i> J1074/R2.....	8
2.6	CoA thioesters as central precursors for pamamycin.....	13
2.7	Precise quantification of CoA thioesters as pamamycin building blocks.....	14
2.8	Branched-chain amino acids as ideal source for pamamycin relevant CoA thioesters .....	16
3	Scientific Articles .....	19
3.1	Gläser et al. 2020 .....	19
3.2	Gläser et al. 2021 .....	33
3.3	Kuhl et al. 2020.....	50
4	General Discussion .....	69
4.1	A common approach for quantification of intracellular CoA thioesters applicable in broad biotechnological application fields.....	69
4.2	The ethylmalonyl-CoA pool is a key node to derive heavy pamamycin derivatives in <i>Streptomyces albus</i> J1074/R2 .....	70
4.3	Systems biology identifies the amino acid L-valine as trigger towards heavy pamamycin derivatives .....	71

4.4 BkdR as global player in the regulation of secondary metabolism .....	72
5 Conclusion and Outlook .....	73
6 References.....	75
7 Supplementary Information .....	89
7.1 Supplementary Information Gläser et al. 2020.....	89
7.2 Supplementary Information Gläser et al. 2021.....	95
7.3 Supplementary Information Kuhl et al. 2020 .....	121

## Summary

*Streptomyces* produce a range of polyketides, a class of small natural molecules with interesting bioactive properties that have significantly contributed to human well-being over the past decades. Therefore, the exploration of these microbes towards a streamlined overproduction of polyketides and the discovery of novel ones receives high interest. In this regard, this work deals with the development and establishment of an analytical approach, using LC-MS/MS to quantify intracellular CoA thioesters, the cellular building blocks to derive polyketides, as well as other products of interest. The developed method was validated for various microbes and then used to gain insight into the biosynthesis of pamamycins, a polyketide family with up to 16 isomers, in the heterologous host *Streptomyces albus*. First, this unraveled the link between CoA thioester availability and pamamycin spectrum. Second, the combined analysis of metabolome and transcriptome of *S. albus*, grown under different conditions, provided a global view on pamamycin production and its regulation. The amino acid L-valine emerged as beneficial medium supplement, as it substantially increased production. Inter alia, this led to the construction of a *bkdR* regulator mutant, which provided larger fractions of so far inaccessible heavy pamamycin derivatives.

## Zusammenfassung

Streptomyceten produzieren zahlreiche Polyketide, eine Klasse kleiner natürlicher Moleküle mit interessanten Eigenschaften, die im Laufe der letzten Jahrzehnte maßgeblich zum Wohlbefinden der Menschheit beigetragen haben. Die Erforschung dieser Mikroben mit dem Ziel einer zielgerichteten Überproduktion, sowie der Entdeckung neuer Substanzen erlangt größtes Interesse. In diesem Zusammenhang befasst sich diese Arbeit mit der Entwicklung und Etablierung einer analytischen Pipeline zur Quantifizierung von intrazellulären CoA-Thioestern mittels LC-MS/MS, wichtige Bausteine für Polyketide sowie anderer interessanter Produkte. Die hier entwickelte Methode wurde an unterschiedlichen Mikroben validiert und danach angewendet um nähere Einblicke in die Biosynthese der Pamamycine, eine Polyketide-Familie mit bis zu 16 Isomeren, in dem heterologen Produzenten *Streptomyces albus* zu erhalten. Dies enthüllte zunächst den Zusammenhang zwischen der Verfügbarkeit von CoA-Thioestern und dem Pamamycin-Spektrum. Zweitens lieferte die kombinierte Analyse von Metabolom und Transkriptom von *S. albus*, die unter verschiedenen Bedingungen kultiviert wurden, einen globalen Überblick über die Pamamycin-Produktion und ihrer Regulation. Die Aminosäure L-valin stellte sich als ideale Medienergänzung heraus, da sie die Produktion wesentlich erhöhte. Dies führte unter anderem zur Konstruktion einer *bkdR*-Regulatormutante, die größere Fraktionen bisher unzugänglicher schwerer Pamamycin-Derivate lieferte.

# 1 Introduction

## 1.1 General introduction

Microbes provide various products for the food and feed, the medical, the energy, and other industries (Becker & Wittmann, 2015). Especially *Streptomyces*, a class of actinobacteria have experienced a real boom in the last 70 years, and have been two-times awarded with the Nobel prize (Woodruff, 2014; Owens, 2015). The microbes are distributed in aquatic and terrestrial ecosystems and exhibit a unique multi-staged life-cycle with complex morphological differentiation, including vegetative filaments as well as spores (Barka et al., 2016). They are further known for their rich secondary metabolism, that has provided approximately 70% of all commercially available antibiotics today (Kitani et al., 2011; Ventola, 2015; Barka et al., 2016). In addition to antibiotics, the product range of *Streptomyces* covers herbicides, antifungals, antitumor drugs, and immunosuppressants (Barka et al., 2016)

As prominent example, the polyketide pamamycin was discovered in the 1970s (McCann & Pogell, 1979). The metabolite revealed growth inhibitory activity against gram-positive bacteria and fungi and was found to stimulate morphology development and secondary metabolism of *Streptomyces*. As example, pamamycins show high antibacterial potential against multi-resistant *Staphylococcus aureus* and *Mycobacterium tuberculosis*, among the top ten causes of deaths worldwide causing yearly more than one million deadly infections (Zaheen & Bloom, 2020). Over the years, different pamamycin derivatives were discovered that differ in molecular mass and biological activity (Natsume et al., 1991; Natsume et al., 1995; Kozone et al., 2008).

One of the challenges in the production of secondary metabolites are titers which are too low to enable further research (Bekiesch et al., 2016). This is also the case for pamamycins.

Fortunately, the genetic background of pamamycin biosynthesis was deciphered in *Streptomyces alboniger* (Rebets et al., 2015). The identification of the biosynthetic genes and their specific role in pamamycin biosynthesis enabled the creation of a heterologous pamamycin-overproducer (Rebets et al., 2015).

## 1.2 Main objectives

This work aimed to study the heterologous pamamycin producer *S. albus* J1074/R2 on the systems level. In this regard, the first goal was the establishment of a robust and precise approach for the quantification of intracellular CoA thioesters, the cellular building blocks of pamamycins. Towards broader impact and use, the method should be validated and applied for different gram-positive and gram-negative bacteria and yeast. Subsequently, the approach should be applied to study the production of pamamycins in *S. albus* J1074/R2, including different experimental conditions such as variations in medium composition and the supplementation with microparticles for enhanced production.

Second, the integration of metabolomic and transcriptomic analysis should gain insights into the biosynthesis of pamamycins and supporting pathways and eventually lead to improved production strains and processes. Of specific interest was the modulation of the pamamycin product spectrum towards increased fractions of so far inaccessible heavy derivatives to enable follow-up research on bioactivity and mode-of-action.

## 2 Theoretical Background

### 2.1 The phylum *Actinobacteria*

*Actinobacteria* form one of the largest phyla within the domain of *Bacteria* (Barka et al., 2016). The microbes belonging to this phylum are mostly free-living organisms with a high guanine-plus-cytosine (G+C) content (Barka et al., 2016; Chater, 2016). Based on their often filamentous phenotype, *Actinomycetes* have been described as intermediates between fungi and bacteria (Barka et al., 2016). In contrast to other bacteria, they grow by a combination of tip extension and hyphae branching (Barka et al., 2016; Kashiwagi et al., 2017). Hence, their name is derived from the Greek words “aktis” or “aktin” (English for ray), and “mukes” (fungi), whereby the similarity to fungi is purely phenotypically (Barka et al., 2016). *Actinobacteria* are widely distributed among aquatic and terrestrial ecosystems. Likewise, they can also live as plant symbionts, plant or animal pathogens, or gastrointestinal commensals (Barka et al., 2016).

### 2.2 *Streptomyces* and secondary metabolism – The world of bioactive molecules

*Streptomyces*, forming the largest genus of *Actinobacteria* (Williams & Vickers, 1988), are aerobic gram-positive bacteria that originated over 400 million years ago. They inhabit terrestrial and aquatic environments and play a key role in soil ecology, regarding their ability to use a wide range of nutrients, including complex polysaccharides, such as cellulose, chitin, xylan, and agar (Flardh & Buttner, 2009; Chater, 2016; Kashiwagi et al., 2017). Their wide abundance in soil honored them as “recycling specialists”, being indispensable for natural vegetation (Chater et al., 2010).

In contrast to most other bacteria, *Streptomyces* exhibit a filamentous fungus-like life cycle, which is divided into several growth phases (Kashiwagi et al., 2017). Under nutrient-rich conditions, the cycle starts with a germinating spore that forms a germ tube. Through tip extension, a branching vegetative mycelium network is then developed. When nutrients become scarce, a morphological differentiation is initiated and aerial hyphae are formed (Barka et al., 2016). The apical aerial hyphae are divided through sporulation, finally forming a new generation of spores to redistribute in search of new nutrient-rich areas, where the life cycle can start again (Figure 1) (Bibb, 2005; van Wezel & McDowall, 2011; Liu et al., 2013; Chater, 2016).

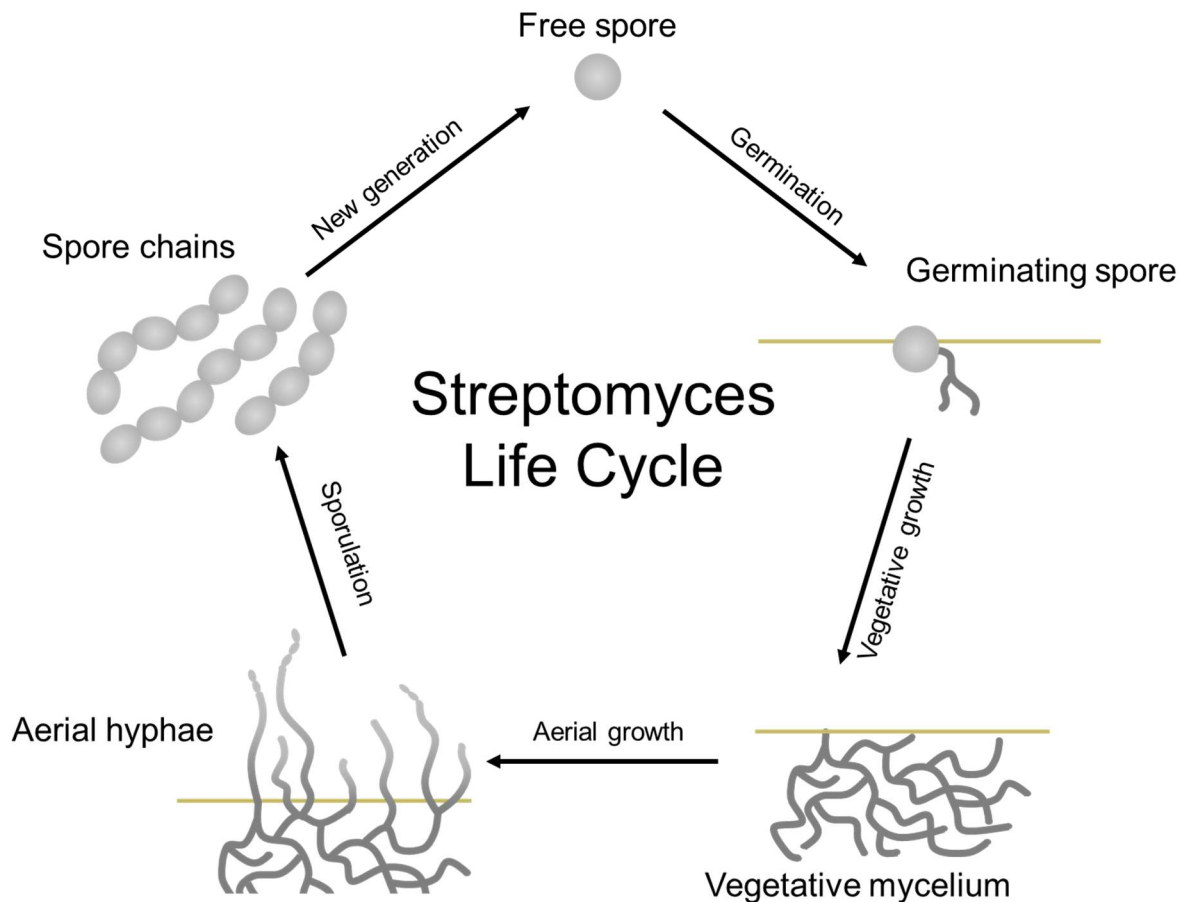


**Figure 1: Developmental lifecycle of *Streptomyces* species.** Germination of the spore in nutrient-rich environment leads to the formation of a germ tube progressively evolving to a vegetative mycelium. After nutrient scarcity, the aerial hyphae escape into the air. Morphological differentiation causes sporulation of those aerial hyphae into mature spore chains, later released into the environment, where the new generation can germinate in new nutrient-rich areas (adopted from (Kieser et al., 2000)).

*Streptomyces* are sedentary microorganisms. As a result, they depend on the prevailing supply of nutrients. When nutrient depletion occurs, *Streptomyces* use a sophisticated strategy to ensure continued life of the population. The branched vegetative mycelium partially undergoes an autolytic programmed cell death (PCD). The decomposition of cells results in the accumulation of amino acids, amino sugars, nucleotides, and lipids (Wildermuth, 1970; Mendez et al., 1985; Miguez et al., 1999; Barka et al., 2016). These substrates then provide building blocks for the aerial mycelium formation (Fernandez & Sanchez, 2002; Rigali et al., 2006; Barka et al., 2016). This release of carbon and other nutrients naturally attracts other microorganisms competing for those molecules, confronting *Streptomyces* with a new challenge through self-protection (Barka et al., 2016).

Closely connected to this morphological differentiation, *Streptomyces* exhibit a uniquely high capacity of secondary metabolites (van Wezel & McDowall, 2011; Barka et al., 2016). Secondary metabolites are not correlated to growth, but function as defense or signaling molecules.

Their biological activities, especially against various other microbes tempt the interest of agriculture, medicine, and veterinary industry (Kashiwagi et al., 2017). Today, more than 70% of all commercially available antibiotics are derived from *Streptomyces* (Kitani et al., 2011; Liu et al., 2020). The repertoire of clinical antibiotics comprises for instance: aminoglycosides (neomycin, kanamycin, streptomycin) (Vakulenko & Mobashery, 2003; Busscher et al., 2005; Park et al., 2013), anthracyclines (e.g., antitumor agent daunorubicin) (Minotti et al., 2004),  $\beta$ -lactams (cephamycin) (Liras, 1999), glycopeptides (vancomycin, teicoplanin) (Van Bambeke, 2006; Butler et al., 2014), macrolides (erythromycin, and tetracyclines) (Okami & Hotta, 1988; Gaynor & Mankin, 2003). Besides antibiotics, *Streptomyces* also supply insecticides (Ōmura & Crump, 2014; Thuan et al., 2014; Owens, 2015), bioherbicides (Bo et al., 2019), and antifungal agents (Lechevalier et al., 1953; Gil & Campelo-Diez, 2003), which emphasizes the importance of these bacteria in today's world and the rising interest of industry and research (Barka et al., 2016). The genomic basis for the versatile spectrum of metabolites is a variety of biosynthetic genes often clustered among the genomes. Most of these secondary clusters are weakly expressed or even silent under laboratory conditions (Nguyen et al., 2020). Genome sequencing research indicated, that roughly 90% of the chemical potential of actinobacterial organisms have remained undiscovered, predicting a pool of over 150,000 bioactive metabolites still waiting to be explored (Watve et al., 2001; Baltz, 2006; Barka et al., 2016).

### **2.3 Systems biology of *Streptomyces***

Until 2012, more than 500 *Streptomyces* species have been described (Kashiwagi et al., 2017). Due to the complex life cycle and the underlying regulatory networks, production at industrial level faces various barriers (Nguyen et al., 2020). However, the complex regulation of secondary metabolite biosynthesis is indispensable for a better understanding of the bioprocess for a desired improved production (Bekiesch et al., 2016). This comprises the correct balancing of preferred substrates and inhibitory nutrients for growth regarding carbon, nitrogen, and phosphate (Liu et al., 2013). Additionally, hormones (Kitani et al., 2011; Thao et al., 2017) and metals have been shown to affect antibiotic production (Abbas & Edwards, 1990; Coisne et al., 1999; Liu et al., 2013). Bioprocess parameters like pH and dissolved oxygen level were also shown to potentially disrupt the successful transfer from nature to industrial application (Liu et al., 2013).

Secondary metabolism of *Streptomyces* is known to be highly regulated especially on transcriptional level. In nature, it is triggered by biotic (microbial, physical, or chemical) and abiotic

(pH, temperature, pressure, or nutrient depletion) stress, different to laboratory conditions (Lee et al., 2021). This phenomenon leads to clusters being weakly expressed or even silent, challenging research to decipher these puzzles. At this point, the analysis of the transcriptome can help to gain a better understanding of the regulatory network behind the biosynthesis of secondary metabolites. Using deep-sequencing technologies, RNA-Seq provides a precise measurement of levels of transcripts and their isoforms. Over the years, the analysis of the transcriptome under different culture conditions or altered gene expression patterns has become a common approach to provide valuable information for further optimization (Lee et al., 2021). However, among sequenced *Streptomyces*, regulatory genes represent approximately 12% of the total genome, encoding more than 1000 transcription factors, highlighting the tremendous complexity of the regulatory network in these bacteria (Bentley et al., 2002; Romero-Rodriguez et al., 2015). Since secondary metabolism and primary metabolism are tightly connected, the modification of culture conditions is a promising way to gain closer insights into the biosynthesis of secondary metabolites (Lee et al., 2021). A systems biology analysis with the help of transcriptomics enables the identification of crucial transcriptional regulators, helping to decipher the underlying regulatory mechanisms.

As stated above, genes encoding the biosynthetic route for a secondary metabolite are typically clustered. They are variable in size, spanning from a few 1000 bp to more than 100 kb (Bekiesch et al., 2016). Most of these clusters contain regulatory genes, affecting the level of production of the respective metabolite (Liu et al., 2013). Formerly, such regulatory genes led to the term “pathway-specific” regulator. Over the years, different studies of these regulators revealed a more global influence than previously thought, which made the term “cluster-situated regulator” (CSR) more appropriate (van Wezel & McDowall, 2011). As shown, CSRs are controlled in a growth-dependent manner by proteins, also known as *Streptomyces* antibiotic regulatory proteins (SARPs) (Barka et al., 2016). SARPs are a specific family of proteins revealing high controlling activity on antibiotic production in *Streptomyces* (Liu et al., 2013). Two of the best-known members of this family are ActII-ORF4 and RedD in *S. coelicolor*, which control and activate the production of the pigmented antibiotics actinorhodin (ACT) and undecylprodigiosin (RED), respectively (Barka et al., 2016). Moreover, using actinorhodin as an example, the gene encoding ActII-ORF4 embedded in the actinorhodin cluster gets controlled on transcriptional expression by more than 15 different regulatory proteins. Transcription factors are highly diverse in *Streptomyces* (Romero-Rodriguez et al., 2015; Lee et al., 2021). Genetic studies in recent decades continuously identified new regulatory proteins, including sigma factors and transcription factors forming a hierarchically network connected by cross-regulation or auto-regulation (Romero-Rodriguez et al., 2015; Lee et al., 2021). They process cellular information regarding the physiological status of the cell regarding nutritional requirements including carbon, phosphate, and nitrogen (van Wezel & McDowall, 2011; Liu et al., 2013; Barka et al., 2016).

In addition to transcriptomics, a second useful technique to study secondary metabolism is metabolomics, which deals with the analysis and quantification of extracellular and intracellular small metabolites (<1000 Da) (Nicholson et al., 1999; Buchholz et al., 2002; Yang et al., 2019; Lee et al., 2021). Intracellular metabolite levels provide important information about reaction and consumption rates, fundamental for the relationship between metabolites and physiological changes (Yang et al., 2019).

The high complexity of metabolism requires efficient and robust analysis platforms. Mass spectrometry (MS) appears as an all-purpose solution for quantitative analysis with high sensitivity and selectivity. The availability of various atmospheric pressure ionization methods, e.g., electrospray ionization (ESI) or chemical ionization (APCI), enables the ionization of versatile metabolites in positive and negative mode (Xiao et al., 2012). The coupling of high-performance liquid chromatography (HPLC) with MS into LC-MS configurations has become a method of choice for precise and absolute quantification of small metabolites in complex biological samples, especially in the field of *Streptomyces* (Bowen & Northen, 2010; Xiao et al., 2012; Lee et al., 2021). The separation of metabolites prior to analysis reduces sample complexity and improves signal quality. In addition to the analysis of the sample and the interpretation of the data, the analytical quality mainly relies on the used sampling procedure (Zhou et al., 2012). Therefore, many efforts have aimed at robust sampling and extraction protocols. Common to all methods is the importance of extraction step and treatment of the samples to ensure precise and reproducible results (Yang et al., 2019). Consequently, isotope-labeled metabolites containing  $^{13}\text{C}$ ,  $^{15}\text{N}$  or  $^{18}\text{O}$  in exchange for their unlabeled atoms as internal standards were chosen as the golden method to avoid ion suppression effects and correct metabolite loss occurring during metabolomics (Berg & Strand, 2011; Gläser et al., 2020). Regarding *Streptomyces*, different metabolomic studies have been published. Most of these studies addressed the identification of new secondary metabolites found in *Streptomyces* rather than understanding the regulatory network between genetic regulation and metabolite concentrations (Lee et al., 2021).

## **2.4 *Streptomyces albus* J1074 as heterologous workhorse**

*Streptomyces albus* J1074 is a laboratory mutant, evolved from *S. albus* G (Chater & Wilde, 1976). This strain was found readily transformable as a basic cloning host even before cloning in *Streptomyces* was conceivable (Chater & Wilde, 1976; Baltz, 2010). The defectiveness of the *Sal*G1 restriction-modification system in J1074 made targeted genetic modifications feasible (Chater & Wilde, 1976; Chater & Wilde, 1980; Myronovskiy et al., 2014).

The potential of J1074 to produce secondary metabolites was recognized from early on (Baltz, 2010). The strain successfully expressed the heterologous clusters for steffimycin, an antibiotic

from the anthracycline family (Gullón et al., 2006). Especially due to its small genome with 6.8 Mb and fast growth, *S. albus* J1074 has turned out as an ideal production host and was used to derive a versatile spectrum of products (Table 1) (Wendt-Pienkowski et al., 2005; Myronovskyi et al., 2014; Bekiesch et al., 2016; Kallifidas et al., 2018).

**Table 1: Secondary metabolites produced in heterologous *Streptomyces albus* J1074.** Displayed are the products, their respective native host and the achieved titer. NR=not reported

Product	Native Host	Titer [mg L <sup>-1</sup> ]	Reference
Albumycin	<i>Micromonospora rosaria</i> SCIO N160	NR	(Huang et al., 2019)
Actinorhodin	<i>S. coelicolor</i>	50	(Kallifidas et al., 2018)
Fredericamycin	<i>S. griseus</i>	120	(Tetzlaff et al., 2006)
	<i>S. griseus</i>	132	(Chen et al., 2008)
Iso-migrastatin	<i>S. platensis</i>	46	(Feng et al., 2009)
Napyradiomycin	<i>Streptomyces</i> sp.	NR	(Winter et al., 2007)
Salumycin	NR	NR	(Tao et al., 2020)
Thiocoraline	<i>Micromonospora</i> sp.	NR	(Lombó et al., 2006)

## 2.5 Biosynthesis of the polyketide pamamycin in *S. albus* J1074/R2

Pamamycins are macrodiolide antibiotics of the polyketide family. In 1979, the first isolated pamamycin 607 from *Streptomyces alboniger* ATCC12461 was published (McCann & Pogell, 1979). Bioactivity studies revealed inhibitory function on growth of gram-positive bacteria, neurospora, mycobacteria, and fungi (McCann & Pogell, 1979; Pogell, 1998). Over the years, closer analysis revealed the presence of a versatile mixture of different pamamycin derivatives with varying molecular weight and biological activity (Natsume et al., 1991; Natsume et al., 1995; Lefevre et al., 2004; Kozone et al., 2008). Besides their antibacterial activity, pamamycins also showed stimulating function on aerial mycelia formation and affecting secondary metabolism of other *Streptomyces* (Hashimoto et al., 2011).

The chemical structure of pamamycin consists of a sixteen-membered macrodiolide as the carbon backbone carrying a dimethylamino group-bearing sidechain, being uncommon within the

polyketide family to contain a nitrogen atom (Figure 2) (Hashimoto et al., 2005). The dominant precursor molecules for pamamycin biosynthesis are CoA thioesters (Rebets et al., 2015; Kuhl et al., 2020). More precisely, CoA thioesters derived from central carbon metabolism succinyl-CoA and malonyl-CoA, as well as methylmalonyl-CoA and ethylmalonyl-CoA. The latter ones differing in the presence of a methyl-group are mainly originated from other pathways like amino acid or fatty acid metabolism (Figure 2) (Rebets et al., 2015; Kuhl et al., 2020; Gläser et al., 2021).

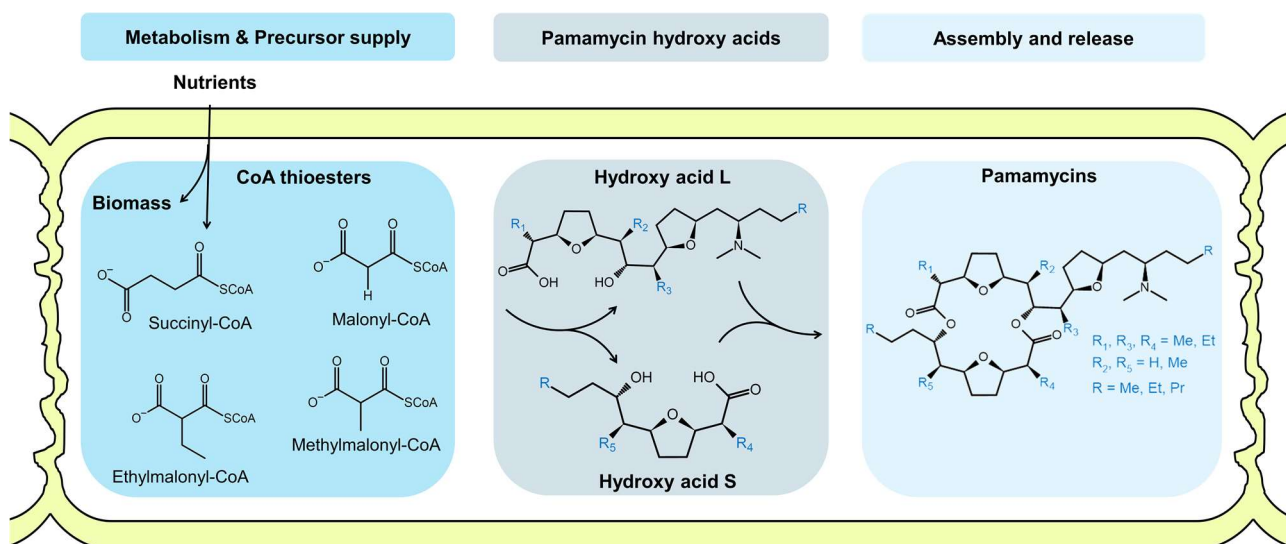


**Figure 2: Schematic biosynthesis of pamamycin in *Streptomyces species* (Gläser et al., 2021).**

Nutrients are metabolized and formed CoA thioesters as precursor molecules for pamamycin biosynthesis are supplied. Relevant precursors are succinyl-CoA, malonyl-CoA, methylmalonyl-CoA, and ethylmalonyl-CoA, where the latter ones decide over the molecular mass of produced pamamycins. Elongation of those CoA thioesters results in the formation of two hydroxy acids L and S, which are consequently combined for the final product. Within the molecule seven positions are highlighted (blue), where different precursors can be incorporated.

In 2015, new insights into biosynthesis of pamamycin were proposed, describing a genetic cluster harboring 20 genes responsible for pamamycin production (Figure 3). Those genes were isolated from a natural producer *S. alboniger* DSMZ40043 and cloned into a cosmid, called R2. Heterologous expression of this cosmid resulted in the pamamycin producer *S. albus* J1074/R2, building an ideal workhorse for further systems biology studies (Rebets et al., 2015).

From a genomic point of view, the biosynthetic genes are organized in two clusters (right and left core), both flanked by a regulatory encoding gene R1 and R2, respectively (Figure 3). Most of the genes encode for the enzymatic biosynthesis through the elongation by CoA thioesters building the carbon backbone, resulting in two uneven mass hydroxy acid L and S, which are finally assembled

into one molecule (Figure 2, Figure 4). In detail, the cluster situated *pam* genes encode for polyketide-ketosynthases, acyltransferases, ketoreductases/dehydrogenases, an acyl-carrier protein, a CoA-ligase, a hydrolase, an aminotransferase, a methyltransferase, and a putative pamamycin transporter. To determine the sequential biosynthetic steps for pamamycin production, a set of mutant cosmids lacking individual *pam* genes were created. Systems biology analyzes proposed the biosynthesis pathway and the role of individual genes for the biosynthesis of pamamycin (Rebets et al., 2015).

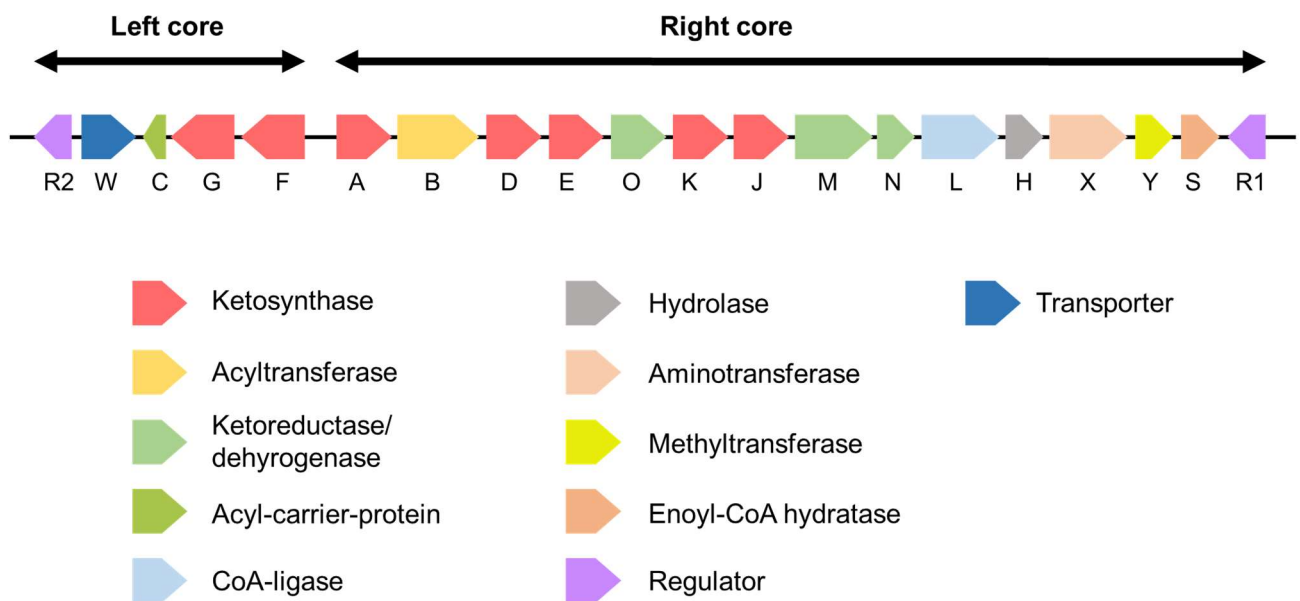


**Figure 3: Genetic organization of the pamamycin biosynthesis cluster in the cosmid R2 from *Streptomyces albus* J1074/R2.** The cluster is divided into a left and right core, each flanked by a regulatory gene R2 and R1, respectively. The respective genes are indicated by color and the main function assigned (adopted from (Rebets et al., 2015)).

In more detail, the pamamycin biosynthesis starts with the condensation of succinyl-CoA with either malonyl-CoA or methylmalonyl-CoA (Figure 4). The formed compounds are then rotated by the acyltransferase PamB resulting in 4-oxoadipyl-CoA or 5-methyl-4-oxoadipyl-CoA, respectively. Extension of these compounds gets accomplished by further incorporation of succinate via a Claisen condensation by PamD as a first extension by a short-chain acyl starter unit. PamE catalyzes the addition of malonyl-CoA or methylated derivatives like methylmalonyl-CoA or ethylmalonyl-CoA. Moving on, the biosynthesis gets separated into two branches. In the first branch, the interaction of the ketoreductases PamO, PamM, and PamN forms the double bond, and the hydratase PamS closes the tetrahydrofuran ring structure, resulting in the small

pamamycin hydroxy acid S. In the second branch, an additional adipate gets added by PamF. The extension of the carbon backbone with a malonate, derived by either methylmalonyl-CoA or ethylmalonyl-CoA is catalyzed by PamG. Same as with the little hydroxy acid, the larger carbon chain gets also reduced by PamO, M, and N and tetrahydrofuran ring structure closed by PamS. A special feature about pamamycin is the reductively amination and methylation by Pam X and PamY, resulting in the large pamamycin hydroxy acid L. Both hydroxy acids S and L are re-activated by the acyl-CoA-ligase PamL and finally assembled by PamJ and PamK to form the final pamamycin molecule (Rebets et al., 2015).

Since a few of the polyketide-ketosynthases are not ligand specific, they partially are able to use malonyl-CoA, methylmalonyl-CoA, or ethylmalonyl-CoA as substrate (Rebets et al., 2015). This yields in a near random incorporation of various precursors, leading to seven different known pamamycins with different masses, beginning from Pam 579, Pam 593, Pam 607, Pam 621, Pam 635, Pam 649, to Pam 663 (Gläser et al., 2020; Kuhl et al., 2020). Those derivatives distinguish by the presence of an additional methyl group due to the increased incorporation of methylmalonyl-CoA or ethylmalonyl-CoA (Rebets et al., 2015; Kuhl et al., 2020). In addition, the biosynthesis also enables the formation of various stereoisomers, depending on the incorporation position of each precursor. Summarized, the versatile mixture of different pamamycin derivatives and isomers builds a large pool of metabolites to be analyzed further in the future, additionally as promising basis for drug design.

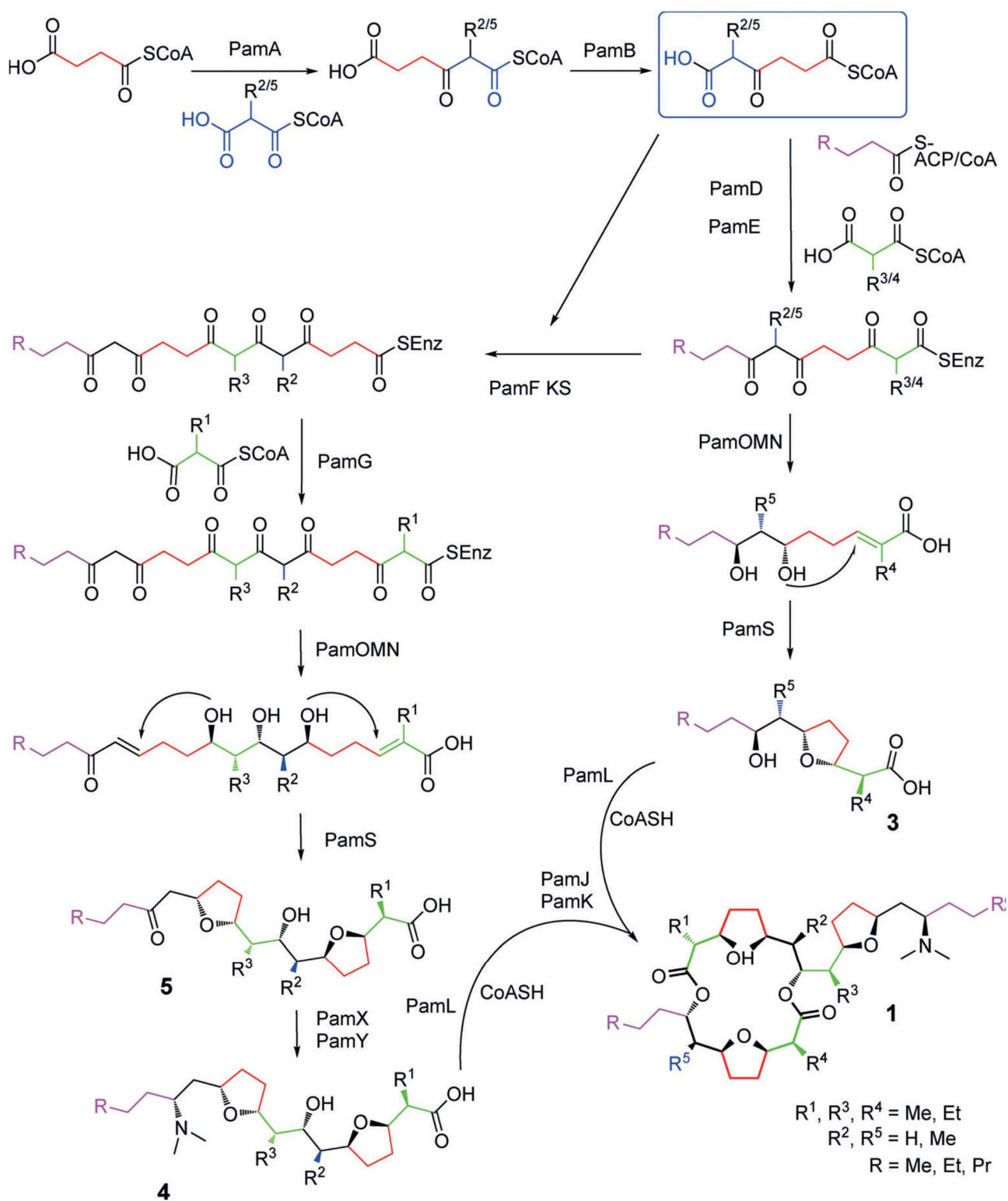


**Figure 4: Proposed pathway for the biosynthesis of pamamycin polyketides (Rebets et al., 2015).** Biosynthetic genes encoding the Pam-enzymes are associated to the respective reaction step, and the carbon backbones coloured to its originated CoA thioesters incorporated into the respective pamamycin hydroxy acid L (4) and S (3). Activation of both hydroxy acids and assembling results in final pamamycin molecule (1) with various methylated sidechains.

## 2.6 CoA thioesters as central precursors for panamycin

Evolution yielded in a highly complex network of different biological reactions comprising versatile metabolites. A relevant group of metabolites are CoA thioesters, ester between the coenzyme A and a carboxylic acid. In this form, CoA thioesters participate in about 5% of all enzymatic reactions, emphasizing the importance for the carbon metabolism, where one-third of carbon is estimated to be metabolized through CoA thioesters (Peter et al., 2016; Gläser et al., 2020). The basic structure a CoA thioester consists of one molecule adenosine diphosphate (ADP), pantothenate (vitamin B<sub>5</sub>), and a cysteine with a respective carbon residue at the thiol group (Figure 5).

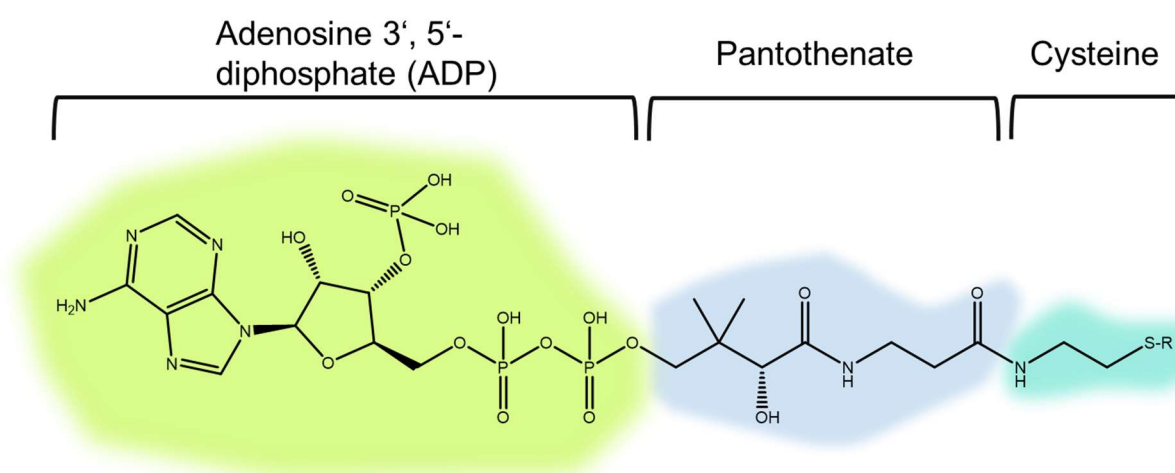


**Figure 5: Schematic structure of an CoA thioester.** The coenzyme A thioester consists of an adenosine 3'- 5'-diphosphate, and pantothenate and a cysteine optionally carrying an attached carboxylic acid (R), yielding a versatile spectrum of CoA thioesters.

The biosynthesis of coenzyme A is evolutionary highly conserved in all microbes (Gout, 2018). Modern bioinformatic databases attest a diversity of more than two hundred naturally occurring CoA thioester derivatives (Zimmermann et al., 2013). Most prominent representatives are acetyl-CoA and succinyl-CoA, both central intermediates in carbon core metabolism.

Besides cofactors and pathway intermediates, CoA thioesters display crucial building blocks of a wide range of microbial metabolites from a commercial perspective. Notable metabolites would be here antibiotics (Li et al., 2001; Milke & Marienhagen, 2020), insecticides (Yoon et al., 2004; Thuan et al., 2014), platform chemicals, like butyric-acid and biofuels (Branduardi et al., 2013; Suo et al., 2018), lipids in form of waxes (Shi et al., 2012) or fatty acids (Xu et al., 2016; Jovanovic et al.,

2021), food supplements like vitamins (Fang et al., 2017), or amino acids (Kind et al., 2013), and modern bioplastics, like polyhydroxyalkanoates (Borrero-de Acuna et al., 2014) (Figure 6).

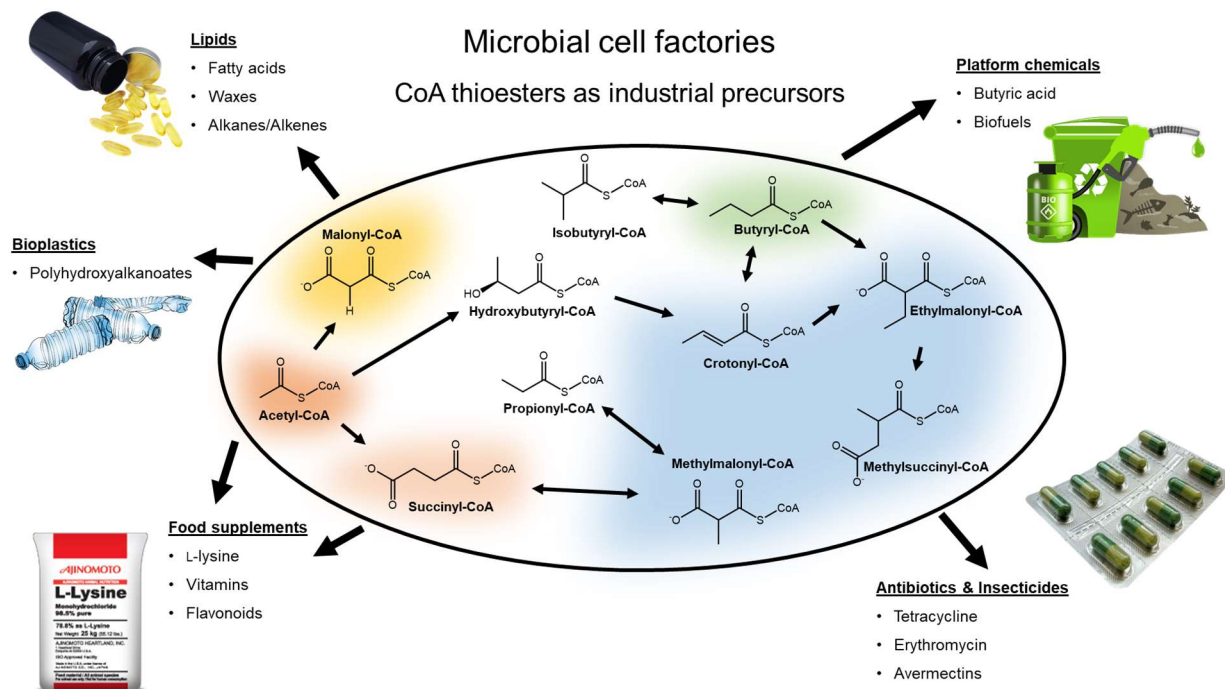


**Figure 6: CoA thioesters as important industrial precursor molecules for a wide range of commercially interesting molecules.** A selection of important CoA thioesters is displayed and their relationship to each other and to industrial products are indicated by arrows.

## 2.7 Precise quantification of CoA thioesters as pamamycin building blocks

Regarding secondary metabolism, the quantification of selected CoA thioesters has been demonstrated. As example, metabolite analysis in a salinomycin producing *S. albus* revealed a bottleneck in the supply of ethylmalonyl-CoA (Lu et al., 2016). In addition, medium optimization resulted in increased ethylmalonyl-CoA levels and increased production of tylactone (Park et al., 2007).

From a technical viewpoint, different approaches have been proposed. They comprise basic quantification via enzymatic assays (Kroeger et al., 2011), HPLC with UV detection (Todd King et al., 1988), capillary electrophoresis with UV detection (Liu et al., 2003), laser-induced fluorescence detection (Jiang et al., 2010) or gas chromatography-mass spectrometry (GC-MS) (Tamvakopoulos & Anderson, 1992; Kasumov et al., 2002; Neubauer et al., 2015). In recent years,

liquid chromatography with tandem mass spectrometric detection (LC-MS/MS) emerged as the state-of-the-art method. Reversed phase liquid chromatography using ion-pairing reagents (ion-pair RPLC) was used for the analysis for a broader spectrum of CoA thioesters (Neubauer et al., 2015). However, ion-pairing reagents have several disadvantages, especially through implying the establishment of a dedicated LC-MS/MS system targeted for the respective application in the field of metabolomics, as well as moderate sensitivities and impaired robustness (Neubauer et al., 2015). The establishment of LC-MS/MS methods for the analysis of CoA thioesters without ion-pairing reagents therefore seems desirable.

In addition to the measurement by LC-MS/MS itself, the extraction and sampling of the rather unstable CoA thioesters is of fundamental importance (King et al., 1988). A selection of different extraction methods is listed in Table 2. In the different studies, the used extraction protocols appeared specifically dedicated to the respective research goals, lacking the potential to be used in other application fields. Therefore, the establishment of a more common approach, applicable to many organisms and questions around CoA thioesters would be advantageous.

**Table 2: Methods for quantification of CoA thioesters in biological samples.** Listed are the samples derived from bacterial, animal and plant tissue, as well as the investigated CoA thioesters, and briefly the extraction method showing the immense diversity of published methods for the quantification of CoA thioesters.

Application field	Investigated CoA thioesters	Extraction method	Reference
<b>Bacterial samples</b>			
<i>Escherichia coli</i>	CoASH, short-chain acyl-CoAs, e.g., acetyl-CoA, crotonyl-CoA, butyryl-CoA, and isovaleryl-CoA	Chloroform -45 °C	(Coulier et al., 2006)
	Acetyl-CoA, butyryl-CoA, malonyl-CoA, methylmalonyl-CoA, propionyl-CoA, succinyl-CoA, and glutaryl-CoA	ACN/MeOH/H <sub>2</sub> O + 0.1 % HCOOH at -20 °C	(Armando et al., 2012)
<i>Saccharomyces cerevisiae</i>	CoASH, acetyl-CoA, succinyl-CoA, phenylacetyl-CoA and other CoA thioesters	Boiling ethanol	(Seifar et al., 2013)
<i>Megasphaera elsdenii</i>	Acetyl-CoA, butyryl-CoA, CoASH, CoASSCoA, crotonyl-CoA, hydroxybutyryl-CoA, hexanoyl-CoA, malonyl-CoA, propionyl-CoA, and succinyl-CoA	Methanol -20 °C + freeze-thaw	(Neubauer et al., 2015)
<b>Plant tissue</b>	Acetyl-CoA, malonyl-CoA and propionyl-CoA	5% trifluoroacetic acid + homogenizer	(Hayashi & Satoh, 2006)
<b>Animal tissue</b>	Acetyl-CoA, malonyl-CoA and other short-chain and long-chain CoA thioesters	2-Propanol, KH <sub>2</sub> PO <sub>4</sub> , NH <sub>4</sub> SO <sub>4</sub> , ACN at 4 °C	(Magnes et al., 2008)

## 2.8 Branched-chain amino acids as ideal source for pamamycin relevant CoA thioesters

Among the proteinogenic amino acids, the branched-chain amino acids (BCAAs) L-valine, L-leucine, and L-isoleucine account for about 18% of all amino acids in protein across many life-forms (Neinast et al., 2019). Therefore, the small hydrophobic and branched amino acids serve as essential building blocks for all biological processes. Despite not all organisms are able to synthesize them on their own, the catabolism pathways are still highly conserved in nature cross-

species (Neinast et al., 2019). The initial enzymatic reactions are similar for all three BCAAs beginning with a transamination forming respective branched-chain  $\alpha$ -ketoacids  $\alpha$ -ketoisovaleric-acid,  $\alpha$ -ketoisocaproic-acid, and  $\beta$ -methylvaleric-acid, respectively (Sprusansky et al., 2005). The following two steps are common to all BCAAs, performed by the branched-chain amino acid dehydrogenase (BCDH) complex. First, the respective acid gets decarboxylated and a subsequent dehydrogenation by NAD results in the corresponding acyl-CoA thioester derivative isobutyryl-CoA, isovaleryl-CoA, and  $\alpha$ -methylbutyryl-CoA. In detail, the BCDH complex consists of four subunits, E1- $\alpha$ - and E1- $\beta$  with a dehydrogenase and decarboxylase function, E2 with acyltransferase function, and E3 with a dihydrolipoamide dehydrogenase function. The genes encoding the first three subunits are clustered together, interestingly, the gene encoding E3 is not linked to the genetic BCDH cluster and is located elsewhere in the genome (Sprusansky et al., 2005). The subsequent steps convert the respective CoA derivatives further finally entering the central carbon metabolism into the tricarboxylic acid (TCA) via acetyl-CoA or succinyl-CoA.

Regarding the production of secondary metabolites, BCAAs seem a promising supplement for improved production titers (Rebets et al., 2015; Yi et al., 2018). For instance, supplemented L-valine increased the bitespiramycin titer by 45% in *S. spiramyceticus*. The use of the L-leucine did not affect the final titer but shifted the production spectrum towards isovalerylspiramycin, a bitespiramycin derivative, resulting in a different incorporation of available CoA thioesters (Li et al., 2009). Regarding the biosynthesis of pamamycin, the degradation of the BCAAs supplies methylmalonyl-CoA and succinyl-CoA.

Since the BCDH complex is conserved within most bacteria, *Streptomyces* are unique since they possess two BCDH clusters within their genome (Sprusansky et al., 2005). Targeting the BCDH complex was found useful to improve secondary metabolite production. The overexpression of the BCDH complex for instance, yielded a 52-fold increased actinorhodin level in *S. coelicolor* (Kim et al., 2014).

The regulation of the BCDH cluster was mainly investigated in *Pseudomonas putida* (Madhusudhan et al., 1999) and *Bacillus subtilis* (Debarbouille et al., 1999). It was found that the transcriptional activator BkdR, upstream of the BCDH cluster, affected the degradation of BCAAs. A homologue to *bkdR* was then discovered in *S. coelicolor*, placed in front of one of the two BCDH clusters (Sprusansky et al., 2005). Its protein product revealed high similarity to the leucine-responsive regulatory proteins (Lrp), a class of transcription factors (Lee et al., 2015). The deletion of this regulator in *S. coelicolor* affected morphological development and secondary metabolism (Sprusansky et al., 2005). A null mutant of this gene was defective in sporulation and failed in associated actinorhodin production, indicating a more global function in *Streptomyces*. Additionally, BKdR was shown to repress transcription of one BCDH cluster, causing constitutive overexpression in the null mutant (Sprusansky et al., 2005). Furthermore, the role of *bkdR* in the L-

valine-dependent valinomycin and bafilomycin production in *Streptomyces* sp. M10 was investigated (Lee et al., 2015). Here, the knockout of *bkdR* yielded a 2.4-fold increased production of bafilomycin but did not affect the valinomycin yield. Both secondary metabolites share 2-ketoisovaleric acid, a deamination product of L-valine, as common precursor. While valinomycin requires D-hydroxyisovaleric-acid through oxidation, bafilomycin precursor is isobutyric-acid which is formed from 2-ketoisovaleric acid through the BCDH complex (Lee et al., 2015). The few different studies on *bkdR* so far, highlight the importance of this regulator for the breakdown of BCAAs, secondary metabolism and morphology.

### 3 Scientific Articles

The thesis is based on three research papers, all reproduced in this chapter.

#### 3.1 Gläser et al. 2020

##### **A common approach for absolute quantification of short chain CoA thioesters in prokaryotic and eukaryotic microbes.**

Lars Gläser, Martin Kuhl, Sofija Jovanovic, Michel Fritz, Bastian Vögeli, Tobias J. Erb, Judith Becker, and Christoph Wittmann

*Microbial Cell Factories* **19**, 160 (2020).

<https://doi.org/10.1186/s12934-020-01413-1>

This is an open access article published under the terms of a Creative Commons Attribution 4.0 International License.

BV synthesized CoA thioesters. LG, MK and MF developed the CoA thioester extraction and analytical protocol. LG produced the <sup>13</sup>C labeled extracts and conducted cultivation of *S. albus*, *C. glutamicum*, and *P. putida*. SJ performed cultivation of *Y. lipolytica*. LG conducted thioester analysis. CW conceived and structured the work. LG, JB and CW wrote the first draft of the manuscript. All authors critically commented and improved the manuscript. All authors read and approved the final manuscript.

RESEARCH

Open Access



# A common approach for absolute quantification of short chain CoA thioesters in prokaryotic and eukaryotic microbes

Lars Gläser<sup>1</sup>, Martin Kuhl<sup>1</sup>, Sofija Jovanovic<sup>1</sup>, Michel Fritz<sup>1</sup>, Bastian Vögeli<sup>2</sup>, Tobias J. Erb<sup>2</sup>, Judith Becker<sup>1</sup> and Christoph Wittmann<sup>1\*</sup>

## Abstract

**Background:** Thioesters of coenzyme A participate in 5% of all enzymatic reactions. In microbial cell factories, they function as building blocks for products of recognized commercial value, including natural products such as polyketides, polyunsaturated fatty acids, biofuels, and biopolymers. A core spectrum of approximately 5–10 short chain thioesters is present in many microbes, as inferred from their genomic repertoire. The relevance of these metabolites explains the high interest to trace and quantify them in microbial cells.

**Results:** Here, we describe a common workflow for extraction and absolute quantification of short chain CoA thioesters in different gram-positive and gram-negative bacteria and eukaryotic yeast, i.e. *Corynebacterium glutamicum*, *Streptomyces albus*, *Pseudomonas putida*, and *Yarrowia lipolytica*. The approach assessed intracellular CoA thioesters down to the picomolar level and exhibited high precision and reproducibility for all microbes, as shown by principal component analysis. Furthermore, it provided interesting insights into microbial CoA metabolism. A succinyl-CoA synthase defective mutant of *C. glutamicum* exhibited an unaffected level of succinyl-CoA that indicated a complete compensation by the L-lysine pathway to bypass the disrupted TCA cycle. Methylmalonyl-CoA, an important building block of high-value polyketides, was identified as dominant CoA thioester in the actinomycete *S. albus*. The microbe revealed a more than 10,000-fold difference in the abundance of intracellular CoA thioesters. A recombinant strain of *S. albus*, which produced different derivatives of the antituberculosis polyketide pamamycin, revealed a significant depletion of CoA thioesters of the ethylmalonyl CoA pathway, influencing product level and spectrum.

**Conclusions:** The high relevance of short chain CoA thioesters to synthesize industrial products and the interesting insights gained from the examples shown in this work, suggest analyzing these metabolites in microbial cell factories more routinely than done so far. Due to its broad application range, the developed approach appears useful to be applied this purpose. Hereby, the possibility to use one single protocol promises to facilitate automatized efforts, which rely on standardized workflows.

**Keywords:** *Corynebacterium glutamicum*, *Streptomyces albus*, *Pseudomonas putida*, *Yarrowia lipolytica*, Lysine, Pamamycin, CoA thioester, LC–MS

## Background

Microbial cell factories are a key to the bio-based industry [1]. Upgrading and streamlining their biocatalytic activity through systems metabolic engineering requires detailed understanding of the underlying metabolism [2–5]. Among other techniques, the assessment of intracellular metabolite

\*Correspondence: christoph.wittmann@uni-saarland.de

<sup>1</sup> Institute of Systems Biotechnology, Saarland University, Saarbrücken, Germany

Full list of author information is available at the end of the article



© The Author(s) 2020. This article is licensed under a Creative Commons Attribution 4.0 International License, which permits use, sharing, adaptation, distribution and reproduction in any medium or format, as long as you give appropriate credit to the original author(s) and the source, provide a link to the Creative Commons licence, and indicate if changes were made. The images or other third party material in this article are included in the article's Creative Commons licence, unless indicated otherwise in a credit line to the material. If material is not included in the article's Creative Commons licence and your intended use is not permitted by statutory regulation or exceeds the permitted use, you will need to obtain permission directly from the copyright holder. To view a copy of this licence, visit <http://creativecommons.org/licenses/by/4.0/>. The Creative Commons Public Domain Dedication waiver (<http://creativecommons.org/publicdomain/zero/1.0/>) applies to the data made available in this article, unless otherwise stated in a credit line to the data.

levels and pathway fluxes has proven valuable to understand metabolic network function and its regulation and derive novel targets for strain engineering [1, 6].

A relevant group of metabolites are thioesters, esters between a carboxylic acid and a thiol. In microbial metabolism, the best-known and most relevant thioesters are short chain CoA thioesters, derivatives of coenzyme A (CoA) [7, 8]. Notably, CoA thioesters such as acetyl-CoA and succinyl-CoA participate in 5% of all enzymatic reactions and at least one-third of all cellular carbon is typically metabolized through a CoA thioester [7]. As example, they provide activated groups to drive the anabolic synthesis of cellular constituents such as peptides, fatty acids, sterols, and terpenes, display intermediates of catabolic pathways, and are essential to central energy metabolism [8]. Today, bioinformatics databases reveal more than two hundred naturally occurring CoA thioester derivatives [8], of which a core spectrum between approximately 5–10 compounds is potentially present in most microbes, based on their genomic repertoire [9, 10].

From a commercial perspective, CoA thioesters display building blocks of a wide range of industrially interesting products. Prominent examples are polyketides [11], polyunsaturated fatty acids (PUFAs) [12], polyhydroxyalkanoates (PHAs) [13], biofuels [14], amino acids [15], and dicarboxylic acids [16], among others [17]. This relevance might explain the increasing interest to trace CoA thioesters. Previous efforts have provided different experimental approaches, each specifically designed for a particular microbe, including indirect analysis of CoA thioesters via measurement of the respective organic acid, isotope dilution and enzymatic assays [17–20].

In this work, we have set up a sensitive, robust, and reproducible workflow to quantify short chain CoA thioesters in microbes. For this purpose, we adapted a previous protocol, used to assess a wide spectrum of CoA thioesters in the methylotrophic bacterium *Methylobacterium extorquens* [21]. After improvement and careful validation, we demonstrated the approach for industrially relevant microorganisms, which utilize CoA thioesters to form value-added products: the gram-positive bacteria *Corynebacterium glutamicum* [15], and *Streptomyces albus* [11], the gram-negative bacterium *Pseudomonas putida* [13], and the eukaryotic yeast *Yarrowia lipolytica* [12].

## Results

### Set up and validation of a single protocol for extraction and quantification of short chain CoA thioesters in gram-positive and gram-negative bacteria and eukaryotic yeast

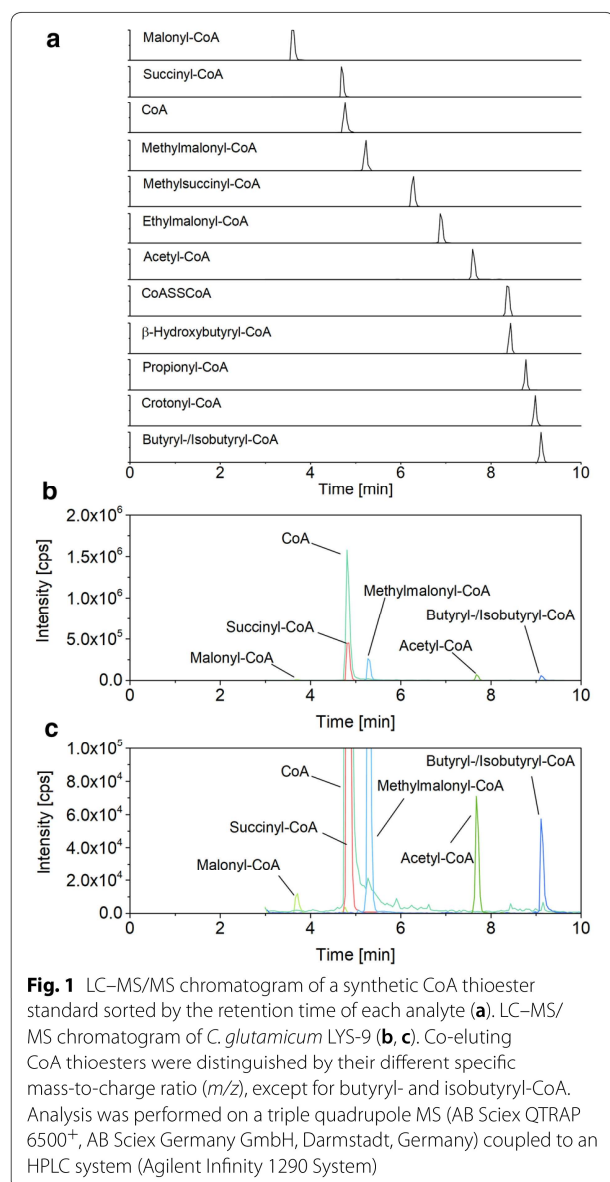
A synthetic mixture of 11 CoA thioesters of interest was used to set up a chromatographic method. Using a porous organo-silica reversed phase column (100 × 2.1 mm,

1.5 μm), efficient separation of the analytes was achieved within 25 min, including the isobaric derivatives succinyl-CoA/methylmalonyl-CoA and methylsuccinyl-CoA/ethylmalonyl-CoA, respectively (Additional file 1: Fig. S1). As exception butyryl-CoA and isobutyryl-CoA co-eluted in all cases tested (data not shown). They could not be distinguished in the MS due to their identical mass either and were therefore regarded as one pool. The linear range for quantification covered 5–8 orders of magnitude, down to the picomolar level (Additional file 1: Fig. S2).

Next, we aimed to develop one common workflow, which was suitable to analyze real samples from the different microbes. Initial tests with *C. glutamicum* revealed that combined quenching and extraction was straightforward to handle experimentally and provided extracts of reproducible quality (data not shown), so that we used it as a starting point for development. Several practical challenges resulted from the nature of the different microbes and the used culture conditions and had to be addressed.

First, the chosen small column geometry and particle size turned out incompatible with certain samples. Over rather few injections (10–20), the column pressure increased from initially 250 to 1000 bar, which required extensive cleaning with water to regenerate the separation column. However, despite such efforts, we faced a rapid loss of separation efficiency. This was especially true for samples of *S. albus* and *C. glutamicum*, grown in media with elevated ionic strength. The use of a larger column (100 × 4.6 mm) and a twofold increased particle size of the separation material (3 μm) solved this issue so that more than 500 samples could be analyzed on the same column without pressure increase and loss in separation performance, independent of the microbe investigated. Due to the larger geometry, the eluent flow was increased to 600 μL min<sup>-1</sup>, which kept the analysis time at 25 min and provided a robust approach for the analytics. By far the best separation was achieved using a core-shell silica column instead of the porous silica column (Fig. 1). Due to superior properties of the core-shell material, the resulting peaks were narrower so that the gradient could be increased substantially. Altogether, this shortened the analysis time for all CoA esters to only 10 min (Fig. 1a). The analysis of cell extracts yielded clean chromatograms with high signal quality, even for low abundance thioesters (Fig. 1 b, c).

Second, small biomass amounts, typically chosen for sampling in metabolomics due to easier handling, were not suitable to precisely quantify all CoA thioesters present in vivo due to an extremely low abundance of some of them. As example, *S. albus* contained ultralow amounts of crotonyl-CoA, which yielded low quality



signals near the threshold, when extracted from 0.6 mg biomass. Similar observations were made for the other microbes studied. An increase of the sample amount to 8 mg, however, allowed clean detection and quantification of all CoA thioesters to be expected from the genomic repertoire for each of the tested strains and conditions.

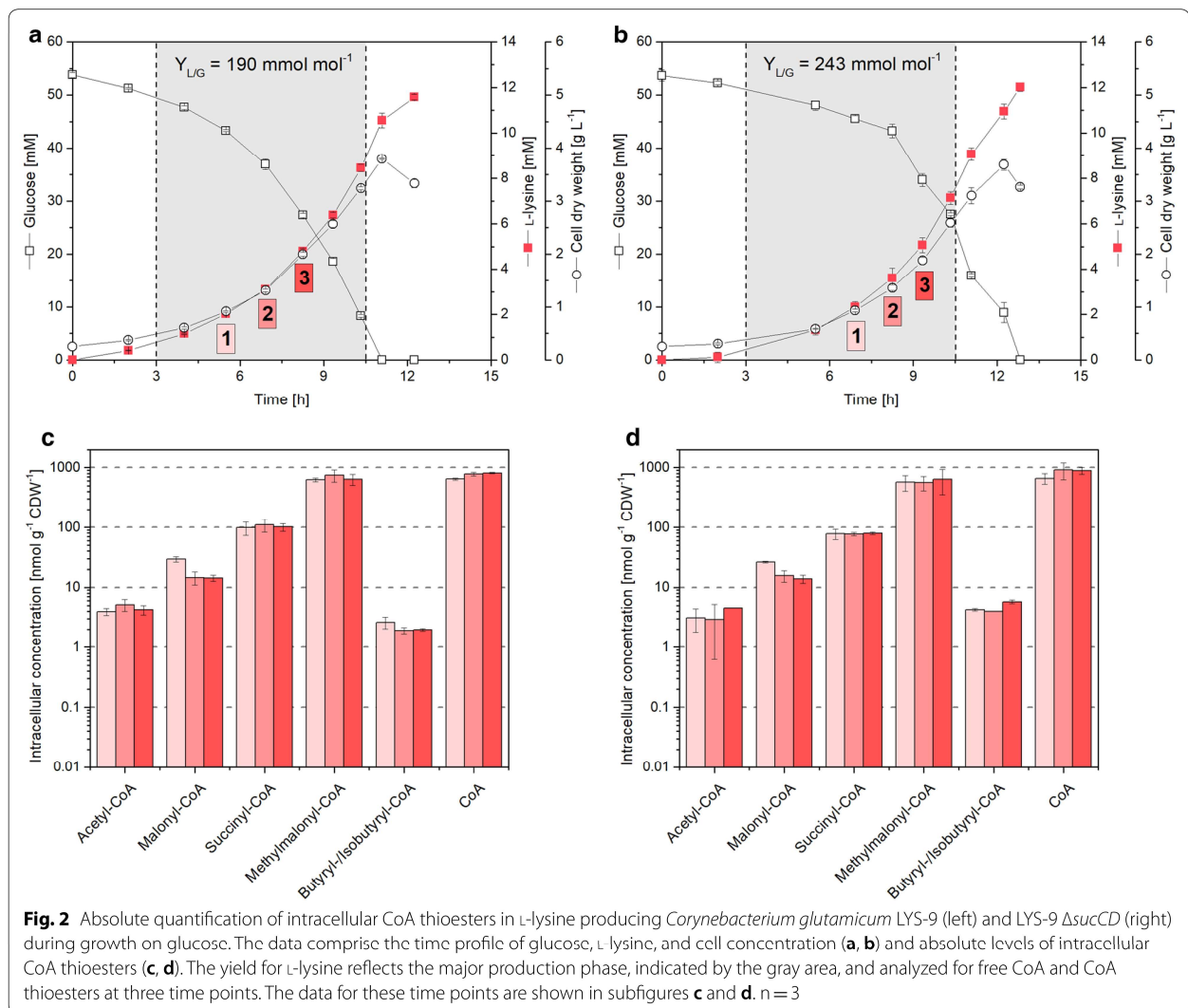
Third, the higher biomass amounts caused difficulties in dissolving lyophilized extracts, after freeze-drying them together with extracted cell fragments. The obtained solutions were too viscous, especially when sampling the filamentous actinomycete, to

appropriately filter them prior to analysis. Due to this, we introduced a centrifugation step between extraction and lyophilization, which allowed a better handling, especially for *S. albus*. Additional tests for all strains revealed that after two washing cycles the cell pellets did not contain any significant residuals of the analytes of interest, which ensured complete extraction. In the following,  $^{13}\text{C}$  labeled cell extracts were prepared by growing each microbe on its corresponding  $[\text{U-}^{13}\text{C}]$  substrate and conducting the established sample processing. The concentration of the  $^{13}\text{C}$  CoA thioesters was precisely quantified against synthetic standards so that the  $^{13}\text{C}$  extracts could then be used to quantify absolute concentrations.

Fourth, free CoA underwent dimerization to a certain degree during the sample processing. When analyzing the synthetic standard, approximately  $15\% \pm 3\%$  of free coenzyme A was observed as CoA-disulfide (CoA-S-S-CoA), eluting 3.5 min after the free monomer (Fig. 1, Additional file 1: Table S1). This phenomenon was also observed for cell extract samples.

### *C. glutamicum* reveals a small spectrum of CoA thioesters with methylmalonyl-CoA as the dominating metabolite

The L-lysine producing mutant *C. glutamicum* LYS-9 was analyzed during batch growth on glucose. It continuously accumulated L-lysine to a final titer of 10.5 mM at a yield of  $190 \text{ mmol mol}^{-1}$  (Fig. 2a). The specific growth rate remained constant over the whole cultivation ( $\mu = 0.27 \text{ h}^{-1}$ ). The cell interior of *C. glutamicum* LYS-9 contained five CoA thioesters: acetyl-CoA, malonyl-CoA, methylmalonyl-CoA, succinyl-CoA, and butyryl/isobutyryl-CoA. The esters differed almost 200-fold in abundance. Methylmalonyl-CoA exhibited the highest concentration (up to  $750 \text{ nmol g}^{-1}$ ), followed by succinyl-CoA ( $110 \text{ nmol g}^{-1}$ ), malonyl-CoA ( $30 \text{ nmol g}^{-1}$ ), acetyl-CoA ( $5 \text{ nmol g}^{-1}$ ), and butyryl/isobutyryl-CoA ( $3 \text{ nmol g}^{-1}$ ). Additionally, free coenzyme A was observed in significant amount ( $820 \text{ nmol g}^{-1}$ ). The level of all CoA thioesters remained stable over time, except for malonyl-CoA, which decreased by approximately 50% in later cultivation stages (Fig. 2c, d). Incubated under the same conditions as its ancestor, *C. glutamicum* LYS-9  $\Delta\text{sucCD}$  (lacking succinyl-CoA synthetase) formed 12 mM L-lysine at an increased yield of  $243 \text{ mmol mol}^{-1}$ , while growing at a specific growth rate of  $\mu = 0.25 \text{ h}^{-1}$  (Fig. 2b). The spectrum of intracellular CoA thioesters was almost unaffected in the TCA-cycle defective mutant, as compared to LYS-9. This was also true for succinyl-CoA, the substrate of the deleted enzyme. Its pool size was identical



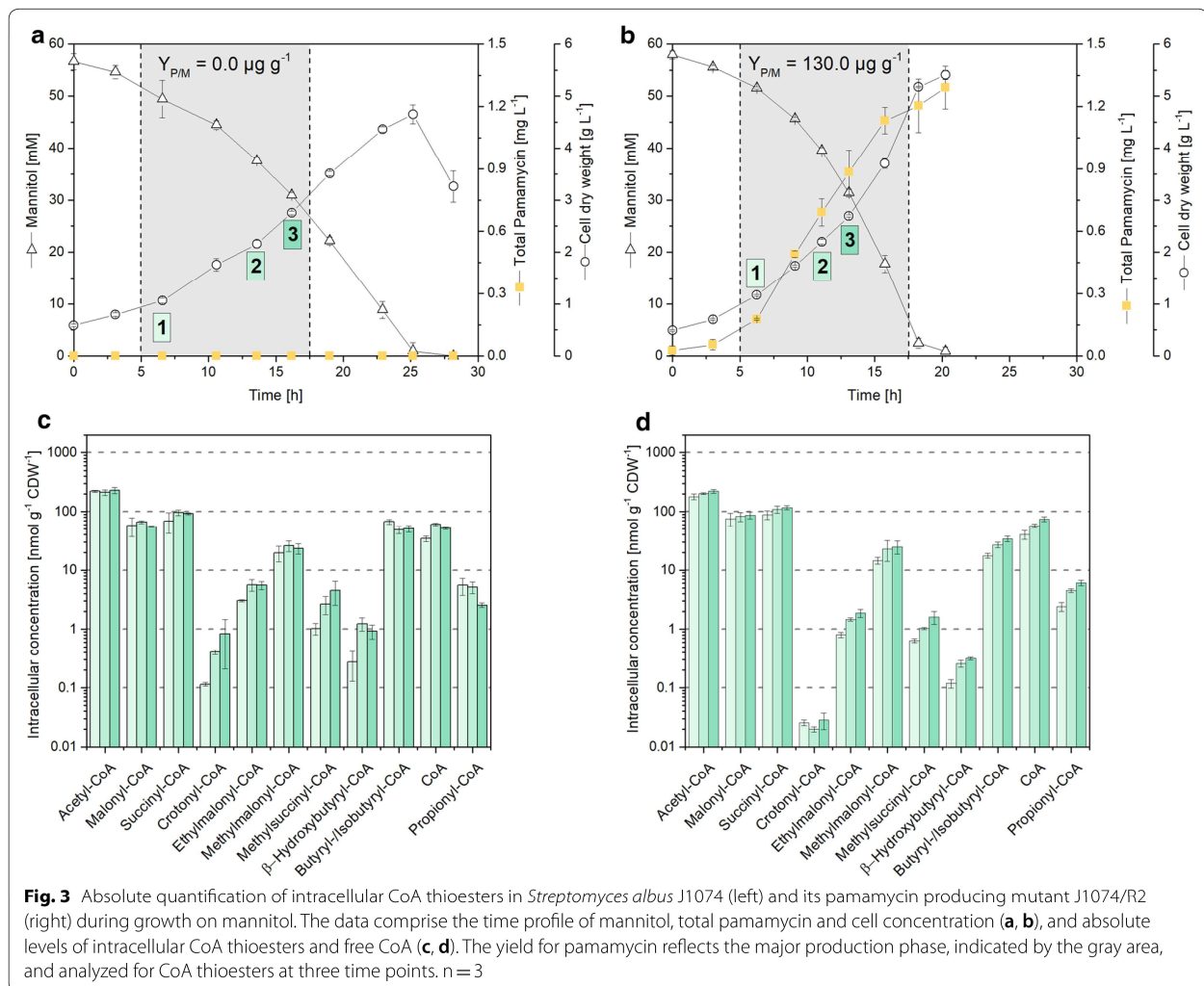
in both strains. Only butyryl/isobutyryl-CoA slightly differed (Student's *t* test,  $p = 0.01$ ).

#### The actinomycete *S. albus* exhibits a rich set of CoA thioesters varying more than 10,000-fold in intracellular availability

The wild type *S. albus* J1074 was grown on mannitol-based minimal medium (Fig. 3a). The substrate was consumed over a time of 25 h and cells reached a cell dry weight of  $4.5 \text{ g L}^{-1}$ . CoA thioesters were sampled at three time points during the mid-growth phase. The actinomycete revealed a rich spectrum of eleven CoA thioesters with side chains of two, three, four and five carbons (Fig. 3c). Acetyl-CoA was most abundant (up to  $230 \text{ nmol g}^{-1}$ ), followed by succinyl-CoA, malonyl-CoA, and butyryl/isobutyryl-CoA. The other six thioesters partly exhibited much lower levels. Crotonyl-CoA and

$\beta$ -hydroxybutyryl-CoA were contained only in trace amounts down to  $0.3 \text{ nmol g}^{-1}$ . Furthermore, *S. albus* contained free coenzyme A up to  $60 \text{ nmol g}^{-1}$ . Along the cultivation, most pools (including those of high abundance) remained stable, but selected CoA thioesters changed to some extent. As example, the level of the carbon-five side-chain esters ethylmalonyl-CoA and methylsuccinyl-CoA increased over time.

The recombinant strain *S. albus* J1074/R2 produced  $1.3 \text{ mg L}^{-1}$  total pamamycin during growth on mannitol (Fig. 3b). The polyketide was produced from early on, accumulated in an exponential manner during the first hours and levelled off toward the end. The mutant revealed the same number of CoA thioesters as its ancestor *S. albus* J1074, but strongly differed in amount for some of them. As example, the level of crotonyl CoA was decreased up to more



than ten-fold to  $0.02 \text{ nmol g}^{-1}$ . In addition, the levels of  $\beta$ -hydroxybutyryl-CoA, ethylmalonyl-CoA, and methylsuccinyl-CoA were reduced up to five-fold (Fig. 3c, d). The other CoA thioesters, including pools of highest abundance (acetyl-CoA, malonyl-CoA, succinyl-CoA) appeared relatively unaffected by pamamycin production. Regarding the pamamycin spectrum, the strain synthesized various derivatives that differed in their mass, due to divergent side chains (Pam 579, Pam 593, Pam 607, Pam 621, Pam 635, Pam 649, Pam 663), which is known to be caused by the alternative incorporation of three-carbon malonyl-CoA, four-carbon methyl-malonyl-CoA, and five-carbon ethylmalonyl-CoA during biosynthesis. At the end of the

process, the distribution was Pam 579 (1.5%), Pam 593 (5.6%), Pam 607 (40.5%), Pam 622 (48.1%), Pam 635 (3.9%), Pam 649 (0.3%) and Pam 663 (0.0%).

#### Glucose-grown *P. putida* KT2440 shows a high abundance of free coenzyme A up to 1000-fold more than bound CoA thioesters

When grown on glucose, *P. putida* KT2440 contained six intracellular CoA thioesters with two, three and four carbon side chains, respectively: acetyl-CoA, malonyl-CoA, succinyl-CoA,  $\beta$ -hydroxybutyryl-CoA, butyryl/isobutyryl-CoA, and crotonyl-CoA. The level of the CoA thioesters ranged from  $280 \text{ nmol g}^{-1}$  (succinyl-CoA) to  $1 \text{ nmol g}^{-1}$  (crotonyl-CoA). *P. putida* KT2440 contained a huge amount of free coenzyme A ( $1,260 \text{ nmol g}^{-1}$ ),

(See figure on next page.)

**Fig. 4** Impact of environmental and genetic perturbation on the spectrum of short-chain CoA thioesters and free coenzyme A in different microbes. The data show direct correlations in absolute CoA thioester levels between different strains of *Corynebacterium glutamicum* (a, b), *Streptomyces albus* (c, d), and *Pseudomonas putida* (e, f), and between glucose and glycerol grown *Yarrowia lipolytica* (g, h). The analysis comprised *C. glutamicum* LYS-9 and its succinyl-CoA synthetase deletion mutant LYS-9  $\Delta$ sucCD, which achieved a higher L-lysine yield, due to flux coupling of the L-lysine pathway with the disrupted TCA cycle (a, b) [15]. In comparison to the wild type *S. albus* J1074, the recombinant producer J1074/R2 formed the polyketide pamamycin from CoA thioester building blocks malonyl-CoA, methylmalonyl-CoA, ethylmalonyl-CoA, succinyl-CoA, and acetyl-CoA (c, d) [11]. In addition, the data comprise *Pseudomonas putida* KT2440 and its glucose dehydrogenase deficient mutant KT2440  $\Delta$ gcd (e, f) [13], and *Yarrowia lipolytica* Po1h:Af4 using glucose and glycerol as sole carbon source (g, h) [12]. The statistical significance for observed differences in CoA thioester levels (t-test  $p < 0.05$ ) is marked by an asterisk.  $n = 3$

exceeding the sum of all thioester pools more than two-fold and the level of individual thioesters up to more than 1000-fold (Fig. 4f). The glucose dehydrogenase (*gcd*) deletion mutant KT2440  $\Delta$ gcd, grown under the same conditions, showed a five-fold decreased level for succinyl-CoA ( $p = 0.01$ ) and  $\beta$ -hydroxybutyryl-CoA (0.6-fold,  $p = 0.01$ ). The most obvious consequence of the *gcd* deletion was a dramatically decreased abundance of free coenzyme A (172 nmol g<sup>-1</sup>) (Fig. 4f).

#### *Y. lipolytica* adapts the level of carbon three thioesters, when grown on glucose and glycerol

Acetyl-CoA, malonyl-CoA, butyryl/isobutyryl-CoA,  $\beta$ -hydroxybutyryl-CoA, crotonyl-CoA, and succinyl CoA were present, when the yeast was grown on glucose or on glycerol (Fig. 4h). The carbon source specifically affected the intracellular level of carbon-three CoA thioesters. Whereas malonyl-CoA was significantly increased on glucose (19 nmol g<sup>-1</sup>) as compared to glycerol (15 nmol g<sup>-1</sup>) (Student's t-test,  $p = 0.04$ ), propionyl-CoA was reduced more than threefold as compared glycerol-grown cells. The other CoA thioesters as well as free CoA showed similar concentrations on both substrates.

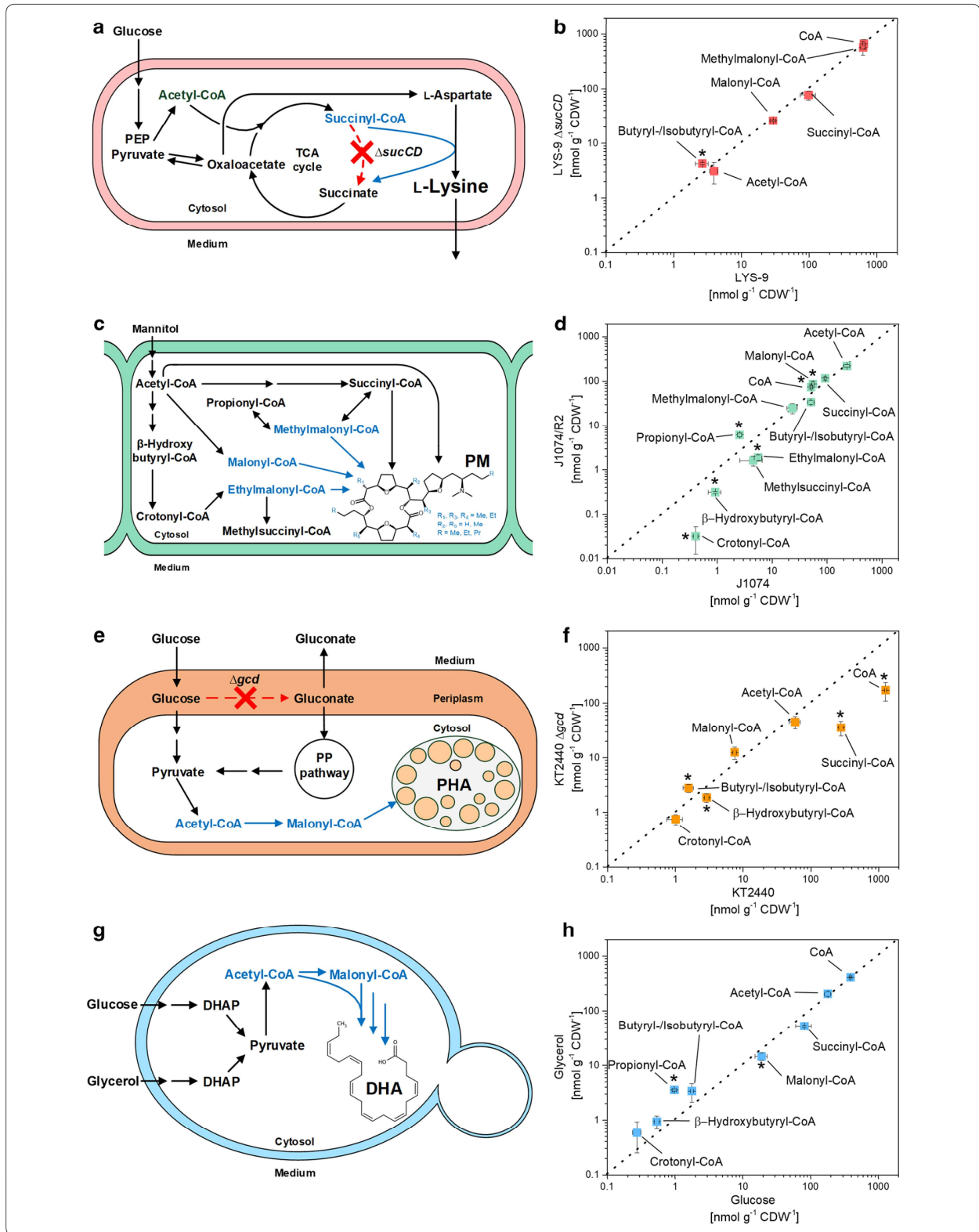
## Discussion

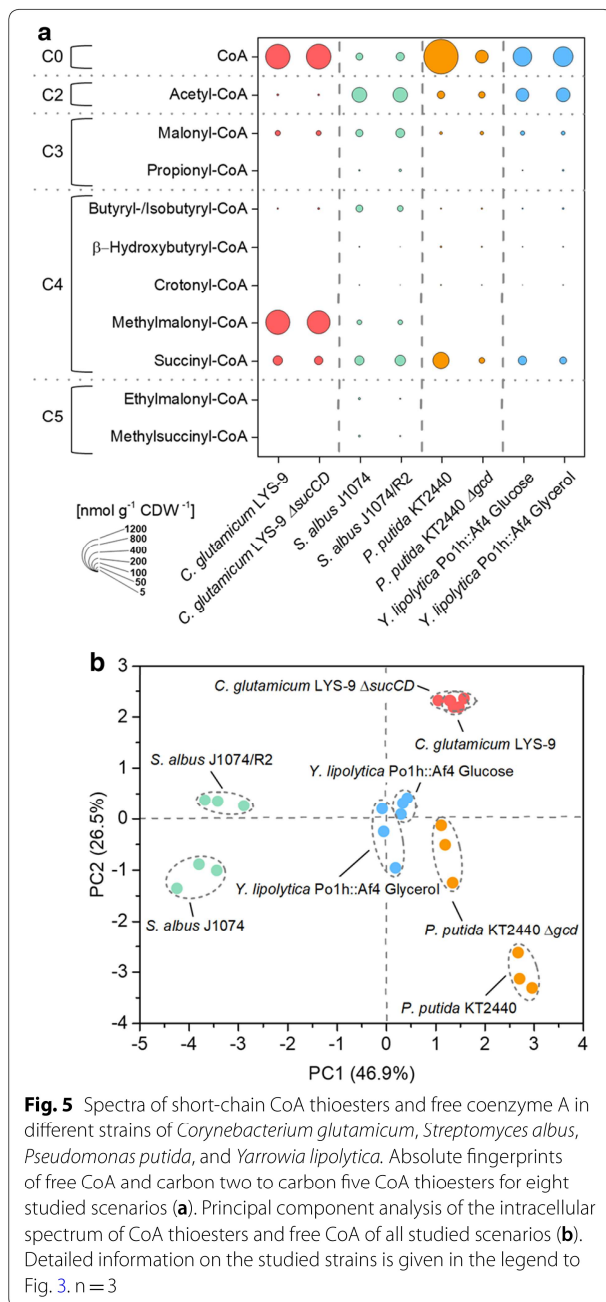
### The developed experimental workflow enables precise and reproducible quantification of CoA thioesters in gram-positive and gram-negative bacteria and eukaryotic yeast

Thioesters of coenzyme A play an important role in metabolism and participate in 5% of all enzymatic conversions [7]. However, only selected studies so far have managed to assess their presence in microbial cells using different protocols, specifically elaborated for the given question [8, 20, 22, 23]. In this work, we successfully adapted a workflow with integrated quenching and extraction using pre-cooled acetonitrile and formic acid, previously described for the methanol-utilizing bacterium *Methylobacterium extorquens* [21] to quantitatively extract intracellular CoA thioesters from *C. glutamicum*, *S. albus*, *P. putida*, and *Y. lipolytica*. The method precisely yielded absolute concentrations due to the use

of internal <sup>13</sup>C-standards. The addition of the standard during the initial extraction step allowed to compensate for potential concentration changes during sample processing, whereby all thioesters were found rather stable under the given conditions. Notably, the workflow should also deliver robust estimates of free CoA levels. This compound, due its reactive free thiol group, exhibited a certain degree of dimerization into the disulfide (and heterodimers might have been potentially formed with other reduced thiols such as glutathione and mycothiol). All these effects should be compensated by the internal standard (assuming that isotope effects in dimerization were negligible), underlining its importance. One should, however, be aware of such side reactions and eventually explore them in more detail, when needed.

Following specific improvement in sampling, sample processing and analytics, we could separate, detect, and quantify CoA thioesters in cell extracts of all studied microbes down to the attomole level within only 10 min (Fig. 1, 3, and 4). Each microbe revealed a unique CoA thioester spectrum, regarding thioester number, type, and level (Fig. 5a). The method allowed to assess also low abundance CoA thioesters, such as crotonyl-CoA in recombinant *S. albus* (Fig. 4c, d). The wide linear range of 10<sup>5</sup>–10<sup>8</sup> achieved for quantification (Additional file 1: Fig. S2) appeared crucial to cover the full spectrum of CoA thioesters, which differed more than 10,000-fold in intracellular concentration (Fig. 3d). Statistical analysis of the data, using principal component analysis, revealed that biological triplicates clustered closely for each experiment, independent of the studied strain (Fig. 5b). The concentrations, determined for single CoA esters, were in the same range as values previously observed in these and similar microbes [17–20]. The achieved high reproducibility appears valuable to identify even small phenotypic differences, particularly when considering the general difficulties to obtain precise metabolite and metabolome data [24]. The microbes selected in this study differed significantly in properties that potentially affect the suitability of experimental approaches in metabolomics: cell size and morphology, composition of the cell wall, and presence of specific cellular barriers, such as outer layers or





compartmental membranes [25–27]. The fact that they all could be appropriately analyzed with the same workflow suggests a broad applicability of the method. The possibility to use of one common method for different microbes seems also interesting for automatized screening efforts, which more and more get into focus and benefit from standardized workflows [28].

In the following, the approach was applied to different industrial microbes to demonstrate its potential. As

example, we could show that growth of *Y. lipolytica* on glycerol results in significantly enhanced levels of propionyl-CoA (Fig. 4h). This finding is interesting for the synthesis of odd-chain fatty acids in the yeast, which relies on propionyl-CoA availability and usually requires toxic propionate supplementation or massive strain engineering [29]. In contrast, glucose resulted in a higher amount of malonyl-CoA. In line, this substrate has proven more efficient than glycerol to derive PUFAs, built from this two CoA thioester, in *Y. lipolytica* [12].

*P. putida* KT2440 revealed a huge amount of free CoA, more than the other microbes (Fig. 5a), which might be involved in metabolic control, but requires more investigation. A disruption of the periplasmic oxidation route, the major pathway for glucose-breakdown [30] has been previously used to drive PHA synthesis in engineered *P. putida* [13]. As shown, the mutation did not significantly alter the availability of the PHA building blocks but affected the pools of free CoA and the TCA cycle intermediate succinyl-CoA, suggesting a broader impact on metabolism (Figs. 4e, f, and 5a). In addition, the CoA thioester analysis revealed interesting insights into the metabolism of *C. glutamicum* and *S. albus*, which are discussed below in more detail.

#### The succinylase branch of L-lysine biosynthesis efficiently bridges the disrupted TCA cycle in succinate dehydrogenase deficient *C. glutamicum*

The amino acid L-lysine is an important industrial feed additive, largely produced with *C. glutamicum* [5]. The TCA cycle competes for carbon with L-lysine biosynthesis but is essential for the aerobic microbe and therefore cannot be eliminated [31]. Increased production, however, can be achieved by flux coupling of the TCA cycle to L-lysine biosynthesis [15]. Succinate dehydrogenase deficient strains cannot convert succinyl-CoA into succinate through the TCA cycle but use the succinylase branch of the L-lysine pathway instead, which results in significantly increased yield (Figs. 2a, b and 4b). One unanswered question so far related to the fact, how the genetic modification affected the availability of succinyl-CoA for L-lysine biosynthesis [15]. Here, we could show that a block of the TCA cycle at the level of succinate dehydrogenase did not affect the succinyl-CoA pool (Figs. 2 and 4b), and also not that of acetyl-CoA at the entry into the TCA cycle. The TCA cycle mutant and its parent strain exhibited an identical CoA thioester spectrum (Fig. 4b). This demonstrates that the three enzymes of the succinylase branch, succinyl-transferase (DapD), aminotransferase (DapC), and desuccinylase (DapE) [32] fully compensated for the disrupted TCA cycle. An insufficient capacity of this pathway would have otherwise presumably caused an accumulation of succinyl-CoA in

the mutant. This finding displays a valuable insight into TCA cycle disrupted L-lysine hyper-producing strains. Future profiling of CoA thioesters seems also interesting for other *C. glutamicum* mutants, in which the L-lysine pathway [33], the TCA cycle [34] and pathways around the CoA thioester metabolism [35–37] have been engineered.

#### **The high abundance of methylmalonyl-CoA in *C. glutamicum* is promising towards heterologous production of complex polyketides**

As shown, methylmalonyl-CoA was the dominating CoA thioester in *C. glutamicum* (Fig. 4b). From our data, we conclude that methylmalonyl-CoA is formed from succinyl-CoA by methylmalonyl-CoA mutase, eventually as response to TCA cycle activity. Propionyl-CoA, the potentially alternative source for methylmalonyl-CoA via propionyl-CoA carboxylase was proven absent so that this route can be excluded, matching with the fact that propionyl-CoA typically occurs as catabolic intermediate during the degradation of odd-chain fatty acids [38, 39] and branched-chain amino acids [40], not present here.

Methylmalonyl-CoA is a common extender substrate for the biosynthesis of complex polyketides by modular polyketide synthases [41]. The lack of this metabolite has been identified as a barrier to heterologous production of complex polyketides and extensive efforts have been made to install pathways to supply methylmalonyl-CoA as a building block [42, 43]. The discovered high abundance of methylmalonyl-CoA is therefore promising for future production of complex polyketides in *C. glutamicum*, which has been recently demonstrated via functional polyketide synthase expression and 6-methylsalicylate biosynthesis in the microbe [36]. For future efforts, the 50-fold excess of methylmalonyl CoA over malonyl-CoA might display an interesting feature, because the relative availability of the two metabolites often impacts the final product structure due to promiscuous enzymes in polyketide synthase assembly lines [41]. Without doubt, the protocol for CoA thioester profiling developed in this work, appears useful for a broad characterization of precursor availability in polyketide producing *C. glutamicum* mutants.

#### **CoA thioester intermediates from the ethylmalonyl pathway are depleted in pamamycin-producing *S. albus* and indicate an impact of precursor availability on product formation**

As shown, the CoA thioester spectrum significantly differed between the pamamycin-producing mutant of *S. albus* and the non-producing wildtype (Fig. 3). In particular, intermediates of the ethylmalonyl-CoA pathway [44] were decreased up to more than ten-fold in the

producer:  $\beta$ -hydroxybutyryl-CoA, crotonyl-CoA, ethylmalonyl-CoA, and methylsuccinyl-CoA (Fig. 4d). The formation of pamamycin in the heterologous host obviously consumed more CoA thioester building blocks than were supplied from central metabolism. This could display a bottleneck towards higher titers and deserves further investigation in the future. It was interesting to note that introduction of the heterologous pamamycin pathway perturbed the ratio between malonyl-CoA, methylmalonyl-CoA, and ethylmalonyl-CoA. It was approximately 100:40:10 in the wild type and changed to 100:30:1 in the producer (Fig. 3c, d). The three building blocks compete for incorporation into pamamycin. Unusual polyketide synthases in the assembly line equally accept them as substrates, which leads to 16 pamamycin homologues that differ in their side chains at six positions [11, 45]. As shown from our data, the dramatically reduced availability of ethylmalonyl-CoA, together with the accumulation of malonyl-CoA, promoted the synthesis of smaller pamamycins. Indeed, 95.7% of all pamamycin derivatives observed (Pam 579, Pam 593, Pam 607, Pam 621) were light ones (had a lower mass), which could be formed without any contribution of ethylmalonyl-CoA. The pamamycins of higher mass (Pam 635, 649 and 663), which required one, two or even more ethylmalonyl-CoA units, became exceedingly rare, based on this effect. It would be interesting to further explore this link in other natural producers, which obviously differ in the spectrum of pamamycin homologues [46–48]. Metabolic engineering of CoA thioester supply appears promising to streamline pamamycin production towards selective derivatives, as proven valuable for other polyketides [18]. Likewise, a variation of bioprocess parameters appears promising to tailor the CoA ester spectrum [49].

## **Materials and methods**

### **Microorganisms**

Strains used in this study were obtained from previous work. This included *Streptomyces albus* J1074 and its pamamycin producing derivative J1074/R2 [11], the two L-lysine producing strains *Corynebacterium glutamicum* LYS-9 and LYS-9  $\Delta$ sucCD [15], *Pseudomonas putida* KT2440 and its mutant KT2440  $\Delta$ gcd [13], and the docosahexaenoic acid (DHA) producing recombinant yeast *Yarrowia lipolytica* Po1h::Af4 [12]. All strains were maintained as glycerol stocks at  $-80^{\circ}\text{C}$ .

### **Media**

*Streptomyces albus* was kept on mannitol-soy flour (MS) agar containing per liter: 20 g mannitol, 20 g soy flour (Schoenenberger Hensel, Magstadt, Germany), and 20 g agar (Becton–Dickinson, Heidelberg, Germany) [49]. Liquid pre-cultures of *S. albus* were grown in LB broth

(20 g L<sup>-1</sup>, Sigma-Aldrich, Darmstadt, Germany) and main cultures were grown in minimal medium, which contained per liter: 10 g mannitol, 200 mM potassium phosphate buffer (pH 7.8), 15 g (NH<sub>4</sub>)<sub>2</sub>SO<sub>4</sub>, 1 g NaCl, 550 mg MgCl<sub>2</sub>·7H<sub>2</sub>O, 200 mg CaCl<sub>2</sub>, 30 mg 3,4-dihydroxybenzoic acid, 20 mg FeSO<sub>4</sub>, 2 mg FeCl<sub>3</sub>·6H<sub>2</sub>O, 2 mg MnSO<sub>4</sub>·H<sub>2</sub>O, 0.5 mg ZnSO<sub>4</sub>·H<sub>2</sub>O, 0.2 mg CuCl<sub>2</sub>·2H<sub>2</sub>O, 0.2 mg Na<sub>2</sub>B<sub>4</sub>O<sub>7</sub>·10H<sub>2</sub>O, 0.1 mg (NH<sub>4</sub>)<sub>6</sub>Mo<sub>7</sub>O<sub>24</sub>·4H<sub>2</sub>O, 1 mg nicotinamide, 1 mg riboflavin, 0.5 mg thiamine hydrochloride, 0.5 mg pyridoxine hydrochloride, 0.2 mg biotin, and 0.1 mg p-aminobenzoic acid. In addition, liquid media were amended with 30 g L<sup>-1</sup> glass beads (soda-lime glass, 5 mm, Sigma-Aldrich) to avoid cell agglomeration.

*Corynebacterium glutamicum* was kept on BHI agar (37 g L<sup>-1</sup> BHI, 20 g L<sup>-1</sup> agar, Becton–Dickinson). Pre-cultures and main cultures of *C. glutamicum* were grown on complex BHI medium and minimal glucose medium, respectively, as described previously [3].

*Pseudomonas putida* was kept on BHI agar (37 g L<sup>-1</sup> BHI, 20 g L<sup>-1</sup> agar, Becton–Dickinson). The mineral M9 medium, used for all liquid cultures, contained per liter: 20 g glucose, 12.8 g Na<sub>2</sub>HPO<sub>4</sub>·7H<sub>2</sub>O, 3 g KH<sub>2</sub>O<sub>4</sub>, 1 g NH<sub>4</sub>Cl, 0.5 g NaCl, 0.25 g MgSO<sub>4</sub>·7H<sub>2</sub>O, 6 mg FeSO<sub>4</sub>·7H<sub>2</sub>O, 2.7 mg CaCO<sub>3</sub>, 2.0 mg ZnSO<sub>4</sub>·H<sub>2</sub>O, 1.2 mg MnSO<sub>4</sub>·H<sub>2</sub>O, 0.4 mg CoSO<sub>4</sub>·7H<sub>2</sub>O, 0.3 mg CuSO<sub>4</sub>·5H<sub>2</sub>O, and 0.1 mg H<sub>3</sub>BO<sub>3</sub> [13].

*Yarrowia lipolytica* was incubated on YNB-N5000 agar, which contained per liter: 10 g glucose, 5 g (NH<sub>4</sub>)<sub>2</sub>SO<sub>4</sub>, 1.7 g YNB (yeast nitrogen base w/o amino acids and ammonium sulfate, Sigma-Aldrich), and 20 g agar. All liquid cultures of the yeast were conducted in minimal medium, containing per liter: 10 g glycerol or 10 g glucose, 200 mM 2-(*N*-morpholino)ethanesulfonic acid (MES, pH 6.8), 5 g (NH<sub>4</sub>)<sub>2</sub>SO<sub>4</sub>, and 1.7 g YNB.

#### Cultivation in shake flasks

Liquid cultures were incubated in baffled shake flasks (500 mL, 10% filling volume) on an orbital shaker (Multitron, Infors AG, Bottmingen, Switzerland, 5 cm shaking diameter, 230 rpm, 75% relative humidity), whereby the temperature was adjusted individually (30 °C for *P. putida* and *C. glutamicum*; 28 °C for *S. albus* and *Y. lipolytica*). For each strain, a specific protocol for inoculation and pre-culturing was used to obtain reproducibly growing main cultures. *S. albus* was incubated on MS agar at 28 °C for 3 days until sporulation occurred. Spores of a single colony were collected to inoculate the pre-culture, which was incubated overnight in LB medium. Afterwards, cells were collected (5000×g, 25 °C, 6 min), resuspended in main culture medium, and used to inoculate the main culture. *C. glutamicum* was grown overnight on BHI agar at 30 °C. A single colony was used to

inoculate an overnight pre-culture, which was then collected (5,000×g, 25 °C, 6 min), resuspended in main culture medium, and used to inoculate the main culture. *P. putida* was grown overnight on M9 agar (30 °C). A single colony served as inoculum for the pre-culture which was then grown overnight, harvested (5,000×g, 25 °C, 6 min), resuspended in main culture medium, and used to inoculate the main culture. *Y. lipolytica* was grown overnight on YNB-N5000 agar at 28 °C. A single colony was used to inoculate the pre-culture, which was incubated overnight, harvested (5000×g, 25 °C, 6 min), resuspended in main culture medium and then served as inoculum for the main culture. All growth experiments were conducted as biological triplicate.

#### Determination of cell concentration

All investigated microbes were analyzed for their cell dry weight. Cells of *S. albus* were vacuum-filtered using a nitrocellulose filter (0.2 µm, Sartorius, Göttingen, Germany), washed twice with 15 mL deionized water, and gravimetrically analyzed using a moisture analyzer (HB43-S, Mettler-Toledo, Columbus, USA). The parallel measurement of the cell concentration as optical density at 600 nm (OD<sub>600</sub>) resulted in a correlation factor of CDW (g L<sup>-1</sup>) = 0.62 × OD<sub>600</sub>. The cell dry weight of *C. glutamicum* was inferred from the optical density measurement at 660 nm as previously described [3]. The cell dry weight of *P. putida* and *Y. lipolytica* was measured as follows. Cells were collected (15,000×g, 4 °C, 10 min), washed twice with 15 mL deionized water, and freeze-dried. Afterwards, the dry biomass was gravimetrically determined.

#### Quantification of substrates

Mannitol and glucose were quantified by HPLC (1260 Infinity Series, Agilent, Darmstadt, Germany) using a Metacarb 87C column (300 × 7.8 mm, Agilent), a Metacarb 87C guard column (50 × 7.8 mm, Agilent), a desalting column (Microguard Deashing Cartridge, Bio-Rad, Munich, Germany), and demineralized water as mobile phase (85 °C, 0.6 mL min<sup>-1</sup>). Refraction index measurement was used for detection, and external standards were used for quantification [2, 3].

#### Extraction and quantification of pamamycins

Prior to analysis, pamamycins were extracted from *S. albus* culture broth. For this purpose, 200 µL broth was mixed with 200 µL acetone and incubated for 15 min (1,000 rpm, room temperature, Thermomixer F1.5, Eppendorf, Wesseling, Germany). Afterwards, 200 µL ethyl acetate was added, and the mixture was incubated for further 15 min. The organic phase was collected by centrifugation (20,000×g, 5 min, room temperature).

Subsequently, the solvent mixture was evaporated under nitrogen. The obtained extract was dissolved in methanol and clarified from debris (20,000  $\times g$ , 5 min, 4 °C). Afterwards, the different pamamycin derivatives were analyzed using LC-ESI-MS/MS (QTRAP 6500<sup>+</sup>, AB Sciex, Darmstadt, Germany) coupled to an HPLC system (Agilent Infinity 1290 System). In short, the analytes were separated on a C18 column (Vision HT C18 HighLoad, 100 mm  $\times$  2 mm, 1.5  $\mu m$ , Dr. Maisch, Ammerbuch-Entringen, Germany) at 45 °C and a flow rate of 300  $\mu L min^{-1}$  (8 mM ammonium formate in 92% acetonitrile). Detection was carried out in positive selected ion monitoring (SIM) mode, using the  $[M+H]^+$  ion for each pamamycin derivative.

#### Quantification of L-lysine

The amino acid L-lysine was quantified using HPLC with pre-column derivatization and fluorescence detection as described before [50]. For quantification,  $\alpha$ -aminobutyric acid was used as internal standard [2].

#### Extraction of intracellular CoA thioesters

A broth sample (approximately 8 mg CDW) was collected and immediately transferred into a pre-cooled extraction and quenching buffer (95% acetonitrile, 25 mM formic acid, -20 °C) [21]. The volume ratio was 1:4. The obtained solution was thoroughly mixed while cooled on ice for 10 min, and then clarified from debris (15,000  $\times g$ , 4 °C, 10 min). The obtained supernatant was mixed with 10 mL super cooled deionized water (-2 °C). The cell pellet was twice washed with 8 mL super cooled deionized water. Afterwards, all supernatants were combined, frozen with liquid nitrogen, freeze-dried, and then re-dissolved in 500  $\mu L$  pre-cooled resuspension buffer (25 mM ammonium formate, pH 3.0, 2% MeOH, 4 °C) [51]. The buffered extract was filtered (Ultrafree-MC 0.22  $\mu m$ , Merck, Millipore, Germany) prior to analysis.

#### Quantification of CoA thioesters using LC-ESI-MS/MS

The analysis of CoA thioesters was performed on a triple quadrupole MS (QTRAP 6500<sup>+</sup>, AB Sciex, Darmstadt, Germany) coupled to an HPLC system (Agilent Infinity 1290 System). Generally, the injection volume was 10  $\mu L$ . Separation of the analytes of interest was conducted on a porous reversed phase column (Gemini C18, 100 mm  $\times$  4.6 mm, 3  $\mu m$ , 110 Å, Phenomenex, Aschaffenburg, Germany) at 40 °C using a gradient of formic acid (50 mM, adjusted to pH 8.1 with ammonium hydroxide 25% in H<sub>2</sub>O, eluent A) and methanol (eluent B) at a flow rate of 600  $\mu L min^{-1}$ . The fraction of eluent B was as follows: 0–12 min, 0–15% B; 12–16 min, 15–100% B; 16–18 min, 100% B; 18–20 min, 100–0% B; 20–25 min, 0% B. Initial tests were further done, using a smaller

column geometry and pore size (Gemini C18, 100 mm  $\times$  2.1 mm, 1.5  $\mu m$ , 110 Å, Phenomenex), using the same gradient, but a reduced flow rate of 300  $\mu L min^{-1}$ . In addition (and finally used in the optimized workflow), a core-shell reversed phase column (Kinetex XB-C18, 100  $\times$  2.1 mm, 2.6  $\mu m$ , 100 Å, Phenomenex) was applied at 40 °C, using a gradient of formic acid (50 mM, adjusted to pH 8.1 with ammonium hydroxide 25% in H<sub>2</sub>O, eluent A) and methanol (eluent B) at a flow rate of 300  $\mu L min^{-1}$ . The fraction of eluent B was as follows: 0–7 min, 0–10% B; 7–10 min, 10–100% B; 10–11 min, 100% B; 11–12 min, 100–0% B; 12–15 min, 0% B. During the first 3 min of the analysis, the outflow from the chromatographic column was discharged to minimize the entry of salts from samples into the mass spectrometer. The individual CoA thioesters were detected using multiple reaction monitoring (MRM), involving the corresponding parent ion and its respective daughter ion (Additional file 1: Table S1). Further instrument settings were as follows: curtain gas, 35 psi; collision gas flowrate, medium; ion spray voltage, 4.5 kV; temperature, 400 °C; ion source gas, 60 psi; and entrance potential, 10 V. The declustering potential, the collision energy and the collision cell exit potential were optimized individually for each CoA thioester using synthetic standards. Acetyl-CoA, propionyl-CoA, succinyl-CoA, methylmalonyl-CoA, and free CoA were purchased (Sigma-Aldrich), whereas malonyl-CoA,  $\beta$ -hydroxybutyryl-CoA, butyryl-CoA, isobutyryl-CoA, crotonyl-CoA, methylsuccinyl-CoA and ethylmalonyl-CoA were chemo-enzymatically synthesized as previously described [7].

#### Absolute quantification of CoA thioesters using <sup>13</sup>C-labeled extracts

Absolute quantification of CoA thioesters was conducted using the MIRACLE approach [52]. For this purpose, <sup>13</sup>C-labeled cell extracts were used as internal standard, whereby an individual standard was produced for each microbe. For this purpose, the different organisms were grown on <sup>13</sup>C-enriched substrates, i.e. the naturally labeled carbon source was replaced by an equimolar amount of the [U-<sup>13</sup>C] enriched isomer: 99% [<sup>13</sup>C<sub>6</sub>] D-mannitol (*S. albus*), 99% [<sup>13</sup>C<sub>6</sub>] D-glucose (*P. putida* and *C. glutamicum*), and 99% [<sup>13</sup>C<sub>3</sub>] D-glycerol (*Y. lipolytica*). The <sup>13</sup>C tracer substrates were obtained from Cambridge Isotope Laboratories (Tewksbury, MA, USA). For each microbe, the second pre-culture and the main culture was conducted in the <sup>13</sup>C-enriched minimal medium. In each case, the inoculum size was below 1% of the later harvested cell concentration to finally provide fully <sup>13</sup>C enriched cell extracts as standard and exclude potential interference [27]. The culture broth from the main <sup>13</sup>C culture was

extracted during the late exponential growth phase, using the extraction protocol described above. After freeze-drying and re-suspension, the  $^{13}\text{C}$  extract was stored as aliquots at  $-80\text{ }^{\circ}\text{C}$ . The level of the individual CoA thioesters in each  $^{13}\text{C}$  extract was precisely quantified using the synthetic standards and corresponding instrument settings (Additional file 1: Tables S1 and S2). During later analysis, an appropriate volume of  $^{13}\text{C}$  extract (of the respective microbe) was thawed on ice, and then simultaneously added with the sample into the quenching solution. This protocol allowed to infer absolute metabolite levels and to take any eventual changes during sample processing into account.

### Principal component analysis

Principle component analysis (PCA) was performed using the ClustVis web tool [53].

### Supplementary information

**Supplementary information** accompanies this paper at <https://doi.org/10.1186/s12934-020-01413-1>.

**Additional file 1: Figure S1.** LC-MS chromatogram of a synthetic CoA thioester standard using a porous organo-silica reversed phase column ( $100 \times 2.1\text{ mm}$ ,  $1.5\text{ }\mu\text{m}$ ) for the chromatographic separation. Co-eluting analytes were distinguished by a different specific mass-to-charge ratio ( $m/z$ ). **Figure S2.** Calibration curves for different CoA thioesters using LC-MS/MS analysis. **Table S1.** Instrumental settings for LC-MS/MS analysis of CoA thioesters. The declustering potential (DP), the collision energy (CE) and the cell exit potential (CEP) were individually tuned for each CoA thioester. The parent ion reflects the positive proton adduct  $[\text{M}+\text{H}]^+$ , except for the CoA homodimer (CoA-S-S-CoA), where the parent ion was  $[\text{M}+2\text{H}]^{2+}$ . In each case, the daughter ion reflects the positive proton adduct after neutral loss of  $507\text{ (}m/z\text{)}$ . **Table S2.** Instrumental settings for LC-MS/MS analysis of fully  $^{13}\text{C}$ -labeled CoA thioesters used as internal standard for absolute CoA thioesters quantification. The respective mass of the fully labeled parent ion was determined by adding the number of carbon atoms to the monoisotopic mass of the non-labelled parent ion (Table S1). The mass of each daughter ion was then calculated by subtraction of  $m/z\ 517$  from this value, considering the neutral loss of a fragment with ten  $^{13}\text{C}$  atoms.

### Authors' contributions

BV synthesized CoA thioesters. LG, MK and MF developed the CoA thioester extraction and analytical protocol. LG produced the  $^{13}\text{C}$  labeled extracts and conducted cultivation of *S. albus*, *C. glutamicum*, and *P. putida*. SJ performed cultivation of *Y. lipolytica*. LG conducted thioester analysis. CW conceived and structured the work. LG, JB and CW wrote the first draft of the manuscript. All authors critically commented and improved the manuscript. All authors read and approved the final manuscript.

### Funding

Open access funding provided by Projekt DEAL. This work was supported by the German Ministry of Education and Research (BMBF) through the Grants MyBio (FKZ 031B034A) and MYX04PUFA (FKZ 031B0346B) and by the German Research Foundation (FKZ INST 256/418-1). Further support was provided by the Max Planck Society and the LOEWE program (Landes-Offensive zur Entwicklung wissenschaftlich-ökonomischer Exzellenz) of the state of Hessen within the framework of the MegaSyn Research Cluster. The funding bodies did not contribute to study design, data collection, analysis, and interpretation, or writing of the manuscript.

### Availability of data and materials

The dataset(s) supporting the conclusions of this article are all included within the article.

### Ethics approval and consent to participate

Not applicable. The manuscript does not contain data collected from humans or animals.

### Consent for publication

Not applicable.

### Competing interests

The authors declare that they have no competing interests.

### Author details

<sup>1</sup>Institute of Systems Biotechnology, Saarland University, Saarbrücken, Germany. <sup>2</sup>Max Planck Institute for Terrestrial Microbiology, Marburg, Germany.

Received: 4 May 2020 Accepted: 20 July 2020

Published online: 10 August 2020

### References

- Becker J, Wittmann C. From systems biology to metabolically engineered cells—an omics perspective on the development of industrial microbes. *Curr Opin Microbiol*. 2018;45:180–8.
- Hoffmann SL, Jungmann L, Schiefelbein S, Peyriga L, Cahoreau E, Portais JC, Becker J, Wittmann C. Lysine production from the sugar alcohol mannitol: design of the cell factory *Corynebacterium glutamicum* SEA-3 through integrated analysis and engineering of metabolic pathway fluxes. *Metab Eng*. 2018;47:475–87.
- Rohles CM, Giesselmann G, Kohlstedt M, Wittmann C, Becker J. Systems metabolic engineering of *Corynebacterium glutamicum* for the production of the carbon-5 platform chemicals 5-aminovalerate and glutarate. *Microb Cell Fact*. 2016;15:154.
- Rohles CM, Gläser L, Kohlstedt M, Giesselmann G, Pearson S, del Campo A, Becker J, Wittmann C. A bio-based route to the carbon-5 chemical glutaric acid and to bionylon-6,5 using metabolically engineered *Corynebacterium glutamicum*. *R Soc Chem Green Chem*. 2018;20:4662–74.
- Becker J, Rohles CM, Wittmann C. Metabolically engineered *Corynebacterium glutamicum* for bio-based production of chemicals, fuels, materials, and healthcare products. *Metab Eng*. 2018;50:122–41.
- Veras HCT, Campos CG, Nascimento IF, Abdelnur PV, Almeida JRM, Parachin NS. Metabolic flux analysis for metabolome data validation of naturally xylose-fermenting yeasts. *BMC Biotechnol*. 2019;19:58.
- Peter DM, Vogeli B, Cortina NS, Erb TJ. A chemo-enzymatic road map to the synthesis of CoA esters. *Molecules*. 2016;21:517.
- Zimmermann M, Thormann V, Sauer U, Zamboni N. Nontargeted profiling of coenzyme A thioesters in biological samples by tandem mass spectrometry. *Anal Chem*. 2013;85:8284–90.
- Kanehisa M, Goto S. KEGG: kyoto encyclopedia of genes and genomes. *Nucleic Acids Res*. 2000;28:27–30.
- Kanehisa M, Sato Y, Furumichi M, Morishima K, Tanabe M. New approach for understanding genome variations in KEGG. *Nucleic Acids Res*. 2019;47:D590–5.
- Rebets Y, Brotz E, Manderscheid N, Tokovenko B, Myronovskiy M, Metz P, Petzke L, Luzhetskyy A. Insights into the pamamycin biosynthesis. *Angew Chem*. 2015;54:2280–4.
- Gemperlein K, Dietrich D, Kohlstedt M, Zipf G, Bernauer HS, Wittmann C, Wenzel SC, Müller R. Polyunsaturated fatty acid production by *Yarrowia lipolytica* employing designed myxobacterial PUFA synthases. *Nat Commun*. 2019;10:4055.
- Poblete-Castro I, Binger D, Rodrigues A, Becker J, Martins Dos Santos VA, Wittmann C. In-silico-driven metabolic engineering of *Pseudomonas putida* for enhanced production of poly-hydroxyalkanoates. *Metab Eng*. 2013;15:113–23.
- Kang A, Lee TS. Converting sugars to biofuels: ethanol and beyond. *Bioengineering*. 2015;2:184–203.
- Kind S, Becker J, Wittmann C. Increased lysine production by flux coupling of the tricarboxylic acid cycle and the lysine biosynthetic

- pathway—metabolic engineering of the availability of succinyl-CoA in *Corynebacterium glutamicum*. *Metab Eng*. 2013;15:184–95.
16. Schada von Borzyskowski L, Sonntag F, Poschel L, Vorholt JA, Schrader J, Erb TJ, Buchhaupt M. Replacing the ethylmalonyl-CoA pathway with the glyoxylate shunt provides metabolic flexibility in the central carbon metabolism of *Methylobacterium extorquens* AM1. *ACS Synth Biol*. 2018;7:86–97.
  17. Huang YY, Jian XX, Lv YB, Nian KQ, Gao Q, Chen J, Wei LJ, Hua Q. Enhanced squalene biosynthesis in *Yarrowia lipolytica* based on metabolically engineered acetyl-CoA metabolism. *J Biotechnol*. 2018;281:106–14.
  18. Lu C, Zhang X, Jiang M, Bai L. Enhanced salinomycin production by adjusting the supply of polyketide extender units in *Streptomyces albus*. *Metab Eng*. 2016;35:129–37.
  19. Martinez-Garcia E, Nikel PI, Aparicio T, de Lorenzo V. Pseudomonas 2.0: genetic upgrading of *P. putida* KT2440 as an enhanced host for heterologous gene expression. *Microbial cell factories*. 2014;13:159.
  20. Botella L, Lindley ND, Eggeling L. Formation and metabolism of methylmalonyl coenzyme A in *Corynebacterium glutamicum*. *J Bacteriol*. 2009;191:2899–901.
  21. Peyraud R, Kiefer P, Christen P, Massou S, Portais JC, Vorholt JA. Demonstration of the ethylmalonyl-CoA pathway by using <sup>13</sup>C metabolomics. *Proc Natl Acad Sci USA*. 2009;106:4846–51.
  22. Seifar RM, Ras C, Deshmukh AT, Bekers KM, Suarez-Mendez CA, da Cruz AL, van Gulik WM, Heijnen JJ. Quantitative analysis of intracellular coenzymes in *Saccharomyces cerevisiae* using ion pair reversed phase ultra high performance liquid chromatography tandem mass spectrometry. *J Chromatogr A*. 2013;1311:115–20.
  23. Park JW, Jung WS, Park SR, Park BC, Yoon YJ. Analysis of intracellular short organic acid-coenzyme A esters from actinomycetes using liquid chromatography-electrospray ionization-mass spectrometry. *Journal of mass spectrometry: JMS*. 2007;42:1136–47.
  24. Rost LM, Brekke Thorfinnsdottir L, Kumar K, Fuchino K, Eide Langorgen I, Bartosova Z, Kristiansen KA, Bruheim P. Absolute quantification of the central carbon metabolome in eight commonly applied prokaryotic and eukaryotic model systems. *Metabolites*. 2020;10:74.
  25. Bolten CJ, Kiefer P, Letisse F, Portais JC, Wittmann C. Sampling for metabolome analysis of microorganisms. *Anal Chem*. 2007;79:3843–9.
  26. Wittmann C, Krömer JO, Kiefer P, Binz T, Heinzle E. Impact of the cold shock phenomenon on quantification of intracellular metabolites in bacteria. *Anal Biochem*. 2004;327:135–9.
  27. Wittmann C. Fluxome analysis using GC-MS. *Microb Cell Fact*. 2007;6:6.
  28. Weber RJM, Lawson TN, Salek RM, Ebbels TMD, Glen RC, Goodacre R, Griffin JL, Haug K, Koulman A, Moreno P, et al. Computational tools and workflows in metabolomics: an international survey highlights the opportunity for harmonisation through Galaxy. *Metabolomics*. 2017;13:12.
  29. Park YK, Ledesma-Amaro R, Nicaud JM. De novo biosynthesis of odd-chain fatty acids in *Yarrowia lipolytica* enabled by modular pathway engineering. *Front Bioeng Biotechnol*. 2019;7:484.
  30. Kohlstedt M, Wittmann C. GC-MS-based (<sup>13</sup>C) metabolic flux analysis resolves the parallel and cyclic glucose metabolism of *Pseudomonas putida* KT2440 and *Pseudomonas aeruginosa* PAO1. *Metab Eng*. 2019;54:35–53.
  31. Becker J, Klopprogge C, Schroder H, Wittmann C. Metabolic engineering of the tricarboxylic acid cycle for improved lysine production by *Corynebacterium glutamicum*. *Appl Environ Microbiol*. 2009;75:7866–9.
  32. Sonntag K, Eggeling L, De Graaf AA, Sahm H. Flux partitioning in the split pathway of lysine synthesis in *Corynebacterium glutamicum*. Quantification by <sup>13</sup>C- and <sup>1</sup>H-NMR spectroscopy. *Eur J Biochem*. 1993;213:1325–31.
  33. Becker J, Zelder O, Haefner S, Schröder H, Wittmann C. From zero to hero—design-based systems metabolic engineering of *Corynebacterium glutamicum* for l-lysine production. *Metab Eng*. 2011;13:159–68.
  34. Zhang Y, Shang X, Wang B, Hu Q, Liu S, Wen T. Reconstruction of tricarboxylic acid cycle in *Corynebacterium glutamicum* with a genome-scale metabolic network model for trans-4-hydroxyproline production. *Biotechnol Bioeng*. 2019;116:99–109.
  35. Milke L, Kallscheuer N, Kappelmann J, Marienhagen J. Tailoring *Corynebacterium glutamicum* towards increased malonyl-CoA availability for efficient synthesis of the plant pentaketide noreugenin. *Microb Cell Fact*. 2019;18:71.
  36. Kallscheuer N, Kage H, Milke L, Nett M, Marienhagen J. Microbial synthesis of the type I polyketide 6-methylsalicylate with *Corynebacterium glutamicum*. *Appl Microbiol Biotechnol*. 2019;103:9619–31.
  37. Chang Z, Dai W, Mao Y, Cui Z, Wang Z, Chen T. Engineering *Corynebacterium glutamicum* for the efficient production of 3-hydroxypropionic acid from a mixture of glucose and acetate via the malonyl-CoA pathway. *Catalysts*. 2020;10:203.
  38. Zhang YQ, Brock M, Keller NP. Connection of propionyl-CoA metabolism to polyketide biosynthesis in *Aspergillus nidulans*. *Genetics*. 2004;168:785–94.
  39. Dolan SK, Wijaya A, Geddis SM, Spring DR, Silva-Rocha R, Welch M. Loving the poison: the methylcitrate cycle and bacterial pathogenesis. *Microbiology*. 2018;164:251–9.
  40. Xu Z, Liu Y, Ye BC. PccD regulates branched-chain amino acid degradation and exerts a negative effect on erythromycin production in *Saccharopolyspora erythraea*. *Appl Environ Microbiol*. 2018;84:e00049-18.
  41. Helfrich EJ, Piel J. Biosynthesis of polyketides by trans-AT polyketide synthases. *Nat Prod Rep*. 2016;33:231–316.
  42. Dayem LC, Carney JR, Santi DV, Pfeifer BA, Khosla C, Kealey JT. Metabolic engineering of a methylmalonyl-CoA mutase-epimerase pathway for complex polyketide biosynthesis in *Escherichia coli*. *Biochemistry*. 2002;41:5193–201.
  43. Gross F, Ring MW, Perlova O, Fu J, Schneider S, Gerth K, Kuhlmann S, Stewart AF, Zhang Y, Müller R. Metabolic engineering of *Pseudomonas putida* for methylmalonyl-CoA biosynthesis to enable complex heterologous secondary metabolite formation. *Chem Biol*. 2006;13:1253–64.
  44. Wang J, Wang C, Song K, Wen J. Metabolic network model guided engineering ethylmalonyl-CoA pathway to improve ascocin production in *Streptomyces hygroscopicus* var. *ascocineticus*. *Microb Cell Fact*. 2017;16:169.
  45. Kuhl M, Gläser L, Rebets Y, Rückert C, Sarkar N, Hartsch T, Kalinowski J, Luzhetskyy A, Wittmann C. Microparticles globally reprogram the metabolism of *Streptomyces albus* towards accelerated morphogenesis, streamlined carbon core metabolism and enhanced production of the antituberculosis polyketide pamamycin. *Biotechnol Bioeng* 2020, submitted.
  46. Natsume M, Tazawa J, Yagi K, Abe H, Kondo S, Marumo S. Structure-activity relationship of pamamycins: effects of alkyl substituents. *J Antibiotics*. 1995;48:1159–64.
  47. Kozono I, Chikamoto N, Abe H, Natsume M. De-N-methylpamamycin-593A and B, new pamamycin derivatives isolated from *Streptomyces alboniger*. *J Antibiotics*. 1999;52:329–31.
  48. Natsume M, Yasui K, Kondo S, Marumo S. The structure of four new pamamycin homologues isolated from *Streptomyces alboniger*. *Tetrahedron Lett*. 1991;32:3087–90.
  49. Kieser T, Bibb M, Buttner M, Chater K, Hopwood D. Practical streptomyces genetics *John Innes Foundation*. United Kingdom: Norwich; 2000.
  50. Krömer JO, Fritz M, Heinzle E, Wittmann C. In vivo quantification of intracellular amino acids and intermediates of the methionine pathway in *Corynebacterium glutamicum*. *Anal Biochem*. 2005;340:171–3.
  51. Schneider K, Peyraud R, Kiefer P, Christen P, Delmotte N, Massou S, Portais JC, Vorholt JA. The ethylmalonyl-CoA pathway is used in place of the glyoxylate cycle by *Methylobacterium extorquens* AM1 during growth on acetate. *J Biol Chem*. 2012;287:757–66.
  52. Mashego MR, Wu L, Van Dam JC, Ras C, Vinke JL, Van Winden WA, Van Gulik WM, Heijnen JJ. MIRACLE: mass isotopomer ratio analysis of U-<sup>13</sup>C-labeled extracts. A new method for accurate quantification of changes in concentrations of intracellular metabolites. *Biotechnol Bioeng*. 2004;85:620–8.
  53. Metsalu T, Vilo J. ClustVis: a web tool for visualizing clustering of multivariate data using Principal Component Analysis and heatmap. *Nucleic Acids Res*. 2015;43:W566–70.

## Publisher's Note

Springer Nature remains neutral with regard to jurisdictional claims in published maps and institutional affiliations.

### 3.2 Gläser et al. 2021

#### **Superior production of heavy pamamycin derivatives using a *bkdR* deletion mutant of *Streptomyces albus* J1074/R2**

Lars Gläser, Martin Kuhl, Julian Stegmüller, Christian Rückert, Maksym Myronovskyi, Jörn Kalinowski, Andriy Luzhetskyy, and Christoph Wittmann

*Microbial Cell Factories*. **20**, 111

<https://doi.org/10.1186/s12934-021-01602-6>

This is an open access article published under the terms of a Creative Commons Attribution 4.0 International License.

CW designed and supervised the study. LG carried out the cultivation experiments and performed the CoA thioester analysis. LG and MK conducted pamamycin analysis. JS and MM performed genetic engineering. CR and JK performed RNA sequencing and data processing. LG und CW analyzed the data, drew the figures, and wrote the first draft of the manuscript. All authors critically commented and improved the manuscript. All authors read and approved the final manuscript.

RESEARCH

Open Access



# Superior production of heavy pamamycin derivatives using a *bkdR* deletion mutant of *Streptomyces albus* J1074/R2

Lars Gläser<sup>1</sup>, Martin Kuhl<sup>1</sup>, Julian Stegmüller<sup>1</sup>, Christian Rückert<sup>2</sup>, Maksym Myronovskyi<sup>3</sup>, Jörn Kalinowski<sup>2</sup>, Andriy Luzhetskyy<sup>3</sup> and Christoph Wittmann<sup>1\*</sup> 

## Abstract

**Background:** Pamamycins are macrodiolides of polyketide origin which form a family of differently large homologues with molecular weights between 579 and 663. They offer promising biological activity against pathogenic fungi and gram-positive bacteria. Admittedly, production titers are very low, and pamamycins are typically formed as crude mixture of mainly smaller derivatives, leaving larger derivatives rather unexplored so far. Therefore, strategies that enable a more efficient production of pamamycins and provide increased fractions of the rare large derivatives are highly desired. Here we took a systems biology approach, integrating transcription profiling by RNA sequencing and intracellular metabolite analysis, to enhance pamamycin production in the heterologous host *S. albus* J1074/R2.

**Results:** Supplemented with L-valine, the recombinant producer *S. albus* J1074/R2 achieved a threefold increased pamamycin titer of 3.5 mg L<sup>-1</sup> and elevated fractions of larger derivatives: Pam 649 was strongly increased, and Pam 663 was newly formed. These beneficial effects were driven by increased availability of intracellular CoA thioesters, the building blocks for the polyketide, resulting from L-valine catabolism. Unfavorably, L-valine impaired growth of the strain, repressed genes of mannitol uptake and glycolysis, and suppressed pamamycin formation, despite the biosynthetic gene cluster was transcriptionally activated, restricting production to the post L-valine phase. A deletion mutant of the transcriptional regulator *bkdR*, controlling a branched-chain amino acid dehydrogenase complex, revealed decoupled pamamycin biosynthesis. The regulator mutant accumulated the polyketide independent of the nutrient status. Supplemented with L-valine, the novel strain enabled the biosynthesis of pamamycin mixtures with up to 55% of the heavy derivatives Pam 635, Pam 649, and Pam 663: almost 20-fold more than the wild type.

**Conclusions:** Our findings open the door to provide rare heavy pamamycins at markedly increased efficiency and facilitate studies to assess their specific biological activities and explore this important polyketide further.

**Keywords:** Polyketide, Transcriptome, Metabolome, *bkdR*, L-valine, CoA thioester, Ethylmalonyl-CoA, Methylmalonyl CoA, Malonyl-CoA

## Background

Pamamycins, polyketide natural products with molecular weights between 579 and 663 (Fig. 1), were first isolated from the actinomycete *S. alboniger* ATCC 21461 [1], which accumulated Pam 621 as major component. Studies using *S. alboniger* IFO 12738 revealed the formation of a pamamycin mixture that mainly contained Pam 607 [2], later leading to the identification of 14 different

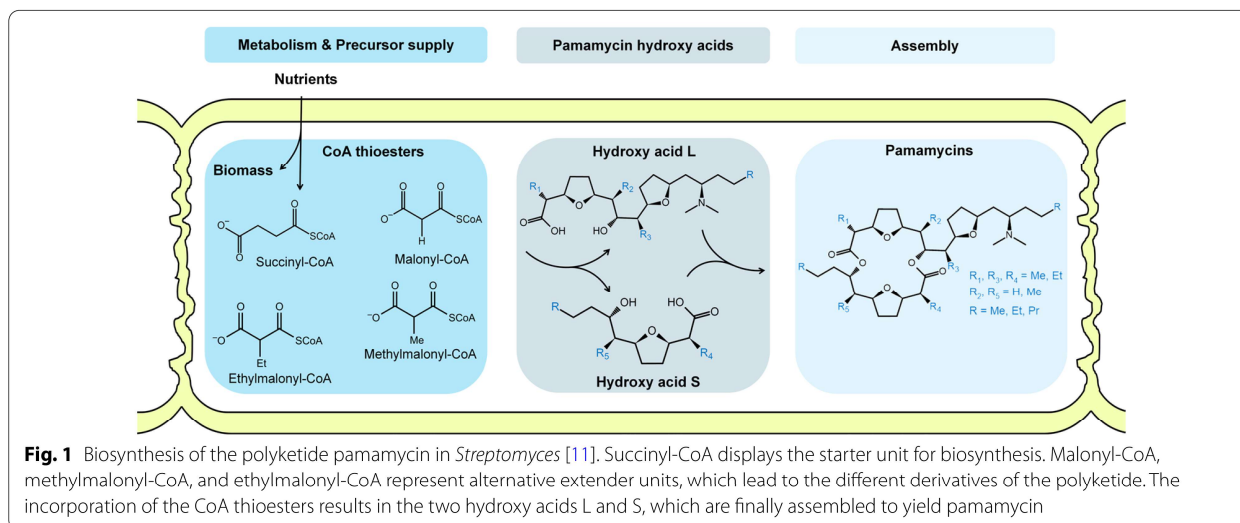
\*Correspondence: christoph.wittmann@uni-saarland.de

<sup>1</sup> Institute of Systems Biotechnology, Saarland University, Saarbrücken, Germany

Full list of author information is available at the end of the article



© The Author(s) 2021. This article is licensed under a Creative Commons Attribution 4.0 International License, which permits use, sharing, adaptation, distribution and reproduction in any medium or format, as long as you give appropriate credit to the original author(s) and the source, provide a link to the Creative Commons licence, and indicate if changes were made. The images or other third party material in this article are included in the article's Creative Commons licence, unless indicated otherwise in a credit line to the material. If material is not included in the article's Creative Commons licence and your intended use is not permitted by statutory regulation or exceeds the permitted use, you will need to obtain permission directly from the copyright holder. To view a copy of this licence, visit <http://creativecommons.org/licenses/by/4.0/>. The Creative Commons Public Domain Dedication waiver (<http://creativecommons.org/publicdomain/zero/1.0/>) applies to the data made available in this article, unless otherwise stated in a credit line to the data.



homologues between 593 and 649 Da which differed in number and position of methyl and ethyl group substituents [3]. From an application viewpoint, pamamycins exhibit a range of interesting pharmacological activities. In actinomycetes, they induce the switch from substrate to aerial mycelium [2, 4, 5]. Moreover, they act against pathogenic fungi and gram-positive bacteria, including *Staphylococcus aureus* and multi-resistant clinical isolates of *Mycobacterium tuberculosis* [6], among the top ten causes of death worldwide with more than 1 million people that died from corresponding infections in 2019 [7]. These promising properties have raised the interest in pamamycins and stimulated a number of follow-up studies on physicochemical properties [3, 8, 9], mode-of-action [6, 10], and also synthetic routes over the past decades [9, 11]. Due to the high complexity and laboriousness, it was not feasible to use chemical synthesis for pamamycin production. On the other hand, fermentation methods were limited by low production levels and extraordinarily complex mixtures with up to 16 derivatives, mainly small ones [11–13]. Therefore, most of the biological activity studies were performed with the most abundant low-weight variants Pam 607 and Pam 621. Hereby, it was discovered that pamamycin derivatives differ in biological activity [3]. Because of inaccessibility, larger pamamycins have escaped further evaluation but remain highly interesting to be studied. In this regard, the development of strategies that (i) generally enable a more efficient formation of pamamycins and (ii) provide increased fractions of large derivatives for facilitated follow-up studies appears as promising direction of research.

Biochemically, pamamycin biosynthesis requires succinyl-CoA as the starter unit. The different pamamycin

variants then result from promiscuous incorporation of malonyl-CoA, methylmalonyl-CoA, and ethylmalonyl-CoA as alternative extender units [11, 13], whereby the intracellular availability of the three CoA thioesters influences the formed spectrum [12, 13]. Interestingly, malonyl-CoA, methylmalonyl-CoA, and ethylmalonyl-CoA are provided from the degradation of branched-chain amino acids (BCAAs, i.e., L-valine, L-leucine, L-isoleucine). Following initial transamination of BCAAs into  $\alpha$ -keto acids, decarboxylation, and dehydrogenation, catalyzed by the branched-chain amino acid dehydrogenase (BCDH) complex, yield the corresponding acyl-CoA derivatives [14]. Subsequently, these are converted into acetyl-CoA, propionyl-CoA, and succinyl-CoA, inter alia potentially leading to the pamamycin precursors malonyl-CoA, methylmalonyl-CoA, and ethylmalonyl-CoA, respectively [15–17]. The genome of *S. albus* contains the entire catabolic route for degradation of all three BCAAs [18] and the incorporation of L-valine-derived carbon into pamamycin has been experimentally shown [19].

Here, we modulated the branched-chain amino acid metabolism to improve the performance of the recombinant pamamycin producer *S. albus* J1074/R2. Supplementation of the medium with L-valine increased total pamamycin production and shifted the polyketide spectrum to heavier homologues, whereas L-isoleucine was found detrimental and L-leucine, like other amino acids did not result in a significant change. Systems-wide analysis of the L-valine-related effects, combining global transcription profiling and quantification of intracellular CoA thioesters revealed surprising dynamics: excess L-valine suppressed pamamycin biosynthesis but pre-conditioned *S. albus* towards a 3.5-fold increased production after L-valine depletion. On the transcriptional level, L-valine

simultaneously perturbed primary and secondary metabolic pathways. This observation inspired the construction of a mutant that mimicked the L-valine effect on the genetic level. A *bkdR* deletion mutant, lacking a key regulator of the BCDH complex that presumably acted at the crossroad of primary and secondary metabolic pathways, provided a novel mode of decoupled pamamycin synthesis, apparently independent of the growth and nutrient status. The regulator mutant enabled the biosynthesis of pamamycin mixtures with up to 55% of the heavy-weight derivatives Pam 635, Pam 649, and Pam 663, almost 20-fold more than the wild type.

**Results**

**L-Valine enhances pamamycin production in recombinant *S. albus* and shifts the spectrum to larger derivatives**

To assess its performance, the pamamycin producer *Streptomyces albus* J1074/R2 was cultivated in a minimal medium using 10 g L<sup>-1</sup> mannitol as sole carbon source. The sugar alcohol is a frequently chosen carbon source to produce secondary metabolites [20–22]. The strain, harboring the pamamycin cluster from *S. alboniger* [11], accumulated pamamycin to a total titer of 1.3 mg L<sup>-1</sup> after 48 h, whereby different derivatives between 579 and 649 Da were formed (Fig. 2a). The

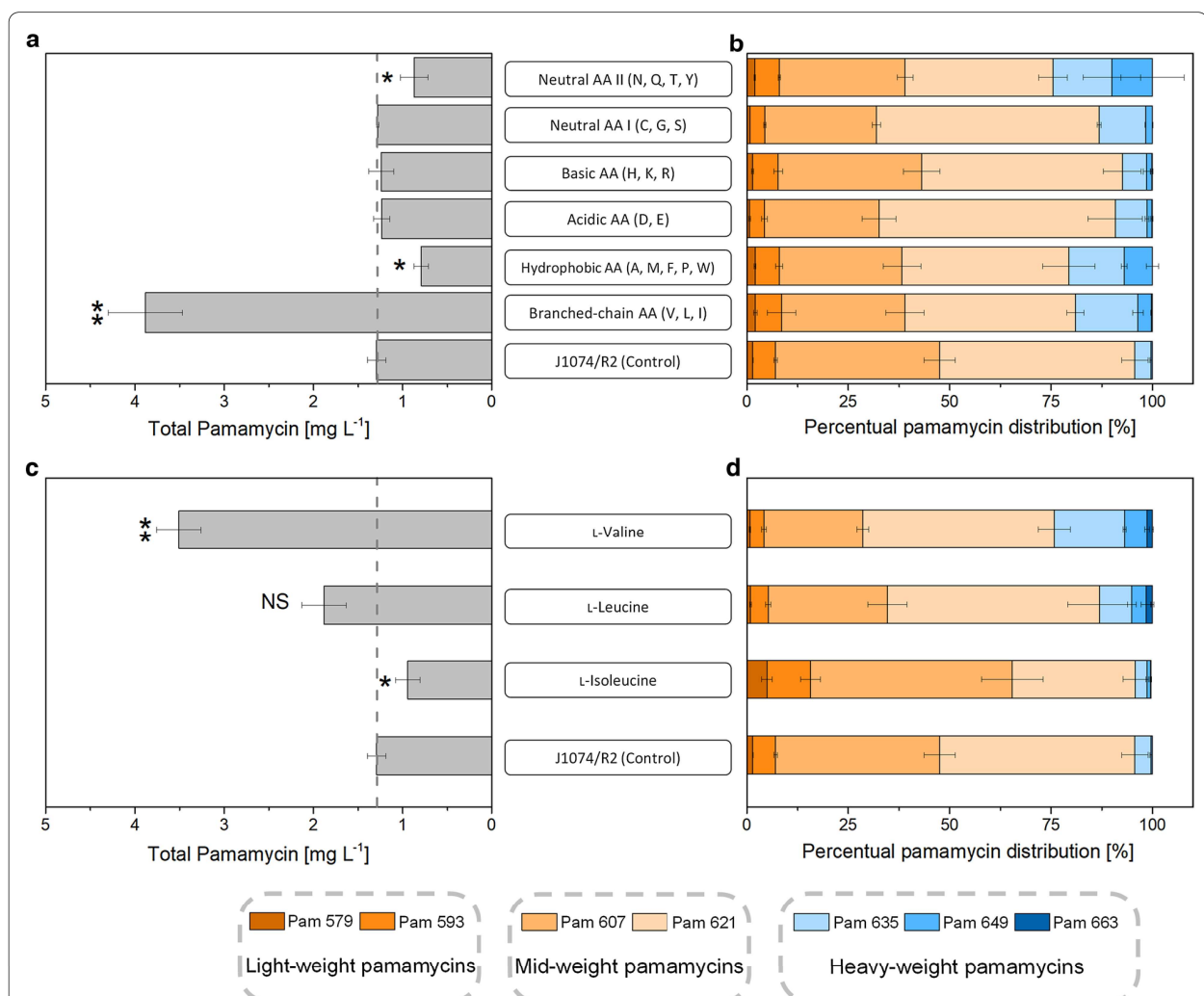


**Fig. 2** Impact of the nutrient environment on pamamycin production in *S. albus* J1074/R2. The strain was grown on a mineral mannitol-based medium containing 10 g L<sup>-1</sup> (55 mM) of the sugar alcohol as sole carbon source (J1074/R2 Control), supplemented with different amino acid mixtures, containing three to five amino acids (designated by the one letter code) at a concentration of 3 mM each (a, b). The strain was grown on a mineral mannitol-based medium containing 10 g L<sup>-1</sup> (55 mM) of the sugar alcohol as sole carbon source (J1074/R2 Control), supplemented individually with branched-chain amino acids (I, L, and V) at a concentration of 3 mM each (c, d). The data comprise the total pamamycin titer after 96 h (a, c), and the final pamamycin spectrum (b, d). Statistical significance was assessed by a t-test ( $p < 0.05$ , \*;  $p < 0.01$ , \*\*). n = 3

mid-weight pamamycins 607 and 621 were the dominant ones (Fig. 2b). They made up approximately 89%. The low weight pamamycins 579 and 593 contributed 7% to the total pool, whereas the fractions of the heavy-weight derivatives Pam 635 and Pam 649 were around 4%, respectively, and Pam 663, the largest derivative, was not observed (limit of detection  $< 1 \mu\text{g L}^{-1}$ ). A doubling of the mannitol content to  $20 \text{ g L}^{-1}$  did not affect production. The use of glucose as alternative carbon source resulted in a pamamycin titer of  $0.9 \text{ mg L}^{-1}$  (30% less than on mannitol), potentially due to negative effects of glucose-mediated carbon catabolite repression [23–25]. The addition of a casamino acid mixture ( $8 \text{ g L}^{-1}$ ) increased the pamamycin titer after 48 h almost three-fold to  $3.7 \text{ mg L}^{-1}$ . This observation indicated that nutrient specific effects rather than general carbon availability impacted polyketide production. Next, the influence of different amino acids was studied systematically. For this purpose, pamamycin production was compared for mixtures of three to five amino acids, each added at equimolar concentration (Fig. 2).

Among all experiments, only the BCAA mixture with L-valine, L-leucine, and L-isoleucine revealed a positive effect. The final pamamycin titer was increased to  $4 \text{ mg L}^{-1}$ , whereby 20% of the product was composed of the heavy derivatives Pam 635, Pam 649, and Pam 663, whereby the latter variant was newly observed (Fig. 2a, b). The addition of acidic (D, E), basic (H, K, R), and neutral (C, G, S) amino acids did not affect the pamamycin level amount but slightly affected the product spectrum. A mixture of hydrophobic amino acids (A, M, F, P, W) and the second group of neutral amino acids (N, Q, T, Y) unfavorably decreased production to below  $1 \text{ mg L}^{-1}$ . The branched-chain amino acids were now evaluated individually. Only the supplementation with L-valine revealed a positive effect: the total pamamycin level was increased to approximately  $3.5 \text{ mg L}^{-1}$  and the product spectrum was shifted towards heavier pamamycins of 635 to 663 Da (23%) (Fig. 2c, d). The addition of L-leucine did not significantly enhance production, whereas L-isoleucine was found even detrimental (Fig. 2c).

#### **The L-valine effect is complex and dynamic: L-valine suppresses pamamycin biosynthesis but primes *S. albus* to a production boost after its depletion**

Given the ability of L-valine to stimulate pamamycin production, the effect of the amino acid on *S. albus* J1074/R2 was studied in more detail. First, we investigated the dynamics of production (Fig. 3). The control culture, containing only mannitol as carbon source, revealed a growth-coupled accumulation of pamamycin. The polyketide was formed from early on and reached a final titer of  $1.3 \text{ mg L}^{-1}$  after 21 h, when mannitol was depleted

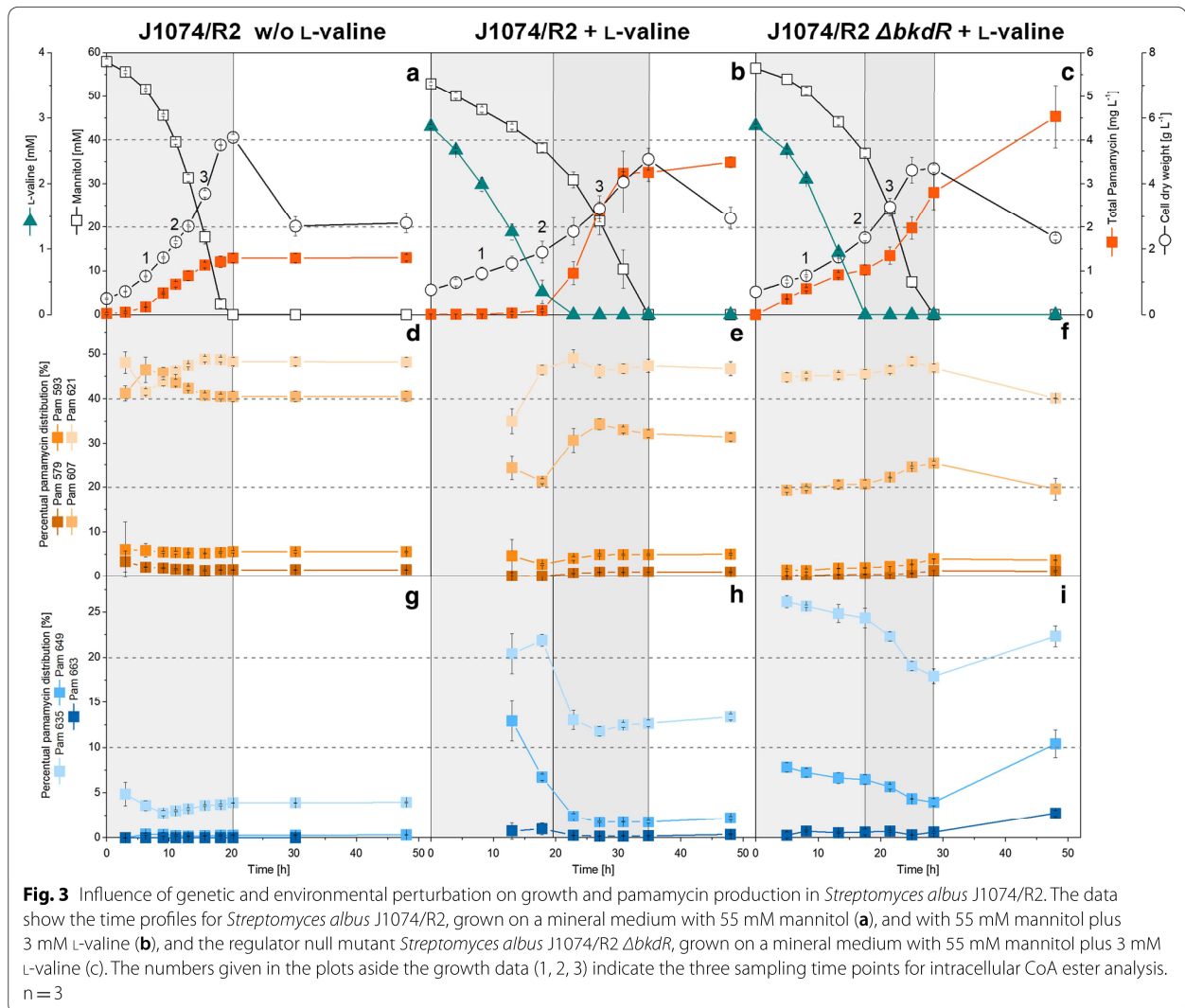
(Fig. 3a), and there was no further accumulation later. The pamamycin spectrum was constant over time and revealed Pam 607 (41%) and Pam 621 (48%) as dominant variants (Fig. 3d, g). During the process, *S. albus* J1074/R2 grew at a maximum specific growth rate of  $0.13 \text{ h}^{-1}$ .

The addition of L-valine to the medium caused several effects (Fig. 3b). First, extracellular L-valine surprisingly suppressed pamamycin biosynthesis. Production of the polyketide was very weak if traces of the amino acid were still present, far below that of the control. Second, L-valine was co-consumed with mannitol, whereby it strongly suppressed the uptake of the sugar alcohol and reduced the maximum specific growth rate of the microbe by more than half to  $0.05 \text{ h}^{-1}$ . This inhibition resulted in a pro-longed cultivation time of finally 35 h until all carbon was depleted, almost 70% more than in the control. Third, when L-valine had been completely consumed and mannitol remained as the sole carbon source, the cells switched to a highly productive mode and formed  $3.5 \text{ (mg pamamycin) L}^{-1}$  within only 16 h. The pamamycin space time yield during this phase ( $0.21 \text{ mg L}^{-1} \text{ h}^{-1}$ ) was 3.5-fold higher than that of the control ( $0.06 \text{ mg L}^{-1} \text{ h}^{-1}$ ), although the nutrient environment during this phase was apparently the same for both cultures. Fourth, regarding the pamamycin spectrum, the culture revealed two phases. The initial phase of weak production (12–18 h) formed high fractions of heavy pamamycins (Fig. 3h). Unfortunately, this had only a minor effect on the final spectrum due to the minute amounts formed during this period. After L-valine depletion, the product spectrum shifted to some extent from heavy to mid and light weight variants (Fig. 3e, h). Nevertheless, the relative (and absolute) production of the heavy pamamycins (Pam 635, Pam 649, Pam 663) was higher than in the control.

#### **L-Valine creates a memory effect on the metabolic level: CoA thioester availability is modulated even hours after the amino acid is depleted**

Pamamycin biosynthesis and L-valine degradation share CoA thioesters as pathway intermediates [12, 13]. To characterize the two routes and study their potential interaction, the CoA thioester spectrum in *S. albus* was quantified at three different time points during the L-valine supplemented process: growth under co-utilization of excess L-valine and mannitol (7 h, timepoint 1), weak pamamycin production in the presence of L-valine traces (18 h, timepoint 2), and strong production, 8 h after L-valine depletion (26 h, timepoint 3) (Fig. 3a, b, and Fig. 4a–c). A culture without L-valine addition was analyzed as control at the same time points.

Generally, L-valine supplementation strongly affected the CoA ester metabolism. During early growth (7 h),

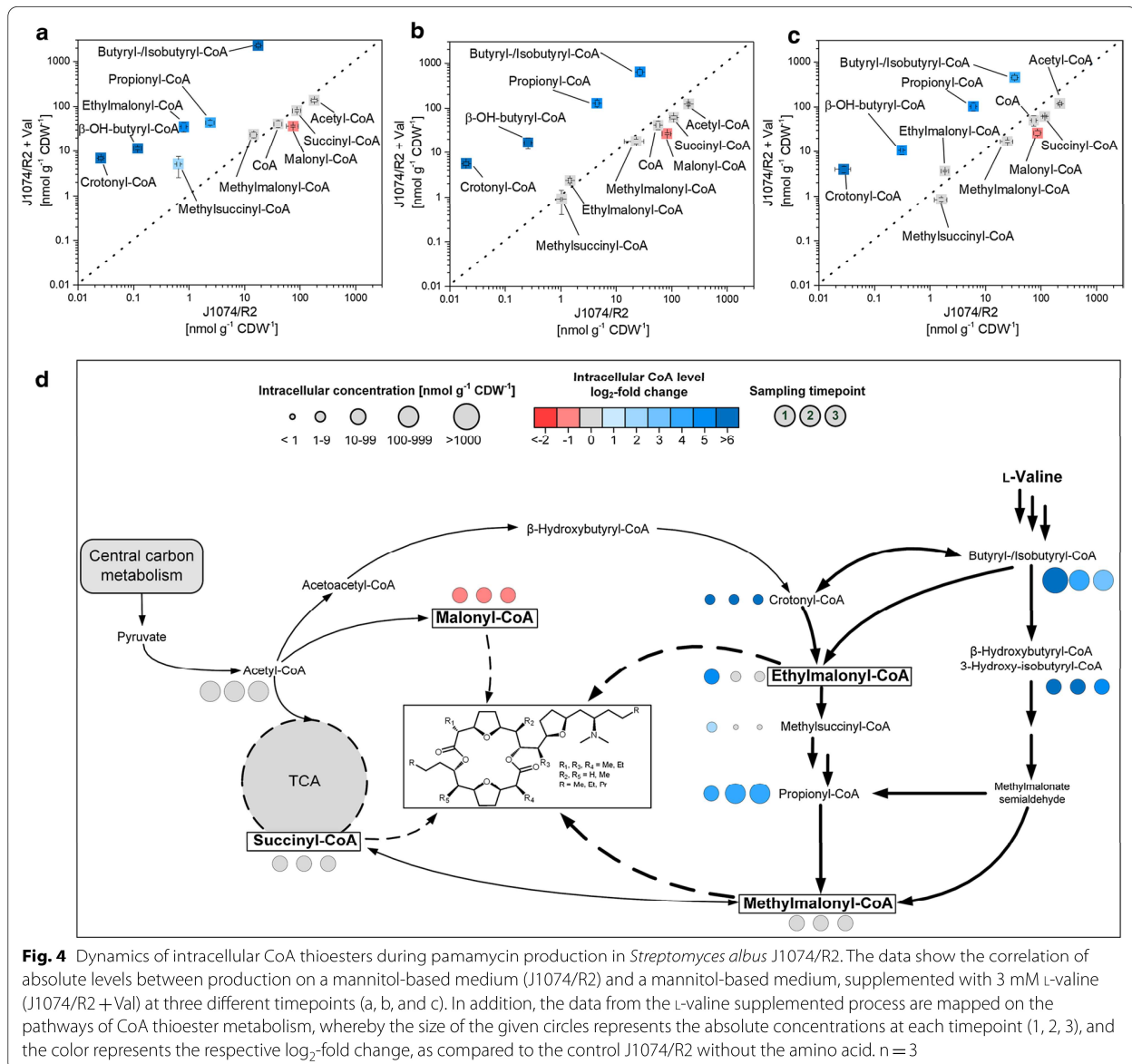


butyryl-/isobutyryl-CoA and hydroxybutyryl-/hydroxyisobutyryl-CoA, catabolic intermediates of L-valine degradation, were increased up to more than 100-fold as compared to the control and reached levels above 2000 nmol g<sup>-1</sup> (Fig. 4a, d). In addition, several intermediates of the ethylmalonyl-CoA pathway, such as crotonyl-CoA, ethylmalonyl-CoA, methylsuccinyl-CoA, and propionyl-CoA were accumulated up to more than 30-fold, whereas malonyl-CoA was reduced by 50%. Interestingly, several of the increased CoA thioester pools remained high even hours after L-valine had been depleted. As an example, the level of butyryl-/isobutyryl-CoA remained above 500 nmol g<sup>-1</sup> and displayed the dominant CoA thioester even 8 h after L-valine had been consumed (Fig. 4b, c). The pool of ethylmalonyl-CoA sharply dropped from 30 to below 5 nmol g<sup>-1</sup> but was still slightly higher than in the control, whereas

malonyl-CoA remained low. The observed changes substantially affected the ratio between the alternative extender units for pamamycin synthesis. In the L-valine supplemented process the ratio between malonyl-CoA, methylmalonyl-CoA, and ethylmalonyl-CoA was 100:65:97 during growth (7 h), 100:68:9 during weak production (18 h), and 100:64:14 in the major production phase (26 h), while it was 100:20:1, 100:28:2, and 100:29:2 at the corresponding time points in the control (Fig. 4).

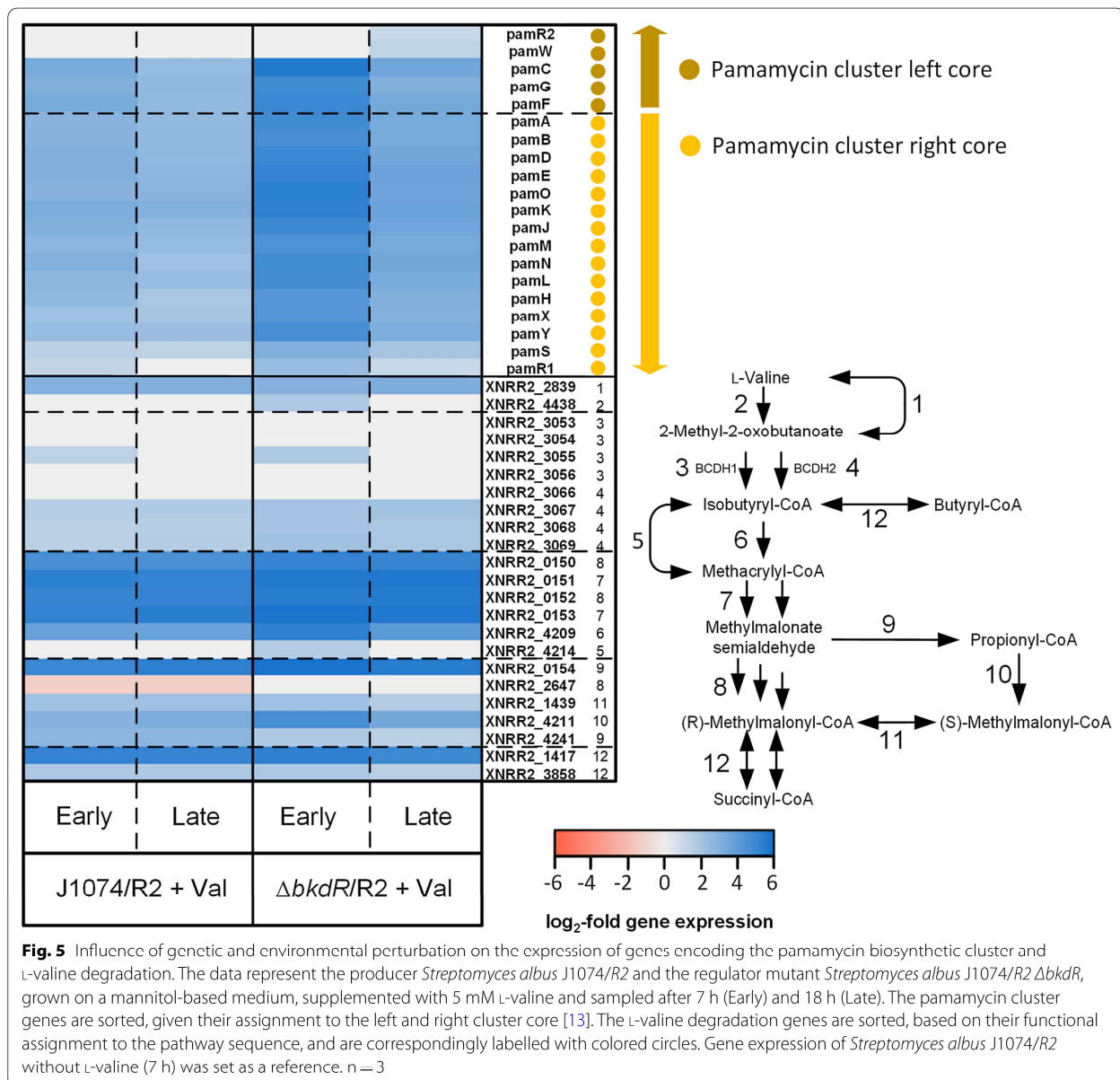
#### L-valine induces global transcriptional changes in *S. albus*

The recombinant producer was now studied on the transcriptional level. Using RNA sequencing, we analyzed the transcriptome of *S. albus* J1074/R2 in a L-valine supplemented process during initial growth (7 h) and strong pamamycin production (26 h) and sampled a process without L-valine addition as control. Sample-level quality



control revealed excellent reproducibility (Additional file 1: Fig. S11, Additional file 1: Fig. S12). The individual replicates of all samples closely clustered together so that the observed expression differences could be fully attributed to the different experimental conditions. Various genes were significantly changed in expression by addition of L-valine during growth (7 h) (Additional file 1: Fig. S5). Interestingly, the gene expression pattern was still largely perturbed in the later process, although L-valine had been depleted approximately 8 h before and the resulting nutrient status (only mannitol present as carbon source), was the same for both processes at this time point.

Surprisingly, L-valine triggered the overexpression of almost the entire pamamycin cluster ( $\log_2$ -fold change up to 3.2) (Fig. 5). This effect was observed for the growth phase (when pamamycin biosynthesis was strongly suppressed) and the production phase (when L-valine had long been depleted). As an exception, the pamamycin exporter (*pamW*) and its regulator *pamR2* were not affected. XNRR2\_0579, XNRR2\_1238, and XNRR2\_5716, encoding phosphopantetheinyl transferases (PPTases) for initial activation of the acyl-carrier protein (*pamC*) during pamamycin synthesis, were found unchanged in expression (Additional file 1: Table S5). The catabolic L-valine route was strongly activated (Fig. 5), whereby



BCDH II was identified as major complex catalyzing the initial step, and these changes remained over a period of 8 h after L-valine depletion. The genes XNRR2\_0150 to XNRR2\_0154, encoding for L-valine degradation from isobutyryl-CoA to methylmalonate semialdehyde, were among the 20 most upregulated genes (Table 1). Notably, excess L-valine did not inhibit expression of L-valine biosynthesis but rather upregulated certain steps of the anabolic route (Additional file 1: Table S3).

Complex changes were observed for central carbon metabolism. As response to excess L-valine, cells exhibited a down-regulation of sugar transport genes encoding:

the fructose-specific IIA/B/C component (XNRR2\_0028) and the phosphor carrier protein HPr (XNRR2\_0029) of the phosphotransferase system (PTS), and a sugar transporter with presumed function as mannitol permease (XNRR2\_0970) (Additional file 1: Table S3). Additionally, two glycolytic genes, i. e. NADPH-dependent glyceraldehyde-3-phosphate dehydrogenase (XNRR2\_0959) and pyruvate kinase (XNRR2\_4449) were down-regulated (Additional file 1: Table S3). Slight expression changes resulted for reactions around the pools of acetyl-CoA and malonyl-CoA. As example, the fatty acid biosynthetic machinery, competing with pamamycin formation

**Table 1** Most pronounced gene expression changes in *Streptomyces albus* J1074/R2 and *Streptomyces albus*  $\Delta bkdR/R2$  caused by supplementation of the minimal mannitol-based medium with L-valine

Gene	Annotation	J1074/R2		$\Delta bkdR/R2$		Function
		+ L-valine		+ L-valine		
		Early	Late	Early	Late	
XNRR2_0839	Pyruvate dehydrogenase E1 component	7.1	6.9	6.7	6.4	●
XNRR2_0151	3-hydroxyisobutyrate dehydrogenase	5.4	5.2	5.6	5.7	●
XNRR2_0153	Butyryl-CoA dehydrogenase	5.2	5.4	5.9	5.7	●
XNRR2_1417	Isobutyryl-CoA mutase	5.1	5.1	5.2	4.9	●
XNRR2_0152	3-hydroxyisobutyryl-CoA hydrolase	5.1	5.2	5.5	5.6	●
XNRR2_0131	Integral membrane protein	5.0	5.3	5.5	5.2	●
XNRR2_0154	Methylmalonate-semialdehyde dehydrogenase	5.0	5.3	5.9	5.5	●
XNRR2_0150	Enoyl-CoA hydratase [valine degradation]	4.6	4.5	5.1	5.1	●
XNRR2_2027	Lantibiotic protein	4.4	3.5	7.0	5.5	●
XNRR2_5094	DUF402 domain containing protein	4.4	4.2	3.5	1.9	●
XNRR2_5095	Acetyltransferase	4.4	3.9	3.2	1.8	●
XNRR2_4266	Acetyltransferase	4.2	3.8	3.1	2.5	●
XNRR2_5673	Hypothetical protein	4.1	2.6	2.6	0.0	●
XNRR2_5027	Endonuclease	3.9	3.1	2.2	1.1	●
XNRR2_3147	Hypothetical protein	3.7	2.1	6.7	2.3	●
XNRR2_3848	Amino acid transporter	3.7	0.0	0.0	0.0	●
XNRR2_4052	Aminoglycoside phosphotransferase	3.6	2.8	2.2	0.0	●
XNRR2_4209	Cyclohexanecarboxyl-CoA dehydrogenase	3.6	3.6	5.3	4.0	●
XNRR2_5626	Alkylhydroperoxidase AhpD	3.6	3.4	2.3	1.0	●
XNRR2_2781	Hypothetical protein	3.5	3.4	2.6	1.5	●
XNRR2_3219	Alanyl-tRNA synthetase	-3.8	-2.8	-2.6	-1.9	●
XNRR2_4152	Hypothetical protein	-3.6	0.0	0.0	0.0	●
XNRR2_5088	Secreted serine protease	-3.5	-4.3	-3.3	-3.8	●
XNRR2_0230	Beta-1,3-glucanase	-3.5	-2.5	-2.8	-2.7	●
XNRR2_4311	Superoxide dismutase [Fe-Zn]	-3.4	-2.2	-1.7	0.0	●
XNRR2_2401	ABC transporter solute-binding protein	-3.4	-4.5	-6.9	-2.8	●
XNRR2_3220	Metal-dependent protease	-3.4	-2.8	-3.3	-1.9	●
XNRR2_5821	Transport permease	-3.2	-1.9	-1.7	0.0	●
XNRR2_5825	Hypothetical protein	-2.9	-5.9	0.0	0.0	●
XNRR2_5822	Transport permease	-2.8	-1.3	0.0	0.0	●

- Valine metabolism   ● CoA metabolism   ● Secondary metabolism  
 ● Cellular processes   ● Unknown

The data show the twenty most upregulated and the ten most downregulated genes. Samples were taken from all cultures after 7 h (Early) and 18 h (Late). The expression level of the control culture J1074/R2 after 7 h was set as a reference. n = 3

for malonyl-CoA was unchanged (Additional file 1: Table S3). However, other genes of CoA metabolism revealed a more pronounced expression change. Isobutyryl-CoA mutase was strongly activated (XNRR2\_1417,

$\log_2$ -fold 5.2), and the initial steps of the ethylmalonyl-CoA pathway, involving acetyl-CoA carboxylase (XNRR2\_1438, XNRR2\_1987) and acetyl-/propionyl-CoA carboxylase (XNRR2\_4211), were up-regulated too

(Fig. 5). In contrast, crotonyl-CoA carboxylase/reductase (XNRR2\_5889) revealed decreased expression ( $\log_2$ -fold -2.1). Regarding higher levels of cellular control, the addition of L-valine caused decreased gene expression of protein PII uridylyl transferase (XNRR2\_1222  $\log_2$ -fold-2.1), the nitrogen regulator protein P-II (XNRR2\_1223,  $\log_2$ -fold change up to -2.1), an ammonium transporter (XNRR2\_1224,  $\log_2$ -fold-2.3) and glutamine synthetase (XNRR2\_4658,  $\log_2$ -fold-1.8), important genes of the nitrogen regulation system in *Streptomyces* [26, 27] (Additional file 1: Table S4). Furthermore, up to nine genes encoding sigma-factors and morphology regulators exhibited significantly changed expression (Additional file 1: Table S4). Finally, L-valine affected a range of pathways of secondary metabolism. In addition to the effects on pamamycin, the cluster encoding for the biosynthetic pathway paulomycin, a glycosylated antibiotic, was upregulated, whereas the clusters for the macrolide candicidin and the nine-membered bis-lactone antimycin were found decreased in expression (Additional file 1: Fig. S7).

#### A null mutant of the *bkdR* regulator reveals decoupled pamamycin biosynthesis, apparently independent of the nutrient status

As shown, L-valine supplementation increased the final pamamycin titer. Despite this improvement, the set-up appeared suboptimal to some extent, because the amino acid caused poor growth of *S. albus* and the production of the polyketide was restricted to a short, post-L-valine phase so that the initial phase with high levels of methylmalonyl-CoA and ethylmalonyl-CoA as building blocks for the desired heavy pamamycins could not be exploited.

For optimization, we now aimed to break the (at least partly unfavorable) regulatory interactions. The transcriptome changes were too complex and provided too many targets to be systematically tackled within reasonable time, considering the demanding genetics of *S. albus*. Therefore, we were inspired to create a mutant that mimicked the promising L-valine effect on the genetic level and perturbed the crossroad between primary and secondary metabolic pathways. We decided to dissect cellular control at the level of *bkdR*, a transcriptional regulator of a branched-chain amino acid dehydrogenase complex which controls branched-chain amino acid metabolism, antibiotic production, and morphogenesis in *Streptomyces* [14, 28], presumably acting at the crossroad between the perturbed primary and secondary metabolic pathways. Therefore, we searched the genome of *S. albus* for a homolog of the known *bkdR* gene (SCO3832) from *S. coelicolor* [14]. The gene XNRR2\_3053 showed 83% identity to SCO3832 (E-value  $2E^{-120}$ ) and was assigned as the corresponding regulator *bkdR* in *S. albus* (Additional

file 1: Figure S1). It turned out that *bkdR* was actively transcribed in the L-valine supplemented cultures and in the control cultures, whereby the expression level (10–20 sequencing reads in the different samples) was generally low. Subsequently, we deleted *bkdR* (XNRR2\_3053) from the genome of *S. albus* J1074/R2. To this end, the linearized pKG1132hyg suicide vector was assembled in vitro with two 2000 bp fragments, containing the upstream and downstream flanking regions of the gene, respectively, using the primers 3053\_HomA\_Fw, 3053\_HomA\_Rev and 3053\_HomB\_Fw, and 3053\_HomB\_Rev (Additional file 1: Table S2). The plasmid was then transformed into *S. albus* using intergenic conjugation. The obtained *S. albus* exconjugants were evaluated by PCR using the primers 3053\_ch\_Fw and 3053\_ch\_Rev (Additional file 1: Table S2). Clones, which carried the desired deletion, revealed a shortened PCR fragment (739 bp), as compared to wildtype (1198 bp). One clone, additionally validated by sequencing for the desired deletion, was designated *S. albus*  $\Delta bkdR$ /R2 and studied further (Additional file 1: Figure S2).

The  $\Delta bkdR$  regulator mutant revealed substantially improved growth and production performance (Fig. 3). The formation of pamamycin occurred during all culture phases. It was no longer suppressed by L-valine but started immediately after inoculation, and it also was maintained during the stationary phase, when all carbon in the medium was exhausted. The final pamamycin level ( $4.5 \text{ mg L}^{-1}$ ) was 1.5-fold higher than that of the wildtype with L-valine supplementation and almost fourfold higher than that of the wildtype without L-valine. The fraction of heavy pamamycins in the mixture (Pam 635, Pam 649, and Pam 663) was increased to 35%. During the stationary phase, the cells even formed a mixture with 55% of these large pamamycins (Additional file 1: Fig. S4). Notably, the  $\Delta bkdR$  strain exhibited a 60% higher specific growth rate ( $\mu = 0.08 \text{ h}^{-1}$ ), than the wildtype.

#### The deletion of *bkdR* beneficially activates the expression of genes related to pamamycin biosynthesis and sugar utilization

The  $\Delta bkdR$  mutant revealed a drastic upregulation of the pamamycin cluster during the early growth phase (7 h,  $\log_2$ -fold up to 5.6) and the expression of the cluster remained much higher than in the parent producer during later stages, although it slightly dropped as compared to the start phase (Fig. 5). Notably, the repressing effects of L-valine on sugar uptake was diminished. The PTS genes (XNRR2\_0028, XNRR2\_0029), and the mannitol permease encoding gene (XNRR2\_0970) were not downregulated in  $\Delta bkdR$ , different to the wild type. In addition, other PTS components (XNRR2\_5450, XNRR2\_5451) were slightly upregulated (Additional

file 1: Table S3). Genes associated to L-valine degradation showed no major difference in expression, matching the similar L-valine degradation rate in both strains (Fig. 5, Table 1). Related to morphogenesis, the mutant revealed modulated expression of several regulators, including XNRR2\_1044 (sporulation transcription factor), XNRR2\_3527 (BldN, RNA polymerase sigma-factor), XNRR2\_2306 (Factor C protein), and different sigma factors (XNRR2\_4476, XNRR2\_5283) (Additional file 1: Table S4). Furthermore, the deletion of *bkdR* had significant effects on the expression of the clusters for paulomycin (no upregulation during later stages), candicidin and antimycin (no downregulation during later stages), and additionally it activated the expression of a lantibiotic cluster and a cluster, encoding for a so far unknown polyketide, during early growth (Additional file 1: Fig. S7, Cluster 12 and 26).

Regarding intracellular CoA thioesters, pools for acetyl-CoA, malonyl-CoA, propionyl-CoA, 3-hydroxy(iso-)butyryl-CoA, crotonyl-CoA (Additional file 1: Fig. S3), and ethylmalonyl-CoA were reduced during L-valine degradation, compared to J1074/R2, whereas the other esters remained unaffected. After L-valine had been depleted, acetyl-CoA and methylmalonyl-CoA exhibited slightly increased levels. The ratio between malonyl-CoA, methylmalonyl-CoA, and ethylmalonyl-CoA was 100:198:43 during L-valine degradation and 100:94:4 during later production.

## Discussion

### The feeding of L-valine enhances the production of rare heavy pamamycins: the formation of Pam 649 is increased up to sevenfold and Pam 663 appears as a newly formed derivative

Using *S. albus* J1074/R2 on a mannitol-based medium in this work (the defined medium was chosen to enable a clear monitoring of the medium supplementation effects), yielded a pamamycin mixture that well matched previous observations [1, 2, 11–13]: lower and mid weight pamamycins were dominating (95.7% Pam 579 to Pam 621), larger derivatives were contained only in low amount (4% Pam 635, 0.3% Pam 649), and the largest one Pam 663 was even absent (<0.1%) (Figs. 2, 3). Remarkably, L-valine stimulated the formation of the larger pamamycins (Pam 635–Pam 663). The total production of Pam 649 was enhanced sevenfold (in J1074/R2) and 16-fold (in  $\Delta bkdR/R2$ ), as compared to the non-supplemented wild type. Considering the period of maximum formation ( $\Delta bkdR/R2$  during stationary phase), the fraction of this rare derivative was even increased 40-fold. Pam 663 was only formed, when L-valine was added. This shift of the product spectrum appears promising. It will help to overproduce rare heavy pamamycins, opening

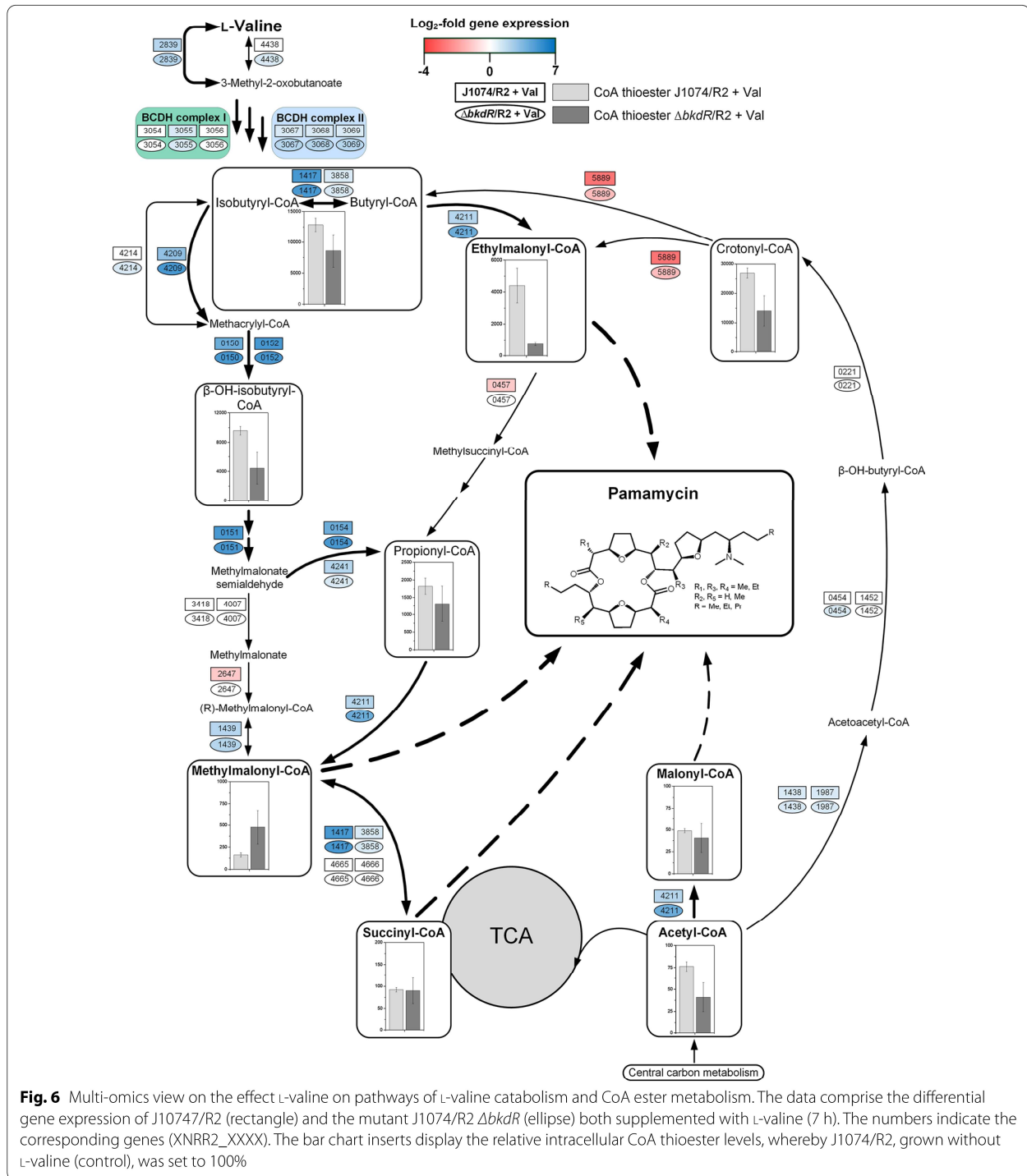
opportunities to study their so far uncharacterized specific biological activity to further explore this important polyketide [3, 6, 29].

### The deletion of *bkdR* improves the growth of *S. albus* J1074/R2 in the presence of L-valine and decouples pamamycin production from the nutrient status

As shown, the feeding of L-valine increased the final pamamycin titer but also revealed undesired side effects: impaired growth and suppression of pamamycin biosynthesis if the amino acid was present (Fig. 2, Fig. 3). It is interesting to note that such negative effects have been also observed in *S. ambofaciens* and *S. venezuelae*, where excess L-valine reduced cell growth and the production of spiramycin [30] and pikromycin [15]. Here, the reduced growth of *S. albus* obviously resulted from transcriptional repression of the mannitol PTS-mediated uptake and the glycolysis (Fig. 3b, Additional file 1: Table S3), similar to the L-valine related downregulation of glycolytic activity, observed in *B. subtilis* [15, 31]. Interestingly, the knockout of *bkdR* restored the PTS expression to high level and thereby eliminated the growth limitation, indicating at least an indirect connection between the regulator and the PTS. This link is rather unexplored in *Streptomyces*. Interestingly, previous studies of *Eubacterium limosum* and *Tepidanaerobacter acetatoxydans* suggest a possible regulatory function of *bkdR* on the PTS system: their Fis-family transcriptional regulators contain a HPr-like domain with significant homology to *bkdR* of *B. subtilis* [32]. Most importantly, the deletion of *bkdR* apparently impaired the control of pamamycin biosynthesis, enabling continuous polyketide formation, even after substrate depletion (Fig. 3, Fig. 5, Additional file 1: Fig. S4). Normally, secondary metabolism starts on the onset of aerial growth when nutrients become scarce [33] and branched-chain amino acids such as L-valine indicate a rich nutrient environment [34], and this control circuit is obviously destroyed by the *bkdR* deletion in *S. albus*. Simultaneously, the deletion of *bkdR* activated other secondary metabolite clusters in the presence of L-valine, (Additional file 1: Fig. S7), underlining the global role of this regulator, besides its well-known control of the BCDH cluster during amino acid degradation [14].

### The degradation of L-valine builds up a huge storage of intracellular CoA thioesters which lasts for a couple of hours after L-valine depletion and tunes the pamamycin spectrum

L-Valine catabolism occurs via methylmalonate semialdehyde and methylmalonyl-CoA as central intermediates [13, 18] which well explains the elevated methylmalonyl-CoA pool, when L-valine was present (Fig. 6). The stimulating effect of L-valine on the pool of ethylmalonyl-CoA



was not such obvious on a first glance. It seemed to involve the ethylmalonyl-CoA pathway, at least considering the increased abundance of the pathway intermediate crotonyl-CoA (Fig. 6) [13, 17]. In addition, we propose a second route for ethylmalonyl CoA supply

based the transcriptome and metabolome data, which formed the CoA thioester from the catabolic L-valine intermediate isobutyryl-CoA via isomerization into butyryl-CoA and subsequent carboxylation into ethylmalonyl-CoA (Fig. 6). The two CoA thioester pools were

strongly increased (Fig. 4, Fig. 6), and the expression of genes encoding for enzymes of this by-pass, isobutyryl-CoA mutase (XNRR2\_1417,  $\log_2$ -fold 5.1) [35] and promiscuous acetyl-/propionyl-CoA carboxylases (e.g. XNRR2\_4211/4212,  $\log_2$ -fold up to 4.7) was increased too (Fig. 6, Table 1). It was interesting to note that butyryl- and isobutyryl-CoA remained high, even hours after L-valine had been depleted and displayed a continuous reservoir to supply ethylmalonyl CoA. The increased abundance of methylsuccinyl-CoA under L-valine excess indicated significant loss of ethylmalonyl-CoA, caused by ethylmalonyl-CoA mutase (*meaA*). A deletion of this gene might enhance the ethylmalonyl-CoA pool even further, as previously shown for other polyketides in *S. venezuelae* [17]. In contrast, the exact reason of the reduced malonyl-CoA pool under L-valine remains rather unclear. As recently discovered, the transcriptional regulator AccR controls several acetyl-CoA carboxylases and affects the levels of malonyl-CoA and methylmalonyl-CoA in *S. avermitilis* [36]. *S. albus* exhibits a homolog to this regulator: XNRR2\_4213, annotated as TetR-family transcriptional regulator, exhibits a high similarity to AccR (E-value  $2E^{-160}$ ) and the transcriptional regulator PccD from *Saccharopolyspora erythraea* which directly controls the BCDH operon [37]. Notably, the gene showed increased expression when L-valine was supplemented to the wildtype but remained unaffected in the *bkdR* mutant (Additional file Table S6). This observation can be taken as a first hint for a link between BCAA degradation, *bkdR* and the level of short-chain acyl-CoA esters but more work is needed in the future to fully resolve this picture in *S. albus*.

Clearly, the effects of L-valine were global and affected (i) morphology regulation and morphogenesis (Additional file 1: Table S4) [38], (ii) nitrogen assimilation and its control (Additional file 1: Table S4) [26, 27, 39, 40], and (iii) XNRR2\_1071 (RelA) as part of the stringent response system [41, 42] (Additional file 1: Table S4). In addition, secondary metabolism was changed at the level of the clusters for paulomycin [43], candicidin [44], and antimycin [45] (Additional file 1: Fig. S7). Altogether, this indicates a complex regulatory network around L-valine [15, 46].

#### The biosynthesis of pamamycin in *S. albus* involves L-valine mediated post-transcriptional control

Interestingly, L-valine activated the expression of the pamamycin biosynthetic gene cluster in *S. albus* J1074/R2, but simultaneously suppressed biosynthesis of the polyketide (Fig. 3, Fig. 5). These diametral effects indicate post-transcriptional control of pamamycin biosynthesis in the heterologous host. A possible mechanism could involve suppressed activation of the acyl-carrier

protein *pamC*, the initial step of the pamamycin assembly, by phosphopantetheinyl transferase (PPtase) activity [47, 48]. The heterologous pamamycin cluster does not encode such an enzyme so that native PPtases apparently catalyzed the activation. The genome of *S. albus* contains three PPtase encoding genes, XNRR2\_0579, XNRR2\_1238, and XNRR2\_5716. None of them was significantly affected in expression (Additional file 1: Table S5), so that we cannot provide a clear conclusion at this stage. However, *pamC* has been shown decisive for pamamycin synthesis [11]. The deletion of this gene *S. albus* J1074/R2 resulted in a dramatic reduction of pamamycin production, especially heavy ones. Remarkably, *pamC* was by far the strongest expressed gene of the pamamycin cluster in the *bkdR* deletion mutant (Fig. 6), eventually overriding the control so that the mutant accumulated pamamycin in the presence of L-valine (with a substantial fraction of large derivatives).

## Materials and methods

### Microorganisms and plasmids

The pamamycin producing strain *S. albus* J1074/R2 was obtained from previous work [11]. The amplification of transformation vectors during molecular cloning was conducted using *Escherichia coli* DH5 $\alpha$  (Invitrogen, Carlsbad, USA). The methylation-sensitive strain *E. coli* ET12567 (*dam-13::Tn9*, *dcm-6*, *hsdM*, *hsdS*), containing the plasmid pUZ8002, was used as donor strain to conjugate DNA into *S. albus* [49]. Plasmid pKG1132, exhibiting  $\beta$ -glucuronidase reporter activity [50], was used to generate the integrative plasmid pKG1132hyg. All strains were maintained as glycerol stocks at  $-80^\circ\text{C}$ .

### Molecular design and genetic engineering

First, DNA fragments from genomic DNA of *S. albus* J1074/R2 were amplified by PCR ( $2\times$  Phusion High-Fidelity PCR Master Mix with GC Buffer, Thermo Scientific, Waltham, MA, USA) using sequence specific primers (Additional file 1: Table S3). To clone the fragments into a linearized vector, homologous overlaps were created by fusing the forward and reverse primers with 20 nucleotide long sequences at their 5' end. Subsequently, the fragments of interest were purified (Wizard SV Gel, PCR Clean-Up System, Promega, Mannheim, Germany) and assembled in vitro [51]. The vector backbone was linearized by EcoRV (FastDigest, Thermo Fisher Scientific, St. Leon-Roth, Germany) involving concomitant alkaline phosphatase treatment (Thermo Fischer Scientific). The reaction mixture for subsequent assembly of fragments and linearized vector contained 157.5 mM Tris-HCl (pH 7.5), 15.75 mM MgCl<sub>2</sub>, 15.75 mM DTT, 42 mg  $\mu\text{L}^{-1}$  PEG-800, 0.6 mg  $\mu\text{L}^{-1}$  NAD, 25 mU  $\mu\text{L}^{-1}$  Phusion High-Fidelity DNA Polymerase (Thermo Fisher Scientific),

7.5 mU  $\mu\text{L}^{-1}$  T5 exonuclease (Epicentre, Madison, USA), 4 U  $\mu\text{L}^{-1}$  Taq Ligase (Thermo Fisher Scientific), and 0.3 mM dNTPs. The obtained plasmid (Additional file 1: Table S2) was transferred into *E. coli* DH5 $\alpha$  competent cells using heat shock, multiplied in the cloning host, isolated, and verified by restriction digestion. Subsequently, electrocompetent cells of *E. coli* ET12567/pUZ8002 were transformed with the correct plasmid and then used to transfer it into *S. albus* J1074/R2 by intergenetic conjugation. For this purpose, the recipient strain was grown for four days for sporulation. Spores were washed off using sterile water, heat shocked for 10 min at 50 °C, mixed with *E. coli* ET12567/pUZ8002 (containing the recombinant plasmid) and plated on MS agar. After overnight incubation at 30 °C, plates were overlaid with phosphomycin (200  $\mu\text{g mL}^{-1}$ ) and apramycin/hygromycin (50/100  $\mu\text{g mL}^{-1}$ ). After four days of incubation at 30 °C, exconjugants were sprinkled with 3  $\mu\text{L}$  X-Gluc (100 mg  $\text{mL}^{-1}$ ), incubated for 20–30 min at 30 °C, and evaluated for blue coloration. Blue stained exconjugants were passaged on MS agar plates containing phosphomycin. Spores were again washed off, diluted serially, and plated onto MS agar, supplemented with X-Gluc. White colonies, that had obviously undergone a second crossover, were evaluated by PCR to differentiate between the desired mutants and wild type. The software SnapGene (GSL Biotech LLC, San Diego, USA) was used for molecular strain, plasmid, and primer design.

### Media

For genetic engineering purposes, *E. coli* was grown in liquid Luria–Bertani medium (LB, Sigma–Aldrich, Darmstadt, Germany) or on solid LB medium containing 20 g  $\text{L}^{-1}$  agar (Becton Dickinson, Heidelberg, Germany), whereas *S. albus* J1074/R2 and its derivative strains were grown in liquid LB medium. To facilitate sporulation, *S. albus* was grown on mannitol-soy flour MS solid media containing per liter: 20 g mannitol (Sigma–Aldrich), 20 g soy flour (Schoenenberger Hensel, Magstadt, Germany) and 20 g agar (Becton Dickinson) [49]. For plasmid maintenance and selection, apramycin (50  $\mu\text{g mL}^{-1}$ ), hygromycin (50  $\mu\text{g mL}^{-1}$ , *S. albus*, 100  $\mu\text{g mL}^{-1}$ , *E. coli*) and phosphomycin (200  $\mu\text{g mL}^{-1}$ ) were added to the medium when needed. Additionally, for blue-white-screening, 5-Bromo-4-chloro-1H-indol-3-yl  $\beta$ -D-glucopyranosiduronic acid (X-Gluc) was supplemented to selection agar plates (40  $\mu\text{g mL}^{-1}$ ) [52].

For pamamycin production, liquid pre-cultures of *S. albus* were grown in LB broth (20 g  $\text{L}^{-1}$ ) and main cultures were grown in basic minimal medium [12], which contained per liter: 10 g mannitol, 200 mM potassium phosphate buffer (pH 7.8), 15 g  $(\text{NH}_4)_2\text{SO}_4$ , 1 g NaCl, 550 mg  $\text{MgCl}_2 \cdot 7\text{H}_2\text{O}$ , 200 mg  $\text{CaCl}_2$ , 30 mg

3,4-dihydroxybenzoic acid, 20 mg  $\text{FeSO}_4$ , 2 mg  $\text{FeCl}_3 \cdot 6\text{H}_2\text{O}$ , 2 mg  $\text{MnSO}_4 \cdot \text{H}_2\text{O}$ , 0.5 mg  $\text{ZnSO}_4 \cdot \text{H}_2\text{O}$ , 0.2 mg  $\text{CuCl}_2 \cdot 2\text{H}_2\text{O}$ , 0.2 mg  $\text{Na}_2\text{B}_4\text{O}_7 \cdot 10\text{H}_2\text{O}$ , 0.1 mg  $(\text{NH}_4)_6\text{Mo}_7\text{O}_{24} \cdot 4\text{H}_2\text{O}$ , 1 mg nicotinamide, 1 mg riboflavin, 0.5 mg thiamine hydrochloride, 0.5 mg pyridoxine hydrochloride, 0.2 mg biotin, and 0.1 mg *p*-aminobenzoic acid. In addition, liquid media were amended with 30 g  $\text{L}^{-1}$  glass beads (soda-lime glass, 5 mm, Sigma–Aldrich) to avoid cell agglomeration. In selected experiments, single amino acids or mixtures of amino acids were added from filter sterilized stocks to the minimal medium, as stated above.

### Cultivation in shake flasks

Liquid cultures were incubated in baffled shake flasks (500 mL, 10% filling volume) on an orbital shaker (Multitron, Infors AG, Bottmingen, Switzerland, 5 cm shaking diameter, 230 rpm, 75% relative humidity), and at 28 °C. *S. albus* was incubated on MS agar at 28 °C for three days until sporulation occurred. Spores of a single colony were collected to inoculate the pre-culture, which was incubated overnight in LB medium. Afterwards, cells were collected (5,000  $\times$ g, 25 °C, 6 min), resuspended in main culture medium, and used to inoculate the main culture. All growth experiments were conducted as biological triplicate.

### Determination of cell concentration

The cell dry weight of the cultures was obtained by measuring the optical density at 600 nm, using the previously obtained correlation factor for *S. albus* of  $\text{CDW (g L}^{-1}) = 0.62 \times \text{OD}_{600}$  [12].

### Quantification of substrates

Mannitol was quantified by HPLC (1260 Infinity Series, Agilent, Darmstadt, Germany) using a Metacarb 87C column (300  $\times$  7.8 mm, Agilent), a Metacarb 87C guard column (50  $\times$  7.8 mm, Agilent), a desalting column (Microguard Deashing Cartridge, Bio-Rad, Munich, Germany), and demineralized water as mobile phase (85 °C, 0.6 mL  $\text{min}^{-1}$ ). Refraction index measurement was used for detection, and external standards were used for quantification [53, 54].

### Quantification of amino acids

The amino acids were quantified using HPLC with pre-column derivatization and fluorescence detection as described before [55]. For quantification,  $\alpha$ -aminobutyric acid was used as internal standard [54].

### Extraction and quantification of pamamycins

Pamamycin analysis was performed following the protocol previously described [12]. In short, pamamycins were

extracted with acetone and ethyl acetate, organic phase evaporated under nitrogen and the obtained extracts resolved in methanol. The filtered extracts were analyzed using LC–ESI–MS/MS (QTRAP 6500<sup>+</sup>, AB Sciex, Darmstadt, Germany) coupled to an HPLC system (Agilent Infinity 1290 System). Analytes were separated on a C18 column (Vision HT C18 HighLoad, 100 mm × 2 mm, 1.5 μm, Dr. Maisch, Ammerbuch-Entringen, Germany) at 45 °C and a flow rate of 300 μL min<sup>-1</sup> (8 mM ammonium formate in 92% acetonitrile). Detection was carried out in positive selected ion monitoring (SIM) mode, using the [M + H]<sup>+</sup> ion for each pamamycin derivative.

#### Extraction of intracellular CoA thioesters

CoA thioesters were extracted using the previously established protocol [12]. In short, a broth sample (approximately 8 mg CDW) was collected and immediately transferred into a pre-cooled extraction and quenching buffer (95% acetonitrile, 25 mM formic acid, -20 °C). Simultaneously a fully <sup>13</sup>C-enriched CoA thioester standard was added during harvesting for later absolute quantification. The volume ratio was 1:4. The obtained solution was thoroughly mixed while cooled on ice for 10 min, and then clarified from debris (15,000×g, 4 °C, 10 min). The obtained supernatant was mixed with 10 mL super cooled deionized water (-2 °C). The cell pellet was twice washed with 8 mL super cooled deionized water. Afterwards, all supernatants were combined, frozen with liquid nitrogen, freeze-dried, and then re-dissolved in 500 μL pre-cooled resuspension buffer (25 mM ammonium formate, pH 3.0, 2% MeOH, 4 °C). The buffered extract was filtered (Ultrafree-MC 0.22 μm, Merck, Millipore, Germany) prior to analysis.

#### Quantification of CoA thioesters using LC–ESI–MS/MS

Analysis of the CoA thioesters were performed as described before [12]. Therefore, the extracts were analyzed on a core–shell reversed phase column (Kinetex XB-C18, 100 × 2.1 mm, 2.6 μ, 100 Å, Phenomenex) was applied at 40 °C, using a gradient of formic acid (50 mM, adjusted to pH 8.1 with ammonium hydroxide 25% in H<sub>2</sub>O, eluent A) and methanol (eluent B) at a flow rate of 300 μL min<sup>-1</sup>. The fraction of eluent B was as follows: 0–7 min, 0–10% B; 7–10 min, 10–100% B; 10–11 min, 100% B; 11–12 min, 100–0% B; 12–15 min, 0% B. During the first 3 min of the analysis, the outflow from the chromatographic column was discharged to minimize the entry of salts from samples into the mass spectrometer. The individual CoA thioesters were detected using

multiple reaction monitoring (MRM), involving the corresponding parent ion and its respective daughter ion.

#### Transcriptomic analysis

Cells were collected by centrifugation (20,000×g, 4 °C, 1 min), and the obtained pellet was immediately frozen in liquid nitrogen. Total RNA was isolated from 3 biological replicates per strain using a Quick-RNA Miniprep Plus kit according to the manufacturer's instructions (Zymo Research). After additional DNase treatment, RNA samples were purified with an RNA Clean&Concentrator-5 kit (Zymo Research) and quantified with a DropSense 16 (Trinean NV). The quality of total RNA was controlled with an RNA 6000 Nano kit in an Agilent 2100 Bioanalyzer (Agilent Technologies). To construct whole transcriptome cDNA libraries, 2.5 μg total RNA each (RIN > 9) was used for the depletion of rRNA with a Ribo-Zero rRNA Removal Kit (Bacteria) according to manufacturer's instructions (Illumina). The rRNA removal was checked with an Agilent RNA Pico 6000 kit and the Agilent 2100 Bioanalyzer (Agilent Technologies). The mRNA obtained was converted to a cDNA library according to the TruSeq Stranded mRNA Sample Preparation guide (Illumina). The quality and quantity of the cDNA library was checked with an Agilent High Sensitivity DNA kit and the Agilent 2100 Bioanalyzer (Agilent Technologies). Sequencing was performed on an Illumina NextSeq 500 using 75 bases read length (Illumina).

Reads were mapped to the *S. albus* J1074/R2 genome sequence (CP059254.1) with Bowtie2 using standard settings [56] except for increasing the maximal allowed distance for paired reads to 600 bases. For visualization of read alignments, ReadXplorer 2.2.3 [57] was used. For counting of reads mapping to gene features, FeatureCounts v.2.0.0 [58] was applied using the parameters -M -O and -s 1. Using the resulting data, DESeq2 [59] was used to QC the datasets via, among others, calculation of the sample-to-sample distances (Additional file 1: Fig. S11) and PCA (Additional file 1: Fig. S12). In addition, DESeq2 was used to calculate DGE datasets. Raw datasets (sequenced reads) as well as processed datasets (input matrix and normalized read counts from DESeq2) are available from GEO (GSE168592). For statistical analysis, Student's t test was carried out and the data were filtered for genes with a log<sub>2</sub>-fold change ≥ 1 (p ≤ 0.05). Data analysis and visualization was conducted using the software package gplots [60, 61].

#### Supplementary Information

The online version contains supplementary material available at <https://doi.org/10.1186/s12934-021-01602-6>.

**Additional file 1:** Additional figures S1 to S12 and tables S1 to S6.

#### Acknowledgements

This work is dedicated to the memory of Dr. Judith Becker (2.2.1981–27.4.2021), our close and cherished colleague at the Institute of Systems Biotechnology, Saarland University, and our true friend.

#### Authors' contributions

CW designed and supervised the study. LG carried out the cultivation experiments and performed the CoA thioester analysis. LG and MK conducted pamamycin analysis. JS and MM performed genetic engineering. CR and JK performed RNA sequencing and data processing. LG und CW analyzed the data, drew the figures, and wrote the first draft of the manuscript. All authors critically commented and improved the manuscript. All authors read and approved the final manuscript.

#### Funding

The authors acknowledge funding from the German Ministry of Education and Research (BMBF) through the grant MyBio (031B034). Christoph Wittmann acknowledges funding from the German Research Foundation (INST 256/418-1). The funding body did not contribute to the design of the study, data collection, analysis, and interpretation, or writing of the manuscript.

#### Availability of data and materials

The dataset(s) supporting the conclusions of this article are all included within the article.

#### Declarations

##### Ethics approval and consent to participate

Not applicable. The manuscript does not contain data collected from humans or animals.

##### Consent for publication

Not applicable.

##### Competing interests

AL has submitted a patent application to produce pamamycin in *S. albus*. All other authors declare no competing interests.

##### Author details

<sup>1</sup>Institute of Systems Biotechnology, Saarland University, Saarbrücken, Germany. <sup>2</sup>Center for Biotechnology, Bielefeld University, Bielefeld, Germany. <sup>3</sup>Department of Pharmacy, Pharmaceutical Biotechnology, Saarland University, Saarbrücken, Germany.

Received: 16 March 2021 Accepted: 27 May 2021

Published online: 03 June 2021

#### References

- McCann PA, Pogell BM. Pamamycin: a new antibiotic and stimulator of aerial mycelia formation. *J Antibiot*. 1979;32:673–8.
- Natsume M, Kondo S, Marumo S. The absolute stereochemistry of pamamycin-607, an aerial mycelium-inducing substance of *Streptomyces alboniger*. *J Chem Soc Chem Commun*. 1989:1911–1913.
- Natsume M, Tazawa J, Yagi K, Abe H, Kondo S, Marumo S. Structure-activity relationship of pamamycins: effects of alkyl substituents. *J Antibiot*. 1995;48:1159–64.
- Hashimoto M, Kondo T, Kozone I, Kawaide H, Abe H, Natsume M. Relationship between response to and production of the aerial mycelium-inducing substances pamamycin-607 and A-factor. *Biosci Biotechnol Biochem*. 2003;67:803–8.
- Hashimoto M, Katsura H, Kato R, Kawaide H, Natsume M. Effect of pamamycin-607 on secondary metabolite production by *Streptomyces* spp. *Biosci Biotechnol Biochem*. 2011;75:1722–6.
- Lefevre P, Peirs P, Braibant M, Fauville-Dufaux M, Vanhoof R, Huygen K, Wang X-M, Pogell B, Wang Y, Fischer P. Antimycobacterial activity of synthetic pamamycins. *J Antimicrob Chemother*. 2004;54:824–7.
- WHO: Global tuberculosis report 2020. Geneva: World Health Organization; 2020. License: CC BY-NC-SA 3.0 IGO.
- Natsume M, Yasui K, Kondo S, Marumo S. The structure of four new pamamycin homologues isolated from *Streptomyces alboniger*. *Tetrahedron Lett*. 1991;32:3087–90.
- Hashimoto M, Komatsu H, Kozone I, Kawaide H, Abe H, Natsume M. Biosynthetic origin of the carbon skeleton and nitrogen atom of pamamycin-607, a nitrogen-containing polyketide. *Biosci Biotechnol Biochem*. 2005;69:315–20.
- Chou WG, Pogell BM. Mode of action of pamamycin in *Staphylococcus aureus*. *Antimicrob Agents Chemother*. 1981;20:443–54.
- Rebets Y, Brotz E, Manderscheid N, Tokovenko B, Myronovskiy M, Metz P, Petzke L, Luzhetskyy A. Insights into the pamamycin biosynthesis. *Angew Chem*. 2015;54:2280–4.
- Gläser L, Kuhl M, Jovanovic S, Fritz M, Vögeli B, Erb TJ, Becker J, Wittmann C. A common approach for absolute quantification of short chain CoA thioesters in prokaryotic and eukaryotic microbes. *Microb Cell Fact*. 2020;19:160.
- Kuhl M, Gläser L, Rebets Y, Rückert C, Sarkar N, Hartsch T, Kalinowski J, Luzhetskyy A, Wittmann C. Microparticles globally reprogram the metabolism of *Streptomyces albus* towards accelerated morphogenesis, streamlined carbon core metabolism and enhanced production of the antituberculosis polyketide pamamycin. *Biotechnol Bioeng*. 2020;117(12):3858–75.
- Sprusansky O, Stirrett K, Skinner D, Denoya C, Westpheling J. The *bkdR* gene of *Streptomyces coelicolor* is required for morphogenesis and antibiotic production and encodes a transcriptional regulator of a branched-chain amino acid dehydrogenase complex. *J Bacteriol*. 2005;187:664–71.
- Yi JS, Kim M, Kim EJ, Kim BG. Production of pikromycin using branched chain amino acid catabolism in *Streptomyces venezuelae* ATCC 15439. *J Ind Microbiol Biotechnol*. 2018;45:293–303.
- Stirrett K, Denoya C, Westpheling J. Branched-chain amino acid catabolism provides precursors for the Type II polyketide antibiotic, actinorhodin, via pathways that are nutrient dependent. *J Ind Microbiol Biotechnol*. 2009;36:129–37.
- Jung WS, Kim E, Yoo YJ, Ban YH, Kim EJ, Yoon YJ. Characterization and engineering of the ethylmalonyl-CoA pathway towards the improved heterologous production of polyketides in *Streptomyces venezuelae*. *Appl Microbiol Biotechnol*. 2014;98:3701–13.
- Kanehisa M, Goto S. KEGG: kyoto encyclopedia of genes and genomes. *Nucleic Acids Res*. 2000;28:27–30.
- Manderscheid N. Strain development for heterologous expression of secondary metabolite clusters in actinobacteria. 2015. Doctoral Thesis, Saarland University, Germany. <https://doi.org/10.22028/D291-23119>.
- Schrader KK, Blevins WT. Effects of carbon source, phosphorus concentration, and several micronutrients on biomass and geosmin production by *Streptomyces halstedii*. *J Ind Microbiol Biotechnol*. 2001;26:241–7.
- Veelken M, Pape H. Production of nikkomycin by immobilized *Streptomyces* cells—Physiological properties. *Appl Microbiol Biotechnol*. 1984;19:146–52.
- Zhang Z, Du C, de Barys F, Liem M, Liakopoulos A, van Wezel GP, Choi YH, Claessen D, Rozen DE. Antibiotic production in *Streptomyces* is organized by a division of labor through terminal genomic differentiation. *Sci Adv*. 2020;6:5781.
- Gubbens J, Janus MM, Florea BI, Overkleeft HS, van Wezel GP. Identification of glucose kinase-dependent and -independent pathways for carbon control of primary metabolism, development and antibiotic production in *Streptomyces coelicolor* by quantitative proteomics. *Mol Microbiol*. 2012;86:1490–507.
- Barka EA, Vatsa P, Sanchez L, Gaveau-Vaillant N, Jacquard C, Meier-Kolthoff JP, Klenk HP, Clement C, Ouhdouch Y, van Wezel GP. Taxonomy, physiology, and natural products of *Actinobacteria*. *Microbiol Mol Biol Rev*. 2016;80:1–43.
- Romero-Rodriguez A, Rocha D, Ruiz-Villafan B, Guzman-Trampe S, Maldonado-Carmona N, Vazquez-Hernandez M, Zelarayan A, Rodriguez-Sanoja R, Sanchez S. Carbon catabolite regulation in *Streptomyces*: new insights and lessons learned. *World J Microbiol Biotechnol*. 2017;33:162.

26. Waldvogel E, Herbig A, Battke F, Amin R, Nentwich M, Nieselt K, Ellingsen TE, Wentzel A, Hodgson DA, Wohlleben W, Mast Y. The PII protein GlnK is a pleiotropic regulator for morphological differentiation and secondary metabolism in *Streptomyces coelicolor*. *Appl Microbiol Biotechnol*. 2011;92:1219–36.
27. Reuther J, Wohlleben W. Nitrogen metabolism in *Streptomyces coelicolor*: transcriptional and post-translational regulation. *J Mol Microbiol Biotechnol*. 2007;12:139–46.
28. Luo S, Chen XA, Mao XM, Li YQ. Regulatory and biosynthetic effects of the bkd gene clusters on the production of daptomycin and its analogs A21978C1–3. *J Ind Microbiol Biotechnol*. 2018;45:271–9.
29. Kozone I, Hashimoto M, Grafe U, Kawada H, Abe H, Natsume M. Structure-activity relationship of pamamycins: effect of side chain length on aerial mycelium-inducing activity. *J Antibiot*. 2008;61:98–102.
30. Lounes A, Lebrihi A, Benslimane C, Lefebvre G, Germain P. Regulation of valine catabolism by ammonium in *Streptomyces ambofaciens*, producer of spiramycin. *Can J Microbiol*. 1995;41:800–8.
31. Ye BC, Zhang Y, Yu H, Yu WB, Liu BH, Yin BC, Yin CY, Li YY, Chu J, Zhang SL. Time-resolved transcriptome analysis of *Bacillus subtilis* responding to valine, glutamate, and glutamine. *PLoS ONE*. 2009;4:e7073.
32. Deutscher J, Ake FM, Derkaoui M, Zebre AC, Cao TN, Bouraoui H, Kenta-tache T, Mokhtari A, Milohanic E, Joyet P. The bacterial phosphoenolpyruvate:carbohydrate phosphotransferase system: regulation by protein phosphorylation and phosphorylation-dependent protein-protein interactions. *Microbiol Mol Biol Rev*. 2014;78:231–56.
33. Cihak M, Kamenik Z, Smidova K, Bergman N, Benada O, Kofronova O, Petrickova K, Bobek J. Secondary Metabolites Produced during the Germination of *Streptomyces coelicolor*. *Front Microbiol*. 2017;8:2495.
34. Yague P, Lopez-Garcia MT, Rioseras B, Sanchez J, Manteca A. New insights on the development of *Streptomyces* and their relationships with secondary metabolite production. *Curr Trends Microbiol*. 2012;8:65–73.
35. Vrijbloed JW, Zerbe Burkhardt K, Ratnatilleke A, Grubelnik Leiser A, Robinson JA. Insertional inactivation of methylmalonyl coenzyme A (CoA) mutase and isobutyryl-CoA mutase genes in *Streptomyces cinnamonensis*: influence on polyketide antibiotic biosynthesis. *J Bacteriol*. 1999;181:5600–5.
36. Lyu M, Cheng Y, Han X, Wen Y, Song Y, Li J, Chen Z. AccR, a TetR family transcriptional repressor, coordinates short-chain acyl coenzyme A homeostasis in *Streptomyces avermitilis*. *Appl Environ Microbiol*. 2020;86:e00508.
37. Xu Z, Liu Y, Ye BC. PccD regulates branched-chain amino acid degradation and exerts a negative effect on erythromycin production in *Saccharopolyspora erythraea*. *Appl Environ Microbiol*. 2018;84:e00049.
38. van Wezel GP, McDowall KJ. The regulation of the secondary metabolism of *Streptomyces*: new links and experimental advances. *Nat Prod Rep*. 2011;28:1311–33.
39. Pullan ST, Chandra G, Bibb MJ, Merrick M. Genome-wide analysis of the role of GlnR in *Streptomyces venezuelae* provides new insights into global nitrogen regulation in actinomycetes. *BMC Genom*. 2011;12:175.
40. Fink D, Weissschuh N, Reuther J, Wohlleben W, Engels A. Two transcriptional regulators GlnR and GlnRII are involved in regulation of nitrogen metabolism in *Streptomyces coelicolor* A3(2). *Mol Microbiol*. 2002;46:331–47.
41. Birko Z, Bialek S, Buzas K, Szajli E, Traag BA, Medzihradsky KF, Rigali S, Vijgenboom E, Penyige A, Kele Z, et al. The secreted signaling protein factor C triggers the A-factor response regulon in *Streptomyces griseus*: overlapping signaling routes. *Mol Cell Proteom*. 2007;6:1248–56.
42. Strauch E, Takano E, Baylis HA, Bibb MJ. The stringent response in *Streptomyces coelicolor* A3(2). *Mol Microbiol*. 1991;5:289–98.
43. Marshall VP, Cialdella JJ, Fox JA, Laborde AL. Precursor directed biosynthesis of paulomycins A and B. The effects of valine, isoleucine, isobutyric acid and 2-methylbutyric acid. *J Antibiotics*. 1984;37:923–5.
44. Gil JA, Campelo-Diez AB. Candidicin biosynthesis in *Streptomyces griseus*. *Appl Microbiol Biotechnol*. 2003;60:633–42.
45. Ward AC, Allenby NE. Genome mining for the search and discovery of bioactive compounds: the *Streptomyces* paradigm. *FEMS Microbiol Lett*. 2018;365:fny240.
46. Li ZL, Wang YH, Chu J, Zhuang YP, Zhang SL. Effect of branched-chain amino acids, valine, isoleucine and leucine on the biosynthesis of bitespiramycin 4'-O-acylsiramycins. *Braz J Microbiol*. 2009;40:734–46.
47. Walsh CT, Gehring AM, Weinreb PH, Quadri LE, Flugel RS. Post-translational modification of polyketide and nonribosomal peptide synthetases. *Curr Opin Chem Biol*. 1997;1:309–15.
48. Zhang B, Tian W, Wang S, Yan X, Jia X, Pierens GK, Chen W, Ma H, Deng Z, Qu X. Activation of natural products biosynthetic pathways via a protein modification level regulation. *ACS Chem Biol*. 2017;12:1732–6.
49. Kieser T, Bibb M, Buttner M, Chater K, Hopwood D. *Practical Streptomyces Genetics*. Norwich: John Innes Foundation; 2000.
50. Barton N, Horbal L, Starck S, Kohlstedt M, Luzhetskyy A, Wittmann C. Enabling the valorization of guaiacol-based lignin: Integrated chemical and biochemical production of cis, cis-muconic acid using metabolically engineered *Amycolatopsis* sp ATCC 39116. *Metab Eng*. 2018;45:200–10.
51. Gibson DG, Young L, Chuang RY, Venter JC, Hutchison CA 3rd, Smith HO. Enzymatic assembly of DNA molecules up to several hundred kilobases. *Nat Methods*. 2009;6:343–5.
52. Myronovskiy M, Welle E, Fedorenko V, Luzhetskyy A. Beta-glucuronidase as a sensitive and versatile reporter in actinomycetes. *Appl Environ Microbiol*. 2011;77:5370–83.
53. Rohles CM, Gläser L, Kohlstedt M, Giesselmann G, Pearson S, del Campo A, Becker J, Wittmann C. A bio-based route to the carbon-5 chemical glutaric acid and to bionylon-6.5 using metabolically engineered *Corynebacterium glutamicum*. *The Royal Society of Chemistry, Green Chemistry*. 2018;20:4662–74.
54. Hoffmann SL, Jungmann L, Schiefelbein S, Peyriga L, Cahoreau E, Portais JC, Becker J, Wittmann C. Lysine production from the sugar alcohol mannitol: Design of the cell factory *Corynebacterium glutamicum* SEA-3 through integrated analysis and engineering of metabolic pathway fluxes. *Metab Eng*. 2018;47:475–87.
55. Krömer JO, Fritz M, Heinzele E, Wittmann C. In vivo quantification of intracellular amino acids and intermediates of the methionine pathway in *Corynebacterium glutamicum*. *Anal Biochem*. 2005;340:171–3.
56. Langmead B, Salzberg SL. Fast gapped-read alignment with Bowtie 2. *Nat Methods*. 2012;9:357–9.
57. Hilker R, Stadermann KB, Schwengers O, Anisiforov E, Jaenicke S, Weishaar B, Zimmermann T, Goesmann A. ReadXplorer 2- detailed read mapping analysis and visualization from one single source. *Bioinformatics*. 2016;32:3702–8.
58. Liao Y, Smyth GK, Shi W. FeatureCounts: an efficient general purpose program for assigning sequence reads to genomic features. *Bioinformatics*. 2014;30:923–30.
59. Love MI, Huber W, Anders S. Moderated estimation of fold change and dispersion for RNA-seq data with DESeq2. *Genome Biol*. 2014;15:550.
60. R Core Team. R: A language and environment for statistical computing. Vienna: R Foundation for Statistical Computing; 2013. <http://www.R-project.org/>.
61. Warnes MGR, Bolker B, Bonebakker L, Gentleman R. Package 'gplots'. Various R programming tools for plotting data. 2016.

## Publisher's Note

Springer Nature remains neutral with regard to jurisdictional claims in published maps and Institutional affiliations.

### 3.3 Kuhl et al. 2020

**Microparticles globally reprogram *Streptomyces albus* toward accelerated morphogenesis, streamlined carbon core metabolism, and enhanced production of the antituberculosis polyketide pamamycin**

Martin Kuhl, Lars Gläser, Yuriy Rebets, Christian Rückert, Namrata Sarkar, Thomas Hartsch, Jörn Kalinowski, Andriy Luzhetskyy, and Christoph Wittmann

*Biotechnology and Bioengineering*. 2020; 117: 3858– 3875.

<https://doi.org/10.1002/bit.27537>

This is an open access article distributed under the terms of the Creative Commons CC BY license.

C. W. designed the project. M. K. conducted the cultures. M. K. and Y. R. performed pamamycin analysis. M. K. and L. G. performed CoA ester analysis. C. R. and J. K. performed RNA sequencing. C. R., J. K., N. S., and T. H. processed and evaluated the RNA sequencing data. M. K. and C. W. analyzed the data, drew the figures, and wrote the first draft of the manuscript. All authors commented, extended, and improved the manuscript. All authors read and approved the final version of the manuscript.

# Microparticles globally reprogram *Streptomyces albus* toward accelerated morphogenesis, streamlined carbon core metabolism, and enhanced production of the antituberculosis polyketide pamamycin

Martin Kuhl<sup>1</sup> | Lars Gläser<sup>1</sup> | Yuriy Rebets<sup>2</sup> | Christian Rückert<sup>3</sup> |  
Namrata Sarkar<sup>4</sup> | Thomas Hartsch<sup>4</sup> | Jörn Kalinowski<sup>3</sup>  | Andriy Luzhetskyy<sup>2</sup>  |  
Christoph Wittmann<sup>1</sup> 

<sup>1</sup>Institute of Systems Biotechnology, Saarland University, Saarbrücken, Germany

<sup>2</sup>Department of Pharmacy, Pharmaceutical Biotechnology, Saarland University, Saarbrücken, Germany

<sup>3</sup>Center for Biotechnology, Bielefeld University, Bielefeld, Germany

<sup>4</sup>Genedata GmbH, Munich, Germany

## Correspondence

Christoph Wittmann, Institute of Systems Biotechnology, Saarland University, 66123 Saarbrücken, Germany.  
Email: christoph.wittmann@uni-saarland.de

## Funding information

Deutsche Forschungsgemeinschaft, Grant/Award Number: INST 256/418-1; Bundesministerium für Bildung und Forschung, Grant/Award Number: 031B0344

## Abstract

*Streptomyces spp.* are a rich source for natural products with recognized industrial value, explaining the high interest to improve and streamline the performance of in these microbes. Here, we studied the production of pamamycins, macrodiolide homologs with a high activity against multiresistant pathogenic microbes, using recombinant *Streptomyces albus* J1074/R2. Talc particles (hydrous magnesium silicate, 3MgO·4SiO<sub>2</sub>·H<sub>2</sub>O) of micrometer size, added to submerged cultures of the recombinant strain, tripled pamamycin production up to 50 mg/L. Furthermore, they strongly affected morphology, reduced the size of cell pellets formed by the filamentous microbe during the process up to sixfold, and shifted the pamamycin spectrum to larger derivatives. Integrated analysis of transcriptome and precursor (CoA thioester) supply of particle-enhanced and control cultures provided detailed insights into the underlying molecular changes. The microparticles affected the expression of 3,341 genes (56% of all genes), revealing a global and fundamental impact on metabolism. Morphology-associated genes, encoding major regulators such as SsgA, RelA, EshA, Factor C, as well as chaplins and rodins, were found massively upregulated, indicating that the particles caused a substantially accelerated morphogenesis. In line, the pamamycin cluster was strongly upregulated (up to 1,024-fold). Furthermore, the microparticles perturbed genes encoding for CoA-ester metabolism, which were mainly activated. The altered expression resulted in changes in the availability of intracellular CoA-esters, the building blocks of pamamycin. Notably, the ratio between methylmalonyl CoA and malonyl-CoA was increased fourfold. Both metabolites compete for incorporation into pamamycin so that the altered availability explained the pronounced preference for larger derivatives in the microparticle-enhanced process. The novel insights into the behavior

This is an open access article under the terms of the Creative Commons Attribution License, which permits use, distribution and reproduction in any medium, provided the original work is properly cited.

© 2020 The Authors. *Biotechnology and Bioengineering* published by Wiley Periodicals LLC

of *S. albus* in response to talc appears of general relevance to further explore and upgrade the concept of microparticle enhanced cultivation, widely used for filamentous microbes.

#### KEYWORDS

filamentous microbe, microparticle, morphogenesis, polyketide, *Streptomyces*, transcriptome

## 1 | INTRODUCTION

Streptomycetes are an important source of natural products for pharmaceutical, medical, agricultural, and nutraceutical application, including more than two-third of all known antibiotics of microbial origin (Bibb, 2013). Over the past, they have provided a range of industrialized blockbuster drugs, including streptomycin (Ehrlich, Bartz, Smith, Joslyn, & Burkholder, 1947), chloramphenicol (Ehrlich et al., 1947), candididin (Lechevalier, Acker, Corke, Haenseler, & Waksman, 1953), doxorubicin (Arcamone et al., 1969), ivermectin (Campbell, Fisher, Stapley, Albers-Schönberg, & Jacob, 1983; Juarez, Scholnik-Cabrera, & Dueñas-Gonzalez, 2018), bialaphos (Bayer et al., 1972), and rapamycin (Sehgal, Baker, & Vézina, 1975; Vézina, Kudelski, & Sehgal, 1975), amongst others (Kieser, Bibb, Buttner, Chater, & Hopwood, 2000). It is easy to understand that strategies to activate and enhance the synthesis of natural products in Streptomycetes have been of a broad interest from early on and still display a topic of major relevance (Ahmed et al., 2020; Horbal, Marques, Nadmid, Mendes, & Luzhetskyy, 2018; Kallifidas, Jiang, Ding, & Luesch, 2018; Lopatniuk et al., 2019; Zhang et al., 2020).

Members of the genus are well known for a complex morphology linked to their multicellular life cycle, which starts with the germination of a single spore that grows into a vegetative mycelium by linear tip extension and hyphae branching (Chater & Losick, 1997; van Dissel, Claessen, & van Wezel, 2014), then forms an aerial mycelium, and finally differentiates into uninucleoid cells that further develop again into spores (Angert, 2005). In submerged culture, more relevant for industrial production, morphogenesis comprises primary and secondary mycelial networks, pellets, and sporulation (van Dissel et al., 2014).

Notably, morphological development and natural product formation are closely linked, and various efforts have been made to increase production through an altered morphology (Chater, 1984). Genetic perturbation, as an example, provided remarkable progress (van Dissel et al., 2014; Koebisch, Overbeck, Piepmeyer, Meschke, & Schrepf, 2009; van Wezel et al., 2006; Xu, Chater, Deng, & Tao, 2008). Other studies aimed to influence morphology on the process level, including the modification of agitation speed (Belmar-Beiny & Thomas, 1991; Xia, Lin, Xia, Cong, & Zhong, 2014), medium viscosity (O'Clearigh, Casey, Walsh, & O'Shea, 2005), pH value (Glazebrook, Vining, & White, 1992), the addition of specific nutrients (Jonsbu, McIntyre, & Nielsen, 2002), and even subinhibitory antibiotic concentrations (Wang, Zhao, & Ding, 2017). These studies,

however, have revealed a mixed outcome and largely remained on a trial and error level.

Strikingly, a breakthrough in tailored control of morphology was achieved with the introduction of inorganic microparticles, added to the cultures (R. Walisko, Krull, Schrader, & Wittmann, 2012). Pioneering studies successfully used such materials to streamline the morphology of eukaryotic filamentous fungi and enhance the formation of enzymes (Driouch, Hänsch, Wucherpennig, Krull, & Wittmann, 2012; Driouch, Roth, Dersch, & Wittmann, 2010; Kaup, Ehrlich, Pescheck, & Schrader, 2008), polyketides, and alcohols (Etschmann et al., 2015). More recently, several studies suggested that microparticles are also beneficial to enhance product formation in filamentous prokaryotes (Holtmann et al., 2017; Liu, Tang, Wang, & Liu, 2019; Ren et al., 2015; J. Walisko et al., 2017).

Here, we studied the use of talc microparticles for the production of pamamycins (Figure 1), a family of 16 macrodiolide homologs that are highly active against multiresistant pathogenic microbes, using recombinant *Streptomyces albus* J1074/R2 (Rebets et al., 2015). Carefully conducted cultures with analysis of growth, product formation and cellular morphology enabled us to specifically study the impact of the microparticle addition on production performance. In addition, transcriptome and intracellular CoA thioester analyses provided insights into the cellular response of *S. albus* and provided a systems-level picture on how the particles reprogrammed morphogenesis and streamlined metabolism for enhanced production and a notable shift toward heavier pamamycin homologs.

## 2 | MATERIALS AND METHODS

### 2.1 | Strain

*S. albus* J1074/R2 expressing the heterologous pamamycin gene cluster was obtained from previous work (Rebets et al., 2015). For strain maintenance, spores collected from agar plate cultures after 5-day incubation were resuspended in 20% glycerol and kept at  $-80^{\circ}\text{C}$ .

### 2.2 | Media

Mannitol-soy flour agar contained per liter: 20 g mannitol (Sigma-Aldrich, Taufkirchen, Germany), 20 g soy flour (Schoenenberger

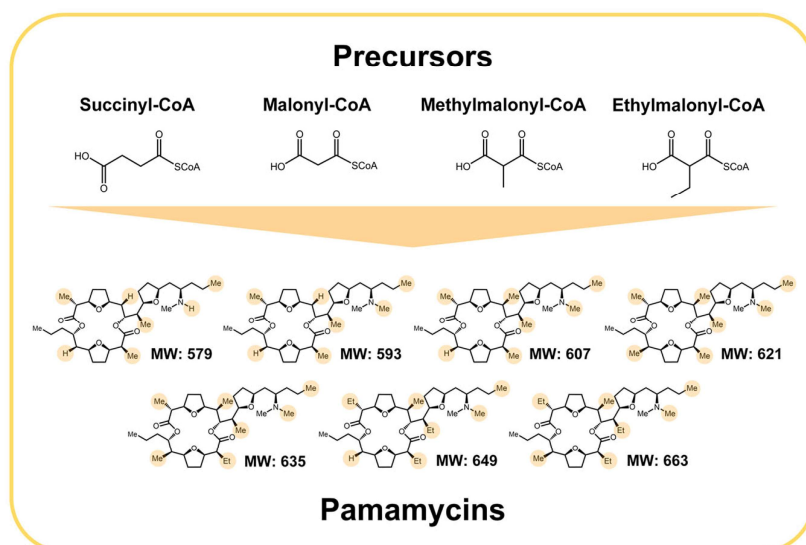


**FIGURE 1** Chemical structure of the polyketide pamamycin family and the building blocks of its different derivatives succinyl-CoA, malonyl-CoA, methylmalonyl-CoA, and ethylmalonyl-CoA. The individual combination of different CoA-esters results in a different decoration of the product (-H, -CH<sub>3</sub>, -C<sub>2</sub>H<sub>5</sub>) at specific positions and determines the molecular weight (MW). Except for Pam 607, several isomers exist for each pamamycin, differing by the exact position of the side chains (Hanquet, Salom-Roig, & Lanners, 2016). For every pamamycin mass derivative, one exemplary structure is shown [Color figure can be viewed at [wileyonlinelibrary.com](http://wileyonlinelibrary.com)]

Hensel, Magstadt, Germany), and 20 g agar (Becton & Dickinson, Heidelberg, Germany). Liquid SGG medium was used for pre- and main cultures for pamamycin production and contained per liter: 10 g soluble starch (Sigma-Aldrich), 10 g glycerol, 2.5 g corn steep powder (Sigma-Aldrich), 5 g bacto peptone (Becton & Dickinson), 2 g yeast extract (Becton & Dickinson), 1 g sodium chloride, and 21 g MOPS. The pH of the medium was adjusted to 7.2, using 6 M NaOH. Talc microparticles (hydrous magnesium silicate, 3MgO·4SiO<sub>2</sub>·H<sub>2</sub>O, 10 μm; Sigma-Aldrich) were resuspended in 50 mM Na-acetate buffer (pH 6.5), autoclaved at 121°C for 20 min, and added to the sterile medium before inoculation of selected experiments (Driouch, Sommer, & Wittmann, 2010).

### 2.3 | Cultivation

One loop of spores was scratched from a 5-day old plate culture and used to inoculate a liquid preculture, which was then grown overnight in a 500-ml baffled shake flask with 50 ml medium and 30 g soda-lime glass beads (5 mm; Sigma-Aldrich). When the preculture reached the late exponential phase, an appropriate amount of cells was collected (8,500g, room temperature, 5 min), resuspended in 10 ml fresh medium, and used to inoculate the main-culture (50 ml medium in 500-ml baffled shake flasks). Main cultures (with and without talc) were inoculated from the same preculture to enable identical starting conditions. All cultivation experiments were conducted in triplicate on a rotary shaker (28°C, 230 rpm, 75% relative humidity, 5-cm shaking diameter, Multitron, Infors AG, Bottmingen, Switzerland).

### 2.4 | Quantification of cell concentration

The cell dry weight (CDW) of *S. albus* was measured as follows. Cells were collected (10,000g, 4°C, 10 min), washed twice with 15 ml deionized water and freeze-dried. Subsequently, the CDW was gravimetrically determined (Gläser et al., 2020). In microparticle cultivations, the measurements were corrected for the added talc (Driouch, Sommer, et al., 2010). The optical density (OD<sub>600</sub>) of a culture was measured at 600 nm (UV-1600PC spectrophotometer; VWR, Hannover, Germany). Individual correlations allowed to infer the CDW from optical density measurement for different talc concentrations: CDW (g/L) = 0.64 × OD<sub>600</sub> (control), CDW (g/L) = 0.70 × OD<sub>600</sub> (2.5 g/L talc), CDW (g/L) = 0.76 × OD<sub>600</sub> (10 g/L talc; Figure S8), as described before (Becker, Klopprogge, Schröder, & Wittmann, 2009). All measurements were performed in triplicate.

### 2.5 | Quantification of substrates

Before analysis, starch was hydrolyzed to glucose monomers for 3 hr using 3 M HCl at 100°C. Glucose and glycerol were quantified by high-performance liquid chromatography (HPLC; 1260 Infinity Series; Agilent, Waldbronn, Germany) using an Aminex HPX-87H column (300 × 7.8 mm; Bio-Rad, München, Germany) and 7 mM H<sub>2</sub>SO<sub>4</sub> as mobile phase (55°C, 0.7 ml/min). Refraction index measurement was used for detection and external standards were used for quantification. Phosphate was analyzed by HPLC (Dionex Integriion; Thermo Fisher Scientific, Karlsruhe, Germany) using a Dionex IonPac AS9-HC column (2 × 250 mm; Thermo Fisher Scientific) and 9 mM Na<sub>2</sub>CO<sub>3</sub> as

mobile phase (35°C, 0.25 ml/min). Conductivity measurement was used for detection and an external standard was used for quantification. All measurements were performed in triplicate.

## 2.6 | Morphology analysis

Five microliter culture broth was transferred onto a glass for bright-field microscopy (Olympus IX70 microscope, Hamburg, Germany). The software ImageJ 1.52 (Schneider, Rasband, & Eliceiri, 2012) was used to automatically determine the size of pellets formed during growth (Krull et al., 2013). The diameter of a pellet was assumed as the smallest circle into which the complete aggregate fitted (Martin & Bushell, 1996). At least 150 aggregates were analyzed per sample.

## 2.7 | Natural compound extraction and quantification

Pamamycin was extracted from culture broth using a two-step process. First, 200  $\mu$ l broth was mixed with 200  $\mu$ l acetone and incubated for 15 min (1,000 rpm, room temperature, Thermomixer F1.5; Eppendorf, Wesseling, Germany). Subsequently, 200  $\mu$ l ethyl acetate was added, and the mixture was incubated for further 15 min under the same conditions. Afterward, the organic phase was collected (20,000g, room temperature, 5 min). The solvents were evaporated under a laminar nitrogen stream. The extract was redissolved in 2 ml methanol, clarified from debris (20,000g, 4°C, 10 min) and analyzed, using HPLC-ESI-MS (Agilent Infinity 1290, Waldbronn, Germany; AB Sciex QTrap 6500, Darmstadt, Germany). The different pamamycin derivatives (Figure 1) were separated on a C18 column (Vision HT C18 HighLoad, 100  $\times$  2 mm, 1.5  $\mu$ m, Dr. Maisch, Ammerbuch-Entringen, Germany) at a flow rate of 300  $\mu$ l/min (8 mM ammonium formate in 92% acetonitrile) and 45°C. Detection was carried out in positive selected ion monitoring mode, using the corresponding  $[M + H]^+$  ion for each derivative (Figure 1). All measurements were performed in triplicate.

## 2.8 | Extraction and quantification of intracellular CoA-esters

The analysis of CoA-esters was conducted as recently described (Gläser et al., 2020). In short, a broth sample (8 mg CDW) was transferred into a precooled tube, which contained quenching and extraction solution (95% acetonitrile, 25 mM formic acid, -20°C) at a volume ratio of 1:4 followed by repetitive mixing and cooling on ice for 10 min, clarification from cell debris (15,000g, 4°C, 10 min) and the addition of 10 ml supercooled deionized water. The cell pellet was washed twice with 8 ml supercooled deionized water. All supernatants were combined, followed by freezing in liquid nitrogen and lyophilization. Before analysis, the obtained dry extract was dissolved in 500  $\mu$ l precold buffer (25 mM ammonium formate, 2% methanol, pH 3.0, 4°C) and filtered

(Ultrafree-MC 0.22  $\mu$ m; Merck, Millipore, Germany). Analysis of the CoA-esters was performed on a triple quadrupole MS (QTRAP 6500+; AB Sciex, Darmstadt, Germany) coupled to an HPLC system (Agilent Infinity 1290 System). Separation of the analytes of interest was conducted at 40°C on a reversed phase column (Gemini 100  $\times$  4.6 mm, 3  $\mu$ m, 110 Å, Phenomenex, Aschaffenburg, Germany) using a gradient of formic acid (50 mM, adjusted to pH 8.1 with 25% ammonium hydroxide, eluent A) and methanol (eluent B) at a flow rate of 600  $\mu$ l/min. The fraction of eluent B was as follows: 0–12 min, 0–15%; 12–16 min, 15–100%; 16–18 min, 100%; 18–20 min, 100–0%; 20–25 min, 0%. The first 3 min of the analysis were discharged to minimize the entry of salts into the mass spectrometer. CoA-esters of interest were analyzed in positive ionization mode, using multiple reaction monitoring. Analyte specific instrument settings such as declustering potential, collision energy, and collision cell exit potential were individually optimized for each CoA-ester, using synthetic standards. All measurements were done in triplicate.

## 2.9 | Transcriptome analysis

Cells (1 ml broth) were collected by centrifugation (20,000g, 4°C, 1 min) and immediately frozen in liquid nitrogen. RNA was extracted with the Qiagen RNA Mini Kit (Qiagen, Hilden, Germany) according to the manufacturer's instructions. Residual DNA was removed by digestion with 10 U RNase-free DNase I (Thermo Fisher Scientific) for 1 hr in the presence of RiboLock RNase inhibitor (Thermo Fisher Scientific). After DNA digestion, the RNA was again purified with the same kit. RNA quality was checked by Trinean Xpose (Gentbrugge, Belgium) and the Agilent RNA 6000 Nano Kit on an Agilent 2100 Bioanalyzer (Agilent Technologies, Böblingen, Germany). Ribosomal RNA molecules were removed from total RNA with the Ribo-Zero rRNA Removal Kit (Illumina, San Diego, CA) and removal of rRNA was checked with the Agilent RNA 6000 Pico Kit on an Agilent 2100 Bioanalyzer. Libraries of complementary DNA (cDNA) were prepared with the TruSeq Stranded mRNA Library Prep Kit (Illumina), and the resulting cDNA was sequenced paired end on an Illumina HiSeq 1500 system using 2  $\times$  75 bp read length. Reads were mapped to the *S. albus* J1074/R2 genome sequence (CP059254.1) with Bowtie2 using standard settings (Langmead & Salzberg, 2012) except for increasing the maximal allowed distance for paired reads to 600 bases. For visualization of read alignments and raw read count calculation, ReadXplorer 2.2.3 was used (Hilker et al., 2014). Due to a high unspecific background over both strands, the raw read count for each CDS was corrected by subtracting the length-adjusted median read count calculated over all CDS from the respective noncoding strand. Using the resulting data, DESeq2 (Love, Huber, & Anders, 2014) was used to QC the datasets via, among others, calculation of the sample to sample distances (Figure S9) and PCA (Figure S10). In addition, DESeq2 was used to calculate DGE datasets. Raw datasets (sequenced reads) as well as processed datasets (input matrix and normalized read counts from DESeq2) are available from GEO (GSE155008). For statistical analysis, Student's *t* test was carried out

and the data were filtered for genes with a  $\log_2$ -fold change  $\geq 1$  ( $p < 0.05$ ). Hierarchical clustering was conducted, using the software package gplots (R Core Team, 2014; Warnes, Bolker, Bonebakker, & Gentleman, 2016). For visualization, Voronoi tree maps were created, using the Voronto tool (Santamaría & Pierre, 2012) for Java (version 8, update 231, Build 1.8.0\_231-b11). RNA extraction and sequencing were conducted as biological triplicates, except for one of the controls, where one replicate was lost during processing. Given the excellent reproducibility of all analyzed samples (Figures S10 and S11), the available dataset was regarded acceptable to enable a robust and reliable evaluation of gene expression.

### 3 | RESULTS

#### 3.1 | Pamamycin production in *S. albus* J1074/R2

In a first set of experiments, the pamamycin production performance of *S. albus* J1074/R2 was assessed in liquid SGG medium, which contained starch and glycerol as carbon source (Figure 2a). After inoculation, cells immediately started to grow into mycelial networks, which then aggregated into pellets as typically observed for actinomycetes. Growth

lasted for about 12 hr. The production of pamamycins started after  $\sim 9$  hr at the end of the growth phase (when phosphate became limiting, Figure S11) and continued during the later stationary phase. The recombinant strain produced a rich spectrum of different pamamycins, which were attributed to derivatives with different side chains according to their molecular mass, that is, Pam 579, Pam 593, Pam 607, Pam 621, Pam 635, Pam 649, and Pam 663. Smaller pamamycins (Pam 579, Pam 593, and Pam 607) were most prominent. The total pamamycin titer was 18 mg/L. Interestingly, starch was the major carbon source until  $\sim 24$  hr (Figure S11). Glycerol remained practically untouched during the initial process, but was consumed later when starch reached a lower level (although it was still present). During the cultivation, the pH value varied between 6.5 and 7.5. It decreased during the growth phase and increased again in later phases.

#### 3.2 | The addition of talc to the culture of *S. albus* J1074/R2 increases the production of pamamycin up to threefold

*S. albus* J1074/R2, cultivated in SGG medium with microparticles (2.5 g/L talc), revealed an increased pamamycin titer of 22 mg/L

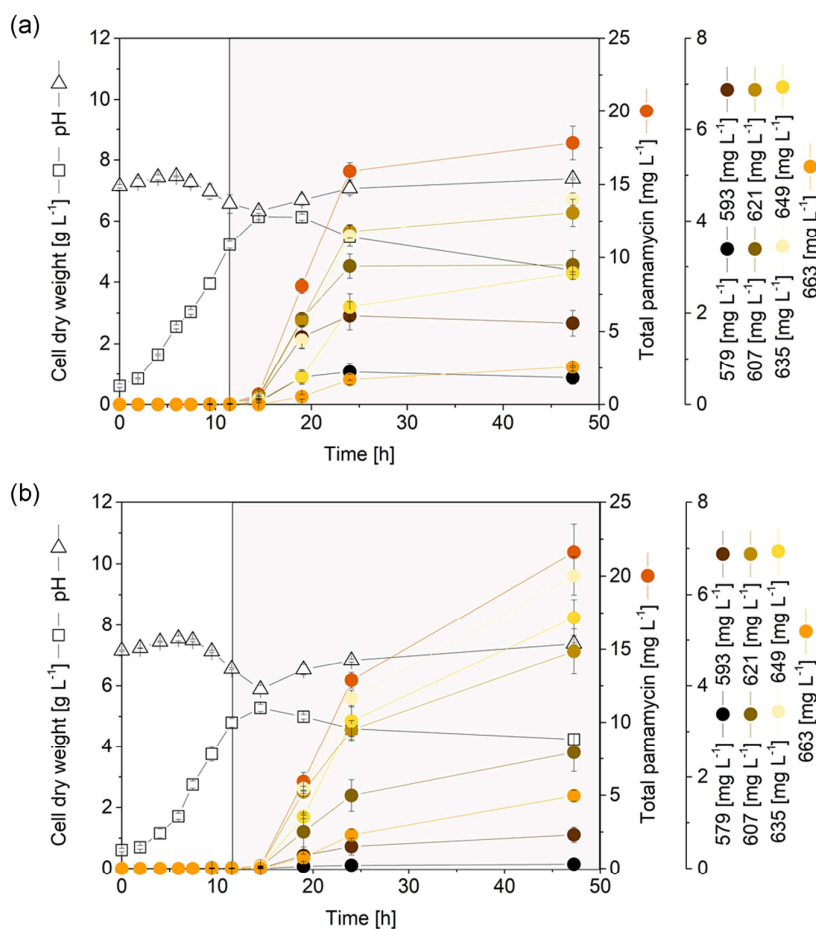


**FIGURE 2** Impact of talc microparticles on growth and pamamycin production in *Streptomyces albus* J1074/R2 using complex SGG medium with starch and glycerol as main carbon source. (a) Control culture without microparticles. (b) Microparticle-enhanced culture with 2.5 g/L talc. Growth phase (white) and major pamamycin production phase (gray) are indicated by color [Color figure can be viewed at [wileyonlinelibrary.com](http://wileyonlinelibrary.com)]

(Figure 2b). Interestingly, talc did not generally enhance production, but specifically affected the pamamycin spectrum. The titer of low molecular weight derivatives (Pam 579, Pam 593, Pam 607) was found reduced, whereas higher molecular weight pamamycins were increased (Pam 635, Pam 649, Pam 663). This effect was most prominent for the two heaviest pamamycins (Pam 649, Pam 663). These two derivatives were increased almost twofold. The presence of the talc particles resulted in a slightly faster use of phosphate (Figure S11). The mode of substrate utilization was the same as for the control, mainly starch consumption during the initial phase and activation of glycerol utilization after ~20 hr. Generally, glycerol uptake was more pronounced than in the control. It's uptake was faster, and a significantly lower amount of it was left at the end of the process (Figure S11). The pH profile was like the control.

Further studies revealed a strong impact of the amount of talc on the product level (Figure 3a). An optimum performance was observed for talc levels of 10 and 15 g/L. These concentrations provided 50 mg/L of total pamamycin. An even higher concentration of talc (20 g/L) resulted in a reduced titer (37 mg/L), slightly below the optimum. Notably, the stimulating effect of the microparticles on the formation of larger pamamycins was maintained even at the highest talc level: 20 g/L of talc specifically enhanced production of pamamycins Pam 649 and Pam 663. Altogether, a concentration of 10 g/L talc appeared optimal and was chosen for further studies.

### 3.3 | Talc microparticles reduce the pellet size of *S. albus* J1074/R2 more than sixfold

The addition of talc caused substantial changes in cellular morphology (Figure 3b). In control cultures without talc, the formed pellets exhibited an average diameter of ~435 μm. Already low levels of talc (2.5 g/L) led to a drastic decrease to 150 μm. With an increasing microparticle concentration, this effect was even more pronounced. The smallest pellet diameter (70 μm) was reached at 10 g/L talc. Further increase of the talc concentration did not result in a further reduction of the pellet size.

Taken together, smaller pellets were obviously beneficial for pamamycin production (Figure 3a). Microscopic analysis of the cultures revealed that the microparticles attached to the cells, which obviously loosened the inner structure of the aggregates (Figure 4c,d). The pellets of talc enhanced cultures appeared of a similar loose structure during growth and production phase. In contrast, the central core of pellets of the control culture showed signs of decomposition during production phase (Figure 4b).

### 3.4 | Microparticles globally reprogram the metabolism of *S. albus* J1074/R2

To assess the response of the actinomycete to the added microparticles in more detail, global gene expression analysis was conducted. We compared the transcriptome during the growth phase

(5 hr) and the production phase (21 hr) between a talc (10 g/L) supplied culture and a control culture without talc using RNA sequencing. Generally, the transition of *S. albus* J1074/R2 from the nonproducing growth phase to the production phase was linked to a wide readjustment of gene expression. The expression of 1,468 genes, representing 24% of the genomic repertoire, was significantly altered in the control culture, when cells shifted from growth to production mode ( $\log_2$ -fold change  $\geq 1$ ,  $p \leq .05$ ; Figures S1 and S7). On top of this general shift, talc supply induced a global change in the transcriptome. These talc-specific effects were observed for the growth as well as the production phase (Figures 5, S1, and S6). Altogether, 3,341 genes (56% of all genes) were specifically affected by the presence of talc, revealing a fundamental impact of the microparticles on the physiology of *S. albus*. During growth, the microparticles changed the expression of 2,133 genes (36%). This number

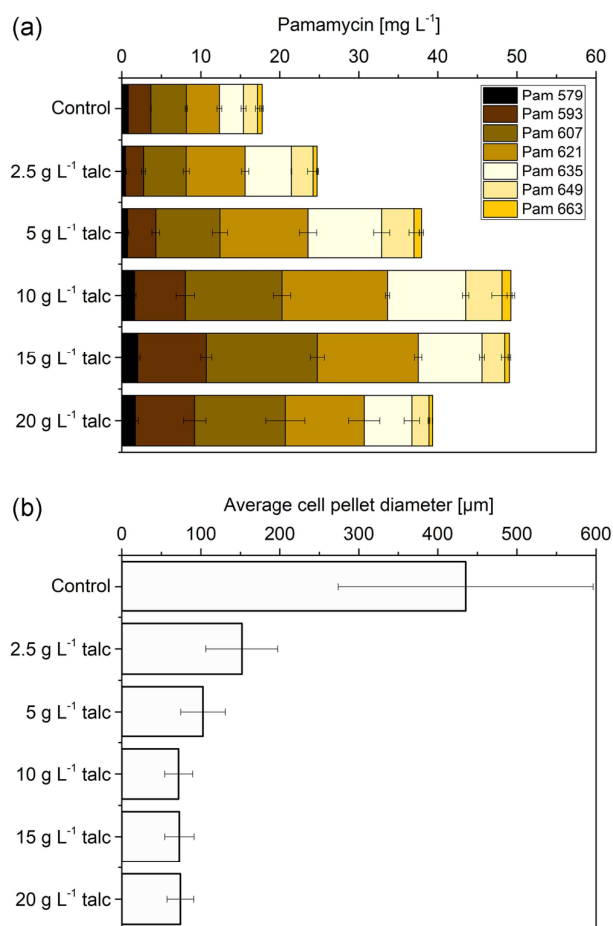


**FIGURE 3** Streamlined pamamycin production using different concentrations of talc added to cultures of recombinant *Streptomyces albus* J1074/R2. (a) Total pamamycin titer and spectrum of different pamamycin derivatives assessed as final value after 48 hr of cultivation. (b) Average pellet diameter during the major production phase (20 hr), as assessed from optical analysis of at least 150 aggregates per condition [Color figure can be viewed at [wileyonlinelibrary.com](http://wileyonlinelibrary.com)]

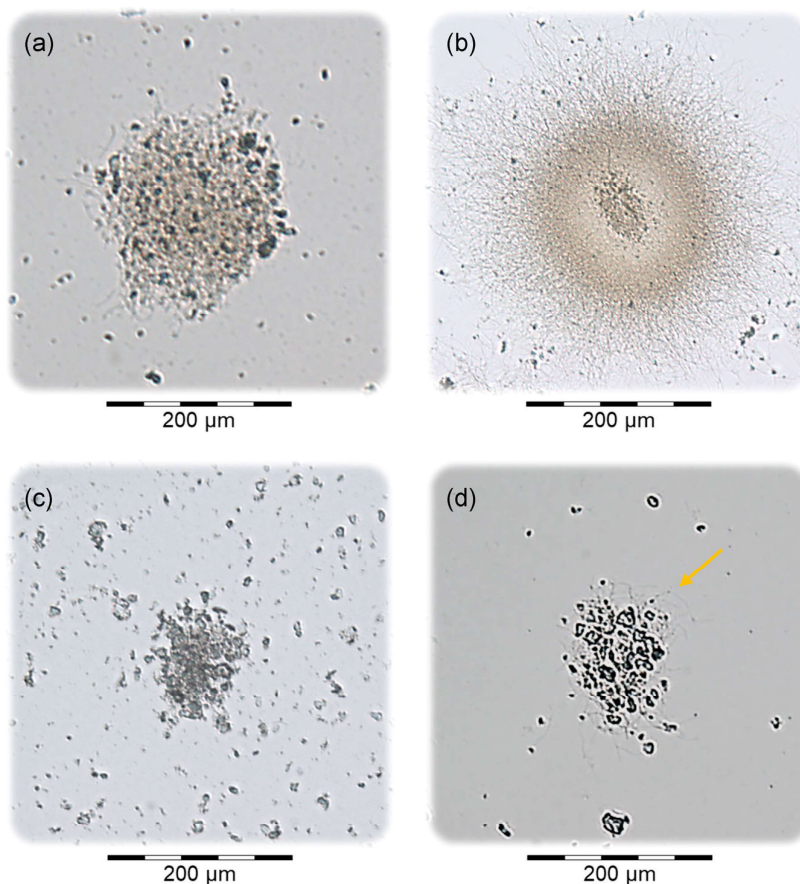


**FIGURE 4** Impact of talc microparticles on the cellular morphology of *Streptomyces albus* J1074/R2. Control culture without microparticles during growth (5 hr) (a) and production (20 hr) (b). Microparticle-enhanced culture with 10 g/L talc during growth (5 hr) (c) and production (20 hr) (d). The arrow indicates the physical attachment of the mycelium to the microparticles [Color figure can be viewed at [wileyonlinelibrary.com](http://wileyonlinelibrary.com)]

increased even further to 2,449 genes (41%), when talc supplemented cultures were in the production phase. The talc-induced changes covered almost all functional gene classes (Figure 5), which were found downregulated (shown in blue) or upregulated (yellow). As example, talc caused an upregulation of the biosynthetic pathways for branched chain amino acids, polyketide metabolism, and the biosynthesis of other secondary metabolites during the growth phase (Figure 5a). Talc specific gene expression changes during the production phase included an upregulation of starch and sucrose metabolism, valine, leucine and isoleucine degradation, butanoate metabolism, propanoate metabolism, fatty acid degradation, and secondary metabolite biosynthesis (Figure 5b). In addition, genes related to stress and cell death differed in transcription depending on culture conditions (Table S2).

### 3.5 | Talc microparticles affect the expression of morphology regulators

Since the microparticles obviously affected the morphology of *S. albus* (Figures 3b and 4), we searched within the transcriptome data for genes involved in morphology and secondary metabolism. Based on their similarity to known morphogenetic genes identified in other

*Streptomyces*, we could identify 55 genes which were affected by the particles (Figures S2 and S3). As prominent example, the addition of microparticles resulted in an upregulation ( $\log_2$ -fold change = 2.0) of the sporulation and cell division protein SsgA, encoded by XNRR2\_5315, already during growth (Table 1). The upregulation was even higher during production ( $\log_2$ -fold change = 3.0). A similar picture was observed for other prominent morphology genes, that is, the signaling protein Factor C (XNRR2\_2306), the chaplin (*chp*) and rodlin (*rdl*) hydrophobic sheath proteins and a neutral zinc metalloprotease (XNRR2\_1391), a homolog to *sgmA* in *S. griseus*, and a well-known morphology regulator (Table 1). In all cases, the microparticles caused an overexpression, which was most pronounced during the pamamycin production phase but partly started already during growth.

### 3.6 | Microparticles drive the expression of the pamamycin biosynthetic cluster

Causally linked to the enhanced production, *S. albus* J1074/R2 responded to the microparticles by a strong overexpression of the pamamycin cluster ( $\log_2$ -fold change up to 10, Figure 6). The activation was most pronounced for the production phase, where 19 out



**TABLE 1** Impact of talc microparticles on the expression of morphology associated genes in pamamycin producing *Streptomyces albus* J1074/R2

Gene	Annotation	Homolog and identity [%]	Growth (Talc)	Prod. (Talc)	Prod. (Control)	Reference
XNRR2_1044	Sporulation factor	<i>whiH</i> , SCO, 79.8	2.1	5.2	3.0	Flårdh, Kindlay, and Chater (1999)
XNRR2_1071	ppGpp synthetase	<i>relA</i> , SCO, 45.3	0.0	2.9	0.0	Hesketh et al. (2007)
XNRR2_5340	ppGpp synthetase I	<i>relA</i> , SCO, 85.6	0.0	0.0	0.0	Hesketh et al. (2007)
XNRR2_1554	Nucl. binding protein	<i>eshA</i> , SCO, 65.9	8.9	10.0	8.2	Saito et al. (2006)
XNRR2_1132	BldB	<i>bldB</i> , SALB	-1.0	-1.4	0.0	Flårdh et al. (1999)
XNRR2_1391	Metalloprotease	<i>sgmA</i> , SGR, 67.6	5.6	10.1	0.0	Kato, Suzuki, Yamazaki, Ohnishi, and Horinouchi (2002)
XNRR2_2151	Membrane protein	<i>chpD</i> , SALB	3.9	7.6	0.0	Zaburannyi et al. (2014)
XNRR2_2152	Secreted protein	<i>chpA</i> , SALB	0.0	7.0	0.0	Zaburannyi et al. (2014)
XNRR2_5022	Hypothetical protein	<i>chpE</i> , SALB	1.1	2.1	0.0	Zaburannyi et al. (2014)
XNRR2_5152	Membrane protein	<i>chpH</i> , SALB	3.3	8.1	4.3	Zaburannyi et al. (2014)
XNRR2_5153	Secreted protein	<i>chpC</i> , SALB	0.0	7.4	0.0	Zaburannyi et al. (2014)
XNRR2_2166	RdIB	<i>rdIB</i> , SALB	4.0	8.3	3.9	Claessen et al. (2004)
XNRR2_2167	RdIA	<i>rdIA</i> , SALB	5.2	10.5	4.1	Claessen et al. (2004)
XNRR2_2306	Factor C	<i>facC</i> , SALB	3.5	4.0	0.0	Birkó et al. (2007)
XNRR2_3527	BldN subunit	$\sigma^{BldN}$ , SVE, 84.9	1.9	4.9	0.0	Bibb, Domonkos, Chandra, and Buttner (2012)
XNRR2_5117	TetR-type regulator	<i>wblA</i> , SCO, 67.8	4.2	4.5	4.2	van Wezel and McDowall (2011)
XNRR2_5315	SsgA	<i>ssgA</i> , SALB	2.0	3.0	1.8	van Wezel et al. (2000a)

Note: Samples were taken from a control and a talc supplied culture (10 g/L) in SGG medium during growth (5 hr) and production (21 hr). The values correspond to  $\log_2$ -fold expression changes, considering the control culture during growth (5 hr) as reference. The listed genes represent previously discovered morphology-associated genes in *S. albus* (SALB) and genes, identified by BLAST search as homologs to morphology-associated genes in *S. coelicolor* (SCO), *S. griseus* (SGR), and *S. venezuelae* (SVE), indicated by the percentage of homology. The identification of homologs was supported by the fact that Streptomycetes share many genetic elements of morphology control (van Dissel et al., 2014), including SsgA like proteins (Traag & van Wezel, 2008) and Factor C (Birkó et al., 1999). In addition to genes identified in *S. albus* before (Zaburannyi, Rabyk, Ostash, Fedorenko, & Luzhetskyy, 2014), further candidates could be inferred from previous studies on morphological development in other *Streptomyces* spp., including *S. coelicolor* (Chakraborty & Bibb, 1997; Hesketh et al., 2007; van Wezel & McDowall, 2011), *S. griseus* (Saito et al., 2006; van Wezel & McDowall, 2011), and *S. lividans* (van Wezel et al., 2006), among others.

of the 20 cluster genes were overexpressed as compared to the control. As exception, only the regulator gene *pamR1* remained relatively unaffected. It was interesting to note that the cluster activation was not fully balanced among the “two cores” of the gene cluster. In fact, genes of the “right core” were induced stronger than genes of the “left core.” Most of the “right core” genes, that is, 11 out of 15, were upregulated with a  $\log_2$ -fold change of more than 8 by talc. A few genes of the pamamycin cluster (*pamC*, *pamD*, *pamE*, *pamF*, *pamH*, *pamK*, *pamO*, *pamS*, and *pamX*) were activated by the microparticles already during the growth phase. In contrast, the pamamycin transporter gene (*pamW*) and the regulator inside the “left core” (*pamR2*) were downregulated. In addition to the pamamycin cluster, also other genes of secondary metabolism were found significantly upregulated (Figure 5). The expression changes covered different gene functions: Type I polyketide structures (candicidin biosynthesis), polyketide sugar unit biosynthesis, siderophores (2,3-dihydroxybenzoate synthesis), sesquiterpenoid and triterpenoid

biosynthesis (germacradienol/geosmin synthase), terpenoid backbone synthesis, and phenazine biosynthesis (Table S3).

### 3.7 | Microparticles modulate supporting pathways in central carbon metabolism

As shown, cells preferably produced higher mass pamamycin derivatives in the presence of microparticles. Generally, different derivatives originate from the incorporation of different precursor metabolites, that is, CoA-esters of different type (Figure 1). We, therefore, hypothesized that the microparticles could have impacted genes encoding enzymes for CoA-ester synthesis and interconversion. Indeed, talc supply affected the expression of CoA-ester related genes (Table 2; Figures S4 and S5). As example, talc led to a strong downregulation ( $\log_2$ -fold change = 6) of the  $\alpha$ -subunit of the acetyl/propionyl-CoA carboxylase (XNRR2\_4211), responsible for the formation of methylmalonyl-CoA

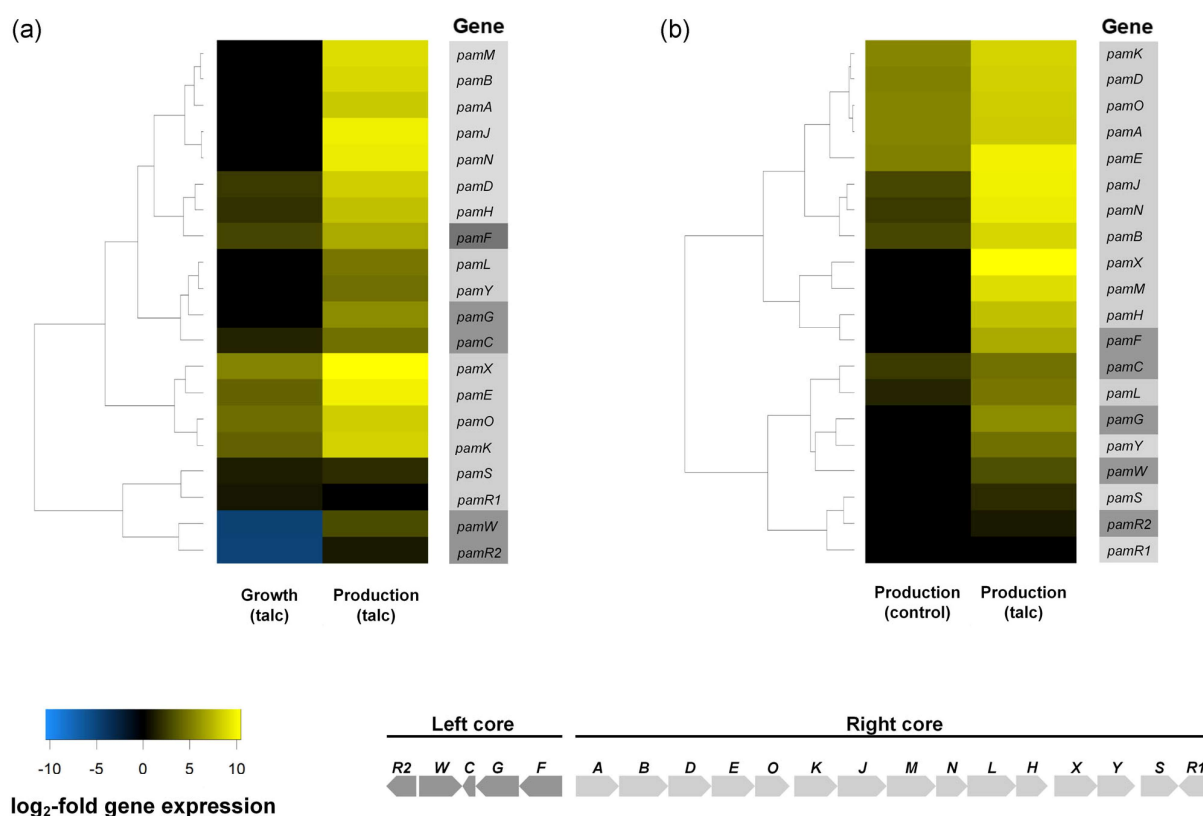


**FIGURE 6** Hierarchical cluster analysis of the expression of the pamamycin biosynthetic pathway genes in *Streptomyces albus* J1074/R2. Samples were taken from a control and a talc supplied culture (10 g/L) in SGG medium during exponential growth (5 hr) and production phase (21 hr). The expression level of the control culture during growth (5 hr) was used as a reference. The cluster comprises the genes *pamA*, 3-oxoacyl-synthase 2; *pamB*, 3-oxoadipate CoA-transferase subunit A; *pamC*, acyl carrier protein; *pamD*, 3-oxoacyl-synthase 3 protein 1; *pamE*, 3-oxoacyl-synthase 3; *pamF*, 3-oxoacyl-synthase 2; *pamG*, 3-oxoacyl-synthase 3; *pamH*, aminohydrolase; *pamJ*, 3-oxoacyl-synthase 2; *pamK*, 3-oxoacyl-synthase 3; *pamL*, putative sulfoacetate-CoA ligase; *pamM*, 3-oxoacyl-reductase FabG; *pamN*, putative oxidoreductase; *pamO*, 3-oxoacyl-reductase FabG; *pamR1*, response regulator protein VraR; *pamR2*, tetracycline repressor protein class E; *pamS*, carnityl-CoA dehydratase; *pamW*, antiseptic resistance protein; *pamX*, L-lysine-8-amino-7-oxononanoate aminotransferase; *pamY*, cypemycin methyltransferase (Rebets et al., 2015) [Color figure can be viewed at [wileyonlinelibrary.com](http://wileyonlinelibrary.com)]

from propionyl-CoA and the conversion of acetyl-CoA into malonyl-CoA. Moreover, talc supply resulted in the downregulation of methylmalonyl-CoA carboxyltransferase (*XNRR2\_1278*). In contrast, elevated expression of acetyl-CoA acetyltransferase (*XNRR2\_0301*, *XNRR2\_1438*, *XNRR2\_1987*), acetoacetyl-CoA synthetase (*XNRR2\_5448*) crotonyl-CoA carboxylase/reductase (*XNRR2\_0456*, *XNRR2\_5889*), methylmalonyl-CoA mutase (*XNRR2\_4665*, *XNRR2\_4666*), and methylmalonyl-CoA epimerase (*XNRR2\_1439*) was observed (Table 2).

### 3.8 | Microparticles affect intracellular CoA-ester pools during pamamycin production in *S. albus* J1074/R2

Due to the significant transcriptomic changes around the pamamycin cluster and the genes of its precursor metabolism, it

appeared interesting to assess the availability of the product precursors during the production process. We focused our analysis on 11 CoA-esters that are either directly incorporated into pamamycins, that is, succinyl-CoA, malonyl-CoA, methylmalonyl-CoA, and ethylmalonyl-CoA (Figure 1), or are connected to these building blocks. For this purpose, we acquired CoA-ester levels in a talc supplied (10 g/L) and a control culture during the major phase of production (20 hr). Interestingly, the microparticles strongly affected the CoA-ester pools (Figure 7). The level of malonyl-CoA (-48%), methylsuccinyl-CoA (-46%), crotonyl-CoA (-32%), and acetyl-CoA (-19%) was strongly decreased. In contrast, the pool of methylmalonyl-CoA was increased by more than 100%. Furthermore, the microparticles increased the level of acetoacetyl-CoA (+250%) and the pool of the isomers butyryl-/isobutyryl-CoA (+169%). The abundance of succinyl-CoA, propionyl-CoA, and ethylmalonyl-CoA remained unchanged.

Gene	Annotation	Growth (Talc)	Prod. (Talc)	Prod. (Control)
XNRR2_0221	Enoyl-CoA hydratase	0.0	5.0	0.0
XNRR2_0301	Acetyl-CoA acetyltransferase	0.0	4.3	0.0
XNRR2_0454	3-Hydroxybutyryl-CoA dehydrogenase	3.2	-1.0	0.0
XNRR2_0456	Crotonyl-CoA carboxylase/reductase	11.3	3.8	0.0
XNRR2_0457	Ethylmalonyl-CoA mutase	8.5	0.0	0.0
XNRR2_1278	Methylmalonyl-CoA decarboxylase	-3.2	-2.3	0.0
XNRR2_1304	Branched-chain amino acid aminotransferase	2.0	1.5	0.0
XNRR2_1417	Isobutyryl-CoA mutase	-1.0	1.3	0.0
XNRR2_1438	Acetyl-CoA acetyltransferase	2.9	4.3	0.0
XNRR2_1439	Methylmalonyl-CoA epimerase; ethylmalonyl-CoA epimerase	3.3	2.3	0.0
XNRR2_1452	3-Hydroxybutyryl-CoA dehydrogenase	1.0	1.3	0.0
XNRR2_1987	Acetyl-CoA acetyltransferase	3.3	3.7	0.0
XNRR2_2839	Valine dehydrogenase	1.1	2.2	0.0
XNRR2_3056	Branched-chain alpha-keto acid dehydrogenase E2	-1.7	0.0	0.0
XNRR2_3069	Branched-chain alpha-keto acid dehydrogenase E2	1.4	0.0	0.0
XNRR2_3858	Isobutyryl CoA mutase, small subunit	1.9	1.8	0.0
XNRR2_4024	Propionyl-CoA carboxylase, beta subunit	2.2	1.2	1.0
XNRR2_4211	Acetyl-/propionyl-CoA carboxylase $\alpha$ -subunit	-6.0	1.7	0.0
XNRR2_4665	Methylmalonyl-CoA mutase large subunit	1.6	2.2	0.0
XNRR2_4666	Methylmalonyl-CoA small subunit	2.2	2.3	0.0
XNRR2_5448	Acetoacetyl-CoA synthetase	8.0	5.9	0.0
XNRR2_5889	Crotonyl-CoA reductase	9.0	8.2	8.6

Note: Samples were taken from a control and a talc supplied culture (10 g/L) in SGG medium during growth (5 hr) and production (21 hr). The values correspond to  $\log_2$ -fold expression changes, considering the control during growth (5 hr) as reference. The annotation was taken from the genome (entry T02545 in KEGG) of *S. albus* (Zaburanyi et al., 2014).

## 4 | DISCUSSION

### 4.1 | Microparticle-enhanced production supports future exploration of pamamycins as lead molecules for novel antituberculosis drugs

As shown in this study, talc microparticles increased the production of pamamycins in recombinant *S. albus* J1074/R2 almost threefold to 50 mg/L, the highest titer observed so far for these polyketides (Figure 3). In this regard, the strongly improved pamamycin production by addition of talc is supposed to facilitate

future exploration of this important polyketide. As shown, only small amounts of talc were required to achieve the stimulating effect (Figures 2 and 3), so that a use of this cheap material for pamamycin production appears feasible also from a cost perspective. Remarkably, the addition of talc selectively triggered the formation of larger variants (Figure 3a), that is, Pam 635, Pam 649, and Pam 663. Due to the fact that the different derivatives apparently differ in biological activity (Lefèvre et al., 2004; Natsume, 2016), a microparticle-based process might help to selectively enrich heavier pamamycin variants in the total product spectrum with potentially other activities.

**TABLE 2** Impact of talc microparticles on the expression of genes associated to CoA-thioester metabolism in pamamycin producing *Streptomyces albus* J1074/R2

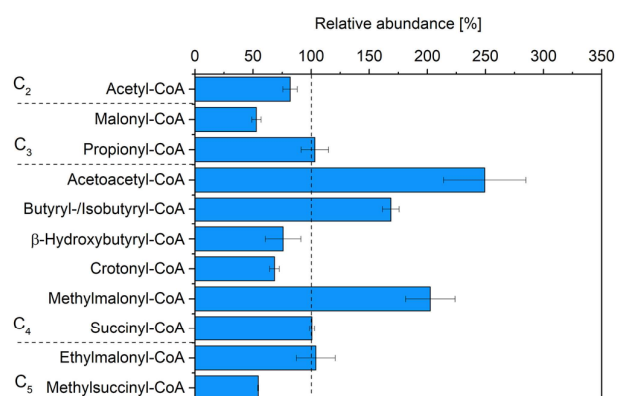


**FIGURE 7** Relative changes of intracellular CoA-ester pools in pamamycin producing *Streptomyces albus* J1074/R2 by the addition of talc microparticles (10 g/L) to the culture during the major production phase (21 hr). The intracellular availability of 11 CoA-esters, directly and indirectly linked to pamamycin assembly was assessed during the production phase (21 hr) of a talc supplied and a control culture (set to 100%, shown as dashed line) [Color figure can be viewed at [wileyonlinelibrary.com](http://wileyonlinelibrary.com)]

#### 4.2 | Pamamycin production in *S. albus* is linked to morphological development

The obtained RNA sequencing data provided a detailed insight into the dynamics of morphology development along the production process (Figures 5, 6, and S1–S7; Tables 1 and 2). As shown for the control, genes encoding morphology regulators and morphogenetic proteins were strongly activated during the shift from growth to production (Figure 8). These comprised prominent players of morphology control in Streptomyces: (a) XNRR2\_1071 (RelA) providing ppGpp, known to control morphogenetic proteins (Hesketh, Chen, Ryding, Chang, & Bibb, 2007), (b) XNRR2\_1554 (EshA) supporting ppGpp accumulation and essential for morphology development in *S. griseus* (Saito et al., 2006; van Wezel & McDowall, 2011); (c) XNRR2\_5315 (SsgA), limiting hyphae growth and branching, supporting septation, and formation of spore-like compartments (van Wezel, van der Meulen, Taal, Koerten, & Kraal, 2000b); (d) XNRR2\_2306 (Factor C protein), stimulating sporulation in submerged culture (Birkó et al., 1999; van Wezel & McDowall, 2011); (e) hydrophobic coat proteins such as chaplins and rodmins, which form the surface rodlet layer on spores (Claessen et al., 2004); and (f) XNRR2\_3527 (sigma factor BldN) controlling their expression in *S. venezuelae* (Bibb et al., 2012) and likely in *S. coelicolor* (McCormick & Flårdh, 2012; Figure 8; Table 1). There seems no doubt that this morphological development during the culture triggered the pamamycin formation (van Wezel & McDowall, 2011). It was interesting to note that the addition of talc influenced the utilization of nutrients, including phosphate and glycerol (Figure S8) and furthermore affected the amount of biomass formed (Figure 2). We cannot provide a clear conclusion

on the underlying effects at this point but would like to notice that the understanding of these effects remains an important question.

#### 4.3 | Microparticles accelerate the morphogenesis of *S. albus* toward sporulation-oriented mycelial development and cell division

Notably, the morphogenesis program was massively upregulated in the presence of the talc particles (Figure 8; Table 1). The activation was already visible during the initial growth phase and was even stronger during the later production phase. It was observed for practically all genes, which were identified as part of the morphology control cascade. We therefore conclude that the microparticles significantly speeded up the aging of the *S. albus* culture and accelerated the shift to second mycelium formation and submerged sporulation response. It appears highly likely that the enhanced pamamycin formation, including a strong overexpression of the *pam* cluster itself, was a consequence of the accelerated morphogenesis program, induced by the microparticles. It is well known that natural product formation is linked to morphological differentiation in Streptomyces (Chater, 1984), so that its perturbation can be efficiently exploited to influence antibiotic production in *S. coelicolor*, *S. lividans*, and other species (Chakraborty & Bibb, 1997; Hesketh et al., 2007; van Wezel & McDowall, 2011). Admittedly, the data did not allow to identify the specific link between morphology development, pamamycin cluster expression, and altered expression of its two regulators (Figure 6). More work will be needed in the future to resolve this in greater detail. *S. albus* possesses a range of different (mainly uncharacterized) ECF sigma factors and regulators, of which the majority was found affected by talc and gives a flavor of the complexity to be explored (Table S1).

#### 4.4 | Talc microparticles orchestrate the regulatory and metabolic network of *S. albus* to a highly efficient program for pamamycin production

We now mapped the obtained transcriptomic and metabolomic data on the carbon core network of *S. albus* to obtain a systems-view on pamamycin production and supporting pathways (Figure 9). First, specific adjustments were observed in central carbon metabolism. Genes, related to conversion of glycerol were generally upregulated during the major production phase, linked to the on-set of glycerol consumption at this point (Figure S8). This substrate shift could also explain the increased expression of the EMP pathway genes alongside the downregulation of the oxidative PP pathway at the level of 6-phosphogluconate dehydrogenase. The effects were slightly more pronounced in the presence of talc. Second, most genes encoding for enzymes of CoA-ester metabolism were upregulated by the microparticles as

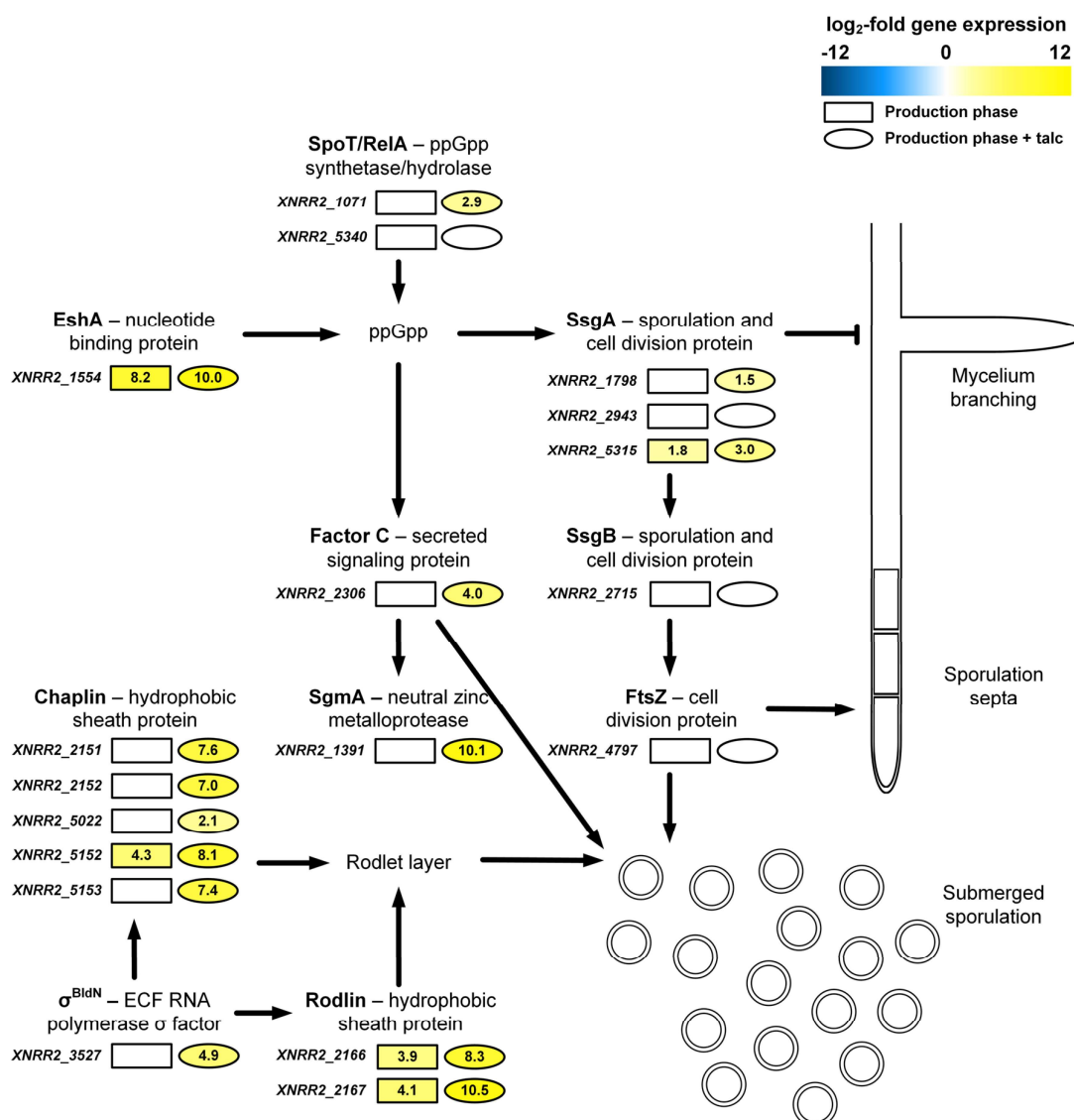


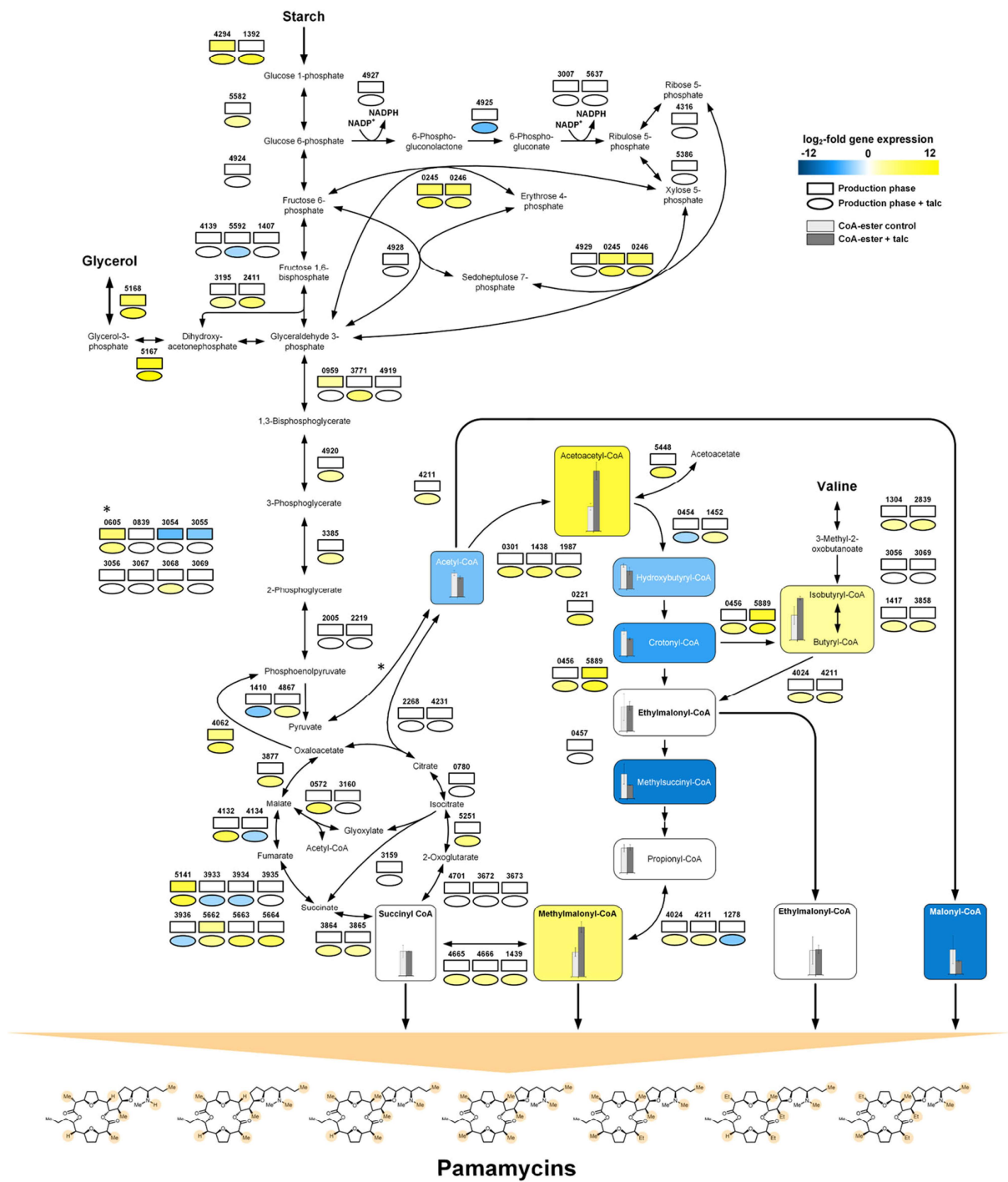
**FIGURE 8** Impact of talc microparticles on the morphogenesis of pamamycin producing *Streptomyces albus* J1074/R2 in submerged culture. The data reflect differential gene expression of morphology-associated genes during the pamamycin production phase (21) in the presence of 10 g/L talc (ellipse) and the control process without particles (rectangle). The gene expression during the growth phase (5 hr) of the control is used as a reference. The numbers denote log<sub>2</sub>-fold expression change. Further details on the displayed components of the morphology cascade are given in Table 2 [Color figure can be viewed at [wileyonlinelibrary.com](http://wileyonlinelibrary.com)]

well and resulted in a modulation of CoA-ester availability. Third, the changes in the CoA-ester metabolism had direct impact on the spectrum of pamamycins formed. It was interesting to note that the particles perturbed the ratio between malonyl-CoA, methylmalonyl-CoA, and ethylmalonyl-CoA (Figure 7). The three building blocks compete for incorporation into pamamycin. The polyketide assembly line equally accepts them as substrates, which leads to 16 pamamycin derivatives that differ in their side chains at six positions (Rebets et al., 2015). As shown, microparticle-affected cells produced more than twofold less small pamamycins (Pam 579 and Pam 593), whereas heavier

derivatives were enriched (Pam 607, Pam 621, Pam 635, Pam 649, and Pam 663).

We conclude that this was the consequence of an increased availability of the larger building block methylmalonyl-CoA, together with a reduction in the malonyl-CoA pool.

It would be interesting to further explore this link in other natural producers, which obviously differ in the spectrum of pamamycin homologues (Natsume, Yasui, Kondo, & Marumo, 1991; Natsume et al., 1995; Kozone, Chikamoto, Abe, & Natsume, 1999). Metabolic engineering of CoA-ester supply appears promising to streamline pamamycin production towards selective derivatives (Lu, Zhang, Jiang, & Bai, 2016).



## 5 | CONCLUSIONS

We could show that talc microparticles globally reprogrammed the metabolism of *S. albus*, forced an accelerated morphological development, and triggered expression of the pamamycin cluster and supporting pathways. Despite the long tradition and the great success microparticles as process agents for filamentous microbes, it has remained largely unclear how the particles actually mediate the observed effects on the molecular level (Antecka, Bizukojc, & Ledakowicz, 2016). In this regard, our insights appear of general value for further exploration and industrialization of microparticle-enhanced processes. The use of microparticles, furthermore promises to support strain engineering by suggesting novel genetic targets, given the rich response on the genomic level observed in this study. Altogether, it appears fair to state that microparticle-enhanced production is advancing into a broadly applicable strategy to tailor *Streptomyces*, *Amycolatopsis*, and other related filamentous Actinomycetes for natural product formation (e.g. rifamycin, ivermectin, etc.) and should be further explored to support their discovery, development, and industrialization (Barton et al., 2018). During the work, the streamlined *S. albus* "clean" chassis turned out to grow fast and exhibit high and stable pamamycin biosynthesis, suggesting further use (Myronovskiy et al., 2018). "Cluster-free" chassis strains appear particularly promising for selective production in the future, given the activation of native clusters observed here (Figure 5).

### ACKNOWLEDGMENTS

The work of Martin Kuhl, Lars Gläser, and Christoph Wittmann was supported by the German Ministry of Education and Research (BMBF) under Grant MyBio (FKZ 031B0344A) and the German Research Foundation (FKZ INST 256/418-1). The work of Yuri Rebets and Andriy Luzhetskyy was supported by the BMBF under Grant MyBio (FKZ 031B0344B). The work of Christian Rückert and Jörn Kalinowski acknowledge funding by the BMBF through the grant MyBio (FKZ 031B0344C). Thomas Hartsch and Namrata Sarkar was supported by the BMBF under Grant MyBio (FKZ 031B0344D). The funding bodies did not contribute to study design, data collection, analysis, and interpretation, or writing of the manuscript. Open access funding enabled and organized by Projekt DEAL.

### CONFLICT OF INTERESTS

Yuriy Rebets and Andriy Luzhetskyy have submitted a patent application to produce pamamycin in *S. albus*. The other authors declare that there are no conflict of interests.

### AUTHOR CONTRIBUTIONS

C. W. designed the project. M. K. conducted the cultures. M. K. and Y. R. performed pamamycin analysis. M. K. and L. G. performed CoA ester analysis. C. R. and J. K. performed RNA sequencing. C. R., J. K., N. S., and T. H. processed and evaluated the RNA sequencing data. M. K. and C. W. analyzed the data, drew the figures, and wrote the first draft of the manuscript. All authors commented, extended, and improved the manuscript. All authors read and approved the final version of the manuscript.

### DATA AVAILABILITY STATEMENT

The raw and processed RNA sequencing data of this article are available as MIAME-compliant datasets in Gene Expression Omnibus under the accession number GSE155008. The authors declare that all other data supporting the findings of this study are available within the article and its supplementary information file.

### ORCID

Jörn Kalinowski  <https://orcid.org/0000-0002-9052-1998>

Andriy Luzhetskyy  <https://orcid.org/0000-0001-6497-0047>

Christoph Wittmann  <http://orcid.org/0000-0002-7952-985X>

### REFERENCES

- Ahmed, Y., Rebets, Y., Estevez, M. R., Zapp, J., Myronovskiy, M., & Luzhetskyy, A. (2020). Engineering of *Streptomyces lividans* for heterologous expression of secondary metabolite gene clusters. *Microbial Cell Factories*, 19(1), 5. <https://doi.org/10.1186/s12934-020-1277-8>
- Angert, E. R. (2005). Alternatives to binary fission in bacteria. *Nature Reviews Microbiology*, 3(3), 214–224. <https://doi.org/10.1038/nrmicro1096>
- Antecka, A., Bizukojc, M., & Ledakowicz, S. (2016). Modern morphological engineering techniques for improving productivity of filamentous fungi in submerged cultures. *World Journal of Microbiology & Biotechnology*, 32(12), 193. <https://doi.org/10.1007/s11274-016-2148-7>

**FIGURE 9** Multiomics view on the effect of talc microparticles on pathways supporting pamamycin biosynthesis in *Streptomyces albus* J1074/R2 during the production phase. The boxes indicate differential gene expression of the control (rectangle) and the talc supplied process (10 g/L talc, ellipse) during the major production phase, as compared to the reference (control in growth phase, boxes indicate XNRR2 numbers). The bar charts display relative CoA-ester availability. Although CCR (XNRR2\_0456 and XNRR2\_5889) and PCC (XNRR2\_4024 and XNRR2\_4211) might be able to convert crotonyl-CoA to butyryl-CoA and butyryl-CoA to ethylmalonyl-CoA, respectively, their main activity catalyzes the formation of ethylmalonyl-CoA and propionyl-CoA, respectively (Chan, Podevels, Kevany, & Thomas, 2009). The observed changes in CoA ester metabolism were complex. Direct correlations between one particular thioester and one enzyme appeared infeasible, due to this complexity and the known promiscuity of several of the CoA-ester converting enzymes (Chan et al., 2009). However, a few conclusions could be drawn. The genes, encoding for reactions upstream of increased CoA-ester pools, that is, acetoacetyl-CoA, (iso)butyryl-CoA, and methylmalonyl-CoA were found upregulated, which suggests that the accumulation was related to an enhanced biosynthesis. In addition, the entry steps into the CoA metabolism were found massively altered. The flux from acetyl-CoA was largely redirected to form acetoacetyl-CoA, instead of malonyl-CoA. The data further suggested that the increased amount of methylmalonyl CoA was mainly derived from succinyl-CoA. The alternative ethylmalonyl CoA route appeared attenuated because major intermediates involved, that is, hydroxybutyryl-CoA, crotonyl-CoA, methylsuccinyl-CoA, were found reduced [Color figure can be viewed at [wileyonlinelibrary.com](http://wileyonlinelibrary.com)]

- Arcamone, F., Cassinelli, G., Fantini, G., Grein, A., Orezzi, P., Pol, C., & Spalla, C. (1969). Adriamycin, 14-hydroxydaimomycin, a new antitumor antibiotic from *S. Peuceetius* var. *caesius*. *Biotechnology and Bioengineering*, 11(6), 1101–1110. <https://doi.org/10.1002/bit.260110607>
- Barton, N., Horbal, L., Starck, S., Kohlstedt, M., Luzhetskyy, A., & Wittmann, C. (2018). Enabling the valorization of guaiacol-based lignin: Integrated chemical and biochemical production of cis, cis-muconic acid using metabolically engineered *Amycolatopsis* sp ATCC 39116. *Metabolic Engineering*, 45, 200–210. <https://doi.org/10.1016/j.ymben.2017.12.001>
- Bayer, E., Gugel, K., Hägele, K., Hagenmaier, H., Jessipow, S., König, W., & Zähler, H. (1972). Stoffwechselprodukte von Mikroorganismen. 98. Mitteilung. Phosphinothricin und Phosphinothricyl-Alanyl-Alanin. *Helvetica Chimica Acta*, 55(1), 224–239. <https://doi.org/10.1002/hlca.19720550126>
- Becker, J., Klopprogge, C., Schröder, H., & Wittmann, C. (2009). Metabolic engineering of the tricarboxylic acid cycle for improved lysine production by *Corynebacterium glutamicum*. *Applied and Environmental Microbiology*, 75(24), 7866–7869. <https://doi.org/10.1128/AEM.01942-09>
- Belmar-Beiny, M., & Thomas, C. (1991). Morphology and clavulanic acid production of *Streptomyces clavuligerus*: Effect of stirrer speed in batch fermentations. *Biotechnology and Bioengineering*, 37(5), 456–462. <https://doi.org/10.1002/bit.260370507>
- Bibb, M. J. (2013). Understanding and manipulating antibiotic production in Actinomycetes. *Biochemical Society Transactions*, 41(6), 1355–1364. <https://doi.org/10.1042/BST20130214>
- Bibb, M. J., Dmonkos, Á., Chandra, G., & Buttner, M. J. (2012). Expression of the chaplin and rodlin hydrophobic sheath proteins in *Streptomyces venezuelae* is controlled by  $\sigma$ BldN and a cognate anti-sigma factor, RsbN. *Molecular Microbiology*, 84(6), 1033–1049. <https://doi.org/10.1111/j.1365-2958.2012.08070.x>
- Birkó, Z., Bíalek, S., Buzás, K., Szajli, E., Traag, B. A., Medzihradsky, K. F., ... Biró, S. (2007). The secreted signaling protein factor C triggers the A-factor response regulon in *Streptomyces griseus*: Overlapping signaling routes. *Molecular & Cellular Proteomics*, 6(7), 1248–1256. <https://doi.org/10.1074/mcp.M600367-MCP200>
- Birkó, Z., Sümegi, A., Vinnai, A., Van Wezel, G., Szeszák, F., Vitális, S., ... Biró, S. (1999). Characterization of the gene for factor C, an extracellular signal protein involved in morphological differentiation of *Streptomyces griseus*. *Microbiology*, 145(9), 2245–2253. <https://doi.org/10.1099/00221287-145-9-2245>
- Campbell, W. C., Fisher, M. H., Stapley, E. O., Albers-Schönberg, G., & Jacob, T. A. (1983). Ivermectin: A potent new antiparasitic agent. *Science*, 221(4613), 823–828. <https://doi.org/10.1126/science.6308762>
- Chakraborty, R., & Bibb, M. (1997). The ppGpp synthetase gene (*relA*) of *Streptomyces coelicolor* A3 (2) plays a conditional role in antibiotic production and morphological differentiation. *Journal of Bacteriology*, 179(18), 5854–5861. <https://doi.org/10.1128/jb.179.18.5854-5861.1997>
- Chan, Y. A., Podevels, A. M., Kevany, B. M., & Thomas, M. G. (2009). Biosynthesis of polyketide synthase extender units. *Natural Product Reports*, 26(1), 90–114. <https://doi.org/10.1039/b801658p>
- Chater, K. F. (1984). Morphological and physiological differentiation in *Streptomyces*. *Microbial Development*, 16, 89–115. <https://doi.org/10.1101/0.89-115>
- Chater, K. F., & Losick, R. (1997). Mycelial life style of *Streptomyces coelicolor* A3 (2) and its relatives, *Multicellular and interactive behavior of bacteria: In nature, industry and the laboratory* (pp. 149–182). Oxford, UK: Oxford University Press.
- Claessen, D., Stokroos, I., Deelstra, H. J., Penninga, N. A., Bormann, C., Salas, J. A., ... Wösten, H. A. (2004). The formation of the rodlet layer of *Streptomyces* is the result of the interplay between rodlines and chaplins. *Molecular Microbiology*, 53(2), 433–443. <https://doi.org/10.1111/j.1365-2958.2004.04143.x>
- van Dissel, D., Claessen, D., & van Wezel, G. P. (2014). Morphogenesis of *Streptomyces* in submerged cultures, *Advances in Applied Microbiology* (89, pp. 1–45). Amsterdam, The Netherlands: Elsevier.
- Driouch, H., Hänsch, R., Wucherpfnig, T., Krull, R., & Wittmann, C. (2012). Improved enzyme production by bio-pellets of *Aspergillus niger*: Targeted morphology engineering using titanate microparticles. *Biotechnology and Bioengineering*, 109(2), 462–471. <https://doi.org/10.1002/bit.23313>
- Driouch, H., Roth, A., Dersch, P., & Wittmann, C. (2010). Filamentous fungi in good shape: Microparticles for tailor-made fungal morphology and enhanced enzyme production. *Bioengineered Bugs*, 2(2), 100–104. <https://doi.org/10.4161/bbug.2.2.13757>
- Driouch, H., Sommer, B., & Wittmann, C. (2010). Morphology engineering of *Aspergillus niger* for improved enzyme production. *Biotechnology and Bioengineering*, 105(6), 1058–1068. <https://doi.org/10.1002/bit.22614>
- Ehrlich, J., Bartz, Q. R., Smith, R. M., Joslyn, D. A., & Burkholder, P. R. (1947). Chloromycetin, a new antibiotic from a soil actinomycete. *Science*, 106(2757), 417. <https://doi.org/10.1126/science.106.2757.417>
- Etschmann, M. M., Huth, I., Walisko, R., Schuster, J., Krull, R., Holtmann, D., ... Schrader, J. (2015). Improving 2-phenylethanol and 6-pentyl- $\alpha$ -pyrone production with fungi by microparticle-enhanced cultivation (MPEC). *Yeast*, 32(1), 145–157. <https://doi.org/10.1002/yea.3022>
- Flärth, K., Kindlay, K. C., & Chater, K. F. (1999). Association of early sporulation genes with suggested developmental decision points in *Streptomyces coelicolor* A3(2). *Microbiology*, 145(9), 2229–2243.
- Glazebrook, M. A., Vining, L. C., & White, R. L. (1992). Growth morphology of *Streptomyces akiyoshiensis* in submerged culture: Influence of pH, inoculum, and nutrients. *Canadian Journal of Microbiology*, 38(2), 98–103. <https://doi.org/10.1139/m92-016>
- Gläser, L., Kuhl, M., Jovanovic, S., Fritz, M., Vögeli, B., Erb, T., ... Wittmann, C. (2020). A common approach for absolute quantification of short chain CoA thioesters in industrially relevant gram-positive and gram-negative prokaryotic and eukaryotic microbes. *Microbial Cell Factories*, 19, 160.
- Hanquet, G., Salom-Roig, X., & Lanners, S. (2016). New insights into the synthesis and biological activity of the pamamycin macrodiolides. *Chimia*, 70(1-2), 20–28. <https://doi.org/10.2533/chimia.2016.20>
- Hesketh, A., Chen, W. J., Ryding, J., Chang, S., & Bibb, M. (2007). The global role of ppGpp synthesis in morphological differentiation and antibiotic production in *Streptomyces coelicolor* A3 (2). *Genome Biology*, 8(8), R161. <https://doi.org/10.1186/gb-2007-8-8-r161>
- Hilker, R., Stadermann, K. B., Doppmeier, D., Kalinowski, J., Stoye, J., Straube, J., ... Goesmann, A. (2014). ReadXplorer—visualization and analysis of mapped sequences. *Bioinformatics*, 30(16), 2247–2254. <https://doi.org/10.1093/bioinformatics/btu205>
- Holtmann, D., Vernen, F., Müller, J., Kaden, D., Risse, J. M., Friehs, K., ... Schrader, J. (2017). Effects of particle addition to *Streptomyces* cultivations to optimize the production of actinorhodin and streptavidin. *Sustainable Chemistry and Pharmacy*, 5, 67–71. <https://doi.org/10.1016/j.scp.2016.09.001>
- Horbal, L., Marques, F., Nadmid, S., Mendes, M. V., & Luzhetskyy, A. (2018). Secondary metabolites overproduction through transcriptional gene cluster refactoring. *Metabolic Engineering*, 49, 299–315. <https://doi.org/10.1016/j.ymben.2018.09.010>
- Jonsbu, E., McIntyre, M., & Nielsen, J. (2002). The influence of carbon sources and morphology on nystatin production by *Streptomyces noursei*. *Journal of Biotechnology*, 95(2), 133–144. [https://doi.org/10.1016/s0168-1656\(02\)00003-2](https://doi.org/10.1016/s0168-1656(02)00003-2)
- Juarez, M., Scholnik-Cabrera, A., & Dueñas-Gonzalez, A. (2018). The multitargeted drug ivermectin: From an antiparasitic agent to a repositioned cancer drug. *American Journal of Cancer Research*, 8(2), 317–331.
- Kallifidas, D., Jiang, G., Ding, Y., & Luesch, H. (2018). Rational engineering of *Streptomyces albus* J1074 for the overexpression of secondary metabolite gene clusters. *Microbial Cell Factories*, 17(1), 25. <https://doi.org/10.1186/s12934-018-0874-2>
- Kato, J.-y., Suzuki, A., Yamazaki, H., Ohnishi, Y., & Horinouchi, S. (2002). Control by A-factor of a metalloendopeptidase gene involved in aerial mycelium formation in *Streptomyces griseus*.

- Journal of Bacteriology*, 184(21), 6016–6025. <https://doi.org/10.1128/JB.184.21.6016-6025.2002>
- Kaup, B. A., Ehrich, K., Pescheck, M., & Schrader, J. (2008). Microparticle-enhanced cultivation of filamentous microorganisms: Increased chloroperoxidase formation by *Caldariomyces fumago* as an example. *Biotechnology and Bioengineering*, 99(3), 491–498. <https://doi.org/10.1002/bit.21713>
- Kieser, T., Bibb, M. J., Buttner, M. J., Chater, K. F., & Hopwood, D. A. (2000). An introduction to *Streptomyces*. *Practical Streptomyces genetics* (p. 291). Norwich, UK: John Innes Foundation.
- Koebisch, I., Overbeck, J., Piepmeyer, S., Meschke, H., & Schrepff, H. (2009). A molecular key for building hyphae aggregates: The role of the newly identified *Streptomyces* protein HyaS. *Microbial Biotechnology*, 2(3), 343–360. <https://doi.org/10.1111/j.1751-7915.2009.00093.x>
- Kozone, I., Chikamoto, N., Abe, H., & Natsume, M. (1999). De-N-methylpamamycin-593A and B, new pamamycin derivatives isolated from *Streptomyces alboniger*. *Journal of Antibiotics*, 52(3), 329–331. <https://doi.org/10.7164/antibiotics.52.329>
- Krull, R., Wucherpfennig, T., Esfandabadi, M. E., Walisko, R., Melzer, G., Hempel, D. C., ... Wittmann, C. (2013). Characterization and control of fungal morphology for improved production performance in biotechnology. *Journal of Biotechnology*, 163(2), 112–123. <https://doi.org/10.1016/j.jbiotec.2012.06.024>
- Langmead, B., & Salzberg, S. L. (2012). Fast gapped-read alignment with Bowtie 2. *Nature Methods*, 9(4), 357–359. <https://doi.org/10.1038/nmeth.1923>
- Lechevalier, H., Acker, R. F., Corke, C. T., Haenseler, C. M., & Waksman, S. A. (1953). Candicidin, a new antifungal antibiotic. *Mycologia*, 45(2), 155–171. <https://doi.org/10.1080/00275514.1953.12024259>
- Lefèvre, P., Peirs, P., Braibant, M., Fauville-Dufaux, M., Vanhoof, R., Huygen, K., ... Content, J. (2004). Antimycobacterial activity of synthetic pamamycins. *Journal of Antimicrobial Chemotherapy*, 54(4), 824–827. <https://doi.org/10.1093/jac/dkh402>
- Liu, X., Tang, J., Wang, L., & Liu, R. (2019). Mechanism of CuO nanoparticles on stimulating production of actinorhodin in *Streptomyces coelicolor* by transcriptional analysis. *Scientific Reports*, 9(1), 11253. <https://doi.org/10.1038/s41598-019-46833-1>
- Lopatniuk, M., Myronovskiy, M., Nottbrock, A., Busche, T., Kalinowski, J., Ostash, B., ... Luzhetskyy, A. (2019). Effect of “ribosome engineering” on the transcription level and production of *S. albus* indigenous secondary metabolites. *Applied Microbiology and Biotechnology*, 103, 7097–7110. <https://doi.org/10.1007/s00253-019-10005-y>
- Love, M. I., Huber, W., & Anders, S. (2014). Moderated estimation of fold change and dispersion for RNA-seq data with DESeq2. *Genome Biology*, 15(12), 550. <https://doi.org/10.1186/s13059-014-0550-8>
- Lu, C., Zhang, X., Jiang, M., & Bai, L. (2016). Enhanced salinomycin production by adjusting the supply of polyketide extender units in *Streptomyces albus*. *Metabolic Engineering*, 35, 129–137. <https://doi.org/10.1016/j.ymben.2016.02.012>
- Martin, S. M., & Bushell, M. E. (1996). Effect of hyphal micromorphology on bioreactor performance of antibiotic-producing *Saccharopolyspora erythraea* cultures. *Microbiology*, 142(7), 1783–1788. <https://doi.org/10.1099/13500872-142-7-1783>
- McCormick, J. R., & Flårdh, K. (2012). Signals and regulators that govern *Streptomyces* development. *FEMS Microbiology Reviews*, 36(1), 206–231. <https://doi.org/10.1111/j.1574-6976.2011.00317.x>
- Myronovskiy, M., Rosenkranzer, B., Nadmid, S., Pujic, P., Normand, P., & Luzhetskyy, A. (2018). Generation of a cluster-free *Streptomyces albus* chassis strains for improved heterologous expression of secondary metabolite clusters. *Metabolic Engineering*, 49, 316–324. <https://doi.org/10.1016/j.ymben.2018.09.004>
- Natsume, M. (2016). Studies on bioactive natural products involved in the growth and morphological differentiation of microorganisms. *Journal of Pesticide Science*, 41(3), 96–101. <https://doi.org/10.1584/jpestics.116-03>
- Natsume, M., Tazawa, J., Yagi, K., Abe, H., Kondo, S., & Marumo, S. (1995). Structure-activity relationship of pamamycins: Effects of alkyl substituents. *The Journal of Antibiotics*, 48(10), 1159–1164. <https://doi.org/10.1038/ja.2008.118>
- Natsume, M., Yasui, K., Kondo, S., & Marumo, S. (1991). The structures of four new pamamycin homologues isolated from *Streptomyces alboniger*. *Tetrahedron Letters*, 32(26), 3087–3090. [https://doi.org/10.1016/0040-4039\(91\)80696-4](https://doi.org/10.1016/0040-4039(91)80696-4)
- O’Cleirigh, C., Casey, J. T., Walsh, P. K., & O’Shea, D. G. (2005). Morphological engineering of *Streptomyces hygroscopicus* var. *geldanus*: Regulation of pellet morphology through manipulation of broth viscosity. *Applied Microbiology and Biotechnology*, 68(3), 305–310. <https://doi.org/10.1007/s00253-004-1883-0>
- R Core Team (2014). *R: A language and environment for statistical computing*. Vienna, Austria: R Foundation for Statistical Computing.
- Rebets, Y., Brötz, E., Manderscheid, N., Tokovenko, B., Myronovskiy, M., Metz, P., ... Luzhetskyy, A. (2015). Insights into the pamamycin biosynthesis. *Angewandte Chemie-International Edition*, 127(7), 2309–2313. <https://doi.org/10.1002/anie.201408901>
- Ren, X.-D., Xu, Y.-J., Zeng, X., Chen, X.-S., Tang, L., & Mao, Z.-G. (2015). Microparticle-enhanced production of  $\epsilon$ -poly-L-lysine in fed-batch fermentation. *RSC Advances*, 5(100), 82138–82143. <https://doi.org/10.1039/C5RA14319E>
- Saito, N., Xu, J., Hosaka, T., Okamoto, S., Aoki, H., Bibb, M. J., & Ochi, K. (2006). EshA accentuates ppGpp accumulation and is conditionally required for antibiotic production in *Streptomyces coelicolor* A3(2). *Journal of Bacteriology*, 188(13), 4952–4961. <https://doi.org/10.1128/JB.00343-06>
- Santamaría, R., & Pierre, P. (2012). Voronto: Mapper for expression data to ontologies. *Bioinformatics*, 28(17), 2281–2282. <https://doi.org/10.1093/bioinformatics/bts428>
- Schneider, C. A., Rasband, W. S., & Eliceiri, K. W. (2012). NIH Image to ImageJ: 25 years of image analysis. *Nature Methods*, 9(7), 671–675. <https://doi.org/10.1038/nmeth.2089>
- Sehgal, S. N., Baker, H., & Vézina, C. (1975). Rapamycin (AY-22, 989), a new antifungal antibiotic. II. Fermentation, isolation and characterization. *The Journal of Antibiotics*, 28(10), 727–732. <https://doi.org/10.7164/antibiotics.28.727>
- Traag, B. A., & van Wezel, G. P. (2008). The SsgA-like proteins in actinomycetes: Small proteins up to a big task. *Antonie Van Leeuwenhoek*, 94(1), 85–97. <https://doi.org/10.1007/s10482-008-9225-3>
- Vézina, C., Kudelski, A., & Sehgal, S. (1975). Rapamycin (AY-22, 989), a new antifungal antibiotic. I. Taxonomy of the producing streptomycete and isolation of the active principle. *The Journal of antibiotics*, 28(10), 721–726. <https://doi.org/10.7164/antibiotics.28.721>
- Walisko, R., Krull, R., Schrader, J., & Wittmann, C. (2012). Microparticle based morphology engineering of filamentous microorganisms for industrial bio-production. *Biotechnology Letters*, 34(11), 1975–1982. <https://doi.org/10.1007/s10529-012-0997-1>
- Walisko, J., Vernen, F., Pommerehne, K., Richter, G., Terfehr, J., Kaden, D., ... Krull, R. (2017). Particle-based production of antibiotic rebeccamycin with *Lechevalieria aerocolonigenes*. *Process Biochemistry*, 53, 1–9. <https://doi.org/10.1016/j.procbio.2016.11.017>
- Wang, H., Zhao, G., & Ding, X. (2017). Morphology engineering of *Streptomyces coelicolor* M145 by sub-inhibitory concentrations of antibiotics. *Scientific Reports*, 7(1), 13226. <https://doi.org/10.1038/s41598-017-13493-y>
- Warnes, M. G. R., Bolker, B., Bonebakker, L., & Gentleman, R. (2016). *Package ‘gplots’*. Various R programming tools for plotting data.
- van Wezel, G. P., Krabben, P., Traag, B. A., Keijser, B. J., Kerste, R., Vijgenboom, E., ... Kraal, B. (2006). Unlocking *Streptomyces* spp. for use as sustainable industrial production platforms by morphological engineering. *Applied and Environmental Microbiology*, 72(8), 5283–5288. <https://doi.org/10.1128/AEM.00808-06>
- van Wezel, G. P., & McDowall, K. J. (2011). The regulation of the secondary metabolism of *Streptomyces*: New links and experimental

- advances. *Natural Product Reports*, 28(7), 1311–1333. <https://doi.org/10.1039/c1np00003a>
- van Wezel, G. P., van der Meulen, J., Kawamoto, S., Luiten, R. G., Koerten, H. K., & Kraal, B. (2000a). *ssgA* is essential for sporulation of *Streptomyces coelicolor* A3 (2) and affects hyphal development by stimulating septum formation. *Journal of Bacteriology*, 182(20), 5653–5662.
- van Wezel, G. P., van der Meulen, J., Taal, E., Koerten, H., & Kraal, B. (2000b). Effects of increased and deregulated expression of cell division genes on the morphology and on antibiotic production of *Streptomyces*. *Antonie Van Leeuwenhoek*, 78(3-4), 269–276. <https://doi.org/10.1023/a:1010267708249>
- Xia, X., Lin, S., Xia, X.-X., Cong, F.-S., & Zhong, J.-J. (2014). Significance of agitation-induced shear stress on mycelium morphology and lavendamycin production by engineered *Streptomyces flocculus*. *Applied Microbiology and Biotechnology*, 98(10), 4399–4407. <https://doi.org/10.1007/s00253-014-5555-4>
- Xu, H., Chater, K. F., Deng, Z., & Tao, M. (2008). A cellulose synthase-like protein involved in hyphal tip growth and morphological differentiation in *Streptomyces*. *Journal of Bacteriology*, 190(14), 4971–4978. <https://doi.org/10.1128/JB.01849-07>
- Zaburannyi, N., Rabyk, M., Ostash, B., Fedorenko, V., & Luzhetskyy, A. (2014). Insights into naturally minimised *Streptomyces albus* J1074 genome. *BMC Genomics*, 15(1), 97.
- Zhang, Y., Wang, M., Tian, J., Liu, J., Guo, Z., Tang, W., & Chen, Y. (2020). Activation of paulomycin production by exogenous  $\gamma$ -butyrolactone signaling molecules in *Streptomyces albidoflavus*. *Applied Microbiology and Biotechnology*, 104(1), J1074–J1705. <https://doi.org/10.1007/s00253-019-10329-9>

#### SUPPORTING INFORMATION

Additional supporting information may be found online in the Supporting Information section.

**How to cite this article:** Kuhl M, Gläser L, Rebets Y, et al. Microparticles globally reprogram *Streptomyces albus* toward accelerated morphogenesis, streamlined carbon core metabolism, and enhanced production of the antituberculosis polyketide pamamycin. *Biotechnology and Bioengineering*. 2020;117:3858–3875. <https://doi.org/10.1002/bit.27537>

## 4 General Discussion

### 4.1 A common approach for quantification of intracellular CoA thioesters applicable in broad biotechnological application fields

CoA thioesters play an important role in metabolism as cofactors, participating in 5% of all enzymatic reactions (Peter et al., 2016). Simultaneously, they serve as precursors for various biotechnology products. In the past, different methods have been investigated on the analysis of intracellular CoA thioester in microbial cells, plant and animal tissues, specifically elaborated for the given question and condition (Gläser et al., 2020). These methods differ in complexity of sampling, extraction solutions, as well as the latter analysis, and data processing. Precise and reproducible results in metabolomics generally demand for the utilization of quick and simple extraction tools, to avoid excessive demands and possible sources of errors (Liu et al., 2019).

In this work, a precise method for the quantification of intracellular CoA thioesters using liquid-chromatography mass spectrometry in microbial cells was established. This common approach is characterized by an easy handling protocol and high reproducibility, using an isotopic labeled internal  $^{13}\text{C}$ -standard for accurate absolute quantification. In general, the method was able to analyze ten different short-chain CoA thioesters and free coenzyme A. Additionally, CoA-CoA dimers (CoASSCoA) as omnipresent side product due to its highly reactive free thiol group was identified. Using a synthetic standard, it was possible to separate all CoA thioesters within 10 minutes of separation time in a linear range covering 5-8 orders of magnitude, down to picomolar level. Even challenging isobaric derivatives, such as succinyl-CoA and methylmalonyl-CoA, as well as methylsuccinyl-CoA and ethylmalonyl-CoA were separated successfully. Initial obstacles concerning high salt concentrations in some samples using media with elevated ionic strength, resulted in dramatic loss of separation quality and durability of the column. Detailed optimization, especially regarding column geometry, enabled sustainable and stable analysis, and provided excellent reproducibility over time without quality losses. The use of tailor-made internal CoA thioester  $^{13}\text{C}$ -standards for each individual organism, allowed to compensate for eventual metabolite losses during sample processing.

As shown, the optimized workflow was applied to gram-positive *Corynebacterium glutamicum* (Kind et al., 2013) and *Streptomyces albus* (Rebets et al., 2015), gram-negative *Pseudomonas putida* (Borrero-de Acuna et al., 2014), and the eukaryotic yeast *Yarrowia lipolytica* (Gemperlein et al., 2019). Hereby, the established method enabled robust extraction and quantification of intracellular short-chain CoA thioesters in all organisms, whereby each microbe exhibited a different spectrum.

In summary, the developed method provides a uniform extraction protocol for up to eleven short-chain CoA thioesters. It appears promising to extend this method for the analysis of other CoA thioesters. Conceivable would be aromatic derived thioesters (Ismail & Gescher, 2012) and long-chain CoA thioesters from fatty acid metabolism (Fujita et al., 2007). Additionally, it appears promising to consider the applicability of the obtained extracts for the analysis of other metabolites, including cofactors such as NADPH, ATP, organic acids, and amino acids. Eventually only few changes would have to be made during adaptation (Bolten et al., 2007; Bordag et al., 2016). This could yield a single method applicable for the determination of vast intracellular metabolites besides CoA thioesters to gain more detailed insights into cellular metabolism through a single metabolite extract.

#### **4.2 The ethylmalonyl-CoA pool is a key node to derive heavy pamamycin derivatives in *Streptomyces albus* J1074/R2**

In this work, a chemically defined minimal medium with mannitol as sole-carbon source was selected as basis for systems biology analysis of *Streptomyces albus* J1074 and its heterologous pamamycin producing successor J1074/R2. In addition to the analysis of growth and production performance, the absolute quantification of intracellular CoA thioester levels appeared promising for first analyzes.

At first glance, the producer J1074/R2 revealed a growth-correlated accumulation of pamamycin derivatives, where the mid-weight pamamycins 607 and 621 made up the main part. The heavy weight pamamycins 635 and 649 represented only 4% of the total pamamycin spectrum, and pamamycin 663 was even fully absent. Consequently, the quantification of the pamamycin precursors (CoA thioesters) appeared interesting to obtain more insight into the biosynthesis of the different derivatives.

As shown, the pamamycin producer J1074/R2 exhibited up to ten-fold decreased levels of intermediates of the ethylmalonyl-CoA pathway, in particular  $\beta$ -hydroxybutyryl-CoA, methylsuccinyl-CoA, and crotonyl-CoA in comparison to the non-producing J1074, respectively. Interestingly, ethylmalonyl-CoA as the essential building block to produce the heavy pamamycin derivatives 635, 649, and 663 was dramatically reduced in the pamamycin producer. It was interesting to note that the ratio of malonyl-CoA, methylmalonyl-CoA, and ethylmalonyl-CoA was perturbed from 100:40:10 in the wildtype to 100:30:1 in the producer J1074/R2. The formation of pamamycin in the producer host clearly consumed more building blocks than supplied from central metabolism, indicating a bottleneck of ethylmalonyl-CoA for the biosynthesis of these poorly explored heavy pamamycin derivatives. Furthermore, the increased levels of malonyl-CoA

consequently promoted the synthesis of smaller pamamycins, which can be formed without any contribution of ethylmalonyl-CoA.

Since the discovery of pamamycins, only few studies described the biological activity of the different pamamycins (Hashimoto et al., 2003; Kozone et al., 2008; Hashimoto et al., 2011), antibacterial activity against *Mycobacteria* (Lefevre et al., 2004), and *Bacilli* (Natsume, 1999). Detailed data is mainly available for pamamycin 607 and 621, the dominant derivatives in most studies. So far, the inaccessibility of heavy pamamycin derivatives has prevented a closer exploration of their biological activity profiles. At this point, manipulation of ethylmalonyl-CoA availability appears a promising strategy for increased production of heavy pamamycin derivatives.

### **4.3 Systems biology identifies the amino acid L-valine as trigger towards heavy pamamycin derivatives**

Amino acids are an additive for the production of secondary metabolites in *Streptomyces* (Sprusansky et al., 2005; Barka et al., 2016). Therefore, a supplementation of the used minimal medium with all 20 proteinogenic amino acids was studied. Notably, the addition of L-valine (3 mM) nearly tripled pamamycin production to 3.5 mg L<sup>-1</sup>. Interestingly, the distribution of pamamycin derivatives was shifted towards more heavy derivatives, which made up about 25% of the mixture. A more detailed analysis revealed mixed side effects caused by the feeding of L-valine, including impaired growth, suppressed pamamycin production until L-valine depletion, but a subsequent phase with boosted production of heavy pamamycins.

Combining the quantification of intracellular CoA thioesters and global transcription profiling revealed dynamic effects of L-valine on transcriptome and precursor supply, providing first sprawling insights into the cellular background of pamamycin biosynthesis. The impaired growth caused by L-valine was clearly found as result of decreased gene expression in primary metabolism including mannitol PTS-mediated uptake system. The suppressed pamamycin production during L-valine degradation observed, was not consistent with the increased gene expression level of the pamamycin gene cluster. This contrast clearly indicates a L-valine mediated post-transcriptional control apparently related to the nutrient status.

Regarding other secondary metabolism, the gene expression of various secondary metabolite clusters was found decreased. This coherent impaired growth and limited biosynthesis of secondary metabolites affected by the presence of L-valine was also observed in the production of spiramycin (Lounes et al., 1995) and pikromycin (Yi et al., 2018) where excess of this amino acid reduced cell growth and production. This response indicates L-valine as a critical signaling molecule influencing growth, morphology and associated secondary metabolism. A connection between the cellular regulation and the presence of the BCAAs is imaginable through the stringent

response (Fang & Bauer, 2018). This physiological process gets mediated by the alarmone molecules guanosine 5'-diphosphate,3'-diphosphate (ppGpp) and guanosine 5'-triphosphate,3'-diphosphate (pppGpp), via the two enzymes RelA and SpoT (Fang & Bauer, 2018). This system is important for nutrient sensing, specially nitrogen starvation (Strauch et al., 1991; Hesketh et al., 2007; van Wezel & McDowall, 2011) and was also shown to affect secondary metabolism and morphology in other *Streptomyces* strains (Ochi, 1987; Saito et al., 2006; Hesketh et al., 2007). Furthermore, studies in *Rhodobacter capsulatus* also revealed a direct binding of the BCAAs to these regulatory enzymes (Fang & Bauer, 2018), indicating a close connection between the presence of those amino acids and the complex regulatory networks behind secondary metabolism in *Streptomyces*.

The determination of intracellular CoA thioester levels then revealed the impact of L-valine on CoA metabolism. Besides a nearly 100-fold increased level of iso-/butyryl-CoA, CoA thioesters participating in the ethylmalonyl-CoA pathway were increased up to 30-fold, revealing even higher levels than in the control after L-valine depletion. Indisputable is the close connection between L-valine degradation and the increased amount of ethylmalonyl-CoA observed here. Key enzymes here are isobutyryl-CoA mutase (XNRR2\_1417) and acetyl-/propionyl-CoA carboxylase (XNRR2\_4211), presumably forming a bypass to common L-valine degradation towards butyryl-CoA and subsequent carboxylation to ethylmalonyl-CoA. Both genes were increased in expression level when L-valine was supplemented. Previous studies in *S. cinnamonensis* identified isobutyryl-CoA mutase as key enzyme during L-valine degradation towards methylmalonyl-CoA and subsequent polyketide biosynthesis (Vrijbloed et al., 1999). The high concentration of iso-/butyryl-CoA, even hours after L-valine depletion, served as continuous reservoir to supply the respective precursors for reinforced pamamycin production. This “memory effect” was true for 3-hydroxybutyryl-CoA as well.

#### **4.4 BkdR as global player in the regulation of secondary metabolism**

The degradation of all three branched-chain amino acids includes a common step, catalyzed by the branched-chain amino acid dehydrogenase complex (BCDH complex). This multienzyme complex converts the respective  $\alpha$ -ketoacid after deamination to a CoA thioester (Li et al., 2009; Stirrett et al., 2009; Yi et al., 2018; Neinast et al., 2019). As shown in this work, the addition of L-valine had not only beneficial impacts, but also repressed growth and perturbed pamamycin production until the amino acid was depleted. A *bkdR* deletion mutant, lacking the key regulator of the BCDH complex, exhibited decoupled pamamycin production, independent from the nutrient status. Simultaneously, growth of the mutant was substantially improved, and even enabled pamamycin production after substrate depletion during the stationary phase. Approximately, 30%

of total pamamycin was produced within this newly observed production phase, which particularly stands out due to the extremely high production (~55%) of heavy pamamycins derivatives.

An earlier study already mentioned, that BkdR probably has a more extensive influence on the primary and secondary metabolism, especially on the shift between vegetative and aerial growth (Sprusansky et al., 2005). The results shown in this work clearly support this thesis. The repressing effects of L-valine on growth and sugar uptake were diminished in the mutant. Furthermore, the impact of L-valine on genes participating in its degradation was similar in both strains, reflecting a minor influence of BkdR on BCAA catabolism itself, then previously expected. All in all, the data shown here indicate a more global role of BkdR in *Streptomyces albus*, apart from its originally estimated function as a regulator of the BCDH complex. So far, however, no precise statement can be made about the exact function of this regulator. More detailed analyzes appear to be useful in the future.

## 5 Conclusion and Outlook

Despite the ongoing discovery of new antibiotics and improvements in production, the number of new antibiotics approved for medical use has decreased steadily over the past decades (Ventola, 2015). The genus of *Streptomyces* is one of the most relevant groups of biotechnologically used bacteria (Kitani et al., 2011; Barka et al., 2016). The huge repertoire of biologically active metabolites encoded in their genome gives us a spark of hope in the fight against the steadily increasing antibiotic resistance crisis (Ventola, 2015; Barka et al., 2016). In addition to the discovery of new substances, the increase of production titers remains important to provide sufficient amounts (Bekiesch et al., 2016). A better understanding of the cellular processes around primary and secondary metabolism appears crucial superior production hosts (Hwang et al., 2014).

This study focused on systems biology of *Streptomyces albus* to produce the antituberculosis polyketide pamamycin, a family of secondary metabolites being naturally produced in a mixture of different homologues. At first, a common approach for the absolute quantification of intracellular CoA thioester, precursors of pamamycins, using liquid chromatography-mass spectrometry was successfully established. Due to the high relevance of CoA thioesters as crucial precursors for biotechnological products, the cross-species applicability to other biotechnological organisms was verified. The broad application range of the approach appears useful as a standardized workflow for the precise quantification of CoA thioester also in other studies. Here, first experiments revealed only marginal production of the heavy weight pamamycin derivatives 635, 649, and 663. The comparison of J1074/R2 with the wildtype-like non-producer J1074 on CoA thioester levels, revealed limited ethylmalonyl-CoA availability as major reason for the that hindered production of heavy pamamycin derivatives. Beneficially, the branched-chain amino acid L-valine could be

identified as suitable additive to trigger the formation of heavy pamamycins. The integration of data from metabolome and transcriptome provided important insights into the regulatory mechanisms, affecting growth and production performance. While excess L-valine suppressed growth and perturbed pamamycin production start, however, the degradation intermediates built a persistent memory effect probably providing pamamycin precursor for a subsequent boosted production. Nevertheless, the set-up appeared suboptimal to some extent, therefore a knockout of the gene *bkdR* encoding a transcriptional regulator of the BCDH complex broke the unknown regulatory interactions. This superior producer exhibited a decoupled pamamycin production from nutrient status, improved growth performance and further optimized the production of the rare heavy pamamycin homologues. Again, the strategy of systems level analysis combining metabolome and transcriptome data revealed interesting insights into potential regulatory mechanisms.

Altogether, the data obtained in this work offers numerous interesting approaches and insights into the cellular behavior of *Streptomyces albus* that seem also helpful in the production of other restricted secondary metabolites, far beyond the production of pamamycins.

## 6 References

- Abbas, A. S., & Edwards, C. (1990). Effects of metals on *Streptomyces coelicolor* growth and actinorhodin production. *Applied and environmental microbiology*, 56(3), 675-680. doi:10.1128/AEM.56.3.675-680.1990
- Armando, J. W., Boghigian, B. A., & Pfeifer, B. A. (2012). LC-MS/MS quantification of short-chain acyl-CoA's in *Escherichia coli* demonstrates versatile propionyl-CoA synthetase substrate specificity. *Letters in applied microbiology*, 54(2), 140-148. doi:10.1111/j.1472-765X.2011.03184.x
- Baltz, R. H. (2006). Marcel Faber Roundtable: Is our antibiotic pipeline unproductive because of starvation, constipation or lack of inspiration? *Journal of Industrial Microbiology and Biotechnology*, 33(7), 507-513. doi:10.1007/s10295-005-0077-9
- Baltz, R. H. (2010). *Streptomyces* and *Saccharopolyspora* hosts for heterologous expression of secondary metabolite gene clusters. *Journal of industrial microbiology & biotechnology*, 37(8), 759-772. doi:10.1007/s10295-010-0730-9
- Barka, E. A., Vatsa, P., Sanchez, L., Gaveau-Vaillant, N., Jacquard, C., Meier-Kolthoff, J. P., Klenk, H. P., Clement, C., Ouhdouch, Y., & van Wezel, G. P. (2016). Taxonomy, physiology, and natural products of *Actinobacteria*. *Microbiology and molecular biology reviews : MMBR*, 80(1), 1-43. doi:10.1128/MMBR.00019-15
- Becker, J., & Wittmann, C. (2015). Advanced biotechnology: metabolically engineered cells for the bio-based production of chemicals and fuels, materials, and health-care products. *Angewandte Chemie*, 54(11), 3328-3350. doi:10.1002/anie.201409033
- Bekiesch, P., Basitta, P., & Apel, A. K. (2016). Challenges in the heterologous production of antibiotics in *Streptomyces*. *Archiv der Pharmazie*, 349(8), 594-601. doi:10.1002/ardp.201600058
- Bentley, S. D., Chater, K. F., Cerdeno-Tarraga, A. M., Challis, G. L., Thomson, N. R., James, K. D., Harris, D. E., Quail, M. A., Kieser, H., Harper, D., Bateman, A., Brown, S., Chandra, G., Chen, C. W., Collins, M., Cronin, A., Fraser, A., Goble, A., Hidalgo, J., Hornsby, T., Howarth, S., Huang, C. H., Kieser, T., Larke, L., Murphy, L., Oliver, K., O'Neil, S., Rabinowitsch, E., Rajandream, M. A., Rutherford, K., Rutter, S., Seeger, K., Saunders, D., Sharp, S., Squares, R., Squares, S., Taylor, K., Warren, T., Wietzorrek, A., Woodward, J., Barrell, B. G., Parkhill, J., & Hopwood, D. A. (2002). Complete genome sequence of the

- model actinomycete *Streptomyces coelicolor* A3(2). *Nature*, 417(6885), 141-147. doi:10.1038/417141a
- Berg, T., & Strand, D. H. (2011). <sup>13</sup>C labelled internal standards—A solution to minimize ion suppression effects in liquid chromatography–tandem mass spectrometry analyses of drugs in biological samples? *Journal of Chromatography A*, 1218(52), 9366-9374. doi:https://doi.org/10.1016/j.chroma.2011.10.081
- Bibb, M. J. (2005). Regulation of secondary metabolism in streptomycetes. *Current opinion in microbiology*, 8(2), 208-215. doi:10.1016/j.mib.2005.02.016
- Bo, A. B., Kim, J. D., Kim, Y. S., Sin, H. T., Kim, H. J., Khaitov, B., Ko, Y. K., Park, K. W., & Choi, J. S. (2019). Isolation, identification and characterization of *Streptomyces* metabolites as a potential bioherbicide. *PloS one*, 14(9), e0222933-e0222933. doi:10.1371/journal.pone.0222933
- Bolten, C. J., Kiefer, P., Letisse, F., Portais, J. C., & Wittmann, C. (2007). Sampling for metabolome analysis of microorganisms. *Analytical chemistry*, 79(10), 3843-3849. doi:10.1021/ac0623888
- Bordag, N., Janakiraman, V., Nachtigall, J., Gonzalez Maldonado, S., Bethan, B., Laine, J. P., & Fux, E. (2016). Fast filtration of bacterial or mammalian suspension cell cultures for optimal metabolomics results. *PloS one*, 11(7), e0159389. doi:10.1371/journal.pone.0159389
- Borrero-de Acuna, J. M., Bielecka, A., Haussler, S., Schobert, M., Jahn, M., Wittmann, C., Jahn, D., & Poblete-Castro, I. (2014). Production of medium chain length polyhydroxyalkanoate in metabolic flux optimized *Pseudomonas putida*. *Microbial cell factories*, 13, 88. doi:10.1186/1475-2859-13-88
- Bowen, B. P., & Northen, T. R. (2010). Dealing with the unknown: Metabolomics and metabolite atlases. *Journal of the American Society for Mass Spectrometry*, 21(9), 1471-1476. doi:10.1016/j.jasms.2010.04.003
- Branduardi, P., Longo, V., Berterame, N. M., Rossi, G., & Porro, D. (2013). A novel pathway to produce butanol and isobutanol in *Saccharomyces cerevisiae*. *Biotechnology for biofuels*, 6(1), 68. doi:10.1186/1754-6834-6-68
- Buchholz, A., Hurlebaus, J., Wandrey, C., & Takors, R. (2002). Metabolomics: quantification of intracellular metabolite dynamics. *Biomolecular Engineering*, 19(1), 5-15. doi:https://doi.org/10.1016/S1389-0344(02)00003-5
- Busscher, G. F., Rutjes, F. P., & van Delft, F. L. (2005). 2-Deoxystreptamine: central scaffold of aminoglycoside antibiotics. *Chemical reviews*, 105(3), 775-791. doi:10.1021/cr0404085

- Butler, M. S., Hansford, K. A., Blaskovich, M. A. T., Halai, R., & Cooper, M. A. (2014). Glycopeptide antibiotics: Back to the future. *The Journal of antibiotics*, 67(9), 631-644. doi:10.1038/ja.2014.111
- Chater, K. F., & Wilde, L. C. (1976). Restriction of a bacteriophage of *Streptomyces albus* G involving endonuclease Sall. *Journal of bacteriology*, 128(2), 644-650.
- Chater, K. F., & Wilde, L. C. (1980). *Streptomyces albus* G Mutants Defective in the SalGI Restriction-Modification System. *Microbiology*, 116(2), 323-334. doi:https://doi.org/10.1099/00221287-116-2-323
- Chater, K. F., Biro, S., Lee, K. J., Palmer, T., & Schrepf, H. (2010). The complex extracellular biology of *Streptomyces*. *FEMS microbiology reviews*, 34(2), 171-198. doi:10.1111/j.1574-6976.2009.00206.x
- Chater, K. F. (2016). Recent advances in understanding *Streptomyces*. *F1000Research*, 5, 2795. doi:10.12688/f1000research.9534.1
- Chen, Y., Wendt-Pienkowski, E., & Shen, B. (2008). Identification and utility of FdmR1 as a *Streptomyces* antibiotic regulatory protein activator for fredericamycin production in *Streptomyces griseus* ATCC 49344 and heterologous hosts. *Journal of bacteriology*, 190(16), 5587-5596. doi:10.1128/jb.00592-08
- Coisne, S., Bechet, M., & Blondeau, R. (1999). Actinorhodin production by *Streptomyces coelicolor* A3(2) in iron-restricted media. *Letters in applied microbiology*, 28(3), 199-202. doi:10.1046/j.1365-2672.1999.00509.x
- Coulier, L., Bas, R., Jespersen, S., Verheij, E., van der Werf, M. J., & Hankemeier, T. (2006). Simultaneous quantitative analysis of metabolites using ion-pair liquid chromatography–electrospray ionization mass spectrometry. *Analytical chemistry*, 78(18), 6573-6582. doi:10.1021/ac0607616
- Debarbouille, M., Gardan, R., Arnaud, M., & Rapoport, G. (1999). Role of BkdR, a transcriptional activator of the sigL-dependent isoleucine and valine degradation pathway in *Bacillus subtilis*. *Journal of bacteriology*, 181(7), 2059-2066. doi:10.1128/JB.181.7.2059-2066.1999
- Fang, H., Kang, J., & Zhang, D. (2017). Microbial production of vitamin B12: a review and future perspectives. *Microbial cell factories*, 16(1), 15. doi:10.1186/s12934-017-0631-y
- Fang, M., & Bauer, C. E. (2018). Regulation of stringent factor by branched-chain amino acids. *Proceedings of the National Academy of Sciences*, 115(25), 6446-6451. doi:10.1073/pnas.1803220115

- Feng, Z., Wang, L., Rajski, S. R., Xu, Z., Coeffet-LeGal, M. F., & Shen, B. (2009). Engineered production of iso-migrastatin in heterologous *Streptomyces* hosts. *Bioorganic & medicinal chemistry*, 17(6), 2147-2153. doi:10.1016/j.bmc.2008.10.074
- Fernandez, M., & Sanchez, J. (2002). Nuclease activities and cell death processes associated with the development of surface cultures of *Streptomyces antibioticus* ETH 7451. *Microbiology*, 148(Pt 2), 405-412. doi:10.1099/00221287-148-2-405
- Flardh, K., & Buttner, M. J. (2009). *Streptomyces* morphogenetics: dissecting differentiation in a filamentous bacterium. *Nature reviews. Microbiology*, 7(1), 36-49. doi:10.1038/nrmicro1968
- Fujita, Y., Matsuoka, H., & Hirooka, K. (2007). Regulation of fatty acid metabolism in bacteria. *Molecular microbiology*, 66(4), 829-839. doi:10.1111/j.1365-2958.2007.05947.x
- Gaynor, M., & Mankin, A. S. (2003). Macrolide antibiotics: Binding site, mechanism of action, resistance. *Current topics in medicinal chemistry*, 3(9), 949-960. doi:10.2174/1568026033452159
- Gemperlein, K., Dietrich, D., Kohlstedt, M., Zipf, G., Bernauer, H. S., Wittmann, C., Wenzel, S. C., & Muller, R. (2019). Polyunsaturated fatty acid production by *Yarrowia lipolytica* employing designed myxobacterial PUFA synthases. *Nature communications*, 10(1), 4055. doi:10.1038/s41467-019-12025-8
- Gil, J. A., & Campelo-Diez, A. B. (2003). Candicidin biosynthesis in *Streptomyces griseus*. *Applied microbiology and biotechnology*, 60(6), 633-642. doi:10.1007/s00253-002-1163-9
- Gläser, L., Kuhl, M., Jovanovic, S., Fritz, M., Vögeli, B., Erb, T. J., Becker, J., & Wittmann, C. (2020). A common approach for absolute quantification of short chain CoA thioesters in prokaryotic and eukaryotic microbes. *Microbial cell factories*, 19(1), 160. doi:10.1186/s12934-020-01413-1
- Gläser, L., Kuhl, M., Stegmüller, J., Rückert, C., Myronovskyi, M., Kalinowski, J., Luzhetskyy, A., & Wittmann, C. (2021). Superior production of heavy pamamycin derivatives using a *bkdR* deletion mutant of *Streptomyces albus* J1074/R2. *Microbial cell factories*, 20(1), 111. doi:10.1186/s12934-021-01602-6
- Gout, I. (2018). Coenzyme A, protein CoAlation and redox regulation in mammalian cells. *Biochemical Society transactions*, 46(3), 721-728. doi:10.1042/BST20170506
- Gullón, S., Olano, C., Abdelfattah, M. S., Braña, A. F., Rohr, J., Méndez, C., & Salas, J. A. (2006). Isolation, characterization, and heterologous expression of the biosynthesis gene cluster for the antitumor anthracycline steffimycin. *Applied and environmental microbiology*, 72(6), 4172-4183. doi:10.1128/aem.00734-06

- Hashimoto, M., Kondo, T., Kozone, I., Kawaide, H., Abe, H., & Natsume, M. (2003). Relationship between response to and production of the aerial mycelium-inducing substances pamamycin-607 and A-factor. *Bioscience, biotechnology, and biochemistry*, 67(4), 803-808. doi:10.1271/bbb.67.803
- Hashimoto, M., Komatsu, H., Kozone, I., Kawaide, H., Abe, H., & Natsume, M. (2005). Biosynthetic origin of the carbon skeleton and nitrogen atom of pamamycin-607, a nitrogen-containing polyketide. *Bioscience, biotechnology, and biochemistry*, 69(2), 315-320. doi:10.1271/bbb.69.315
- Hashimoto, M., Katsura, H., Kato, R., Kawaide, H., & Natsume, M. (2011). Effect of pamamycin-607 on secondary metabolite production by *Streptomyces* spp. *Bioscience, biotechnology, and biochemistry*, 75(9), 1722-1726. doi:10.1271/bbb.110251
- Hayashi, O., & Satoh, K. (2006). Determination of acetyl-CoA and malonyl-CoA in germinating rice seeds using the LC-MS/MS technique. *Bioscience, biotechnology, and biochemistry*, 70(11), 2676-2681. doi:10.1271/bbb.60269
- Hesketh, A., Chen, W. J., Ryding, J., Chang, S., & Bibb, M. (2007). The global role of ppGpp synthesis in morphological differentiation and antibiotic production in *Streptomyces coelicolor* A3(2). *Genome biology*, 8(8), R161. doi:10.1186/gb-2007-8-8-r161
- Huang, C., Yang, C., Zhang, W., Zhu, Y., Ma, L., Fang, Z., & Zhang, C. (2019). Albumycin, a new isoindolequinone from *Streptomyces albus* J1074 harboring the fluostatin biosynthetic gene cluster. *The Journal of antibiotics*, 72(5), 311-315. doi:10.1038/s41429-019-0161-4
- Hwang, K. S., Kim, H. U., Charusanti, P., Palsson, B. O., & Lee, S. Y. (2014). Systems biology and biotechnology of *Streptomyces* species for the production of secondary metabolites. *Biotechnology advances*, 32(2), 255-268. doi:10.1016/j.biotechadv.2013.10.008
- Ismail, W., & Gescher, J. (2012). Epoxy coenzyme A thioester pathways for degradation of aromatic compounds. *Applied and environmental microbiology*, 78(15), 5043-5051. doi:10.1128/AEM.00633-12
- Jiang, Y., Nikolau, B., & Ma, Y. (2010). Separation and quantification of short-chain coenzyme A in plant tissues by capillary electrophoresis with laser-induced fluorescence detection. *Analytical Methods*, 2(12), 1900-1904. doi:10.1039/c0ay00425a
- Jovanovic, S., Dietrich, D., Becker, J., Kohlstedt, M., & Wittmann, C. (2021). Microbial production of polyunsaturated fatty acids — high-value ingredients for aquafeed, superfoods, and pharmaceuticals. *Current opinion in biotechnology*, 69, 199-211. doi:https://doi.org/10.1016/j.copbio.2021.01.009

- Kallifidas, D., Jiang, G., Ding, Y., & Luesch, H. (2018). Rational engineering of *Streptomyces albus* J1074 for the overexpression of secondary metabolite gene clusters. *Microbial cell factories*, 17(1), 25. doi:10.1186/s12934-018-0874-2
- Kashiwagi, N., Ogino, C., & Kondo, A. (2017). Production of chemicals and proteins using biomass-derived substrates from a *Streptomyces* host. *Bioresource technology*, 245(Pt B), 1655-1663. doi:10.1016/j.biortech.2017.06.001
- Kasumov, T., Martini, W. Z., Reszko, A. E., Bian, F., Pierce, B. A., David, F., Roe, C. R., & Brunengraber, H. (2002). Assay of the concentration and <sup>13</sup>C isotopic enrichment of propionyl-CoA, methylmalonyl-CoA, and succinyl-CoA by gas chromatography–mass spectrometry. *Analytical biochemistry*, 305(1), 90-96. doi:https://doi.org/10.1006/abio.2002.5639
- Kieser, T., Bibb, M., Buttner, M., Chater, K., & Hopwood, D. (2000). Practical *Streptomyces* Genetics *John Innes Foundation, Norwich, United Kingdom*.
- Kim, M., Sang Yi, J., Kim, J., Kim, J. N., Kim, M. W., & Kim, B. G. (2014). Reconstruction of a high-quality metabolic model enables the identification of gene overexpression targets for enhanced antibiotic production in *Streptomyces coelicolor* A3(2). *Biotechnology journal*, 9(9), 1185-1194. doi:10.1002/biot.201300539
- Kind, S., Becker, J., & Wittmann, C. (2013). Increased lysine production by flux coupling of the tricarboxylic acid cycle and the lysine biosynthetic pathway—metabolic engineering of the availability of succinyl-CoA in *Corynebacterium glutamicum*. *Metabolic engineering*, 15, 184-195. doi:10.1016/j.ymben.2012.07.005
- King, M. T., Reiss, P. D., & Cornell, N. W. (1988). Determination of short-chain coenzyme A compounds by reversed-phase high-performance liquid chromatography. *Methods in enzymology*, 166, 70-79. doi:10.1016/s0076-6879(88)66012-5
- Kitani, S., Miyamoto, K. T., Takamatsu, S., Herawati, E., Iguchi, H., Nishitomi, K., Uchida, M., Nagamitsu, T., Omura, S., Ikeda, H., & Nihira, T. (2011). Avenolide, a *Streptomyces* hormone controlling antibiotic production in *Streptomyces avermitilis*. *Proceedings of the National Academy of Sciences of the United States of America*, 108(39), 16410-16415. doi:10.1073/pnas.1113908108
- Kozone, I., Hashimoto, M., Grafe, U., Kawaide, H., Abe, H., & Natsume, M. (2008). Structure-activity relationship of pamamycins: effect of side chain length on aerial mycelium-inducing activity. *The Journal of antibiotics*, 61(2), 98-102. doi:10.1038/ja.2008.118

- Kroeger, J. K., Zarzycki, J., & Fuchs, G. (2011). A spectrophotometric assay for measuring acetyl-coenzyme A carboxylase. *Analytical biochemistry*, *411*(1), 100-105. doi:<https://doi.org/10.1016/j.ab.2010.11.046>
- Kuhl, M., Gläser, L., Rebets, Y., Rückert, C., Sarkar, N., Hartsch, T., Kalinowski, J., Luzhetskyy, A., & Wittmann, C. (2020). Microparticles globally reprogram *Streptomyces albus* toward accelerated morphogenesis, streamlined carbon core metabolism, and enhanced production of the antituberculosis polyketide pamamycin. *Biotechnology and bioengineering*, *117*(12), 3858-3875. doi:10.1002/bit.27537
- Lechevalier, H., Acker, R. F., Corke, C. T., Haenseler, C. M., & Waksman, S. A. (1953). Candicidin, a new antifungal antibiotic. *Mycologia*, *45*(2), 155-171. doi:10.1080/00275514.1953.12024259
- Lee, D. W., Ng, B. G., & Kim, B. S. (2015). Increased valinomycin production in mutants of *Streptomyces sp.* M10 defective in bafilomycin biosynthesis and branched-chain alpha-keto acid dehydrogenase complex expression. *Journal of industrial microbiology & biotechnology*, *42*(11), 1507-1517. doi:10.1007/s10295-015-1679-5
- Lee, N., Hwang, S., Kim, W., Lee, Y., Kim, J. H., Cho, S., Kim, H. U., Yoon, Y. J., Oh, M. K., Palsson, B. O., & Cho, B. K. (2021). Systems and synthetic biology to elucidate secondary metabolite biosynthetic gene clusters encoded in *Streptomyces* genomes. *Natural product reports*. doi:10.1039/d0np00071j
- Lefevre, P., Peirs, P., Braibant, M., Fauville-Dufaux, M., Vanhoof, R., Huygen, K., Wang, X.-M., Pogell, B., Wang, Y., & Fischer, P. (2004). Antimycobacterial activity of synthetic pamamycins. *Journal of Antimicrobial Chemotherapy*, *54*(4), 824-827.
- Li, T.-L., Choroba, O. W., Hong, H., Williams, D. H., & Spencer, J. B. (2001). Biosynthesis of the vancomycin group of antibiotics: characterisation of a type III polyketide synthase in the pathway to (S)-3,5-dihydroxyphenylglycine. *Chemical communications*(20), 2156-2157. doi:10.1039/b106638b
- Li, Z. L., Wang, Y. H., Chu, J., Zhuang, Y. P., & Zhang, S. L. (2009). Effect of branched-chain amino acids, valine, isoleucine and leucine on the biosynthesis of bitespiramycin 4"-O-acylsiramycins. *Brazilian journal of microbiology : [publication of the Brazilian Society for Microbiology]*, *40*(4), 734-746. doi:10.1590/S1517-83822009000400003
- Liras, P. (1999). Biosynthesis and molecular genetics of cephamycins. *Antonie van Leeuwenhoek*, *75*(1), 109-124. doi:10.1023/a:1001804925843

- Liu, G., Chen, J., Che, P., & Ma, Y. (2003). Separation and quantitation of short-chain coenzyme A's in biological samples by capillary electrophoresis. *Analytical chemistry*, 75(1), 78-82. doi:10.1021/ac0261505
- Liu, G., Chater, K. F., Chandra, G., Niu, G., & Tan, H. (2013). Molecular regulation of antibiotic biosynthesis in *Streptomyces*. *Microbiology and molecular biology reviews : MMBR*, 77(1), 112-143. doi:10.1128/MMBR.00054-12
- Liu, H., Zhang, Y., Li, S., Wang, J., Wang, X., & Xiang, W. (2020). Elucidation of the activation pathways of ScyA1/ScyR1, an Aco/ArpA-Like system that regulates the expression of nemadectin and other secondary metabolic biosynthetic genes. *Frontiers in bioengineering and biotechnology*, 8, 589730. doi:10.3389/fbioe.2020.589730
- Liu, X., Wang, T., Sun, X., Wang, Z., Tian, X., Zhuang, Y., & Chu, J. (2019). Optimized sampling protocol for mass spectrometry-based metabolomics in *Streptomyces*. *Bioresources and Bioprocessing*, 6(1), 32. doi:10.1186/s40643-019-0269-1
- Lombó, F., Velasco, A., Castro, A., de la Calle, F., Braña, A. F., Sánchez-Puelles, J. M., Méndez, C., & Salas, J. A. (2006). Deciphering the biosynthesis pathway of the antitumor thiocoraline from a marine actinomycete and its expression in two *Streptomyces* species. *Chembiochem : a European journal of chemical biology*, 7(2), 366-376. doi:https://doi.org/10.1002/cbic.200500325
- Lounes, A., Lebrihi, A., Benslimane, C., Lefebvre, G., & Germain, P. (1995). Regulation of valine catabolism by ammonium in *Streptomyces ambofaciens*, producer of spiramycin. *Canadian journal of microbiology*, 41(9), 800-808. doi:10.1139/m95-110
- Lu, C., Zhang, X., Jiang, M., & Bai, L. (2016). Enhanced salinomycin production by adjusting the supply of polyketide extender units in *Streptomyces albus*. *Metabolic engineering*, 35, 129-137. doi:10.1016/j.ymben.2016.02.012
- Madhusudhan, K. T., Luo, J., & Sokatch, J. R. (1999). In vitro transcriptional studies of the bkd operon of *Pseudomonas putida*: L-branched-chain amino acids and D-leucine are the inducers. *Journal of bacteriology*, 181(9), 2889-2894. doi:10.1128/jb.181.9.2889-2894.1999
- Magnes, C., Suppan, M., Pieber, T. R., Moustafa, T., Trauner, M., Haemmerle, G., & Sinner, F. M. (2008). Validated comprehensive analytical method for quantification of coenzyme A activated compounds in biological tissues by online solid-phase extraction LC/MS/MS. *Analytical chemistry*, 80(15), 5736-5742. doi:10.1021/ac800031u
- McCann, P. A., & Pogell, B. M. (1979). Pamamycin: a new antibiotic and stimulator of aerial mycelia formation. *The Journal of antibiotics*, 32(7), 673-678.

- Mendez, C., Brana, A. F., Manzanal, M. B., & Hardisson, C. (1985). Role of substrate mycelium in colony development in *Streptomyces*. *Canadian journal of microbiology*, 31(5), 446-450. doi:10.1139/m85-083
- Migueluez, E. M., Hardisson, C., & Manzanal, M. B. (1999). Hyphal death during colony development in *Streptomyces antibioticus*: morphological evidence for the existence of a process of cell deletion in a multicellular prokaryote. *The Journal of cell biology*, 145(3), 515-525. doi:10.1083/jcb.145.3.515
- Milke, L., & Marienhagen, J. (2020). Engineering intracellular malonyl-CoA availability in microbial hosts and its impact on polyketide and fatty acid synthesis. *Applied microbiology and biotechnology*, 104(14), 6057-6065. doi:10.1007/s00253-020-10643-7
- Minotti, G., Menna, P., Salvatorelli, E., Cairo, G., & Gianni, L. (2004). Anthracyclines: molecular advances and pharmacologic developments in antitumor activity and cardiotoxicity. *Pharmacological reviews*, 56(2), 185-229. doi:10.1124/pr.56.2.6
- Myronovskiy, M., Tokovenko, B., Brötz, E., Rückert, C., Kalinowski, J., & Luzhetskyy, A. (2014). Genome rearrangements of *Streptomyces albus* J1074 lead to the carotenoid gene cluster activation. *Applied microbiology and biotechnology*, 98(2), 795-806. doi:10.1007/s00253-013-5440-6
- Natsume, M., Yasui, K., Kondo, S., & Marumo, S. (1991). The structure of four new pamamycin homologues isolated from *Streptomyces alboniger*. *Tetrahedron letters*, 32(26), 3087-3090.
- Natsume, M., Tazawa, J., Yagi, K., Abe, H., Kondo, S., & Marumo, S. (1995). Structure-activity relationship of pamamycins: effects of alkyl substituents. *The Journal of antibiotics*, 48(10), 1159-1164.
- Natsume, M. (1999). Differentiation of aerial mycelia - Pamamycins and calcium ion in *Streptomyces alboniger* -. *Actinomycetologica*, 13(1), 11-19. doi:10.3209/saj.13\_11
- Neinast, M., Murashige, D., & Arany, Z. (2019). Branched chain amino acids. *Annual review of physiology*, 81, 139-164. doi:10.1146/annurev-physiol-020518-114455
- Neubauer, S., Chu, D. B., Marx, H., Sauer, M., Hann, S., & Koellensperger, G. (2015). LC-MS/MS-based analysis of coenzyme A and short-chain acyl-coenzyme A thioesters. *Analytical and bioanalytical chemistry*, 407(22), 6681-6688. doi:10.1007/s00216-015-8825-9
- Nguyen, C. T., Dhakal, D., Pham, V. T. T., Nguyen, H. T., & Sohng, J. K. (2020). Recent advances in strategies for activation and discovery/characterization of cryptic biosynthetic gene clusters in *Streptomyces*. *Microorganisms*, 8(4). doi:10.3390/microorganisms8040616
- Nicholson, J. K., Lindon, J. C., & Holmes, E. (1999). 'Metabonomics': understanding the metabolic responses of living systems to pathophysiological stimuli via multivariate statistical analysis

of biological NMR spectroscopic data. *Xenobiotica; the fate of foreign compounds in biological systems*, 29(11), 1181-1189. doi:10.1080/004982599238047

- Ochi, K. (1987). A *rel* mutation abolishes the enzyme induction needed for actinomycin synthesis by *Streptomyces antibioticus*. *Agricultural and biological chemistry*, 51(3), 829-835.
- Okami, Y., & Hotta, K. (1988). Search and discovery of new antibiotics. In M. Goodfellow, S. T. Williams, & M. Mordarski (Eds.), *Actinomycetes in Biotechnology* (pp. 33-67). London: Academic Press.
- Ōmura, S., & Crump, A. (2014). Ivermectin: panacea for resource-poor communities? *Trends in parasitology*, 30(9), 445-455. doi:https://doi.org/10.1016/j.pt.2014.07.005
- Owens, B. (2015). 2015 Nobel Prize goes to antiparasitic drug discoverers. *Lancet*, 386(10002), 1433. doi:10.1016/S0140-6736(15)00455-9
- Park, J. W., Jung, W. S., Park, S. R., Park, B. C., & Yoon, Y. J. (2007). Analysis of intracellular short organic acid-coenzyme A esters from actinomycetes using liquid chromatography-electrospray ionization-mass spectrometry. *Journal of mass spectrometry : JMS*, 42(9), 1136-1147. doi:10.1002/jms.1240
- Park, S. R., Park, J. W., Ban, Y. H., Sohng, J. K., & Yoon, Y. J. (2013). 2-Deoxystreptamine-containing aminoglycoside antibiotics: recent advances in the characterization and manipulation of their biosynthetic pathways. *Natural product reports*, 30(1), 11-20. doi:10.1039/c2np20092a
- Peter, D. M., Vogeli, B., Cortina, N. S., & Erb, T. J. (2016). A chemo-enzymatic road map to the synthesis of CoA esters. *Molecules*, 21(4), 517. doi:10.3390/molecules21040517
- Pogell, B. M. (1998). The pamamycins: developmental autoregulators and antibiotics from *Streptomyces alboniger*. A review and update. *Cellular and molecular biology*, 44(3), 461-463.
- Rebets, Y., Brotz, E., Manderscheid, N., Tokovenko, B., Myronovskiy, M., Metz, P., Petzke, L., & Luzhetskyy, A. (2015). Insights into the pamamycin biosynthesis. *Angewandte Chemie*, 54(7), 2280-2284. doi:10.1002/anie.201408901
- Rigali, S., Nothhaft, H., Noens, E. E., Schlicht, M., Colson, S., Muller, M., Joris, B., Koerten, H. K., Hopwood, D. A., Titgemeyer, F., & van Wezel, G. P. (2006). The sugar phosphotransferase system of *Streptomyces coelicolor* is regulated by the GntR-family regulator DasR and links N-acetylglucosamine metabolism to the control of development. *Molecular microbiology*, 61(5), 1237-1251. doi:10.1111/j.1365-2958.2006.05319.x

- Romero-Rodriguez, A., Robledo-Casados, I., & Sanchez, S. (2015). An overview on transcriptional regulators in *Streptomyces*. *Biochimica et biophysica acta*, 1849(8), 1017-1039. doi:10.1016/j.bbagr.2015.06.007
- Saito, N., Xu, J., Hosaka, T., Okamoto, S., Aoki, H., Bibb, M. J., & Ochi, K. (2006). EshA accentuates ppGpp accumulation and is conditionally required for antibiotic production in *Streptomyces coelicolor* A3(2). *Journal of bacteriology*, 188(13), 4952-4961. doi:10.1128/JB.00343-06
- Seifar, R. M., Ras, C., Deshmukh, A. T., Bekers, K. M., Suarez-Mendez, C. A., da Cruz, A. L., van Gulik, W. M., & Heijnen, J. J. (2013). Quantitative analysis of intracellular coenzymes in *Saccharomyces cerevisiae* using ion pair reversed phase ultra high performance liquid chromatography tandem mass spectrometry. *Journal of chromatography. A*, 1311, 115-120. doi:10.1016/j.chroma.2013.08.076
- Shi, S., Valle-Rodríguez, J. O., Khoomrung, S., Siewers, V., & Nielsen, J. (2012). Functional expression and characterization of five wax ester synthases in *Saccharomyces cerevisiae* and their utility for biodiesel production. *Biotechnology for biofuels*, 5(1), 7. doi:10.1186/1754-6834-5-7
- Sprusansky, O., Stirrett, K., Skinner, D., Denoya, C., & Westpheling, J. (2005). The *bkdR* gene of *Streptomyces coelicolor* is required for morphogenesis and antibiotic production and encodes a transcriptional regulator of a branched-chain amino acid dehydrogenase complex. *Journal of bacteriology*, 187(2), 664-671. doi:10.1128/JB.187.2.664-671.2005
- Stirrett, K., Denoya, C., & Westpheling, J. (2009). Branched-chain amino acid catabolism provides precursors for the Type II polyketide antibiotic, actinorhodin, via pathways that are nutrient dependent. *Journal of industrial microbiology & biotechnology*, 36(1), 129-137. doi:10.1007/s10295-008-0480-0
- Strauch, E., Takano, E., Baylis, H. A., & Bibb, M. J. (1991). The stringent response in *Streptomyces coelicolor* A3(2). *Molecular microbiology*, 5(2), 289-298. doi:10.1111/j.1365-2958.1991.tb02109.x
- Suo, Y., Ren, M., Yang, X., Liao, Z., Fu, H., & Wang, J. (2018). Metabolic engineering of *Clostridium tyrobutyricum* for enhanced butyric acid production with high butyrate/acetate ratio. *Applied microbiology and biotechnology*, 102(10), 4511-4522. doi:10.1007/s00253-018-8954-0
- Tamvakopoulos, C. S., & Anderson, V. E. (1992). Detection of acyl-coenzyme a thioester intermediates of fatty acid  $\beta$ -oxidation as the N-acylglycines by negative-ion chemical ionization gas chromatography—mass spectrometry. *Analytical biochemistry*, 200(2), 381-387. doi:https://doi.org/10.1016/0003-2697(92)90483-N

- Tao, K., Ye, T., Cao, M., Meng, X., Li, Y., Wang, H., & Feng, Z. (2020). Salumycin, a new pyrazolequinone from a *Streptomyces albus* J1074 mutant strain. *Molecules*, 25(18). doi:10.3390/molecules25184098
- Tetzlaff, C. N., You, Z., Cane, D. E., Takamatsu, S., Omura, S., & Ikeda, H. (2006). A gene cluster for biosynthesis of the sesquiterpenoid antibiotic pentalenolactone in *Streptomyces avermitilis*. *Biochemistry*, 45(19), 6179-6186. doi:10.1021/bi060419n
- Thao, N. B., Kitani, S., Nitta, H., Tomioka, T., & Nihira, T. (2017). Discovering potential *Streptomyces* hormone producers by using disruptants of essential biosynthetic genes as indicator strains. *The Journal of antibiotics*, 70(10), 1004-1008. doi:10.1038/ja.2017.85
- Thuan, N. H., Pandey, R. P., & Sohng, J. K. (2014). Recent advances in biochemistry and biotechnological synthesis of avermectins and their derivatives. *Applied microbiology and biotechnology*, 98(18), 7747-7759. doi:10.1007/s00253-014-5926-x
- Todd King, M., Reiss, P. D., & Cornell, N. W. (1988). Determination of short-chain coenzyme A compounds by reversed-phase high-performance liquid chromatography. In *Methods in enzymology* (Vol. 166, pp. 70-79): Academic Press.
- Vakulenko, S. B., & Mobashery, S. (2003). Versatility of aminoglycosides and prospects for their future. *Clinical microbiology reviews*, 16(3), 430-450. doi:10.1128/cmr.16.3.430-450.2003
- Van Bambeke, F. (2006). Glycopeptides and glycodepsipeptides in clinical development: a comparative review of their antibacterial spectrum, pharmacokinetics and clinical efficacy. *Current opinion in investigational drugs (London, England : 2000)*, 7(8), 740-749.
- van Wezel, G. P., & McDowall, K. J. (2011). The regulation of the secondary metabolism of *Streptomyces*: new links and experimental advances. *Natural product reports*, 28(7), 1311-1333. doi:10.1039/c1np00003a
- Ventola, C. L. (2015). The antibiotic resistance crisis: part 1: causes and threats. *P & T : a peer-reviewed journal for formulary management*, 40(4), 277-283.
- Vrijbloed, J. W., Zerbe-Burkhardt, K., Ratnatilleke, A., Grubelnik-Leiser, A., & Robinson, J. A. (1999). Insertional inactivation of methylmalonyl coenzyme A (CoA) mutase and isobutyryl-CoA mutase genes in *Streptomyces cinnamonensis*: influence on polyketide antibiotic biosynthesis. *Journal of bacteriology*, 181(18), 5600-5605. doi:10.1128/JB.181.18.5600-5605.1999
- Watve, M. G., Tickoo, R., Jog, M. M., & Bhole, B. D. (2001). How many antibiotics are produced by the genus *Streptomyces*? *Archives of microbiology*, 176(5), 386-390. doi:10.1007/s002030100345

- Wendt-Pienkowski, E., Huang, Y., Zhang, J., Li, B., Jiang, H., Kwon, H., Hutchinson, C. R., & Shen, B. (2005). Cloning, sequencing, analysis, and heterologous expression of the fredericamycin biosynthetic gene cluster from *Streptomyces griseus*. *Journal of the American Chemical Society*, *127*(47), 16442-16452. doi:10.1021/ja054376u
- Wildermuth, H. (1970). Development and organization of the aerial mycelium in *Streptomyces coelicolor*. *Journal of general microbiology*, *60*(1), 43-50. doi:10.1099/00221287-60-1-43
- Williams, S., & Vickers, J. (1988). Detection of actinomycetes in the natural environment: problems and perspectives. *Biology of actinomycetes*, *88*, 265-270.
- Winter, J. M., Moffitt, M. C., Zazopoulos, E., McAlpine, J. B., Dorrestein, P. C., & Moore, B. S. (2007). Molecular basis for chloronium-mediated meroterpene cyclization: cloning, sequencing, and heterologous expression of the napyradiomycin biosynthetic gene cluster. *The Journal of biological chemistry*, *282*(22), 16362-16368. doi:10.1074/jbc.M611046200
- Woodruff, H. B. (2014). Selman A. Waksman, winner of the 1952 Nobel Prize for physiology or medicine. *Applied and environmental microbiology*, *80*(1), 2-8. doi:10.1128/AEM.01143-13
- Xiao, J. F., Zhou, B., & Ressom, H. W. (2012). Metabolite identification and quantitation in LC-MS/MS-based metabolomics. *TrAC Trends in Analytical Chemistry*, *32*, 1-14. doi:https://doi.org/10.1016/j.trac.2011.08.009
- Xu, P., Qiao, K., Ahn, W. S., & Stephanopoulos, G. (2016). Engineering *Yarrowia lipolytica* as a platform for synthesis of drop-in transportation fuels and oleochemicals. *Proceedings of the National Academy of Sciences*, *113*(39), 10848-10853. doi:10.1073/pnas.1607295113
- Yang, Q., Zhang, A.-h., Miao, J.-h., Sun, H., Han, Y., Yan, G.-l., Wu, F.-f., & Wang, X.-j. (2019). Metabolomics biotechnology, applications, and future trends: a systematic review. *RSC Advances*, *9*(64), 37245-37257. doi:10.1039/c9ra06697g
- Yi, J. S., Kim, M., Kim, E. J., & Kim, B. G. (2018). Production of pikromycin using branched chain amino acid catabolism in *Streptomyces venezuelae* ATCC 15439. *Journal of industrial microbiology & biotechnology*, *45*(5), 293-303. doi:10.1007/s10295-018-2024-6
- Yoon, Y. J., Kim, E. S., Hwang, Y. S., & Choi, C. Y. (2004). Avermectin: biochemical and molecular basis of its biosynthesis and regulation. *Applied microbiology and biotechnology*, *63*(6), 626-634. doi:10.1007/s00253-003-1491-4
- Zaheen, A., & Bloom, B. R. (2020). Tuberculosis in 2020 - New approaches to a continuing global health crisis. *The New England journal of medicine*, *382*(14), e26. doi:10.1056/NEJMp2000325
- Zhou, B., Xiao, J. F., Tuli, L., & Ressom, H. W. (2012). LC-MS-based metabolomics. *Molecular bioSystems*, *8*(2), 470-481. doi:10.1039/c1mb05350g

Zimmermann, M., Thormann, V., Sauer, U., & Zamboni, N. (2013). Nontargeted profiling of coenzyme A thioesters in biological samples by tandem mass spectrometry. *Analytical chemistry*, 85(17), 8284-8290. doi:10.1021/ac401555n

## 7 Supplementary Information

### 7.1 Supplementary Information Gläser et al. 2020

**A common approach for absolute quantification of short chain CoA thioesters in prokaryotic and eukaryotic microbes.**

Lars Gläser, Martin Kuhl, Sofija Jovanovic, Michel Fritz, Bastian Vögeli, Tobias J. Erb, Judith Becker, and Christoph Wittmann

*Microbial Cell Factories* **19**, 160 (2020).

<https://doi.org/10.1186/s12934-020-01413-1>

This is an open access article published under the terms of a Creative Commons Attribution 4.0 International License.

BV synthesized CoA thioesters. LG, MK and MF developed the CoA thioester extraction and analytical protocol. LG produced the <sup>13</sup>C labeled extracts and conducted cultivation of *S. albus*, *C. glutamicum*, and *P. putida*. SJ performed cultivation of *Y. lipolytica*. LG conducted thioester analysis. CW conceived and structured the work. LG, JB and CW wrote the first draft of the manuscript. All authors critically commented and improved the manuscript. All authors read and approved the final manuscript.

**Additional file 1 for**

**A common approach for absolute quantification of short chain CoA thioesters  
in prokaryotic and eukaryotic microbes**

Lars Gläser<sup>1</sup>, Martin Kuhl<sup>1</sup>, Sofija Jovanovic<sup>1</sup>, Michel Fritz<sup>1</sup>, Bastian Vögeli<sup>2</sup>, Tobias J. Erb<sup>2</sup>,  
Judith Becker<sup>1</sup> and Christoph Wittmann<sup>1#</sup>

<sup>1</sup>Institute of Systems Biotechnology, Saarland University, Saarbrücken, Germany

<sup>2</sup>Max Planck Institute for Terrestrial Microbiology, Marburg, Germany

# Phone/FAX: +49 681 302 71970/71972, e-mail: [christoph.wittmann@uni-saarland.de](mailto:christoph.wittmann@uni-saarland.de)

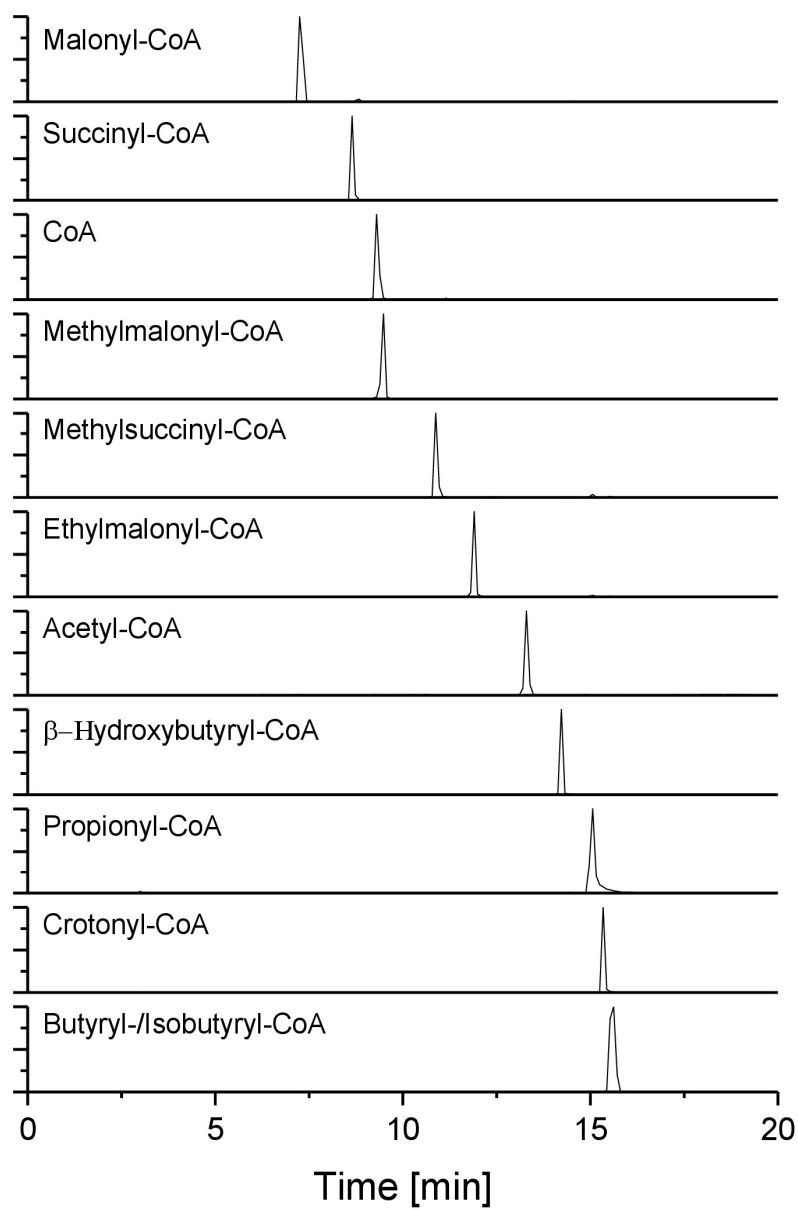


**Figure S1:** LC-MS chromatogram of a synthetic CoA thioester standard using a porous organo-silica reversed phase column (100  $\times$  2.1 mm, 1.5  $\mu$ m) for the chromatographic separation. Co-eluting analytes were distinguished by a different specific mass-to-charge ratio ( $m/z$ ).

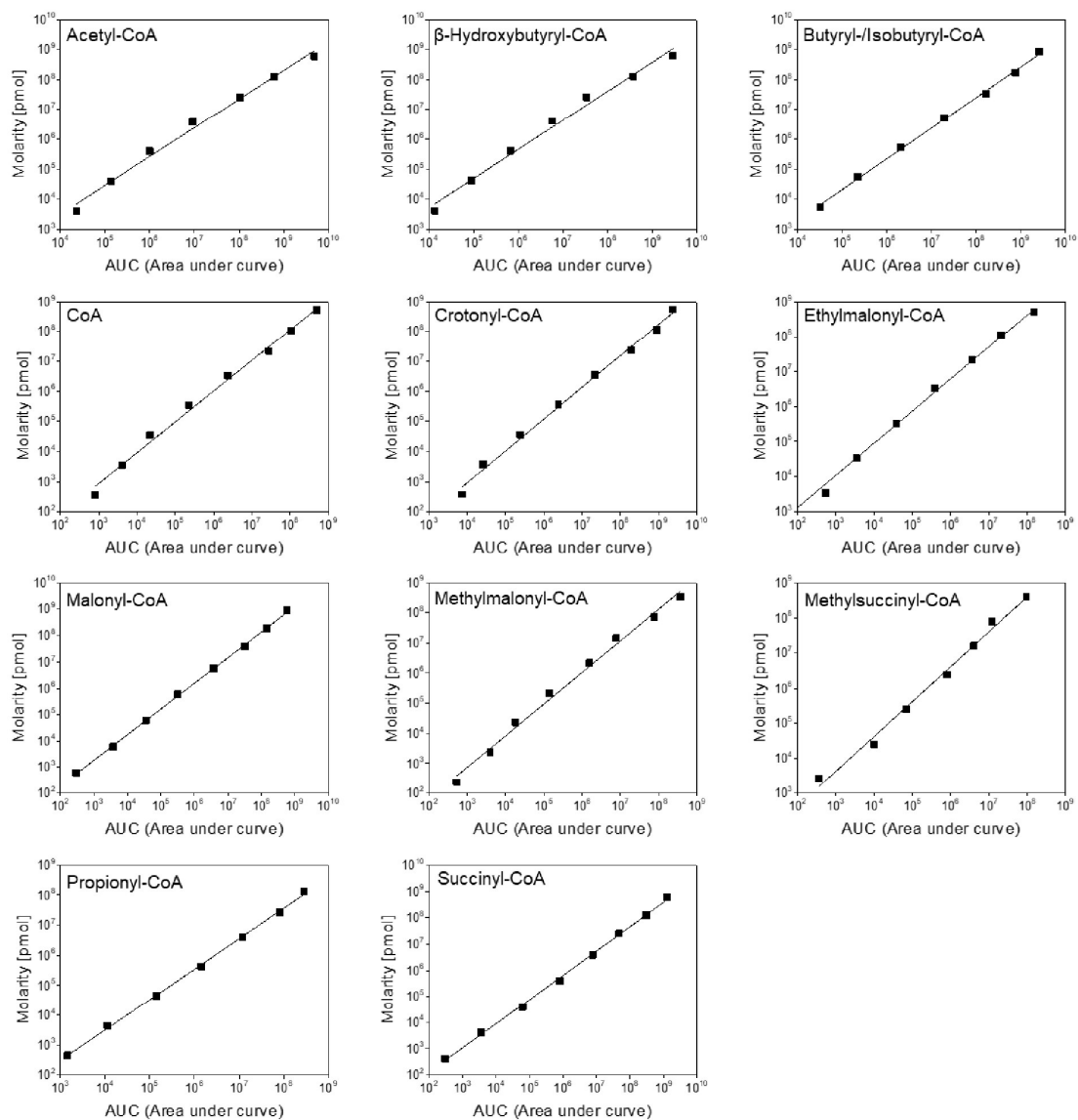


**Figure S2:** Calibration curves for different CoA thioesters using LC-MS/MS analysis.

**Table S1:** Instrumental settings for LC-MS/MS analysis of CoA thioesters. The declustering potential (DP), the collision energy (CE) and the cell exit potential (CXP) were individually tuned for each CoA thioester. The parent ion reflects the positive proton adduct  $[M+H]^+$ , except for the CoA homodimer (CoA-S-S-CoA), where the parent ion was  $[M+2H]^{2+}$ . In each case, the daughter ion reflects the positive proton adduct after neutral loss of 507 ( $m/z$ ).

Analyte	Parent ion ( $m/z$ )	Daughter ion ( $m/z$ )	DP [V]	CE [V]	CXP [V]
CoA-S-S-CoA	767.4	136.0	80.00	47.00	11.00
CoA	768.5	261.0	80.00	47.00	11.00
Acetyl-CoA	810.2	303.0	154.57	38.87	17.01
Malonyl-CoA	854.0	346.6	46.50	43.84	21.75
Propionyl-CoA	824.6	317.1	80.00	47.00	11.00
Butyryl-/Isobutyryl-CoA	838.1	331.1	128.22	45.50	22.16
$\beta$ -Hydroxybutyryl-CoA	854.1	347.1	142.36	39.95	10.73
Crotonyl-CoA	836.1	329.1	143.00	44.00	20.37
Methylmalonyl-CoA	868.0	361.1	90.06	42.50	11.87
Succinyl-CoA	868.1	361.1	15.96	46.78	21.68
Ethylmalonyl-CoA	882.1	375.1	177.58	37.80	25.30
Methylsuccinyl-CoA	882.0	375.1	131.79	50.40	23.73

**Table S2:** Instrumental settings for LC-MS/MS analysis of fully <sup>13</sup>C-labeled CoA thioesters used as internal standard for absolute CoA thioesters quantification. The respective mass of the fully labeled parent ion was determined by adding the number of carbon atoms to the monoisotopic mass of the non-labelled parent ion (Table S1). The mass of each daughter ion was then calculated by subtraction of *m/z* 517 from this value, considering the neutral loss of a fragment with ten <sup>13</sup>C atoms.

Analyte	Parent ion ( <i>m/z</i> )	Daughter ion ( <i>m/z</i> )	DP [V]	CE [V]	CXP [V]
CoA-S-S-CoA	788.1	141.1	80.00	47.00	11.00
CoA	789.5	272.5	80.00	47.00	11.00
Acetyl-CoA	833.2	316.2	154.57	38.87	17.01
Malonyl-CoA	878.0	361.0	46.50	43.84	21.75
Propionyl-CoA	848.6	331.6	80.00	47.00	11.00
Butyryl-/Isobutyryl-CoA	863.1	346.1	128.22	45.50	22.16
β-Hydroxybutyryl-CoA	879.1	362.1	142.36	39.95	10.73
Crotonyl-CoA	861.1	344.1	143.00	44.00	20.37
Methylmalonyl-CoA	893.0	376.0	90.06	42.50	11.87
Succinyl-CoA	893.1	376.1	15.96	46.78	21.68
Ethylmalonyl-CoA	908.1	391.1	177.58	37.80	25.30
Methylsuccinyl-CoA	908.0	391.0	131.79	50.40	23.73

## 7.2 Supplementary Information Gläser et al. 2021

### Superior production of heavy pamamycin derivatives using a *bkdR* deletion mutant of *Streptomyces albus* J1074/R2

Lars Gläser, Martin Kuhl, Julian Stegmüller, Christian Rückert, Maksym Myronovskyi, Jörn Kalinowski, Andriy Luzhetskyy, and Christoph Wittmann

*Microbial Cell Factories*. **20**, 111

<https://doi.org/10.1186/s12934-021-01602-6>

This is an open access article published under the terms of a Creative Commons Attribution 4.0 International License.

CW designed and supervised the study. LG carried out the cultivation experiments and performed the CoA thioester analysis. LG and MK conducted pamamycin analysis. JS and MM performed genetic engineering. CR and JK performed RNA sequencing and data processing. LG und CW analyzed the data, drew the figures, and wrote the first draft of the manuscript. All authors critically commented and improved the manuscript. All authors read and approved the final manuscript.

# Superior production of heavy pamamycin derivatives using a *bkdR* null mutant of *Streptomyces albus*

Submitted for publication in *Microbial Cell Factories*

Lars Gläser<sup>1</sup>, Martin Kuhl<sup>1</sup>, Julian Stegmüller<sup>1</sup>, Christian Rückert<sup>2</sup>, Jörn Kalinowski<sup>2</sup>, Andriy Luzhetskyy<sup>3</sup>, and Christoph Wittmann<sup>1#</sup>

<sup>1</sup>Institute of Systems Biotechnology, Saarland University, Saarbrücken, Germany

<sup>2</sup>Center for Biotechnology, Bielefeld University, Bielefeld, Germany

<sup>3</sup>Department of Pharmacy, Pharmaceutical Biotechnology, Saarland University, Saarbrücken, Germany

Contact information

[lars.glaeser@uni-saarland.de](mailto:lars.glaeser@uni-saarland.de)

[martin.kuhl@uni-saarland.de](mailto:martin.kuhl@uni-saarland.de)

[julian.stegmueller@uni-saarland.de](mailto:julian.stegmueller@uni-saarland.de)

[cruecker@cebitec.uni-bielefeld.de](mailto:cruecker@cebitec.uni-bielefeld.de)

[jkalinowski@cebitec.uni-bielefeld.de](mailto:jkalinowski@cebitec.uni-bielefeld.de)

[a.luzhetskyy@mx.uni-saarland.de](mailto:a.luzhetskyy@mx.uni-saarland.de)

[christoph.wittmann@uni-saarland.de](mailto:christoph.wittmann@uni-saarland.de)

#Corresponding author: Phone: +49 681 302 71970, FAX: +49 681 302 71972, e-mail:

[christoph.wittmann@uni-saarland.de](mailto:christoph.wittmann@uni-saarland.de)



**Table S1:** Strain and plasmids used for performing deletion mutants.

<b>Strains</b>	<b>Description</b>	<b>Reference</b>
E. coli ET12567 (pUZ8002)	Cells for conjugative DNA transfer	[1]
<b>Plasmids</b>	<b>Description</b>	<b>Reference</b>
pKG1132	Suicide vector for genome-based modifications. comprising a MCS, an ORI for <i>E. coli</i> . and <i>AmR</i> and <i>gusA</i> as selection marker	[2]
pKG1132hyg	Suicide vector for genome-based modifications. comprising a MCS, an ORI for <i>E. coli</i> . and <i>HygR</i> and <i>gusA</i> as selection marker	This work
pKG1132hyg_Δ <i>bdkR</i>	Suicide vector for the deletion of the gene XNRR2_3053	This work

**Table S2:** Primers for genome-based engineering of *S. albus* J1074/R2

<b>Name</b>	<b>Sequence</b>
3053_HomA Fw	5'-GATCCGCGGCCGCGCGCGATTCTGCCCACGGTCTTCCTG-3'
3053_HomA Rev	5'-AGTGGGGAGCGATACGAATGTGACGCGAACCGGGCCGAG-3'
3053_HomB Fw	5'-CTGCGGCCCGGTTTCGCGTCACATTCGTATCGCTCCCCACTC-3'
3053_HomB Rev	5'-GACATGATTACGAATTCGATCTTCGACCAGTACAGCCGCTTG-3'
3053_ch_Fw	5'-GGATGATCAACTCGGTGGTCG-3'
3053_ch_Rev	5'-CGGAACGGGGACTCGTCG-3'
Seq1_DbdkR_Fw	5'-GCTCGATCCGTGGCATCC-3'
Seq2_DbdkR_Fw	5'-AGGTCTCCAGCTACAACCTG-3'
Seq3_DbdkR_Fw	5'-CGAACAATCGGTAGGTGAGG-3'

**Table S3:** Gene expression of identified genes participating in biosynthesis of fatty acids, cofactors biotin, pantothenate, and CoA, branched-chain amino acids, as well as participating in phosphotransferase system (PTS) and at the entrance to central carbon metabolism in heterologous pamamycin producing *Streptomyces albus* J1074/R2 and *Streptomyces albus*  $\Delta bkdR/R2$  with supplemented L-valine in mannitol minimal medium during early growth (Early) and main production phase (Late). The expression level of the wildtype culture (J1074/R2) in minimal medium without amino acids during early growth (7h) was set as a reference (Control). n = 3

Gene	Annotation	Control	J1074/R2 + Valine		$\Delta bkdR/R2$ + Valine	
		Late	Early	Late	Early	Late
<b>Fatty acid biosynthesis (FAS)</b>						
XNRR2_0316	acyl-ACP desaturase, Stearoyl-ACP desaturase	0.0	0.0	1.1	0.0	0.0
XNRR2_0345	Long-chain-fatty-acid--CoA ligase	0.0	0.0	0.0	0.0	0.0
XNRR2_0396	3-oxoacyl-[acyl-carrier-protein] synthase, KASIII	0.0	0.0	0.0	0.0	0.0
XNRR2_0403	Long-chain-fatty-acid--CoA ligase	0.0	-1.5	-1.4	0.0	0.0
XNRR2_0583	acyl-CoA synthase	0.0	0.0	0.0	1.4	0.0
XNRR2_0588	3-oxoacyl-ACP synthase III	0.0	0.0	1.0	0.0	0.0
XNRR2_0913	short chain dehydrogenase/reductase family oxidoreductase	0.0	0.0	0.0	0.0	0.0
XNRR2_3581	3-oxoacyl-[acyl-carrier protein] reductase	0.0	0.0	0.0	2.7	0.0
XNRR2_3583	Acyl-CoA synthetase	0.0	0.0	0.0	0.0	0.0
XNRR2_4019	Acyl-CoA carboxylase complex A subunit	0.0	0.0	0.0	0.0	0.0
XNRR2_4211	Acetyl/propionyl CoA carboxylase alpha subunit	0.0	2.8	3.1	4.6	3.4
XNRR2_4377	Acyl-CoA synthetase	0.0	0.0	0.0	1.1	0.0
XNRR2_4461	Short-chain dehydrogenase/reductase SDR	0.0	0.0	0.0	2.5	0.0
XNRR2_4509	3-oxoacyl-[acyl-carrier-protein] synthase 2	0.0	0.0	0.0	0.0	0.0
XNRR2_4511	3-oxoacyl-[acyl-carrier-protein] synthase 3	0.0	0.0	0.0	0.0	0.0
XNRR2_4512	FabD	0.0	0.0	0.0	0.0	0.0
XNRR2_4749	Acyl-CoA synthetase	0.0	0.0	0.0	0.0	0.0
XNRR2_4989	Oxidoreductase	0.0	0.0	0.0	0.0	0.0
XNRR2_5007	3-oxoacyl-[acyl-carrier-protein] reductase	0.0	0.0	0.0	0.0	0.0
XNRR2_5131	Acyl-CoA synthetase	0.0	0.0	0.0	0.0	0.0
XNRR2_5492	3-oxoacyl-[acyl-carrier protein] reductase	0.0	0.0	0.0	0.0	0.0
XNRR2_5537	3-oxoacyl-[acyl-carrier protein] reductase	0.0	0.0	0.0	0.0	0.0
<b>Biotin biosynthesis</b>						
XNRR2_4025	Biotin-protein ligase	0.0	0.0	0.0	0.0	0.0
XNRR2_5558	Dethiobiotin synthetase	0.0	0.0	0.0	0.0	0.0
XNRR2_5559	Adenosylmethionine-8-amino-7-oxononanoate aminotransferase	0.0	0.0	0.0	0.0	0.0
XNRR2_5560	Biotin synthase	0.0	0.0	0.0	0.0	0.0
XNRR2_5561	8-amino-7-oxononanoate synthase	0.0	0.0	0.0	0.0	0.0
XNRR2_4025	Biotin-protein ligase	0.0	0.0	0.0	0.0	0.0

XNRR2_5558	Dethiobiotin synthetase	0.0	0.0	0.0	0.0	0.0
<b>Branched-chain amino acid biosynthesis</b>						
XNRR2_0081	Threonine dehydratase	0.0	0.0	0.0	0.0	0.0
XNRR2_0356	Thiamine pyrophosphate-requiring enzyme	0.0	0.0	0.0	0.0	0.0
XNRR2_1254	3-isopropylmalate dehydratase small subunit	0.0	0.0	0.0	0.0	0.0
XNRR2_1255	3-isopropylmalate dehydratase large subunit	0.0	0.0	0.0	0.0	0.0
XNRR2_1299	(R)-citramalate synthase	0.0	3.3	2.9	2.5	2.5
XNRR2_1304	Branched-chain amino acid aminotransferase	0.0	0.0	0.0	0.0	0.0
XNRR2_1305	3-isopropylmalate dehydrogenase	0.0	0.0	0.0	0.0	0.0
XNRR2_1319	Ketol-acid reductoisomerase	0.0	1.5	1.6	1.7	1.5
XNRR2_1320	Acetolactate synthase small subunit	0.0	2.1	2.1	2.0	2.0
XNRR2_1321	Acetolactate synthase large subunit	0.0	2.4	2.2	2.2	2.2
XNRR2_2513	Aminotransferase AlaT	0.0	0.0	0.0	0.0	0.0
XNRR2_3281	Threonine dehydratase	0.0	0.0	0.0	0.0	0.0
XNRR2_3504	Dihydroxy-acid dehydratase	0.0	0.0	0.0	0.0	0.0
XNRR2_4041	Threonine dehydratase	0.0	0.0	0.0	0.0	0.0
XNRR2_4064	Aspartate aminotransferase	0.0	1.1	0.0	0.0	0.0
XNRR2_4225	Acetolactate synthase	0.0	0.0	0.0	0.0	0.0
XNRR2_4410	2-isopropylmalate synthase	0.0	0.0	0.0	0.0	0.0
XNRR2_4438	Branched-chain amino acid aminotransferase	0.0	0.0	0.0	1.8	0.0
XNRR2_5309	Aminodeoxychorismate lyase	0.0	0.0	0.0	0.0	0.0
<b>Pantothenate and CoA biosynthesis</b>						
XNRR2_0356	Thiamine pyrophosphate-requiring enzyme	0.0	0.0	0.0	0.0	0.0
XNRR2_0487	Dihydropyrimidinase	0.0	1.2	0.0	2.1	0.0
XNRR2_0488	N-carbamoylputrescine amidase / Omegaamidase (Nit2-like protein)	0.0	0.0	0.0	1.9	0.0
XNRR2_0579	4'-phosphopantetheinyl transferase	0.0	0.0	0.0	0.0	0.0
XNRR2_1238	Phosphopantetheine adenylyltransferase	0.0	0.0	0.0	0.0	0.0
XNRR2_1304	Branched-chain amino acid aminotransferase	0.0	0.0	0.0	0.0	0.0
XNRR2_1319	Ketol-acid reductoisomerase	0.0	1.5	1.6	1.7	1.5
XNRR2_1320	Acetolactate synthase small subunit	0.0	2.1	2.1	2.0	2.0
XNRR2_1321	Acetolactate synthase large subunit	0.0	2.4	2.2	2.2	2.2
XNRR2_3418	Aldehyde dehydrogenase	0.0	0.0	0.0	0.0	0.0
XNRR2_3473	Pantoate--beta-alanine ligase	0.0	0.0	0.0	-1.5	0.0
XNRR2_3476	Type III pantothenate kinase	0.0	0.0	0.0	0.0	0.0
XNRR2_3504	Dihydroxy-acid dehydratase	0.0	0.0	0.0	0.0	0.0
XNRR2_3726	Aspartate 1-decarboxylase	0.0	0.0	0.0	0.0	0.0
XNRR2_3763	Pantothenate kinase	0.0	1.0	0.0	0.0	0.0
XNRR2_3772	Holo-[acyl-carrier protein] synthase	0.0	0.0	0.0	0.0	0.0
XNRR2_4007	Aldehyde dehydrogenase	0.0	0.0	0.0	0.0	0.0
XNRR2_4225	Acetolactate synthase	0.0	0.0	0.0	0.0	0.0
XNRR2_4438	Branched-chain amino acid aminotransferase	0.0	0.0	0.0	1.8	0.0
XNRR2_4623	3-methyl-2-oxobutanoate hydroxymethyltransferase	0.0	0.0	0.0	1.0	0.0
XNRR2_4832	2-dehydropantoate 2-reductase	0.0	0.0	0.0	0.0	0.0
XNRR2_4886	Dephospho-CoA kinase	0.0	0.0	0.0	0.0	0.0
XNRR2_5309	Aminodeoxychorismate lyase	0.0	0.0	0.0	0.0	0.0
XNRR2_5374	Phosphopantothencysteine decarboxylase / Phosphopantothencysteine synthetase	0.0	0.0	0.0	0.0	0.0

<b>Phosphotransferase system (PTS) &amp; central carbon metabolism entry</b>						
XNRR2_0026	Transcriptional repressor of the fructose operon, DeoR family	0.0	0.0	0.0	0.0	0.0
XNRR2_0027	1-phosphofructokinase	0.0	0.0	0.0	0.0	0.0
XNRR2_0028	PTS system, fructose-specific IIA component / PTS system, fructose-specific IIB component / PTS system, fructose-specific IIC component	0.0	-1.1	0.0	0.0	0.0
XNRR2_0029	Phosphotransferase system, phosphocarrier protein HPr	0.0	-1.6	-1.3	0.0	0.0
XNRR2_0030	Phosphoenolpyruvate-protein phosphotransferase of PTS system	0.0	0.0	0.0	0.0	0.0
XNRR2_0959	NADPH-dependent glyceraldehyde-3-phosphate dehydrogenase	0.0	-1.0	-1.6	0.0	0.0
XNRR2_0969	Substrate binding protein	0.0	0.0	0.0	0.0	0.0
XNRR2_0970	Integral membrane sugar transporter	0.0	-1.1	0.0	0.0	0.0
XNRR2_0971	Sugar ABC transporter permease	0.0	0.0	0.0	0.0	0.0
XNRR2_1023	Phosphocarrier protein HPr	0.0	0.0	0.0	0.0	0.0
XNRR2_2410	1-phosphofructokinase	0.0	0.0	0.0	0.0	0.0
XNRR2_4139	Fructose 1, 6-bisphosphatase II	0.0	-1.1	-1.9	0.0	0.0
XNRR2_4449	Pyruvate, phosphate dikinase	0.0	-1.2	0.0	0.0	0.0
XNRR2_4550	Hydrolase	0.0	0.0	-1.2	-1.3	-1.6
XNRR2_5287	Phosphatase	0.0	0.0	0.0	0.0	0.0
XNRR2_5450	Phosphoenolpyruvate-protein phosphotransferase of PTS system	0.0	0.0	0.0	1.1	0.0
XNRR2_5451	Phosphoenolpyruvate-dependent sugar phosphotransferase	0.0	0.0	0.0	1.3	0.0

**Table S4:** Gene expression of identified genes having potential regulatory functions in heterologous pamamycin producing *Streptomyces albus* J1074/R2 and *Streptomyces albus*  $\Delta bkdR/R2$  with supplemented L-valine in mannitol minimal medium during early growth (Early) and main production phase (Late). The expression level of the wildtype culture (J1074/R2) in minimal medium without amino acids during early growth (7h) was set as a reference. n = 3

Gene	Annotation	Control	J1074/R2 + Valine		$\Delta bkdR/R2$ + Valine	
		Late	Early	Late	Early	Late
XNRR2_0615	RNA polymerase sigma factor ECF subfamily	0.0	0.0	0.0	0.0	0.0
XNRR2_0683	RNA polymerase sigma factor ECF subfamily	0.0	0.0	0.0	0.0	0.0
XNRR2_0749	RNA polymerase sigma factor ECF subfamily	0.0	0.0	0.0	0.0	0.0
XNRR2_0776	ROK-family transcriptional regulator	0.0	0.0	0.0	0.0	0.0
XNRR2_1043	RNA polymerase, sigma 70 subunit, RpoD	0.0	0.0	0.0	0.0	0.0
XNRR2_1044	Sporulation transcription factor WhiH	4.8	0.0	0.0	-3.7	0.0
XNRR2_1071	PpGpp synthetase/hydrolase	0.0	1.2	0.0	0.0	0.0
XNRR2_1132	BldB protein	0.0	0.0	0.0	1.0	0.0
XNRR2_1222	[Protein-PII] uridylyltransferase	0.0	-2.1	-2.3	-1.4	-1.5
XNRR2_1223	Nitrogen regulatory protein P-II	0.0	-2.1	-2.3	-2.8	-2.3
XNRR2_1224	Ammonium transporter	-1.1	-2.3	-2.6	-2.5	-2.8
XNRR2_1225	NsdA	0.0	0.0	0.0	0.0	0.0
XNRR2_1256	Transcriptional regulator, IclR family	0.0	0.0	0.0	0.0	0.0
XNRR2_1391	Neutral zinc metalloprotease	0.0	-2.4	-2.3	0.0	-1.0
XNRR2_1515	RNA polymerase ECF-subfamily sigma factor	0.0	0.0	0.0	0.0	0.0
XNRR2_1539	arginine/ornithine binding protein	0.0	0.0	0.0	0.0	0.0
XNRR2_1554	Nucleotide-binding protein	5.0	0.0	0.0	0.0	0.0
XNRR2_1574	HTH-type transcriptional repressor dasR	0.0	0.0	0.0	0.0	0.0
XNRR2_1584	RNA polymerase sigma factor RpoE, ECF subfamily	0.0	0.0	0.0	0.0	0.0
XNRR2_1656	RNA polymerase sigma factor SigE, ECF subfamily	0.0	1.0	1.1	0.0	0.0
XNRR2_1798	sporulation and cell division protein SsgA	1.3	0.0	1.1	0.0	0.0
XNRR2_1962	Two-component system histidine kinase	0.0	0.0	0.0	0.0	0.0
XNRR2_1963	Two-component system response regulator	0.0	0.0	0.0	0.0	0.0
XNRR2_2142	RNA polymerase principal sigma factor hrdD	0.0	0.0	0.0	0.0	0.0
XNRR2_2151	Small membrane protein	3.5	0.0	0.0	-2.3	0.0
XNRR2_2166	RdIB protein	4.4	0.0	0.0	0.0	0.0
XNRR2_2167	RdIA protein	5.2	0.0	0.0	0.0	0.0
XNRR2_2231	Transcriptional regulator AfsR	0.0	0.0	0.0	0.0	0.0
XNRR2_2232	AfsS	0.0	0.0	0.0	0.0	0.0
XNRR2_2250	RNA polymerase ECF-subfamily sigma factor	0.0	0.0	0.0	0.0	0.0
XNRR2_2306	Factor C protein	0.0	0.0	0.0	1.1	0.0
XNRR2_2570	Phosphate regulon transcriptional regulatory protein PhoB (SphR)	0.0	0.0	0.0	0.0	0.0
XNRR2_2571	Phosphate regulon sensor protein PhoR (SphS)	0.0	0.0	0.0	0.0	0.0

XNRR2_2597	Universal stress protein UspA	0.0	0.0	0.0	0.0	0.0
XNRR2_2728	Transcriptional regulator, Crp/Fnr family	0.0	0.0	0.0	0.0	0.0
XNRR2_2735	WblA	0.0	0.0	0.0	0.0	0.0
XNRR2_2757	RNA polymerase ECF-subfamily sigma factor	0.0	0.0	0.0	0.0	0.0
XNRR2_2760	Hypothetical protein	0.0	0.0	0.0	0.0	0.0
XNRR2_2769	serine/threonine protein kinase	0.0	0.0	0.0	0.0	0.0
XNRR2_2903	RNA polymerase ECF-subfamily sigma factor	1.2	0.0	0.0	-1.8	-1.0
XNRR2_2943	SsgA	0.0	0.0	0.0	0.0	0.0
XNRR2_2992	RNA polymerase sigma factor SigM, ECF subfamily	0.0	0.0	0.0	0.0	0.0
XNRR2_3046	Hypothetical protein	0.0	0.0	0.0	1.2	0.0
XNRR2_3174	LuxR-family transcriptional regulator	-1.6	0.0	0.0	0.0	0.0
XNRR2_3275	RNA polymerase ECF sigma factor	0.0	0.0	0.0	0.0	0.0
XNRR2_3298	ECF subfamily RNA polymerase sigma-70 factor	0.0	0.0	0.0	0.0	0.0
XNRR2_3323	GlnR-family transcriptional regulator	0.0	0.0	0.0	0.0	0.0
XNRR2_3489	RNA polymerase sigma factor, ECF subfamily	0.0	0.0	0.0	0.0	0.0
XNRR2_3527	BldN RNA polymerase, sigma-24 subunit, ECF subfamily	4.3	0.0	-1.3	-1.7	0.0
XNRR2_3720	30S ribosomal protein S12	0.0	0.0	0.0	0.0	0.0
XNRR2_3805	RpoH RNA polymerase, sigma 32 subunit, ECF subfamily	1.4	0.0	0.0	0.0	0.0
XNRR2_3945	ECF sigma factor	0.0	0.0	0.0	0.0	0.0
XNRR2_3984	RNA polymerase, sigma subunit, ECF family	0.0	0.0	0.0	0.0	0.0
XNRR2_3996	Two-component system sensor histidine kinase AfsQ2	0.0	0.0	0.0	0.0	0.0
XNRR2_3997	Two-component system response regulator AfsQ1	0.0	0.0	0.0	0.0	0.0
XNRR2_3998	RNA polymerase ECF-subfamily sigma factor	0.0	1.5	1.6	0.0	0.0
XNRR2_4039	RNA polymerase ECF-subfamily sigma factor	0.0	0.0	0.0	0.0	0.0
XNRR2_4181	AraC-family transcriptional regulator	1.2	0.0	0.0	0.0	0.0
XNRR2_4476	RNA polymerase, sigma 70 subunit, RpoD	0.0	0.0	0.0	1.4	0.0
XNRR2_4658	Glutamine synthetase	-1.0	-1.9	-2.1	-2.3	-2.0
XNRR2_4681	Gamma butyrolactone receptor protein	0.0	0.0	0.0	0.0	0.0
XNRR2_5022	Hypothetical protein	0.0	0.0	0.0	0.0	0.0
XNRR2_5117	TetR-family transcriptional regulator	0.0	0.0	0.0	0.0	0.0
XNRR2_5152	small membrane protein	3.5	0.0	0.0	0.0	0.0
XNRR2_5153	secreted protein	3.1	0.0	0.0	0.0	0.0
XNRR2_5208	RNA polymerase sigma factor SigK, ECF subfamily	0.0	0.0	0.0	0.0	0.0
XNRR2_5283	RNA polymerase ECF-subfamily sigma factor	0.0	0.0	2.0	1.5	0.0
XNRR2_5315	Sporulation and cell division protein SsgA	0.0	0.0	0.0	0.0	0.0
XNRR2_5340	(P)ppGpp synthetase, SpoT/RelA	0.0	0.0	0.0	0.0	0.0
XNRR2_5362	Pleiotropic negative regulator BldD	0.0	0.0	0.0	0.0	0.0
XNRR2_5529	RNA polymerase ECF-subfamily sigma factor	0.0	0.0	0.0	0.0	0.0
XNRR2_5625	RNA polymerase, sigma-24 subunit, ECF subfamily	0.0	3.5	3.1	2.4	0.0
XNRR2_5652	RNA polymerase sigma factor SigL, ECF subfamily	0.0	0.0	1.9	1.6	0.0
XNRR2_5893	ECF subfamily RNA polymerase sigma factor	0.0	-2.6	-2.5	-2.3	0.0

**Table S5:** Gene expression of phosphopantetheinyl transferases in heterologous pamamycin producing *Streptomyces albus* J1074/R2 and *Streptomyces albus*  $\Delta bkdR/R2$  with supplemented L-valine in mannitol minimal medium during early growth (Early) and main production phase (Late). The expression level of the wildtype culture (J1074/R2) in minimal medium without amino acids during early growth (7h) was set as a reference. n = 3

Gene	Annotation	Control Late	J1074/R2 + Valine		$\Delta bkdR/R2$ + Valine	
			Early	Late	Early	Late
XNRR2_0579	4'-phosphopantetheinyl transferase	0.0	0.0	0.0	0.0	0.0
XNRR2_1238	Phosphopantetheine adenylyltransferase	0.0	0.0	0.0	0.0	0.0
XNRR2_5716	Sfp-type phosphopantetheinyl transferase	0.0	0.0	0.0	0.0	0.0

**Table S6:** Gene expression of acetyl-CoA carboxylases and transcriptional regulator *AccR* homolog in heterologous pamamycin producing *Streptomyces albus* J1074/R2 and *Streptomyces albus*  $\Delta bkdR/R2$  with supplemented L-valine in mannitol minimal medium during early growth (Early) and main production phase (Late). The expression level of the wildtype culture (J1074/R2) in minimal medium without amino acids during early growth (7h) was set as a reference. n = 3

Gene	Annotation	Control	J1074/R2 + Valine		$\Delta bkdR/R2$ + Valine	
		Late	Early	Late	Early	Late
XNRR2_2273	Acetyl/propionyl CoA carboxylase alpha subunit	0.0	0.0	0.0	0.0	0.0
XNRR2_2274	Acetyl/propionyl CoA carboxylase, beta subunit	0.0	0.0	0.0	0.0	0.0
XNRR2_4211	Acetyl/propionyl CoA carboxylase alpha subunit	0.0	2.8	3.1	4.6	3.4
XNRR2_4212	Acetyl/propionyl CoA carboxylase	0.0	2.6	2.7	4.3	2.9
XNRR2_4213	TetR-family transcriptional regulator	0.0	1.6	1.1	0.0	0.0

```

sco_SCO3832      -----ATG
salb_XNR_3053    ATGGCCGAACAGCCGGCACCCAGACCACTGGACGCCGTCGACAGGGACATCCTGCGACTG
                      **

sco_SCO3832      CTCAGGGCGGACGGCCGCGCCTCCATACGGTCGGTCGCGGAGCGGGTGACAGTCTCGCGC
salb_XNR_3053    CTCAGGGCGGACGGCCGCGCCTCGATCCGGTCGGTGGCCGACACCGTCCACGTCTCGCGC
                      ***** ** ***** ** * *****

sco_SCO3832      GCGAACGCCTACGCCCGCATCAACCGCCTGGTTGAGGACGGCGTGATCCGGGCTTCGGC
salb_XNR_3053    GCCAACGCCTACGCCCGCATCAACCGCCTCATGGAGGACGGCGTCATCCGGGGTTTCGGC
                      ** ***** * ***** ** *****

sco_SCO3832      GCCGCGTCGACCACGAGCGCGCCGGGCACGGCACCTCGGCGTACATCACCTGAAGATC
salb_XNR_3053    GCCGCGTCGACCACGAGCGCGCCGGGCACGGCGCTCGGCGTACATCACCTGAAGATC
                      ***** ** ** ** * *****

sco_SCO3832      GTCCAGAACTCCTGGCGGACGGTCCGCGCCAGCTGCGGCAGCTGCCCGGGCCTCGCAC
salb_XNR_3053    GTCCAGAACTCCTGGCGCACCATCCGCGAGGAACTCCGCCAGCTCCCGGGCGCCGCCAC
                      ***** ** ***** * ** * ***** ** * **

sco_SCO3832      ATCGCCCTGGTGGGCGGCGACTTCGACGTCCTGCTGCTGGTGACACGCGGACAACCGG
salb_XNR_3053    ATCGCCCTGGTCAGCGGCGACTTCGACGTCCTCCTCATGATCCACGCGCCGACAACCGC
                      ***** ***** ** * ** * ** * * *****

sco_SCO3832      GCCCTGCGCGAGCTGGTGCTCAGCCGCTCCAGGCCATCCCCGAGGTGCTCAGCACCCGC
salb_XNR_3053    GCCCTGCGCGAACTCGTCCTCACCCGCTCCAGTCCATCCCCGACGTCCTCTCGACCAGA
                      ***** ** ** ***** ***** ***** ** ** *

sco_SCO3832      ACCCTGCTGGTCTTCGAGACGGAGGACCTCGAACCGCAGGGCTGA
salb_XNR_3053    ACCCTCCTGGTCTTCGAGGAGGAGGAACTGTCACCGGAGGGGTGA
                      ***** ***** ** ***** **

```

Identities =339/407 83%  
Expect 2e-120

**Figure S1:** Alignment of the gene encoding the branched-chain amino acid dehydrogenase regulator *bkdR* of *Streptomyces coelicolor* (sco\_SCO3832) and its homolog *salb\_XNR\_3053* in *Streptomyces albus* J1074. The sequences exhibit a homology of 83% and an expected value of 2e-120.

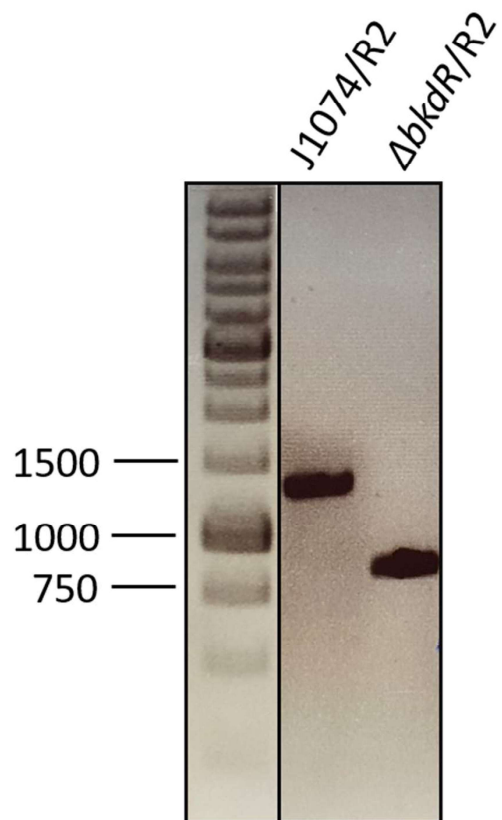


**Figure S2:** Verification of the deletion of XNRR2\_3053 in *Streptomyces albus* J1074/R2 using PCR. The primer pair 3053\_ch\_Fw and 3053\_ch\_rev was used to prove the deletion.

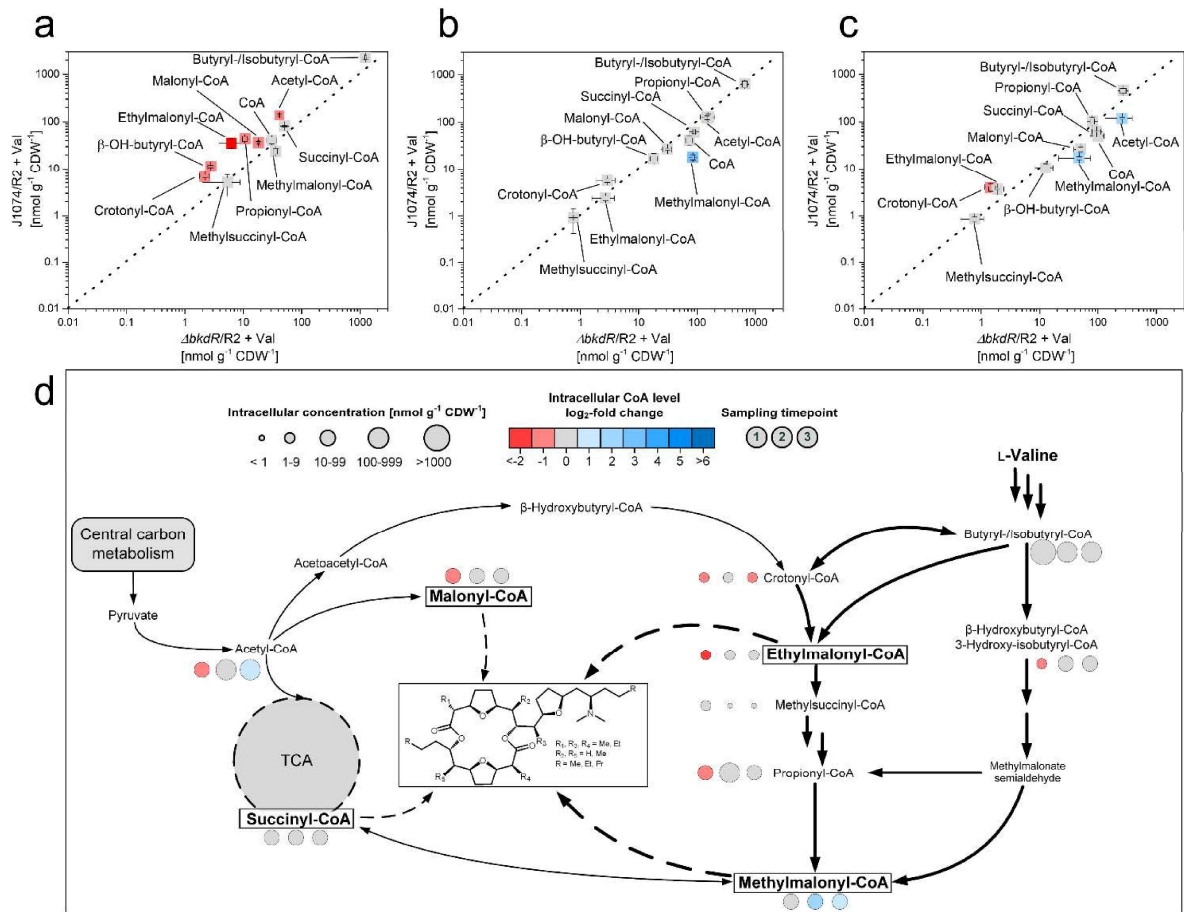


**Figure S3: Dynamics of intracellular CoA thioesters during pamamycin production in *Streptomyces albus* J1074/R2  $\Delta bkdR$ .** The data show the correlation of absolute levels between wildtype (J1074/R2) and mutant at three different timepoints (a, b, and c). In addition, the data are mapped on the pathways of CoA thioester metabolism, whereby the size of the given circles represents the absolute concentrations at each timepoint (1, 2, 3), and the color represents the respective  $\log_2$ -fold change, as compared to the wild type /R2. n = 3

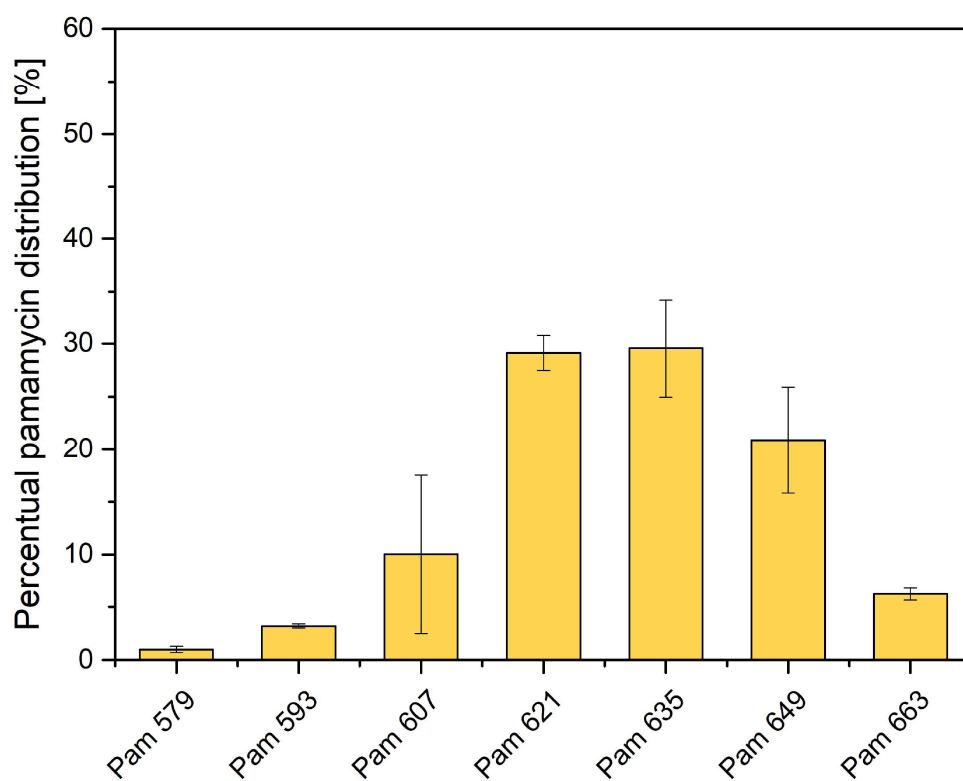


**Figure S4:** Molecular weight distribution of pamamycin, newly produced during the stationary phase by *Streptomyces albus* J1074/R2  $\Delta bkdR$  on a mannitol-based medium, supplemented with 3 mM L-valine. The spectrum is inferred by differential calculation, considering the pamamycin spectrum at the end of the growth phase (28 h) when all carbon was depleted and at the process end after 48 hours. n = 3

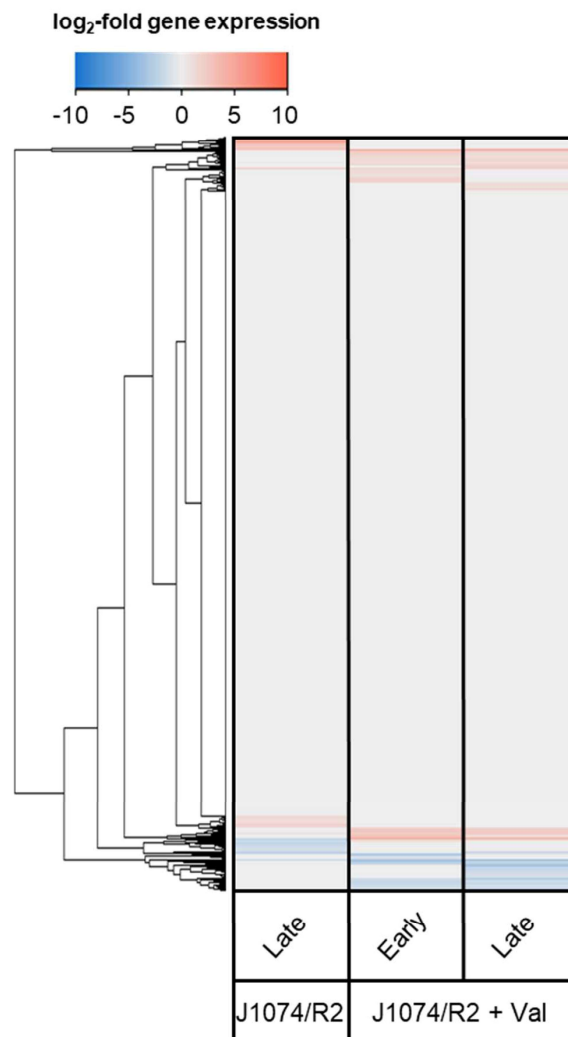


**Figure S5:** Hierarchical cluster analysis of global gene expression of *S. albus* J1074/R2 on a minimal mannitol medium, supplemented with 3 mM L-valine and without L-valine. Samples were taken after 7 h (Early) and 18 h (Late). The gene expression of the control culture during early growth (7 h) was set as reference. n = 3



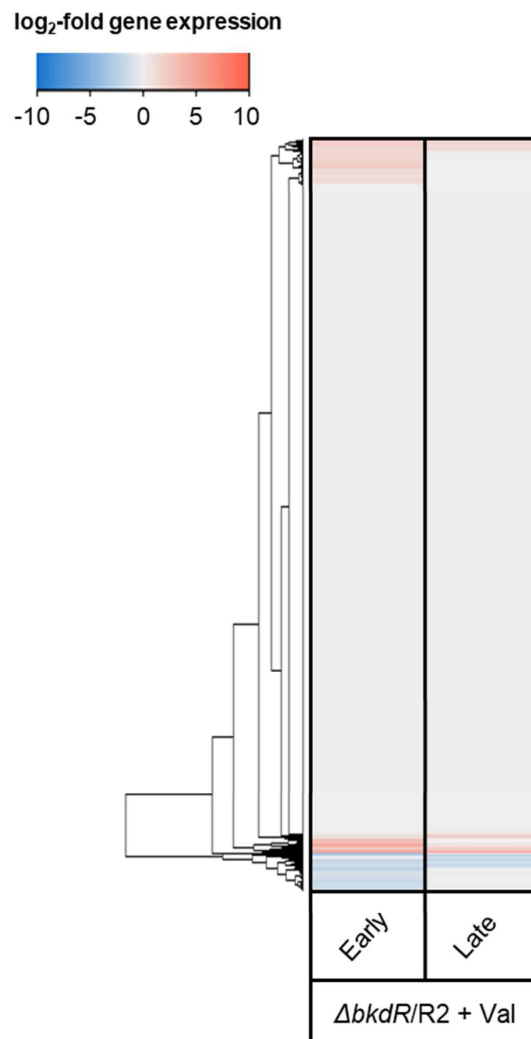


**Figure S6:** Hierarchical cluster analysis of global gene expression of *S. albus* J1074/R2 *ΔbkdR* on a minimal mannitol medium, supplemented with 3 mM L-valine. Samples were taken after 7 h (Early) and 18 h (Late). The gene expression of the control (wild type without L-valine) during early growth (7 h) was set as reference. n = 3

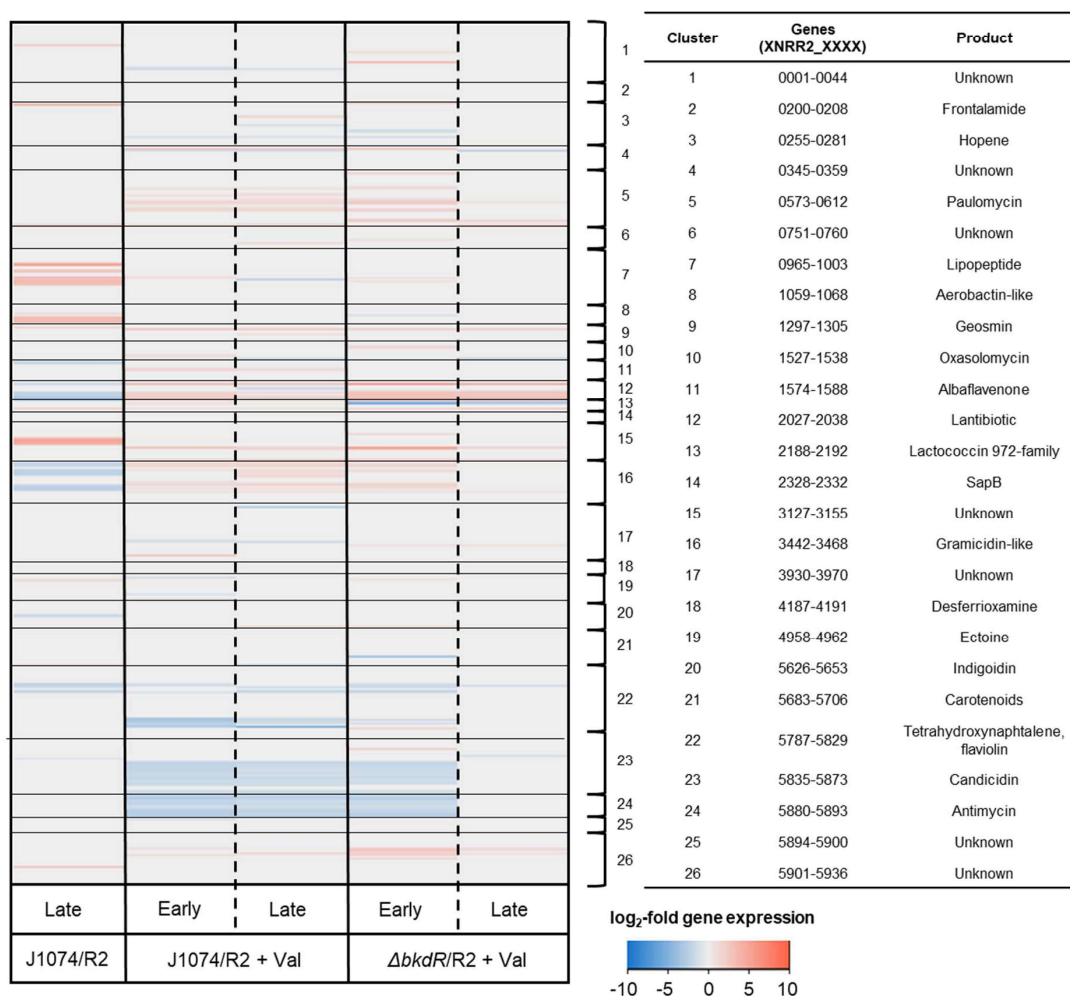


**Figure S7:** Gene expression of secondary metabolite clusters of *S. albus* J1074/R2 and its mutant *S. albus* J1074/R2  $\Delta bkdR$  in minimal mannitol medium, partially supplemented with 3 mM L-valine (+Val). Samples were taken after 7 h (Early) and 18 h (Late). The identified secondary metabolite clusters relate to previous work [3]. The gene expression of the control (wild type without L-valine) during early growth (7 h) was set as reference. n = 3

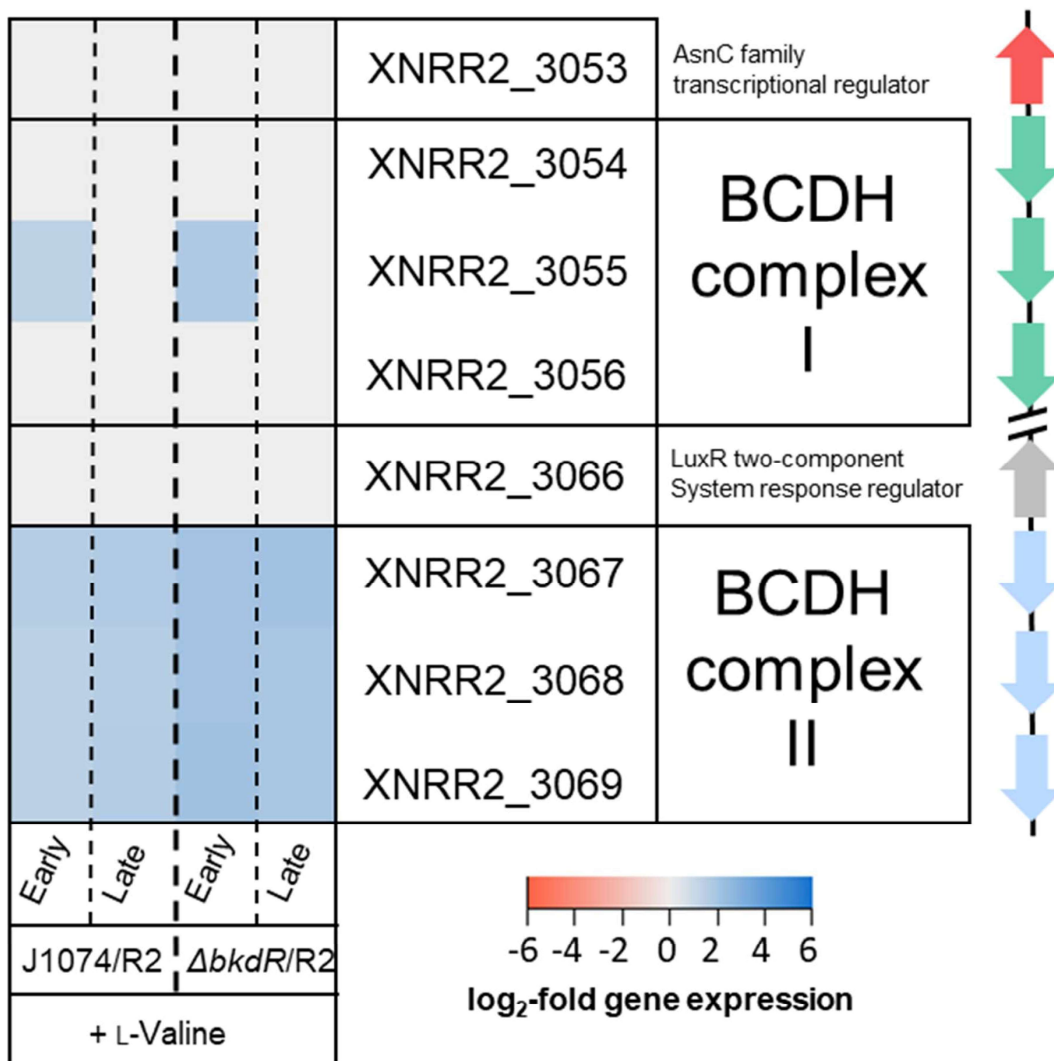


**Figure S8:** Gene expression of the two branched-chain amino acid dehydrogenase (BCDH) complexes in *Streptomyces albus* J1074/R2 and *S. albus* J1074/R2  $\Delta bkdR$  in minimal mannitol medium, supplemented with 3 mM L-valine. Samples were taken after 7 h (Early) and 18 h (Late). The gene expression of the control (wild type without L-valine) during early growth (7 h) was set as reference. n = 3

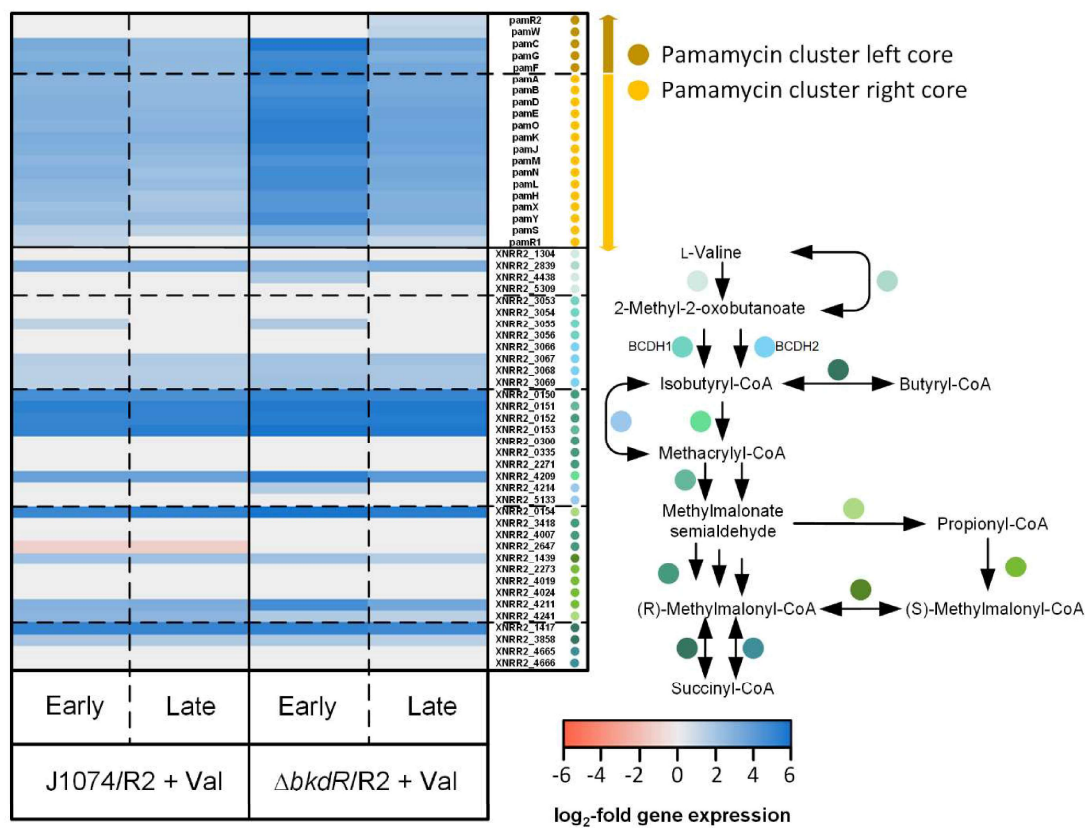


**Figure S9:** Expression of the pamamycins biosynthetic gene cluster and genes related to L-valine degradation in *Streptomyces albus* J1074/R2 and *Streptomyces albus*  $\Delta bkdR/R2$ . The pamamycin cluster genes are sorted according to their affiliation of the individual cores (left and right core) [4]. The L-valine degradation genes are sorted in relation to the KEGG-based pathway. Samples were taken after 7 h (Early) and 18 h (Late). The gene expression of the control (wild type without L-valine) during early growth (7 h) was set as reference. n = 3

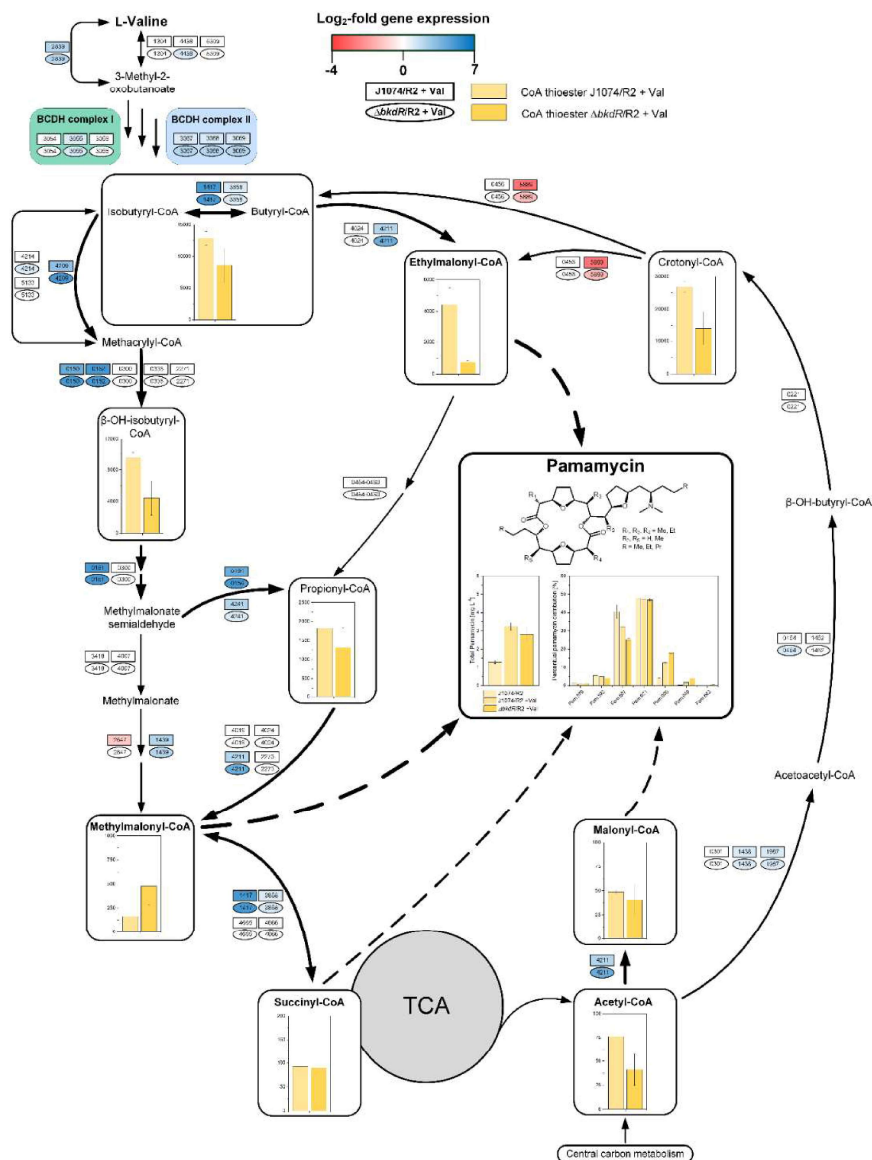


**Figure S10:** Multi-omics view on the effect of supplemented L-valine on pamamycin biosynthesis and supporting pathways in *Streptomyces albus* J1074/R2 and its mutant *Streptomyces albus*  $\Delta bkdR/R2$ . The box colors display the differential gene expression of J1074/R2 (rectangle) and its mutant (ellipse) during the early growth phase (7 h). The numbers inside the boxes indicate the specific gene number (XNRR2\_XXXX). The bar charts display the relative intracellular CoA thioester levels at the same time point. The values from the wild type without L-valine (Control) was set to 100%.

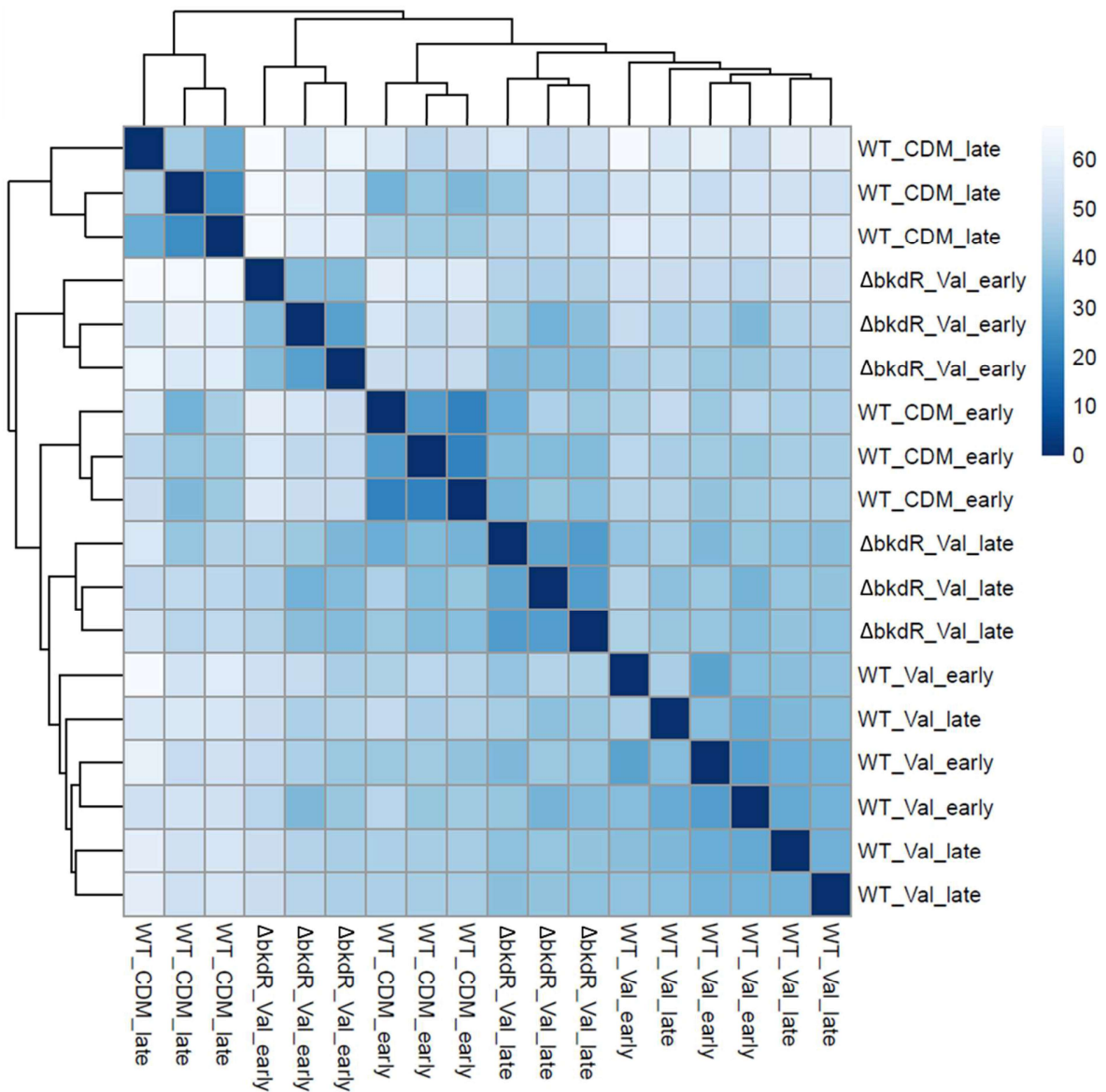


**Figure S11:** Heatmap of the sample-to-sample distances from the RNA sequencing data. The background corrected read count data were fed to DESeq2 [5] to calculate normalized read counts. After regularized log transformation with blind dispersion estimation enabled, the sample-to-sample distances were calculated and used for hierarchical clustering, which in turn was visualized using pheatmap [6].

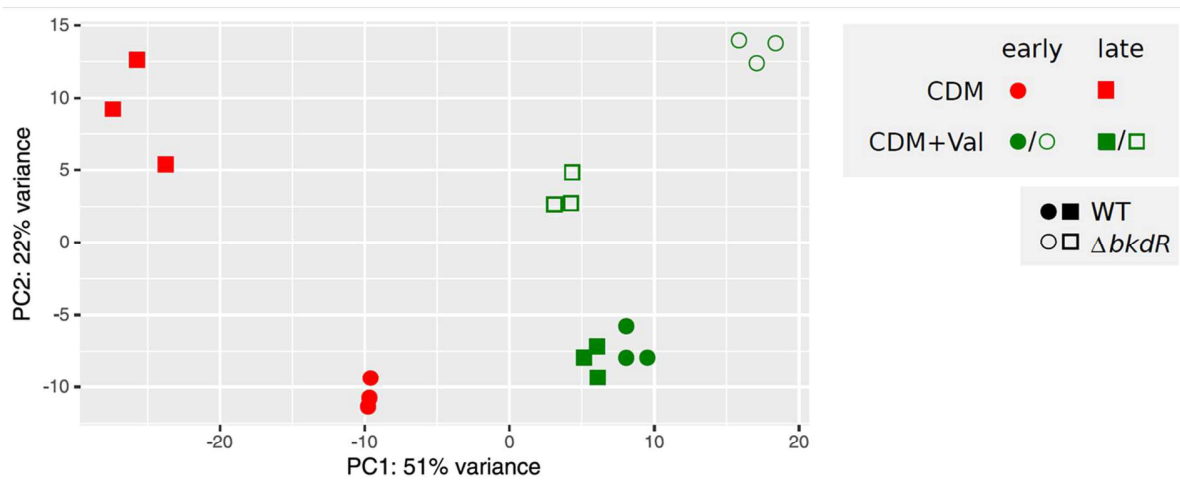


**Figure S12:** PCA of the RNA seq data. The background corrected read count data were fed to DESeq2 to calculate normalized read counts. After regularized log transformation with blind dispersion estimation enabled, a PCA was performed and visualized using ggplot2 [7].

## Literature

1. Kieser T. Bibb M. Buttner M. Chater K. Hopwood D: **Practical Streptomyces Genetics** John Innes Foundation. Norwich. United Kingdom 2000.
2. Barton N. Horbal L. Starck S. Kohlstedt M. Luzhetskyy A. Wittmann C: **Enabling the valorization of guaiacol-based lignin: Integrated chemical and biochemical production of cis.cis-muconic acid using metabolically engineered *Amycolatopsis* sp ATCC 39116.** *Metabolic engineering* 2018. **45**:200-210.
3. Lopatniuk M. Myronovskyi M. Nottebrock A. Busche T. Kalinowski J. Ostash B. Fedorenko V. Luzhetskyy A: **Effect of "ribosome engineering" on the transcription level and production of *S. albus* indigenous secondary metabolites.** *Applied microbiology and biotechnology* 2019. **103**:7097-7110.
4. Kuhl M. Gläser L. Rebets Y. Rückert C. Sarkar N. Hartsch T. Kalinowski J. Luzhetskyy A. Wittmann C: **Microparticles globally reprogram the metabolism of *Streptomyces albus* towards accelerated morphogenesis. streamlined carbon core metabolism and enhanced production of the antituberculosis polyketide pamamycin.** *Biotechnology & Bioengineering* 2020. *submitted*.
5. Love MI. Huber W. Anders S: **Moderated estimation of fold change and dispersion for RNA-seq data with DESeq2.** *Genome biology* 2014. **15**:550.
6. Kolde R: **Pheatmap: Pretty Heatmaps. R Package Version 1.0.12.** 2019.
7. Wickham H: **ggplot2: elegant graphics for data analysis.** *Springer* 2016.

### 7.3 Supplementary Information Kuhl et al. 2020

#### **Microparticles globally reprogram *Streptomyces albus* toward accelerated morphogenesis, streamlined carbon core metabolism, and enhanced production of the antituberculosis polyketide pamamycin**

Martin Kuhl, Lars Gläser, Yuriy Rebets, Christian Rückert, Namrata Sarkar, Thomas Hartsch, Jörn Kalinowski, Andriy Luzhetskyy, and Christoph Wittmann

*Biotechnology and Bioengineering*. 2020; 117: 3858– 3875.

<https://doi.org/10.1002/bit.27537>

This is an open access article distributed under the terms of the Creative Commons CC BY license.

C. W. designed the project. M. K. conducted the cultures. M. K. and Y. R. performed pamamycin analysis. M. K. and L. G. performed CoA ester analysis. C. R. and J. K. performed RNA sequencing. C. R., J. K., N. S., and T. H. processed and evaluated the RNA sequencing data. M. K. and C. W. analyzed the data, drew the figures, and wrote the first draft of the manuscript. All authors commented, extended, and improved the manuscript. All authors read and approved the final version of the manuscript.

**Supplementary information to**

**Microparticles globally reprogram *Streptomyces albus* towards accelerated morphogenesis, streamlined carbon core metabolism and enhanced production of the antituberculosis polyketide pamamycin**

***Biotechnology and Bioengineering***

Martin Kuhl<sup>1</sup>, Lars Gläser<sup>1</sup>, Yuriy Rebets<sup>2</sup>, Christian Rückert<sup>3</sup>, Namrata Sarkar<sup>4</sup>, Thomas Hartsch<sup>4</sup>, Jörn Kalinowski<sup>3</sup>, Andriy Luzhetskyy<sup>2</sup>, and Christoph Wittmann<sup>1\*</sup>

<sup>1</sup> Institute of Systems Biotechnology, Saarland University, Saarbrücken, Germany

<sup>2</sup> Pharmaceutical Biotechnology, Saarland University, Saarbrücken, Germany

<sup>3</sup> Center for Biotechnology, Bielefeld University, Bielefeld, Germany

<sup>4</sup> Genedata AG, Basel, Switzerland

\* Phone: 0049-681-302-71971, FAX: -71972, Email: christoph.wittmann@uni-saarland.de

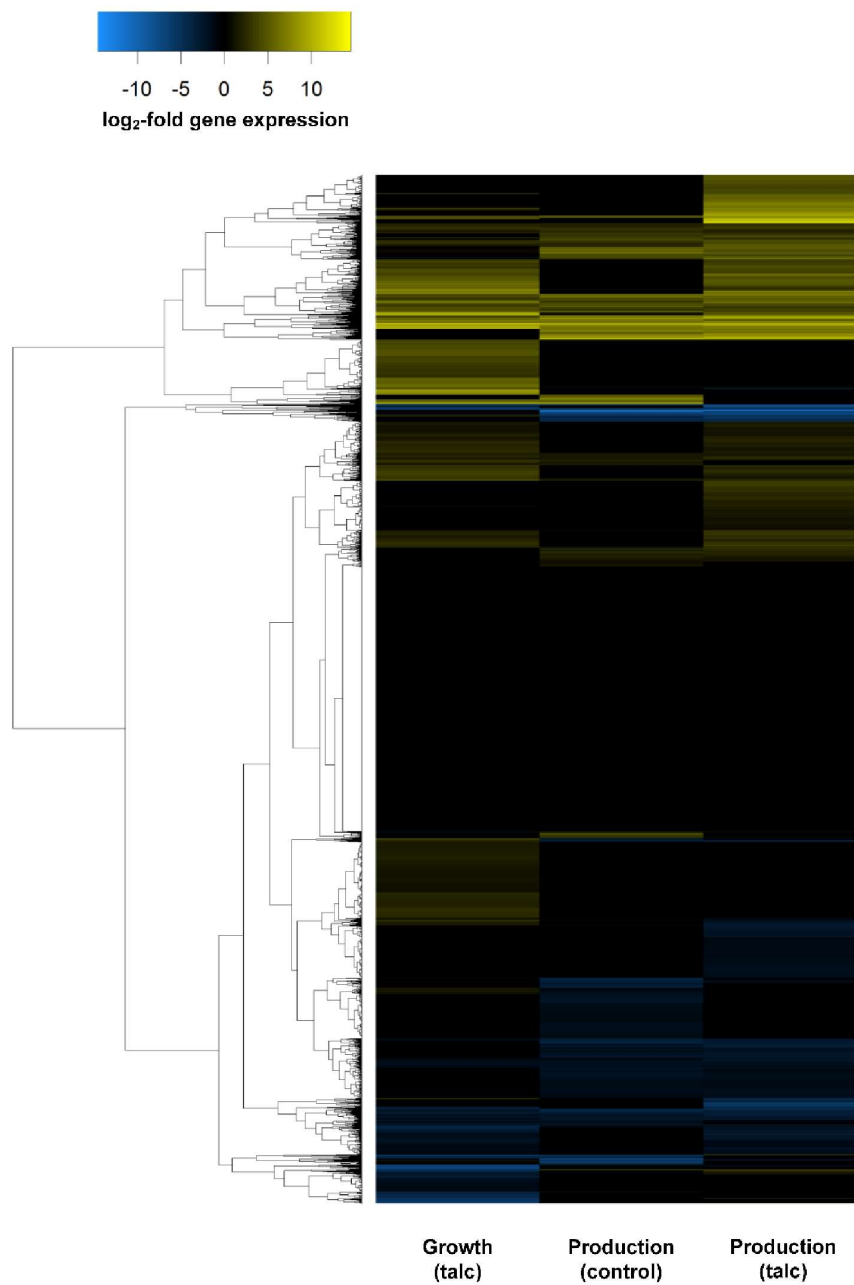


**Figure S1: Hierarchical cluster analysis of global gene expression of *S. albus* J1074/R2 in liquid SGG medium.** Samples were taken from a control and a talc supplied culture (10 g L<sup>-1</sup>) during exponential growth and production phase. The sample out of the control culture during growth was set as reference.

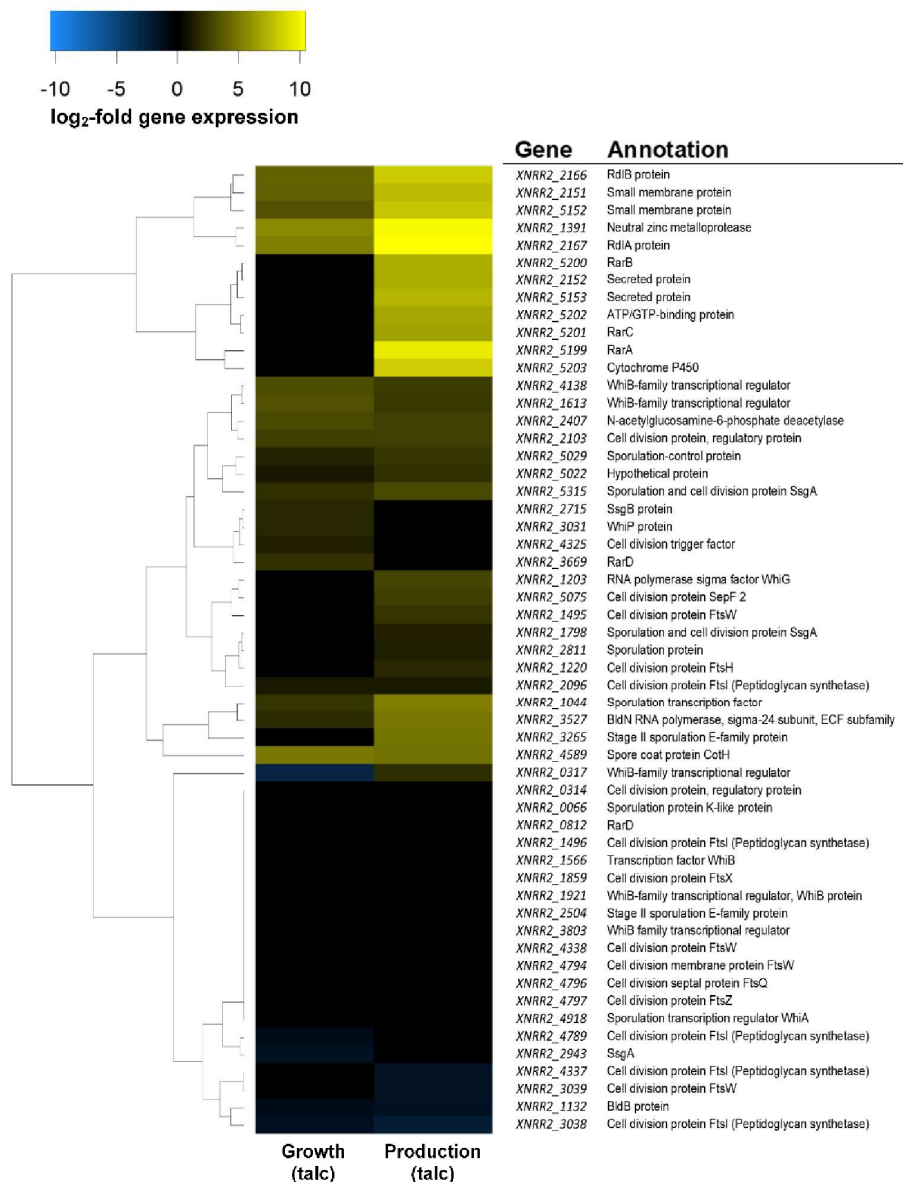


**Figure S2: Hierarchical cluster analysis of gene expression for genes linked to the control of morphology and secondary metabolism in pamamycin producing *Streptomyces albus* J1074/R2.** Samples were taken from a control and a talc supplied culture ( $10 \text{ g L}^{-1}$ ) in SGG medium during exponential growth (5 h) and production phase (21 h). For comparison, the expression levels of the control culture during growth were set as reference. Shown are the relative changes of the talc supplied culture during growth and production.

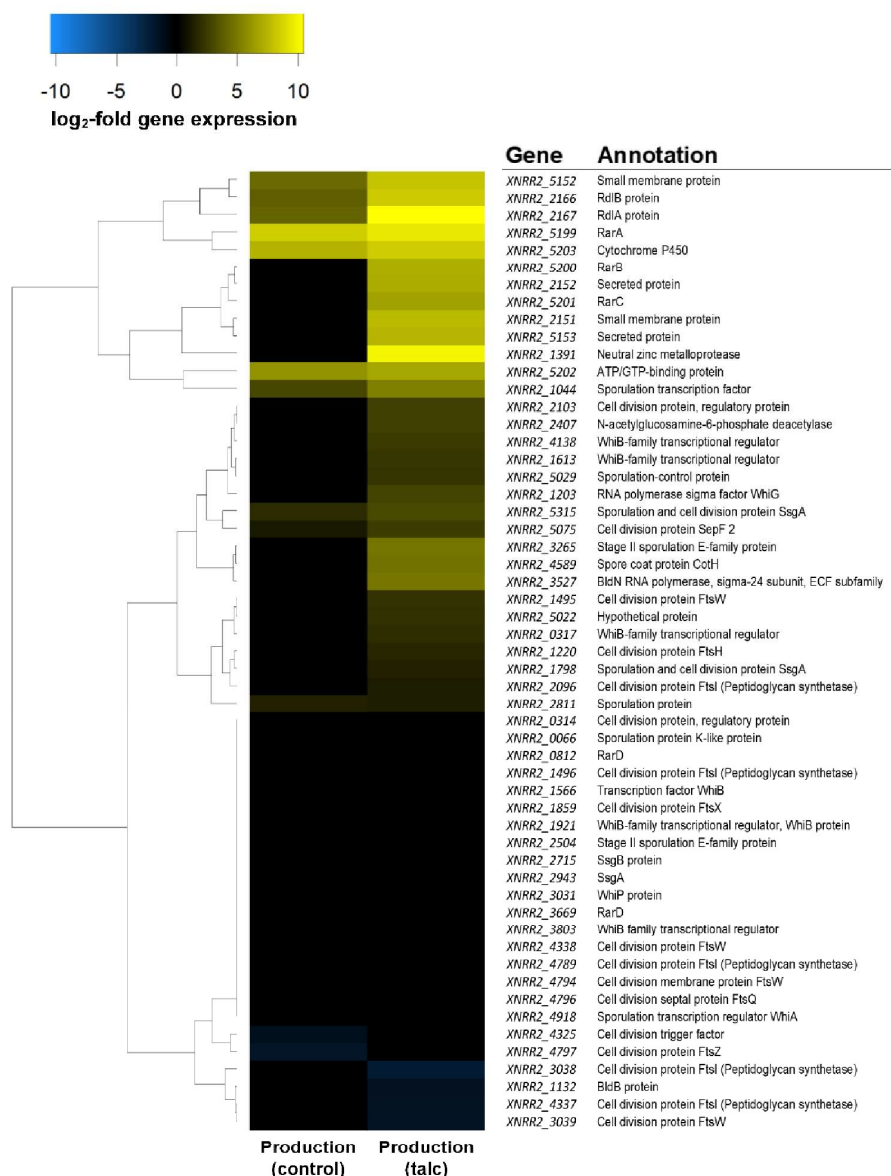


**Figure S3: Hierarchical cluster analysis of gene expression for genes linked to the control of morphology and secondary metabolism in pamamycin producing *Streptomyces albus* J1074/R2.** Samples were taken from a control and a talc supplied culture ( $10 \text{ g L}^{-1}$ ) in SGG medium during exponential growth (5 h) and production phase (21 h). For comparison, the expression levels of the control culture during growth were set as reference. Shown are the relative changes of the control culture and the talc supplied culture during production.

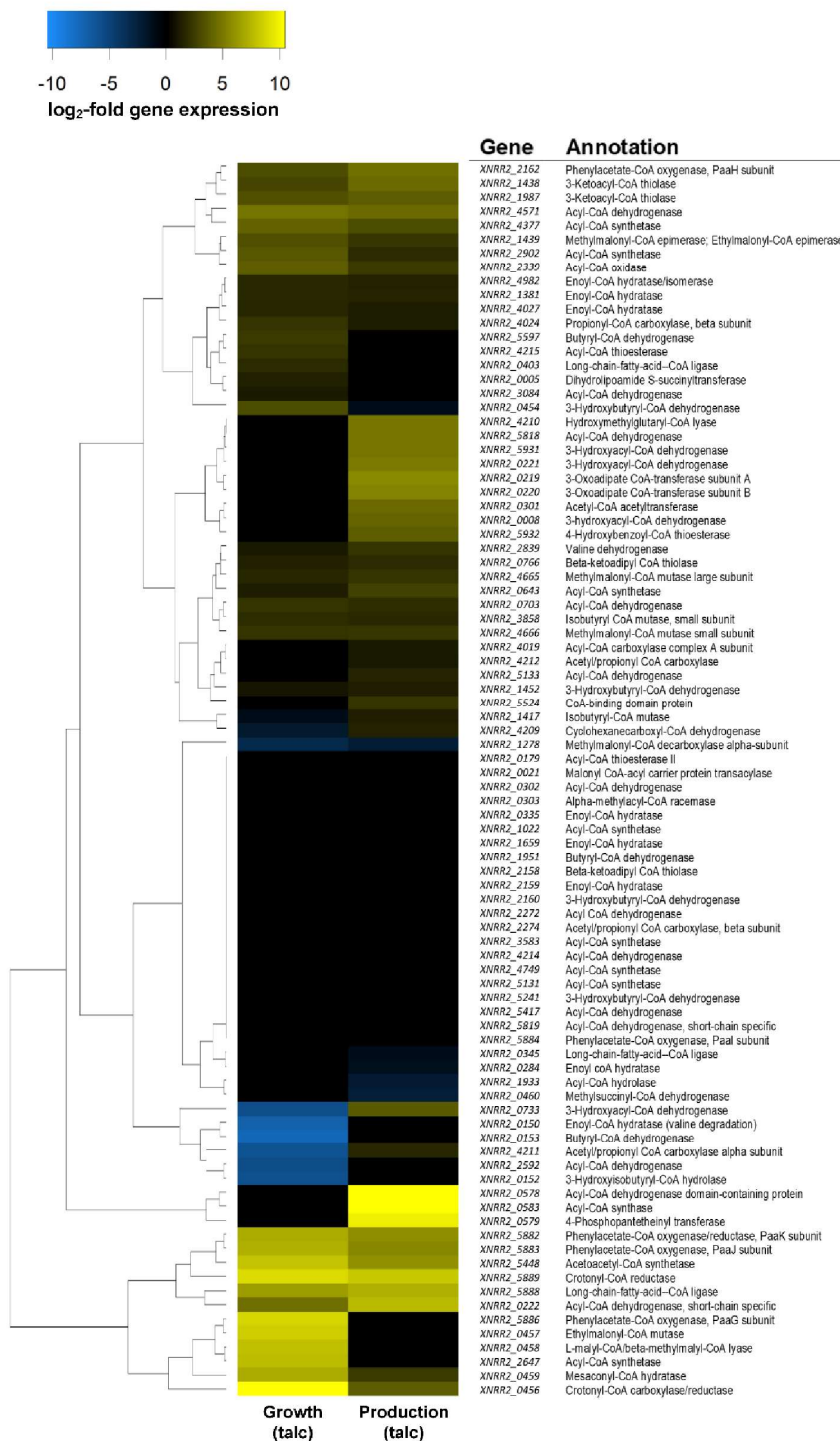


**Figure S4: Hierarchical cluster analysis of gene expression for genes linked to CoA-ester metabolism in pamamycin producing *Streptomyces albus* J1074/R2.** Samples were taken from a control and a talc supplied culture (10 g L<sup>-1</sup>) in SGG medium during exponential growth (5 h)

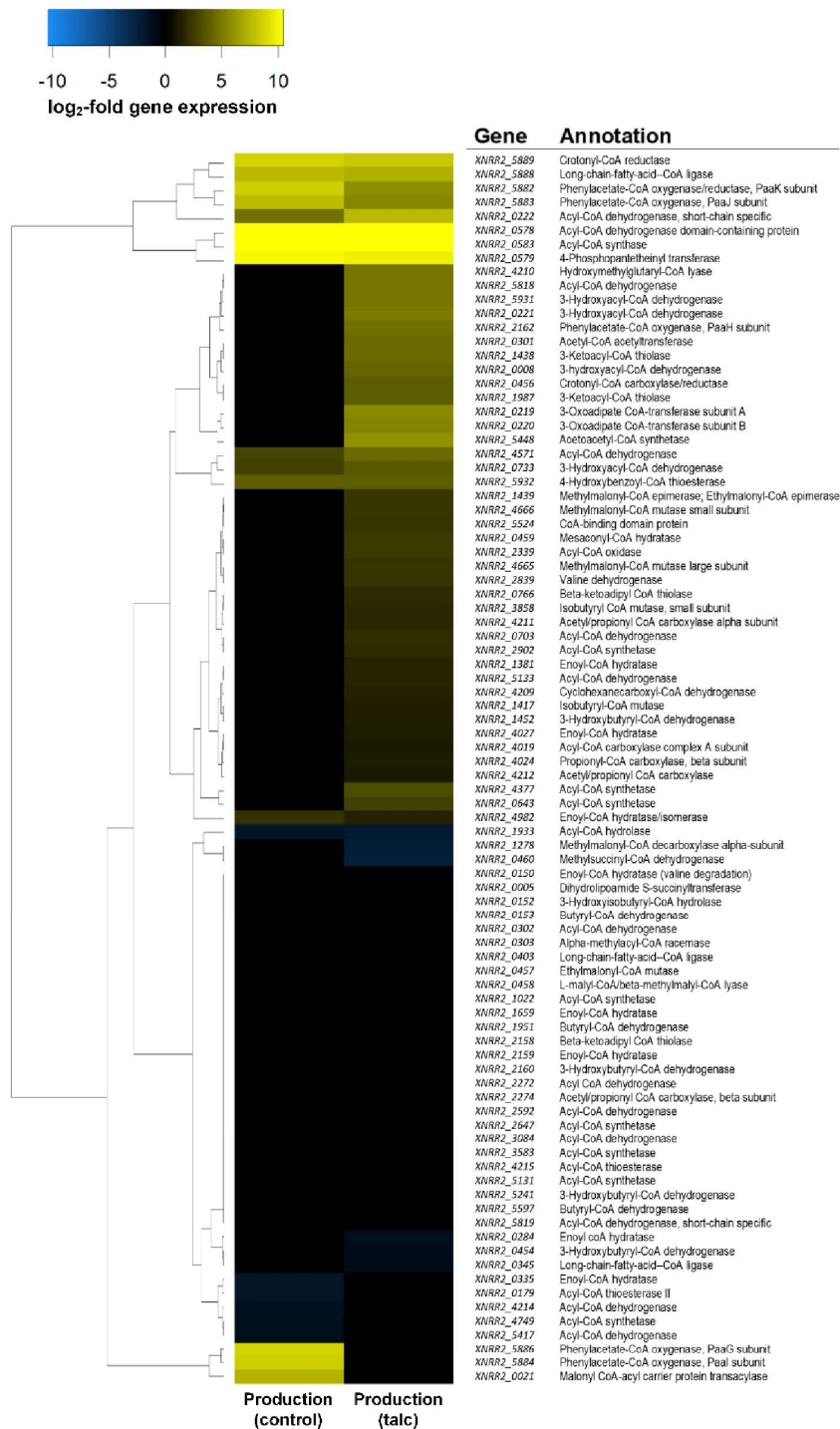


**Figure S5: Hierarchical cluster analysis of gene expression for genes linked to CoA-ester metabolism in pamamycin producing *Streptomyces albus* J1074/R2.** Samples were taken from a control and a talc supplied culture (10 g L<sup>-1</sup>) in SGG medium during exponential growth (5 h)

and production phase (21 h). For comparison, the expression levels of the control culture during growth were set as reference. Shown are the relative changes of the control culture and the talc supplied culture during production.

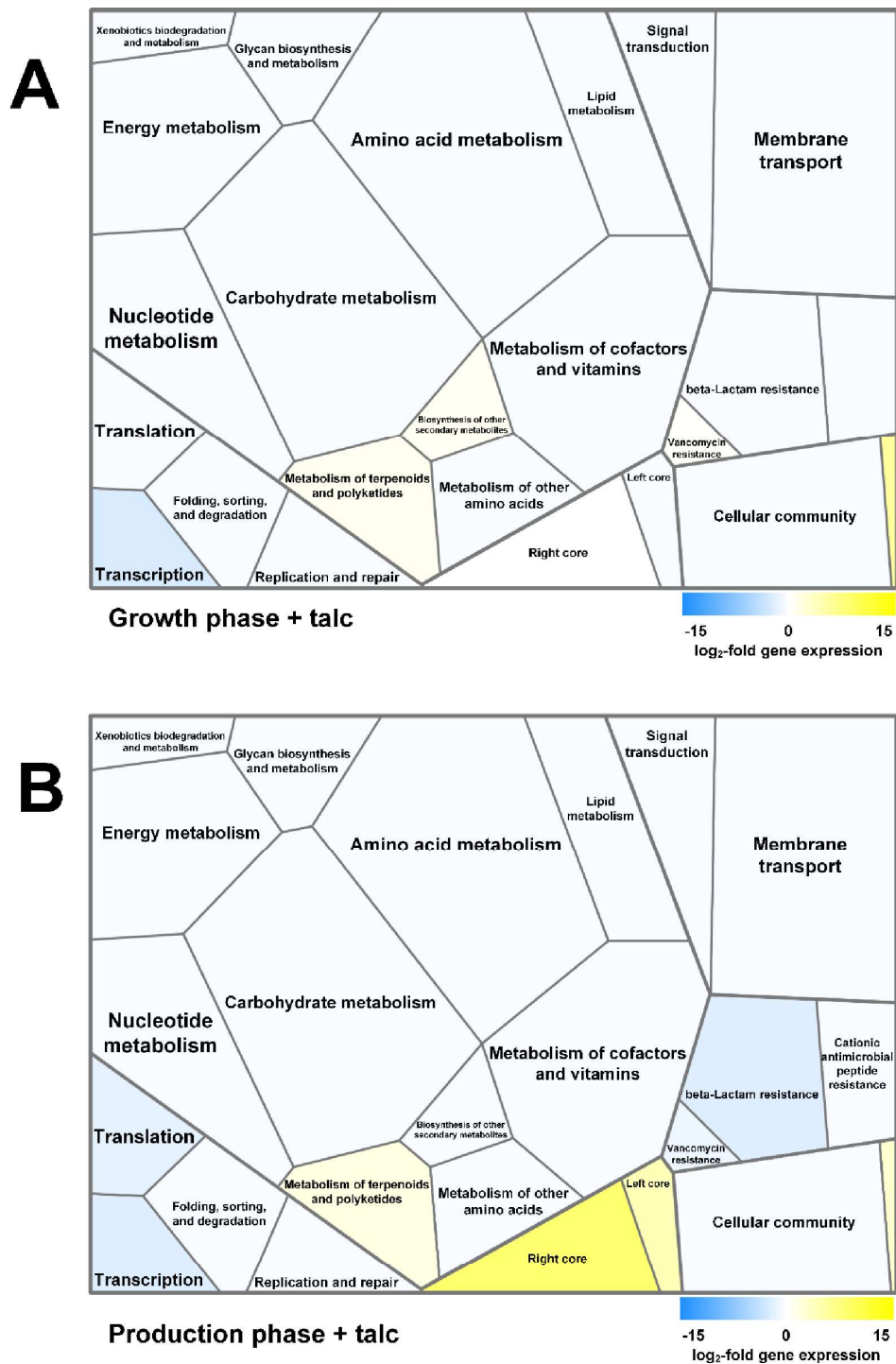


**Figure S6: KEGG-orthology tree maps of talc supplied *Streptomyces albus* J1074/R2. Average gene expressions of growing (A) and producing (B) *S. albus* J1074/R2 in complex SGG medium**

with addition of 10 g L<sup>-1</sup> talc compared to a control culture in growth phase. Each cell represents a functional class of the orthology: Carbohydrate metabolism, amino acid metabolism, lipid metabolism, nucleotide metabolism, energy metabolism, glycan biosynthesis and metabolism, xenobiotics biodegradation and metabolism, metabolism of cofactors and vitamins, metabolism of terpenoids and polyketides, biosynthesis of other secondary metabolites, metabolism of other amino acids, signal transduction, membrane transport, replication and repair, transcription, translation, folding, sorting and degradation, cellular community, cell motility, and the right and left core of the pamamycin gene cluster.

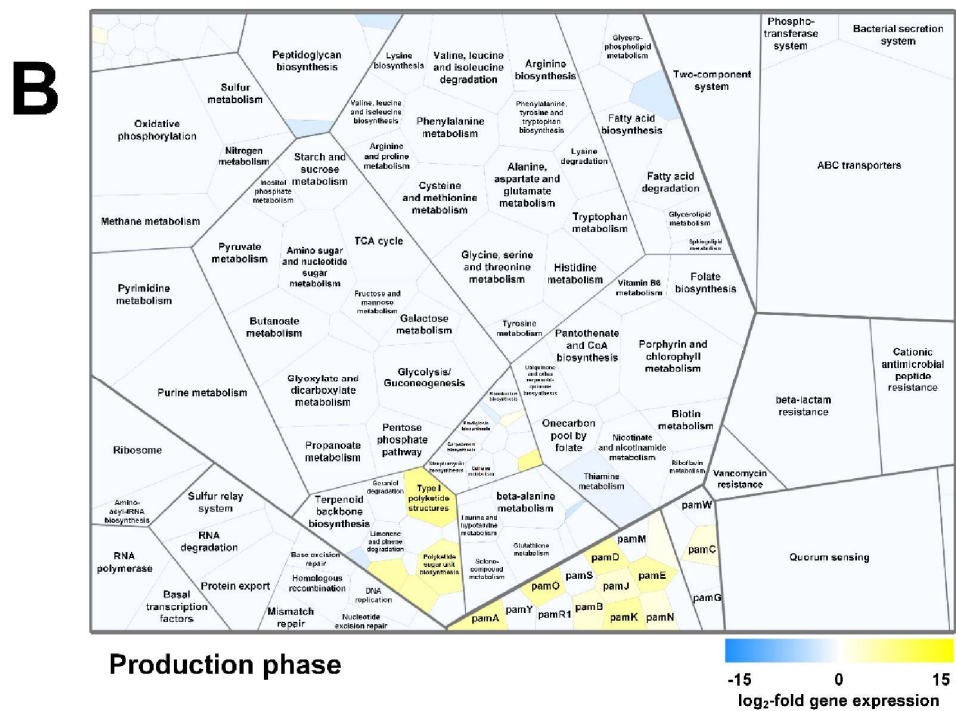
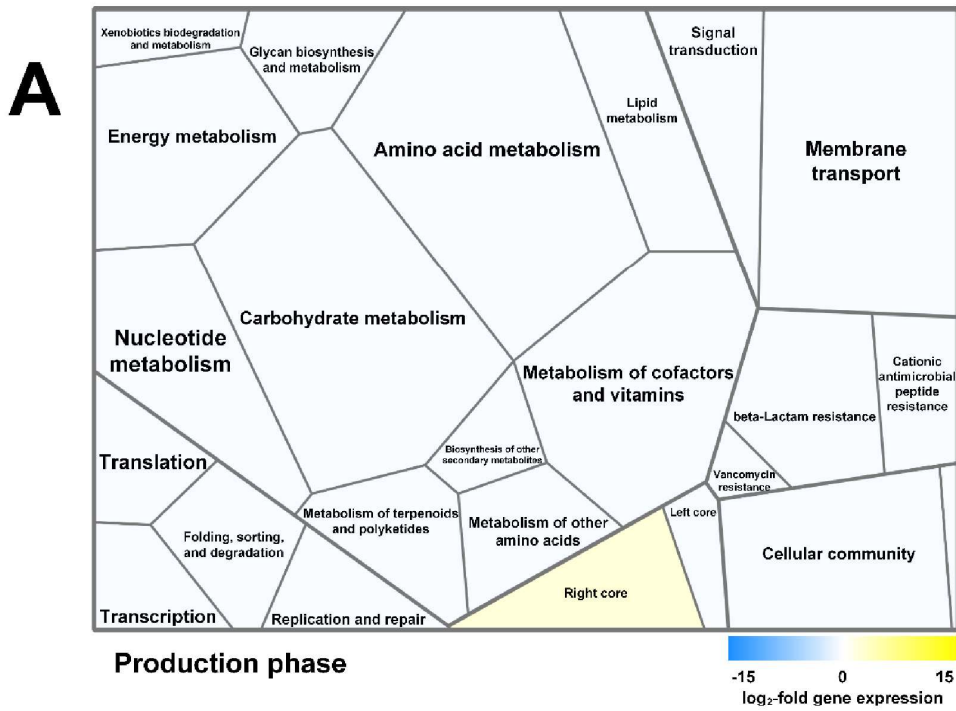
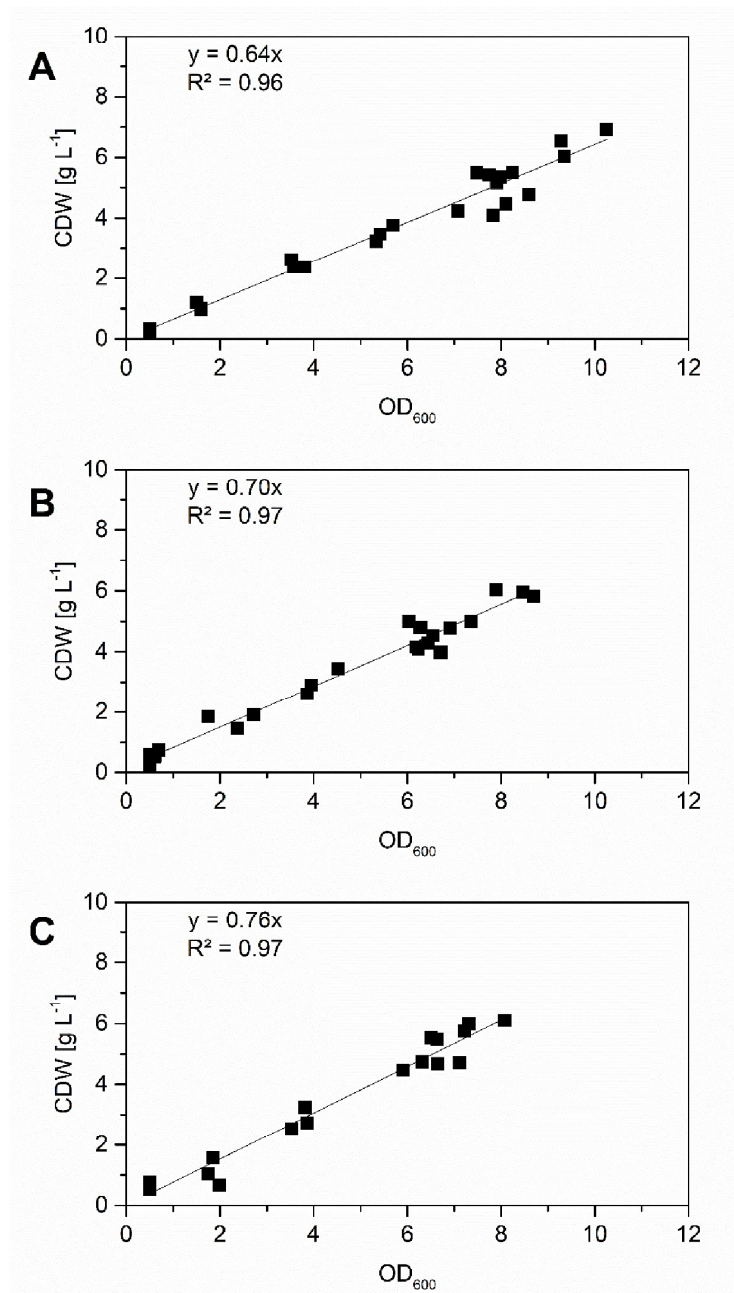


Figure S7: KEGG-orthology tree maps of *S. albus* J1074/R2 during production phase.

Average gene expressions of *S. albus* J1074/R2 in complex SGG medium without talc addition

during production compared to growth phase of the control. **A:** Each cell represents a functional class of the orthology: Carbohydrate metabolism, amino acid metabolism, lipid metabolism, nucleotide metabolism, energy metabolism, glycan biosynthesis and metabolism, xenobiotics biodegradation and metabolism, metabolism of cofactors and vitamins, metabolism of terpenoids and polyketides, biosynthesis of other secondary metabolites, metabolism of other amino acids, signal transduction, membrane transport, replication and repair, transcription, translation, folding, sorting and degradation, cellular community, cell motility, and the right and left core of the pamamycin gene cluster. Additionally, the subclasses of these classes are included in B.



**Figure S8: Correlation of cell dry weight (CDW) to optical density (OD<sub>600</sub>) for different cultivation conditions.** *Streptomyces albus* J1074/R2 was cultivated without talc supply (A) and in presence of 2.5 (B) and 10 g L<sup>-1</sup> talc (C) over 24 hours. At different time points, optical density and cell dry weight of each culture were determined simultaneously.

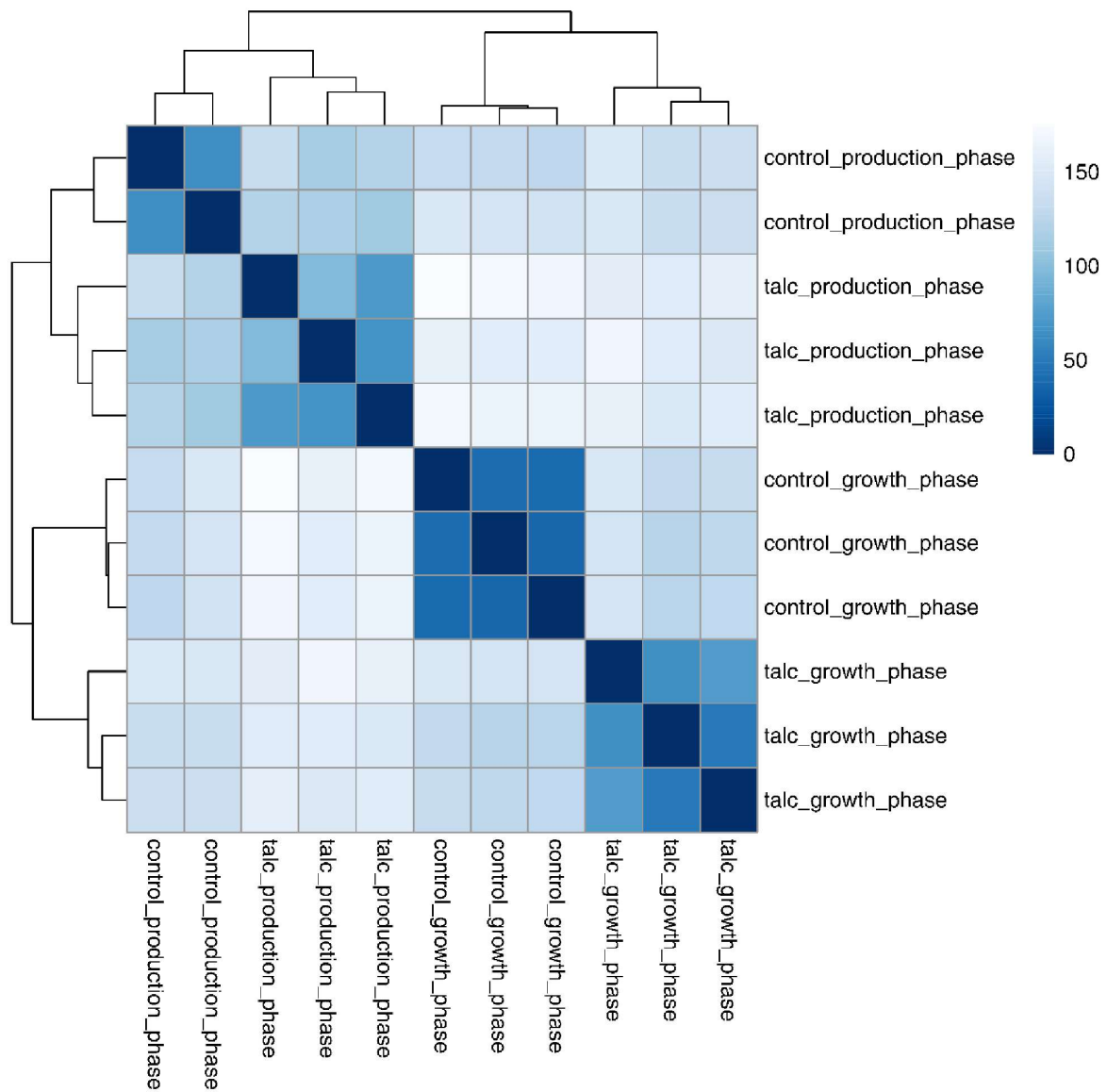


**Figure S9: Heatmap of the sample-to-sample distances from the RNA seq data.** The background corrected read count data were fed to DESeq2 (Love et al., 2014) to calculate normalized read counts. After regularized log transformation with blind dispersion estimation enabled, the sample to sample distances were calculated and used for hierarchical clustering, which in turn was visualized using pheatmap (Kolde, 2019).

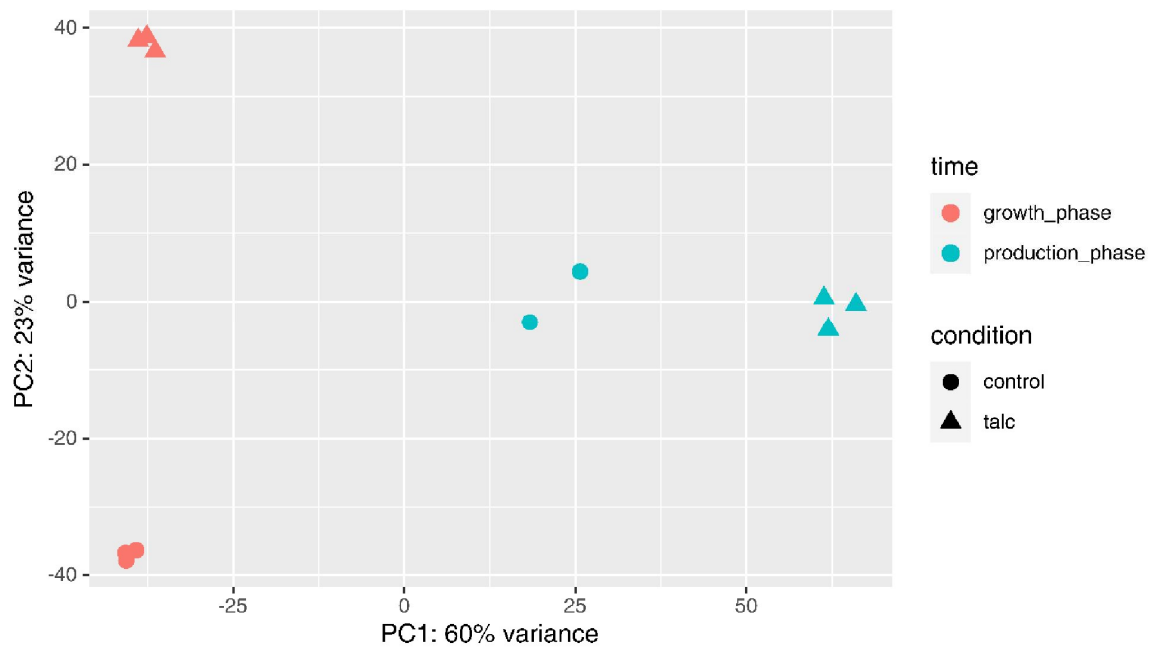


**Figure S10: PCA of the RNA seq data.** The background corrected read count data were fed to DESeq2 to calculate normalized read counts. After regularized log transformation with blind dispersion estimation enabled, a PCA was performed and visualized using ggplot2 (Wickham, 2016)

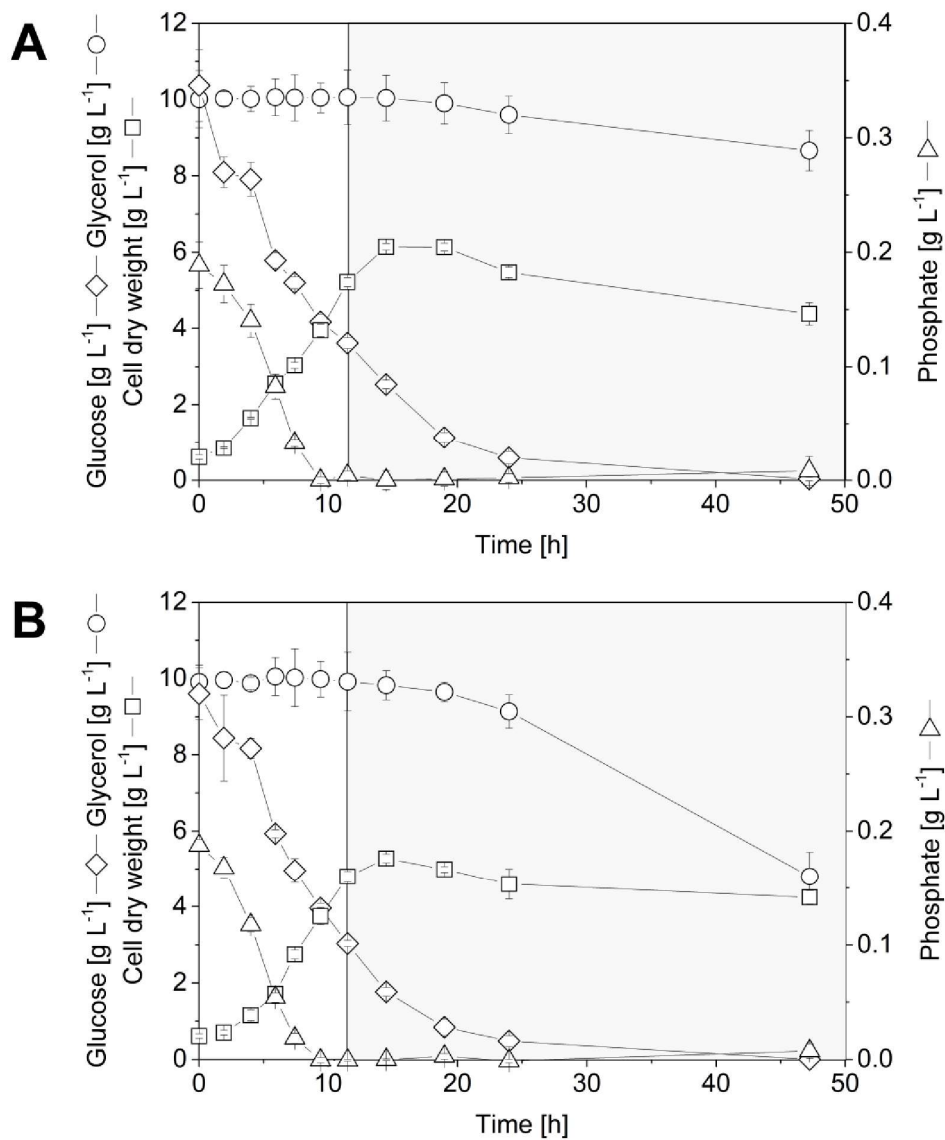


**Figure S11: Impact of talc microparticles on growth and substrate consumption in *Streptomyces albus* J1074/R2 using complex SGG medium with starch and glycerol as main carbon source.** Besides the cell density, the time dependent concentrations of glucose, glycerol, and phosphate are displayed. Control culture without microparticles (A). Microparticle-enhanced culture with 2.5 g L<sup>-1</sup> talc (B).

**Table S1: Gene expression of selected transcriptional regulators, primary  $\sigma$ -factors, and  $\sigma$ -factors of the ECF subfamily in pamamycin producing *Streptomyces albus* J1074/R2. Samples were taken from a control and a talc supplied culture (10 g L<sup>-1</sup>) in SGG medium during exponential growth (5 h) and production phase (21 h). For comparison, the expression levels of the control culture during growth were set as reference.**

Gene	Annotation	Growth (talc) log <sub>2</sub> -fold change	Production (talc) log <sub>2</sub> -fold change	Production (control) log <sub>2</sub> -fold change
XVRR2_1574	HTH-type transcriptional repressor DasR	0.0	0.0	0.0
XVRR2_3562	Pleiotropic negative regulator BldD	1.5	0.0	0.0
XVRR2_1043	RNA polymerase, sigma 70 subunit, RpoD	0.0	0.0	0.0
XVRR2_2142	RNA polymerase principal sigma factor hrdD	0.0	0.0	0.0
XVRR2_4476	RNA polymerase, sigma 70 subunit, RpoD	0.0	4.8	6.7
XVRR2_0615	RNA polymerase sigma factor ECF subfamily	0.0	0.0	0.0
XVRR2_0683	RNA polymerase sigma factor, ECF subfamily	0.0	-1.8	0.0
XVRR2_0749	RNA polymerase sigma factor, ECF subfamily	-1.9	-2.3	0.0
XVRR2_1515	RNA polymerase ECF-subfamily sigma factor	0.0	0.0	0.0
XVRR2_1584	RNA polymerase sigma factor RpoE, ECF subfamily	0.0	0.0	0.0
XVRR2_1656	RNA polymerase sigma factor SigE, ECF subfamily	0.0	2.3	0.0
XVRR2_2250	RNA polymerase ECF-subfamily sigma factor	-1.0	-1.3	0.0
XVRR2_2757	RNA polymerase ECF-subfamily sigma factor	1.1	0.0	0.0
XVRR2_2903	RNA polymerase ECF-subfamily sigma factor	3.5	2.5	0.0
XVRR2_2992	RNA polymerase sigma factor SigM, ECF subfamily	0.0	0.0	0.0
XVRR2_3275	RNA polymerase ECF sigma factor	0.0	0.0	-1.3
XVRR2_3298	ECF subfamily RNA polymerase sigma-70 factor	4.3	0.0	0.0
XVRR2_3489	RNA polymerase sigma factor, ECF subfamily	0.0	-2.9	-2.2
XVRR2_3527	BldN RNA polymerase, sigma-24 subunit, ECF subfamily	1.8	4.9	0.0
XVRR2_3805	RpoH RNA polymerase, sigma 32 subunit, ECF subfamily	-1.4	0.0	0.0
XVRR2_3945	ECF sigma factor	0.0	-2.3	-2.0
XVRR2_3984	RNA polymerase, sigma subunit, ECF family	1.7	2.9	0.0
XVRR2_3998	RNA polymerase ECF-subfamily sigma factor	-5.3	-4.0	-3.4
XVRR2_4039	RNA polymerase ECF-subfamily sigma factor	1.0	1.0	2.5
XVRR2_5208	RNA polymerase sigma factor SigK, ECF subfamily	1.7	-1.8	1.0
XVRR2_5283	RNA polymerase ECF-subfamily sigma factor	2.4	2.6	2.0
XVRR2_5529	RNA polymerase ECF-subfamily sigma factor	0.0	0.0	0.0
XVRR2_5625	RNA polymerase, sigma-24 subunit, ECF subfamily	1.0	1.5	1.0
XVRR2_5652	RNA polymerase sigma factor SigL, ECF subfamily	7.7	6.0	6.2
XVRR2_5893	ECF subfamily RNA polymerase sigma factor	8.0	4.6	7.8

**Table S2: Gene expression of homologues in pamamycin producing *Streptomyces albus* J1074/R2 to genes, previously shown to be involved in *Streptomyces* programmed cell death.** Samples were taken from a control and a talc supplied culture (10 g L<sup>-1</sup>) in SGG medium during exponential growth (5 h) and production phase (21 h). For comparison, the expression levels of the control culture during growth were set as reference.

Gene	Annotation	Homologue & identity [%]	Growth (talc)	Production (talc)	Production (control)
XVRR2_2393	Heat shock protein 60 family chaperone GroEL	SCO4296, <i>S. coelicolor</i> , 92.4	2.0	0.0	0.0
XVRR2_3800	Heat shock protein 60 family chaperone GroEL	SCO4296, <i>S. coelicolor</i> , 74.0	0.0	0.0	2.3
XVRR2_3753	50S ribosomal protein L36	SCO4726, <i>S. coelicolor</i> , 98.2	0.0	-1.2	-1.2
XVRR2_4513	Transcriptional regulator, CdaR	SCO2386, <i>S. coelicolor</i> , 82.9	0.0	0.0	0.0
XVRR2_2416	Tellurium resistance protein TerD	SCO4277, <i>S. coelicolor</i> , 92.5	3.2	2.9	0.0
XVRR2_4120	AlpC	SCO5032, <i>S. coelicolor</i> , 94.4	0.0	1.1	0.0
XVRR2_1430	Transcriptional regulator, MarR family	SCO5405, <i>S. coelicolor</i> , 75.9	2.2	0.0	0.0
XVRR2_0641	Glyoxylate carboligase	SCO6201, <i>S. coelicolor</i> , 84.4	0.0	0.0	0.0
XVRR2_0992	RNA methyltransferase, TrmA family	SCO5901, <i>S. coelicolor</i> , 82.4	-1.3	-2.2	0.0
XVRR2_0640	Catalase	SCO6204, <i>S. coelicolor</i> , 83.1	0.0	0.0	0.0
XVRR2_1593	Catalase	SCO6204, <i>S. coelicolor</i> , 72.5	1.7	6.7	0.0
XVRR2_1945	Catalase	SCO6204, <i>S. coelicolor</i> , 52.5	4.7	5.5	0.0
XVRR2_4128	Catalase	SCO6204, <i>S. coelicolor</i> , 57.4	0.0	0.0	0.0
XVRR2_4489	Catalase	SCO6204, <i>S. coelicolor</i> , 53.8	0.0	0.0	0.0
XVRR2_1130	Polyribonucleotide nucleotidyltransferase	SCO5737, <i>S. coelicolor</i> , 91.2	-1.7	-1.9	0.0

**Table S3: Gene expression of genes involved in the production of other secondary metabolites besides pamamycins.** Samples were taken from a control and a talc supplied culture (10 g L<sup>-1</sup>) in SGG medium during exponential growth (5 h) and production phase (21 h). For comparison, the expression levels of the control culture during growth were set as reference.

Gene	Annotation	Function	Growth (talc) log2-fold change	Production (talc) log2-fold change	Production (control) log2-fold change
XVRR2_5853	FscMIII	Candidicin bios.	5.4	2.6	1.0
XVRR2_5854	FscD	Candidicin bios.	11.4	9.3	11.4
XVRR2_5855	FscE	Candidicin bios.	5.7	5.1	6.4
XVRR2_5856	FscF	Candidicin bios.	8.4	9.1	11.0
XVRR2_5857	FscB	Candidicin bios.	7.0	4.6	6.5
XVRR2_5858	FscC	Candidicin bios.	6.6	5.7	7.5
XVRR2_5859	ABC-transporter	Candidicin bios.	9.4	6.7	7.3
XVRR2_5860	FscTI	Candidicin bios.	4.4	1.6	4.0
XVRR2_5861	FscA	Candidicin bios.	5.6	3.5	5.3
XVRR2_5862	Para-aminobenzoate synthase, amidotransferase component	Candidicin bios.	6.6	5.7	6.9
XVRR2_5863	FscTE	Candidicin bios.	6.6	5.0	1.0
XVRR2_5864	FscFE	Candidicin bios.	4.0	3.0	4.6
XVRR2_5865	Cytochrome P450	Candidicin bios.	6.1	4.9	1.0
XVRR2_5866	Aminotransferase	Candidicin bios.	5.9	3.8	5.5
XVRR2_5867	FscMI	Candidicin bios.	5.6	2.7	1.0
XVRR2_5868	LuxR family transcriptional regulator FscRIV	Candidicin bios.	5.4	3.3	5.0
XVRR2_5869	LuxR family transcriptional regulator FscRIII	Candidicin bios.	1.8	1.0	1.0
XVRR2_5870	LuxR family transcriptional regulator FscRII	Candidicin bios.	1.0	1.0	1.0
XVRR2_5871	LuxR family transcriptional regulator FscRI	Candidicin bios.	2.5	1.3	1.0
XVRR2_5872	PabC	Candidicin bios.	1.5	1.0	1.0
XVRR2_5873	FscO	Candidicin bios.	1.0	1.0	1.0
XVRR2_0573	dTDP-4-keto-6-deoxyhexose 3, 5-epimerase	PK sugar unit bios.	1.0	3.4	5.9
XVRR2_0574	dTDP-6-deoxy-L-hexose 3-O-methyltransferase	PK sugar unit bios.	1.3	4.4	6.2
XVRR2_0575	dTDP-4-keto-6-deoxy-L-hexose 2, 3-reductase	PK sugar unit bios.	1.0	2.4	5.0
XVRR2_0593	Glucose-1-phosphate thymidyl transferase	PK sugar unit bios.	2.0	2.5	3.4
XVRR2_0594	dTDP-glucose 4, 6-dehydratase	PK sugar unit bios.	1.4	1.5	1.0
XVRR2_0596	2, 3-dihydro-2, 3-dihydroxybenzoate dehydrogenase	Siderophore bios.	4.3	4.5	1.0
XVRR2_1297	Germaacridenol/geosmin synthase	Sesquiterp., triperenoid, bios.	1.5	1.7	1.1
XVRR2_1532	Polyprenyl diphosphate synthase	Terpenoid backbone bios.	6.7	7.8	5.4
XVRR2_0597	Phenazine biosynthesis protein PhzD	Phenazine bios.	4.3	5.3	6.8
XVRR2_0598	Phenazine biosynthesis protein PhzE	Phenazine bios.	1.9	3.2	1.0

## References

- Kolde, R. (2019). Pheatmap: Pretty Heatmaps. R Package Version 1.0.12. <https://CRANR-project.org/package=pheatmap>.
- Love, M. I., Huber, W., & Anders, S. (2014). Moderated estimation of fold change and dispersion for RNA-seq data with DESeq2. *Genome biology*, *15*(12), 550. doi:10.1186/s13059-014-0550-8
- Wickham, H. (2016). *ggplot2: elegant graphics for data analysis*: springer.